Process Development for Microalgal Cultivation System Towards Enhancement of CO_2 Fixation and Biochemical Production Efficiency

A Thesis Submitted in Partial Fulfilment of the

Requirements for the Degree of

DOCTOR OF PHILOSOPHY

Deepesh Singh Chauhan

School of Energy Science and Engineering

Indian Institute of Technology, Guwahati

Guwahati– 781039, Assam, India

August 2024

Dedicated

to

Almighty and My Family

INDIAN INSTITUTE OF TECHNOLOGY GUWAHATI

School of Energy Science and Engineering

STATEMENT

I do hereby declare that the content embodied in this thesis titled "*Process Development for Microalgal Cultivation System Towards Enhancement of CO_2 Fixation and Biochemical Production Efficiency*" is the result of investigations carried out by me in the School of Energy Science and Engineering, Indian Institute of Technology Guwahati, Guwahati, India, under the supervision of Prof. Kaustaubh Mohanty and Prof. Lingaraj Sahoo. In accordance with the established research reporting practices, due acknowledgements have been made wherever the work described is based on the findings of other investigators.

Date:

Deepesh Singh Chauhan

(Roll No.: 176151004)

INDIAN INSTITUTE OF TECHNOLOGY GUWAHATI

School of Energy Science and Engineering

SUPERVISION CERTIFICATE

This is to certify that Mr. Deepesh Singh Chauhan (Roll No.: 176151004) has conducted his doctoral thesis research under our supervision since July 2017. His thesis titled "*Process Development for Microalgal Cultivation System Towards Enhancement of CO_2 Fixation and Biochemical Production Efficiency"* is hereby submitted for the award of the Doctor of Philosophy degree. We affirm that Mr. Chauhan has successfully completed all requirements for the Doctor of Philosophy program as set forth by the regulations of the Indian Institute of Technology Guwahati. We further confirm that the research presented in this thesis is original and has not been submitted for a degree at any other institution

Prof. Kaustubha Mohanty
(Thesis Supervisor)
Professor (HAG) and Head,
Department of Chemical engineering,
School of Energy Science and Engineering,
Indian Institute of Technology Guwahati,
Guwahati - 781039, Assam, India

Date:

ACKNOWLEDGEMENTS

This thesis would not have been possible without the invaluable support and guidance of all the incredible people. I am truly grateful to each and every one for their enriching contributions to this thesis and my life.

Deepesh Singh Chauhan

August 2024

Abstract

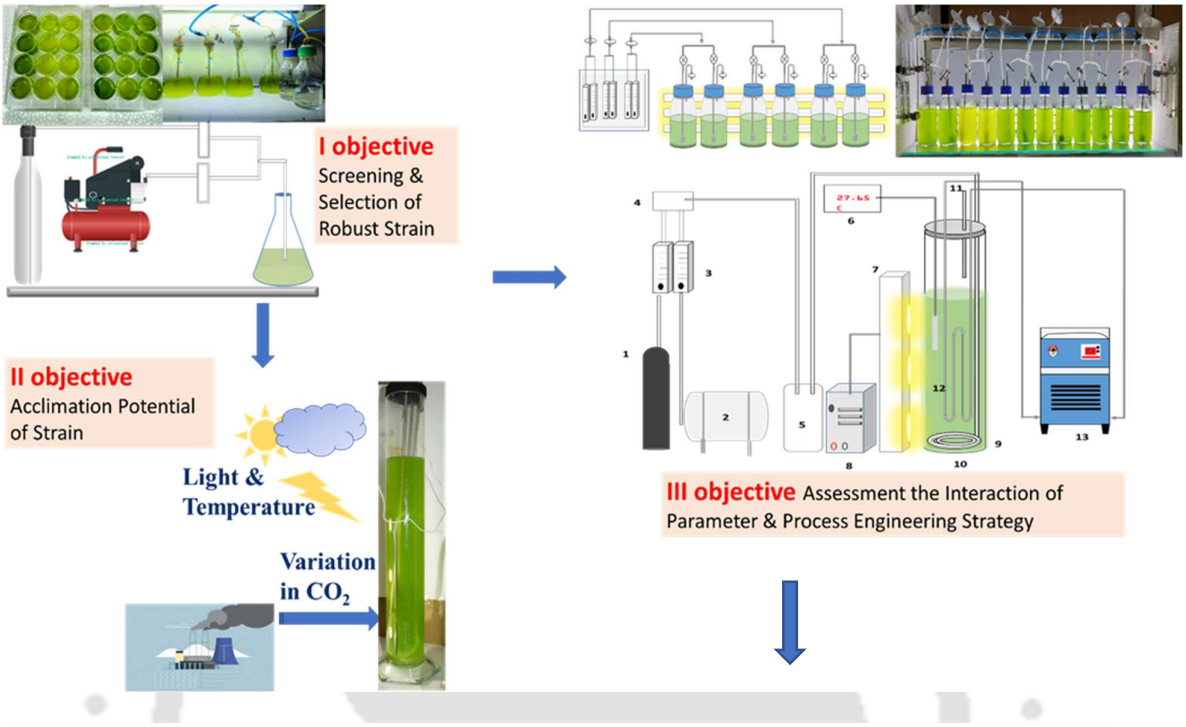
I objective
Screening & Selection of Robust Strain
II objective
Acclimation Potential of Strain
Light & Temperature
Variation in CO_2
III objective Assessment the Interaction of Parameter & Process Engineering Strategy
IV objective Development of Self Sustainable Microalgal Carbon Capture & Biochemical Production Process

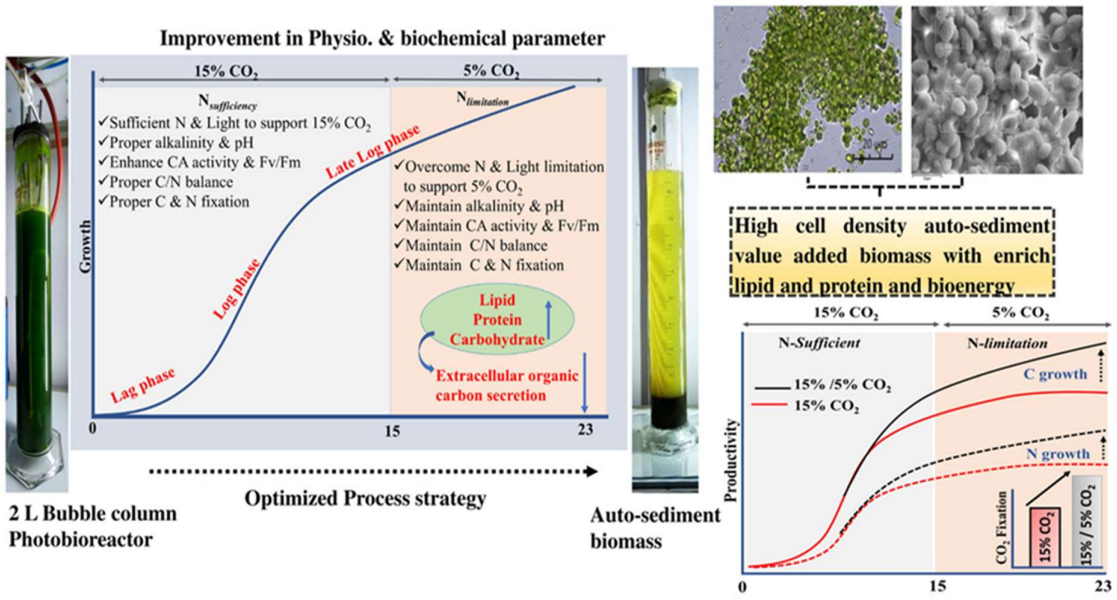
Improvement in Physio. & biochemical parameter
15% CO_2
5% CO_2
$N_{sufficiency}$
✓Sufficient N & Light to support 15% CO_2
✓Proper alkalinity & pH
✓Enhance CA activity & Fv/Fm
✓Proper C/N balance
✓Proper C & N fixation
$N_{limitation}$
✓Overcome N & Light limitation to support 5% CO_2
✓Maintain alkalinity & pH
✓Maintain CA activity & Fv/Fm
✓Maintain C/N balance
✓Maintain C & N fixation
Lipid
Protein
Carbohydrate
Extracellular organic carbon secretion
Growth
Lag phase
Log phase
Late Log phase
0
15
23
2 L Bubble column Photobioreactor
Optimized Process strategy
Auto-sediment biomass
High cell density auto-sediment value added biomass with enrich lipid and protein and bioenergy
15% CO_2
5% CO_2
N-Sufficient
N-limitation
15% /5% CO_2
15% CO_2
C growth
N growth
Productivity
CO_2 Fixation
15% CO_2
15% / 5% CO_2
0
15
23

Microalgae have emerged as a promising solution for CO_2 sequestration and biofuel production due to their rapid growth and high lipid accumulation. However, the commercial and industrial viability of microalgal technologies faces significant challenges. To fully harness the potential of microalgae-based carbon capture systems, several hurdles must be addressed, including low CO_2 capture efficiency, sensitivity to abiotic stresses, and high demands for water and nutrients. Additionally, effective large-scale harvesting poses further challenges. This thesis explores solutions to these challenges, focusing on strain selection, optimization of physiochemical factors, CO_2 utilization stability, high biomass production, cost-effective harvesting, and water reuse.

Initially, 12 microalgal strains were screened for their tolerance to the complex composition of industrial flue gas. Growth rate metrics and photosynthetic performance indicators were used to assess their suitability. Promising strains were further acclimatized through a two-stage cultivation strategy involving bicarbonate and high CO_2 conditions. The selected strains were evaluated for their stability in CO_2 fixation and lipid production under continuous industrial flue gas conditions. Among the strains, NCIM5584 and KMC8 showed the greatest resistance to flue gas chemicals, with significant biomass yield and photosynthetic efficiency. KMC8, in particular, demonstrated exceptional performance with a biomass production rate of 52.5 mg L^{-1} day^{-1}, a CO_2 fixation rate of 346.43 mg L^{-1} day^{-1}, and neutral lipid accumulation up to 20%.

Further investigation into the adaptive mechanisms of *Micractinium pusillum* KMC8 in response to varying light and temperature conditions during semi-continuous culture revealed that evaluating growth parameters, CO_2 fixation rates, and metabolite changes is crucial for commercial scale-up in outdoor environments. *M. pusillum* effectively adapted to simulated severe summer and winter temperatures and varying light intensities, maintaining photosynthetic efficiency and bioenergy content. CO_2 utilization efficiency ranged from 0.32% to 2.03%, exceeding 1.5% under high light and temperature conditions. The lipid content ranged from 23% to 34%, consisting of C-18 and C-16 fatty acids suitable for biodiesel production. Acclimation to high light and temperature conditions improved biomass quality by regulating and remodeling metabolites with carbon content (>50%) without affecting photosynthesis or growth. *M. pusillum's* rapid metabolic adaptations and acclimation responses with excellent CO_2 bio-mitigation illustrate its outdoor resilience in light/dark temperature regimes.

Further research explores the impact of initial nitrogen levels, phosphate availability, and light conditions on the growth dynamics, CO_2 utilization, and lipid production of *M. pusillum*. A semi-continuous cultivation system incorporating media recycling was employed to evaluate long-term productivity and CO_2 mitigation strategies. Logistic and Gompertz models were employed to analyze the kinetics of KMC8 cell growth. Doubling and quadrupling nitrate-based nitrogen concentrations from standard BG-11 media (17.65 mmol/L) boosted biomass growth by 12.5% and 28.78%, respectively, compared to the control. Increasing nitrogen levels to 70.6 mmol/L resulted in a pH above 7 and improved photosynthetic performance, leading to a CO_2 utilization efficiency of 2.27%. Nitrogen deprivation boosted lipid content to 26%, but reduced growth and photosynthesis performance resulted in a 67.15% reduction of CO_2 assimilation performance.

Besides nitrogen, the availability of phosphorus and the intensity of light also impacted the mitigation of CO_2. Higher phosphorus levels and initial high light intensity resulted in better biomass (2.87 g L^{-1}) and lipid productivity (34.34 mg L^{-1} day^{-1}). Gradually increasing light intensity from 150 to 1200 μmol m^{-2} s^{-1}, combined with higher phosphorus content, resulted in an 85% increase in biomass productivity (255 mg L^{-1} day^{-1}) and a 2.5-fold increase in lipid productivity (84.76 mg L^{-1} day^{-1}), with a CO_2 utilization efficiency of 3.3%. A water recycling-fed batch cycle with gradual light feeding resulted in high CO_2 fixation (1.1 g L^{-1} day^{-1}), 7% CO_2 utilization, and significant biomass and lipid productivity (577.23 and 150 mg L^{-1} day^{-1}). This approach promotes lipid synthesis, maintains carbon fixation, and minimizes biomass loss, supporting sustainable bioenergy development in a circular bio-economy framework.

Finally, the study addresses the challenges of CO_2 acidification, saturation, and limited access to flue gas (5-15%) which pose hurdles to stable carbon fixation, often resulting in 5-15 days of suboptimal biomass productivity. Strategies to enhance microalgae growth and CO_2 utilization were investigated over a 23-day period, focusing on the *Micractinium pusillum* strain. Urea served as a cost-effective nitrogen supplement, facilitating growth peaking under 5% CO_2 exposure with a longer growth phase, followed by exposure to 15% CO_2. However, in the later phase under 15% CO_2 conditions, media acidity and reduced alkalinity due to nitrogen deprivation led to pigment loss and diminished photosynthetic efficiency, impacting carbon assimilation in biomass. To address this challenge, cultivation commenced with 15% CO_2 and transitioned to 5% CO_2 after 15 days using a calcium-induced phosphorus fed-batch approach, effectively mitigating media acidification and stabilizing photosynthesis and carbonic anhydrase activity. Consequently, a notable 20% increase in CO_2 fixation and a 15% boost in

biomass productivity was observed. Moreover, lipid, protein, and carbohydrate production surged, ensuring efficient carbon and nitrogen assimilation and augmenting biomass bioenergy potential. Nonetheless, performance declined during transitions to air and continuous 15% CO_2 conditions, indicating the need for further optimization. SEM-EDX analysis underscored auto-sedimentation dynamics, highlighting the pivotal roles of calcium and phosphorus in cell aggregation. These findings offer valuable insights into improving algal bioprocessing for effective CO_2 mitigation and biochemical production, demonstrating a promising 23-day stability in carbon mitigation and induction of auto-flocculation during growth, paving the way for sustainable biomanufacturing practices.

This research underscores the critical role of strategic process engineering in enhancing microalgal growth, photosynthesis, CO_2 mitigation, and bioenergy production. The findings provide valuable insights for the scalable and sustainable application of microalgae for CO_2 capture and biofuel generation, demonstrating the potential for effective bioprocessing, carbon sequestration, and efficient biomass harvesting.

CONTENTS

LIST OF TABLES

LIST OF FIGURES

भारतीय प्रौद्योगिकी संस्थान गुवाहाटी
Indian Institute of Technology Guwahati

CHAPTER 1

Introduction

Chapter 1

Introduction

1.1 Energy Scarcity and Climate change

Tackling the pressing issues of the energy crisis and climate change have emerged as the top priority in today's global society. Carbon dioxide (CO_2) and other greenhouse gases have a significant influence on climate change, ecosystems, economy, and society as a whole. The 2023 report from the International Energy Agency (IEA) emphasizes a troubling trend: worldwide CO_2 emissions linked to energy consumption have risen by 1.1%, reaching an unprecedented level of 37.4 gigatons (Gt). The current year (according to the IEA CO_2 emssion report , 2023) shows an increase of 410 metric tons (Mt) compared to the previous year. The graph in Fig.1.1 clearly demonstrates the consistent increase in average CO_2 emissions from 1900 to 2023.

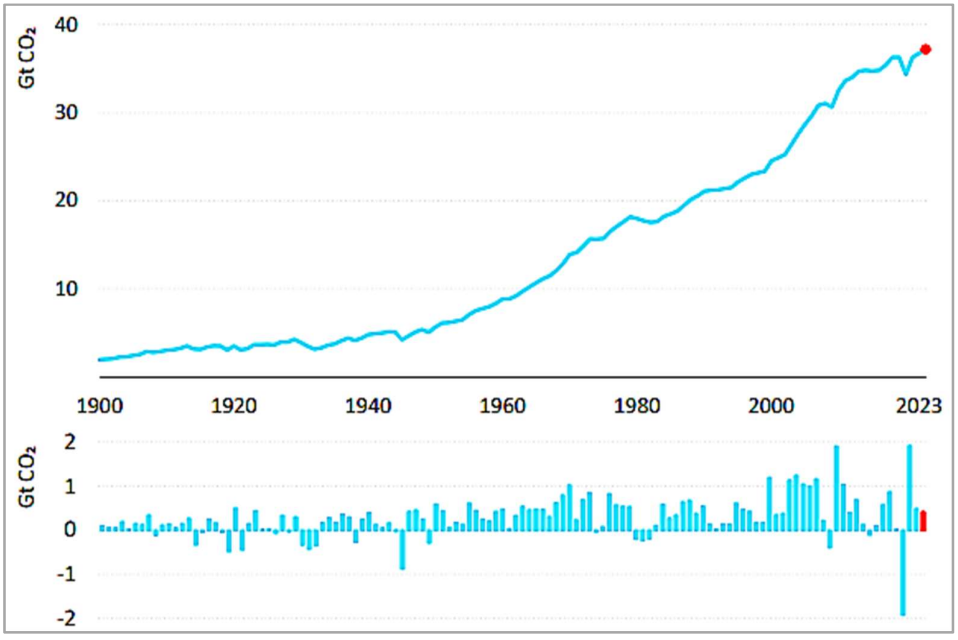

Fig. 1.1. Global energy related CO_2 emission and their annual changes from 1900-2023 (Source: International Energy Agency, 2023)

The adverse impacts of climate change, including extreme weather events, rising sea levels, and biodiversity loss, pose significant obstacles to the attainment of sustainable development objectives and amplify risks across several sectors. It is important to acknowledge that several nations have unique contributions to CO_2 emissions, with variances in how these emissions are distributed across various sectors. Emissions mostly arise from the burning of fossil fuels, namely in the domains of energy, transportation, and buildings [2]. In India, the burning of coal in thermal power plants leads to around 550 million metric tons of CO_2 being released into the atmosphere each year. This is mostly done to generate energy, as stated in the IEA CO_2 emission report of 2023. The Paris Agreement is a significant global pact in the international endeavor to tackle climate change. The main objective is to keep the increase in global temperatures to below 2 ℃ compared to pre-industrial levels, with an additional goal of advocating for a cap of 1.5 ℃ [3]. To do this, it is crucial to reduce emissions and promote sustainable growth. However, the energy industry is now facing several complicated issues, such as the depletion of fossil fuel supplies, disputes over resources, and concerns around energy security and price. India is committing to achieve carbon neutrality by 2070, which entails balancing the emission and removal of greenhouse gases in the atmosphere [4]. To accomplish this pledge, it is necessary to adopt low-carbon technologies and use carbon capture methods in important sectors such as electricity, industry, and transportation. This will make a significant contribution to the goals of sustainable development. It is crucial to prioritize the Sustainable Development Goals (SDGs) while promoting carbon-negative industrial production processes in order to effectively tackle climate change and promote sustainable development [5]. This highlights the need for enhanced efforts in improving the development of carbon capture and utilization (CCU) technologies. CCU technologies have the capacity to decrease CO_2 emissions while promoting economic expansion and sustainability [3]. The rapid advancements in CCU research underscore the urgent need to ascertain the most efficient carbon utilization methodologies. Due to the pressing need, there has been a 5% enhancement in the development pipeline of the CCU project (Fig.1.2). It is important to mention that as of now, only 41 facilities are actively harvesting CO_2, while there are approximately 500 initiatives in the research and development phase (IA CCUS Policies, 2022).

.

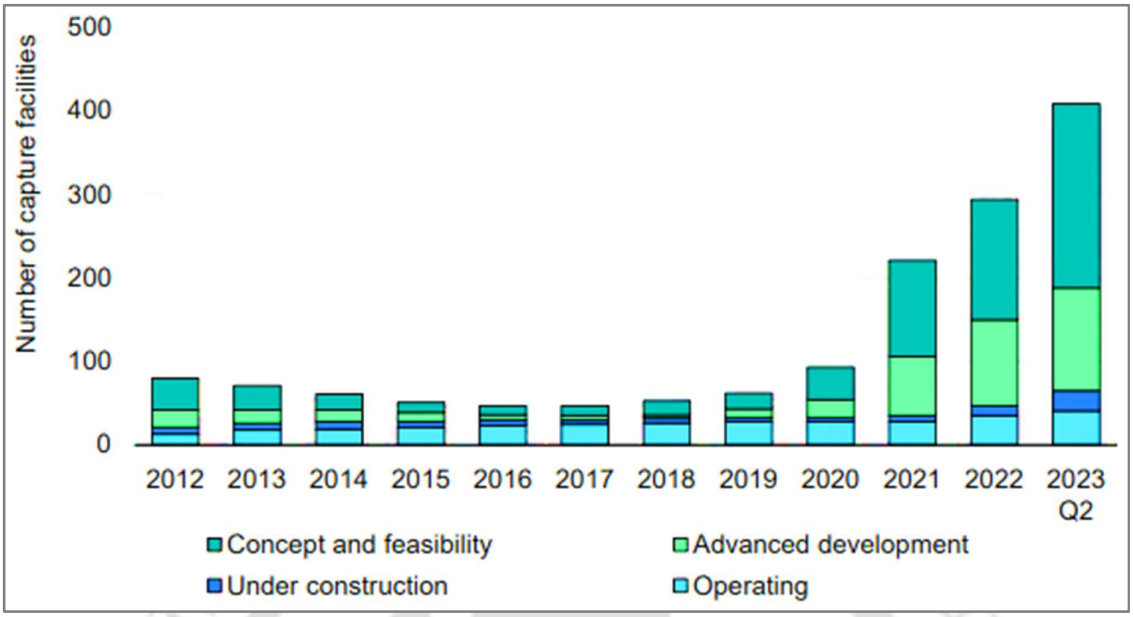

Fig. 1.2 Evolution of the CO_2 capture project pipeline from 2012- 2023 (Source: International Energy Agency, 2023)

1.2 Current Carbon Capture Technologies and Challenges

Over the past decade, carbon capture and storage (CCS) or CCS-utilization (CCSU) technology has become a crucial approach for reducing CO_2 emissions from human-made sources [7]. Post-combustion capture is the predominant technology used in power stations and industrial facilities that depend on fossil fuels [8]. This procedure involves the extraction of carbon dioxide from the flue gas produced during the process of burning. Post-combustion capture systems often use solvent-based absorption, adsorption, and membrane separation processes [9]. The solvent-based physical and chemical absorption technique, which is widely used for carbon capture, involves the use of solvents such as Rectisol and amine-based solutions (e.g., Selexol) to selectively absorb CO_2 from the flue gases released by industrial operations, mostly in power plants and refineries [10]. The CO_2 that has been taken in is then extracted from the solvent via a process of regeneration. Adsorption is a process that utilizes solid materials such as activated carbon or metal-organic frameworks silica/alumina/zeolites, porous crystalline solids, and metal oxides to trap and remove CO_2 from flue gases [11]. After being fully saturated with CO_2, the adsorbent goes through a regeneration process to release the absorbed CO_2 for storage or use. Furthermore, novel techniques involving the use of polyphenylene and polydimethylsiloxane membranes have been developed for membrane-

based separation and adsorption procedure. These membranes exhibit selective permeability to CO_2 molecules, enabling their passage while preventing other gases from flue gas or adsorbing onto the surface [12]. Cryogenic separation [13] and hydrate-based gas separation [14] and many hybrid processes with combination of two process [15] are further advanced methods used for the capture of CO_2.

Pre-combustion capture is a crucial technology used in integrated gasification combined cycle (IGCC) power plants and coal-to-liquid (CTL) facilities [16]. This process entails the conversion of solid or liquid fuels, such as coal or natural gas, into syngas, a gas mixture containing a high concentration of hydrogen and carbon monoxide. Following purification methods separate CO_2 from other gases by using techniques such as pressure swing adsorption (PSA) or membranes. Notwithstanding the advantages of these carbon capture methods, they encounter many obstacles. The primary obstacles faced include energy-intensive methods, poor CO_2 collection efficiency, high operating costs, and technical hurdles [17]. Furthermore, the safe handling and preservation of collected CO_2 pose logistical and environmental challenges. Ultimately, carbon capture technologies have great potential for reducing CO_2 emissions. However, it is crucial to address the associated challenges in order to promote their extensive use on an industrial level [18].

Utilizing biological techniques to capture and stabilize carbon presents a hopeful approach to tackle the urgent issues of climate change and carbon emissions. Biological methods, unlike traditional carbon capture technologies, utilize living organisms such as plants, algae, and microorganisms to capture carbon dioxide from the atmosphere or industrial emissions [19]. One of the most advanced technologies in this field is microbial electrolysis carbon capture (MECC). However, the commercialization of the MECC system remains distant in practical implementation. Only laboratory-scale studies have been conducted due to technological obstacles and insufficient efficiency, which must be addressed to ensure the practicality of scaling up the system [20].

1.3 Advantage of Microalga based CO_2 Capture and Utilization

Microalgae has several benefits compared to conventional land plants and other biological techniques, such as microbial electrolysis cells, for the purpose of carbon capture as illustrate in Fig.1.3. Microalgae may be cultivated in non-arable locations such as deserts or coastal areas

utilizing saline or wastewater resources, unlike terrestrial plants that need arable land and may compete with food production [21].

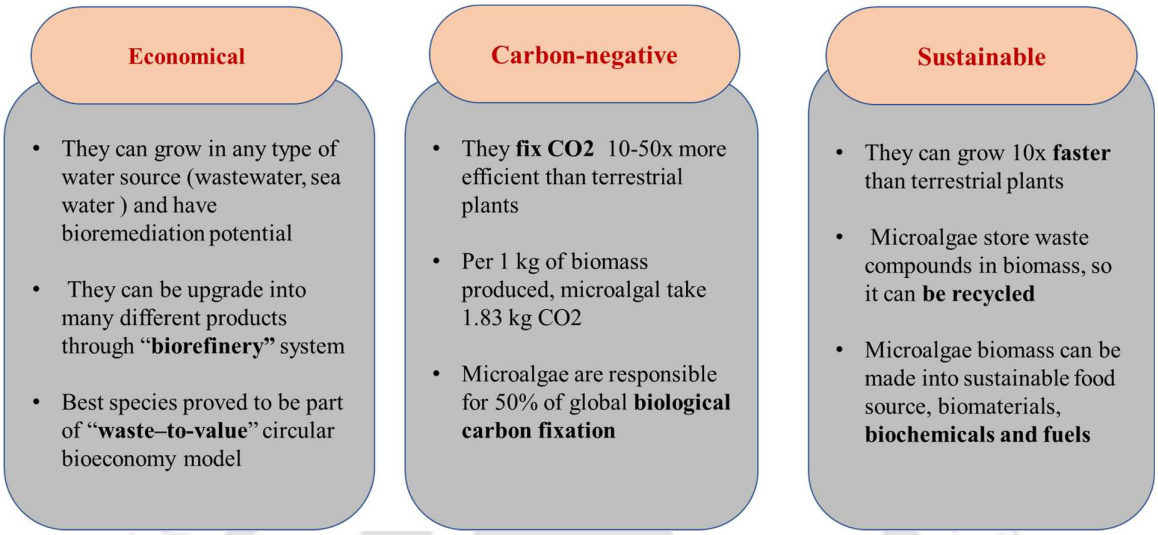

Fig. 1.3. Advantage of microalgal based carbon-dioxide capture and utilization

This approach reduces the environmental consequences of carbon capture activities and prevents any clashes with agricultural activities. Moreover, microalgae generally exhibit high growth rate and possess greater capabilities for CO_2 fixation in comparison to land-based plants. Microalgae have a carbon sequestration capacity that is 10 to 50 times greater than that of terrestrial plants, making them more effective in fixation of CO_2 from the environment. Microalgae provide benefits over microbial electrolysis carbon capture (MECC) in terms of scalability and ease of operation [22]. MECC uses electroactive microorganisms to convert CO_2 into useful chemicals, whereas microalgae offer a more straightforward and efficient approach and convert into high value-added biomass with high valued added bioproduct and biofuels under biorefinery approach [23]. Microalgae-based carbon capture systems are characterized by their simplified infrastructure and low maintenance requirements, which enhances their accessibility and cost-effectiveness for large-scale implementation where other technology is lacking [24]. Moreover, microalgae may be grown in either open ponds or closed photobioreactors, providing versatility in system configuration and the ability to adjust to various environmental conditions and conversion onto CO_2 into desired targeted with control process strategy [25]. In summary, the distinct qualities of microalgae make them very viable options for large-scale and environmentally friendly carbon capture systems, in contrast to other convection technology.

Although microalgae-based carbon capture technologies provide several advantages, it is crucial to acknowledge and tackle the impending obstacles. To fully use the potential of microalgae in carbon capture, it is necessary to tackle various hurdles. The challenges involve selecting an appropriate strain, understanding the influence of different physicochemical parameters and their interactions on the microalgal CO_2 fixation process, improving CO_2 utilization and stability, attaining high cell and biomass production under industrial-scale CO_2 conditions, and creating cost-effective harvesting and processing techniques. The challenges mentioned will be thoroughly examined in Chapter 2 of the thesis, which will include a full assessment of existing literature to address these difficulties and provide potential solutions. Through comprehensive study and analysis, the goal is to demonstrate the potential of microalgae as a viable and sustainable solution to addressing climate change and advancing environmental sustainability.

1.4 Microalgal Photosynthesis CO_2 fixation Regulation and Mechanism

Microalgae use photosynthesis for transforming solar energy and atmospheric CO_2 into energy, lipids, proteins, and carbohydrates via complex mechanisms. Carbohydrates are the first molecules produced in microalgae via the process of CO_2 fixation during photosynthesis. This process has two discrete stages: the light-dependent reactions and the dark reactions, commonly referred to as the Calvin-Benson cycle. As seen in Fig. 1.4, the light reaction takes place in the grana, which are stacks of thylakoids containing pigment molecules complex known as Photosystem I and II. On the other hand, the dark reaction happens in the liquid portion of the chloroplast called the stroma. During the light-dependent processes, photons from sunlight or artificial light provide energy to pigment complexes, consisting mostly of chlorophyll a and b, as well as carotenoids, in photosystems I and II. Photosystems composed of mostly chlorophyll pigments are primarily found in the Chlorophyceae class of green algae. However, their composition might vary across different class of algae [26]. The energy that is absorbed is transmitted to the electron transport chain, resulting in the production of high-energy molecules (ATP) and reducing molecules (NADPH). This process also leads to the photolysis of water, that delivers oxygen. The ATP and NADPH generated are used in the Calvin-Benson cycle, which takes carbon dioxide via the enzyme ribulose bisphosphate carboxylase-oxygenase (Rubisco). This reaction leads to the production of two molecules of 3-phosphoglycerate (3PG).

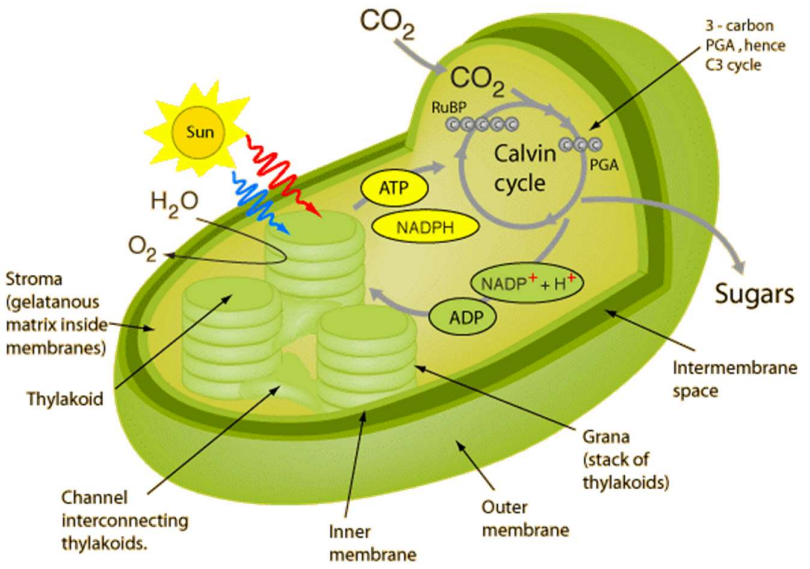

Fig. 1.4. Light and dark reaction in microalgal chloroplast (Adopted from Geider, Richard J. 1955, *Algal photosynthesis*)

Rubisco serves as the catalyst for this process. The 3PG is assimilated into the central carbon metabolism via glycolysis and the pentose phosphate pathway, supplying carbon skeletons and energy for the synthesis of macromolecules and promoting growth [28]. However, Rubisco also has an oxygenase function, enabling it to bond with oxygen and diminish the ability for CO_2 fixation. Microalgae overcome this constraint by using a carbon dioxide concentrating mechanism (CCM) that increases CO_2 concentration by up to 1000 times relative to the levels in the liquid media. This effectively reduces the binding of oxygen to Rubisco. Carbonic anhydrases (CAH) are essential for maintaining the balance between CO_2 and HCO_3^- and aiding their movement across membranes. These enzymes improve the efficacy of Rubisco in pyrenoids, which in turn increases the amount of CO_2 available for photosynthesis [29], as seen in Fig.1.5. In the process of microalgal culture CO_2 from the atmosphere or other sources enters the liquid medium. Once in the medium, it dissolves and combines with water to create carbonic acid (H_2CO_3). The carbonic acid undergoes dissociation, resulting in the formation of bicarbonate ions (HCO_3^-) and hydrogen ions (H^+). The balance between these species is influenced by the pH level. The enzyme carbonic anhydrase speeds up the conversion of CO_2 to bicarbonate, ensuring effective carbon utilization. Microalgae immediately fix CO_2 or transport bicarbonate into their cells. Inside the cells, an internal enzyme called CAH transforms the bicarbonate back into CO_2.

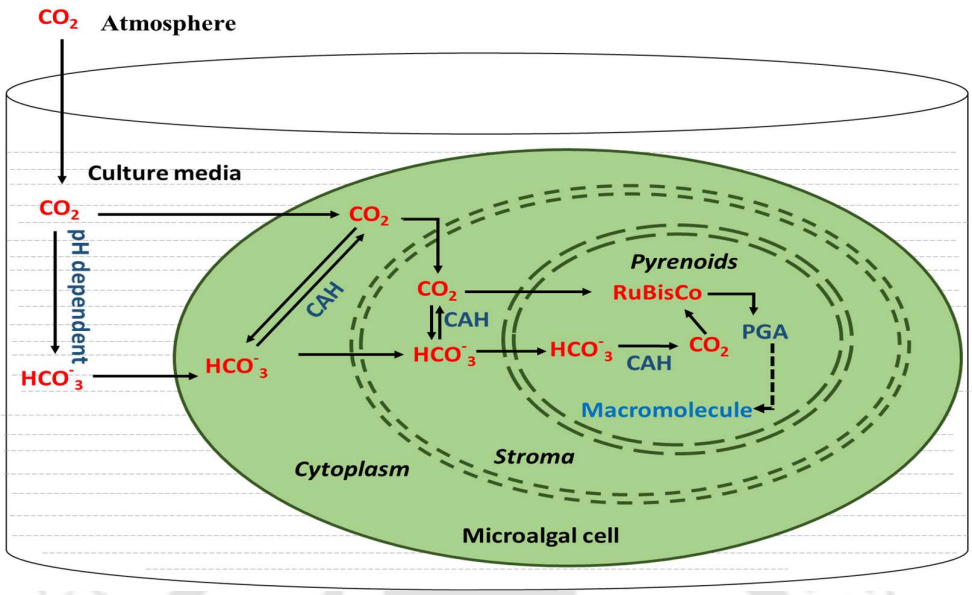

Fig. 1.5. CO_2 biochemistry and uptake in microalgal cells. This figure shows CO_2 conversion to HCO_3^- in the media and its uptake by microalgal cells. Inside the cells, CO_2 is fixed in the chloroplast stroma by RuBisCO in the Calvin cycle, with carbonic anhydrase (CAH) facilitating these processes.

Therefore, it is important to create optimized extracellular conditions in order to maximize CO_2 based carbon availability in media and fixation.

1.5 CO_2 Fixation and Carbon Allocation Pathways in Microalgal Photosynthesis

Microalgae have the ability to efficiently capture CO_2 and generate biomass that can be processed into various biochemicals and biofuels. This makes them a very promising candidates for carbon capture and utilization. Carbohydrates, lipids, and proteins are the primary macromolecules that are synthesized by metabolic pathway. These biomolecules may be processed using a biorefinery technology to produce biofuels, human food, animal feed, polymer and other products. The metabolic pathways responsible for the production of carbohydrates, lipids, and proteins in microalgae are highly controlled and influenced by many external stimuli and cellular conditions during photosynthesis [30]. These pathways regulate the allocation of carbon fixed during photosynthesis into specific biomolecules, enabling microalgae to adapt to varying environmental conditions [31]. These routes are regulated by changes in carbon source and light availability, which in turn modify the trophic mode of culture, as shown in Fig. 1.6.

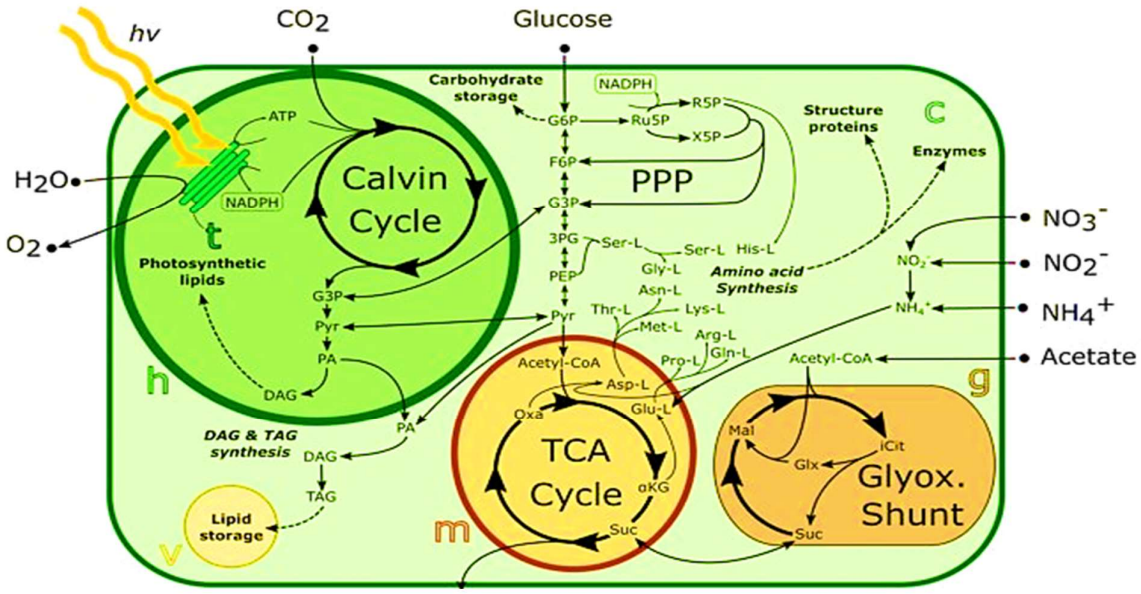

Fig. 1.6. Overview of metabolic pathways in microalgal cells. This figure depicts the key metabolic pathways in microalgal cells, including the Calvin cycle, the tricarboxylic acid (TCA) cycle, the glyoxylate shunt, and the pentose phosphate pathway (PPP). It highlights the conversion of CO_2 to glucose through photosynthesis, the synthesis of lipids, and the assimilation of nitrogen sources (Adapted and modified from Tibocha-Bonilla et al., 2018)

Under ideal growth situations, characterized by high light intensity and sufficient nutrients such as nitrogen and phosphorus, microalgae prefer to allocate a substantial amount of their carbon, acquired from photosynthesis, towards the production of carbohydrates. Starch, a polysaccharide, is the main carbohydrate produced and acts as an energy storage molecule [33]. Enzymes such as ADP-glucose pyro phosphorylase and starch synthase facilitate this process. Cellular metabolism and development are fueled by the creation of soluble sugars such as glucose and sucrose, which serve as easily accessible sources of energy. Microalgae are able to store extra energy by accumulating carbohydrates, which may then be used when there is little light or a shortage of nutrients [34]. Conversely, when microalgae are subjected to stressful circumstances, namely a lack of nutrients such as nitrogen or phosphorus, their metabolic activity redirects towards the production of lipids. In such circumstances, the limited presence of nitrogen hampers the production of proteins, leading to a buildup of carbon compounds that are subsequently used for the synthesis of fatty acids [35]. The fatty acids are then converted into triacylglycerols (TAGs) by esterification. These TAGs then aggregate as lipid droplets within the cells. The buildup of lipids serves as a survival strategy for microalgae,

enabling them to store energy in a concentrated and simplified form that may be used throughout extended periods of stress [36]. The principal enzymes implicated in this route are acetyl-CoA carboxylase, fatty acid synthase, and diacylglycerol acyltransferase [37]. The process of protein synthesis in microalgae is highly reliant on the presence of nitrogen, a crucial ingredient for the production of amino acids and proteins. When there is an abundance of nitrogen, microalgae devote a substantial amount of their carbon and energy to the production of proteins, which are essential for cellular structure, enzymatic activities, and metabolic control. The Calvin cycle produces precursors, such as glycerate-3-phosphate and pyruvate, which are then transaminated to make amino acids [38,39]. The ribosomes govern the polymerization of these amino acids into proteins, a process that is influenced by the supply of ATP and reducing power derived from the light-dependent activities of photosynthesis [40].

The challenging modulation of various metabolic pathways in microalgae arises from intricate interplay between external factors and cellular regulatory systems. The activity of important enzymes and the allocation of carbon towards distinct biosynthetic pathways are influenced by factors such as light intensity, nutrition availability, and the internal metabolic status of the cells[3,41–46]. In situations with high light intensity and abundant nutrients, the production of carbohydrates is promoted to facilitate fast growth and storage of energy. In contrast, when there is a lack of nutrients, the production of lipids is increased to provide a more reliable and enduring energy storage, whereas the production of proteins is reduced because of the restricted supply of nitrogen. The production of carbohydrates, lipids, and proteins in microalgae is a tightly controlled process that is influenced by environmental signals and the requirements of the cells maintenance energy [30,47]. Through comprehending these regulatory processes, researchers may modify growth conditions to maximize the synthesis of certain biomolecules, hence augmenting the potential of microalgae for utilization in biofuels, food, and bioproducts. The ability of microalgae to adapt and change their metabolic pathways highlights their importance as a diverse and sustainable resource for biotechnological advancements [48].

1.6 Hurdles in Microalgae-based CO_2 Capture and Utilization

In order to fully harness the potential of microalgae-based carbon capture systems, it is necessary to address certain hurdles as highlighted in Fig. 1.7. One major challenge in the microalgal carbon capture process is the low CO_2 capture efficiency and the lack of stability in the CO_2 capture process. This is due to the sensitivity of microalgae to various abiotic stresses,

such as outdoor light and temperature conditions. Additionally, there are challenges in meeting the high water and nutrient demands for cultivation, as well as difficulties in the large-scale harvesting process. These challenges need to be addressed in order to enhance the industrial feasibility and real-world application of microalgae, despite their significant advantages and potential. The subsequent section includes a review of various obstacles, accompanied by suggested solutions that tackle the energy and economic aspects of mitigating these obstacles.

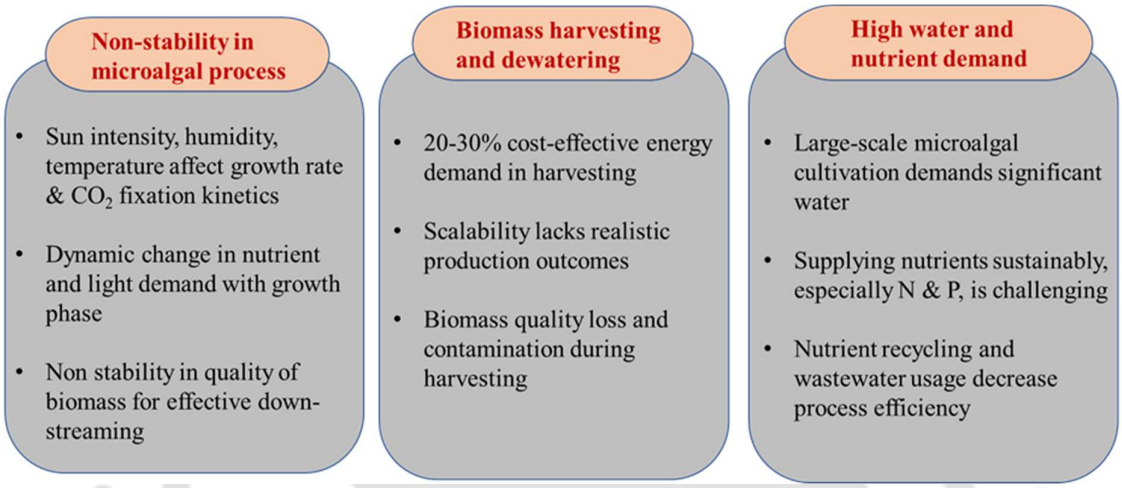

Fig. 1.7. Hurdles in microalgal cultivation system

1.6.1 Challenge in selecting an appropriate Strain

Choosing the right microalgal strain is crucial when it comes to carbon capture and utilization using microalgae. Various microalgal species have different abilities when it comes to fixing CO_2, growing at different rates, having varying nutrient requirements, and tolerating environmental stresses [43]. Choosing the most suitable strain involves considering various factors such as the intended use, growing conditions, and desired biochemical outputs. Firstly, it is important to select a strain with a high CO_2 fixation rate in order to effectively capture carbon from the atmosphere or industrial emissions. Strains that have rapid doubling times and can produce a high amount of biomass under favorable environmental conditions are excellent choices for large-scale cultivation [49].

Furthermore, it is crucial for the strain to possess the capacity to flourish in diverse culture circumstances, including fluctuating light intensity, temperature in accordance with the local climatic conditions, pH levels, and nutrient availability. Strains that are adaptable and can

thrive in outside seasonal or climatic variations, as well as withstand changes in physicochemical parameters, are more suited for large-scale application. In addition, it is important for the strain to demonstrate stability and resilience in the face of environmental stresses, such as nutrient depletion, pH fluctuations, and contamination [50]. This is necessary to ensure that it can consistently perform well over long periods of cultivation.

In order to maximize the effectiveness and sustainability of microalgae-based carbon capture systems, it is important to consider a variety of factors when selecting the right microalgal strain. These factors include CO_2 fixation efficiency, growth kinetics, adaptability to cultivation conditions, and stability under local climatic condition. When selecting a strain, mostly one or two parameters are typically considered. However, it is important to note that this can result in a loss of process efficiency observed in scale up condition[51]. Thus, it is crucial to conduct thorough bench lab scale systematic screening, as shown in Fig. 1.8. This will help ensure the compatibility and strength of the chosen strains. In order to do this, it is crucial to include a wide variety of environmental variables in the screening programmed, rather of just focusing on high CO_2 concentration. To ensure the stability and effectiveness of CO_2 sequestration using microalgae, it is necessary to evaluate the algae's capacity to mitigate CO_2 under various conditions of abiotic factors, such as acidic flue gas components, for industrial applications.

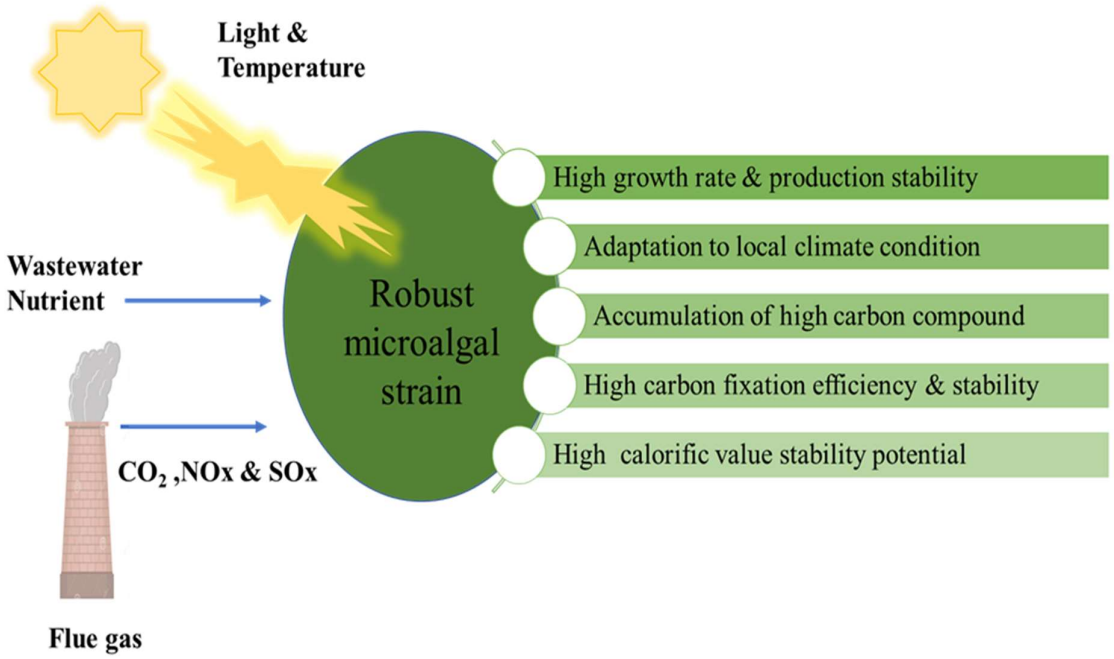

Fig. 1.8. Characteristics for selecting a robust microalgal strain. This figure illustrates the key characteristics for selecting a robust microalgal strain.

1.6.2 Challenges in managing and optimization of physiochemical factors

Managing the complicated interaction of physiochemical factors in microalgal production is a very challenging task. Microalgal culture encompasses several biotic and abiotic factors that undergo dynamic fluctuations during different stages of development [52] as illustrated in detail in Fig. 1.9. While some parameters may be easily controlled and kept stable, others experience large fluctuations, which have a direct influence on microalgal CO_2 fixation and metabolite synthesis. As a result, the efficiency of the production system is affected [53]. Light is a crucial factor that has a significant influence on the regulation of photosynthesis for efficient CO_2 fixation. Light spectrum quality, photoperiod, and light arrangement are crucial factors in microalgal production [54]. Light intensity may provide both advantageous and detrimental outcomes, necessitating a precise equilibrium to efficiently harness its energy. Maximum photosynthetic efficiency, pigment formation, and prevention of light stress need optimal light conditions [55]. Temperature has a dual function in microalgal cultures. Precise modulation is essential to enhance enzymatic and metabolic functions, mitigate heat stress, and control carbonate chemistry [56–58]. Ensuring the pH levels are at

their ideal state is crucial for maintaining metabolic equilibrium, since it enhances the amount of dissolved CO_2 that may be assimilated. Precise regulation of pH is essential to maintain the delicate balance between alkalinity and acidity, and to prevent dilution of CO_2 [59]. The existence and variation of inorganic carbon species are crucial for the process of growth. Microalgae need a sufficient and balanced supply of vital nutrients, namely nitrogen and phosphorus, in order to fulfil their nutritional requirements.

These nutrients are essential for the growth and functioning of cells. An imbalance, whether it is excessive or insufficient, might impede growth and result in nutritional shortages. Thus, the precise formulation of the nutritive medium is essential for the preservation of cultures. Gaining knowledge about the nutritional needs during times of stress and how they interact with other variables is very crucial. The incorporation of CO_2 into the culture medium introduces more complexity due to its concentration, delivery method, and interaction with other process parameters. Carbon dioxide interacts with several dynamic parameters, which affect the process of converting carbon from its gaseous state to its liquid state [60–63]. Adequate levels of CO_2 are necessary to facilitate the process of photosynthesis and enhance the development of biomass. However, careful regulation of CO_2 levels is important to avoid problems such as excessive saturation or depletion [64].

All of these features are interrelated. Studies must do a thorough examination of the intricate relationships between regulated physiochemical components and uncontrolled environmental factors, such as fluctuations in external light and temperature. Comprehensive knowledge of these relationships is essential for optimizing culture conditions. Elements such as the design of the photobioreactor, which affects the distribution of light and exchange of gases, the availability of nutrients, and the rates of flow that affect mixing and delivery of nutrients, are all crucial for this optimization process [21,65]. Researchers can enhance growth conditions throughout the cultivation process by using sensor technologies and automated control systems to dynamically adjust parameters in real-time [66,67]. This approach enhances both the effectiveness and output of microalgal cultures, while also supporting the creation of biofuels in a manner that is environmentally friendly and can be expanded on a large scale. However, the implementation of such systems leads to an increase in both expenses and complexity, presenting obstacles for economically viable and commercially feasible applications [68].

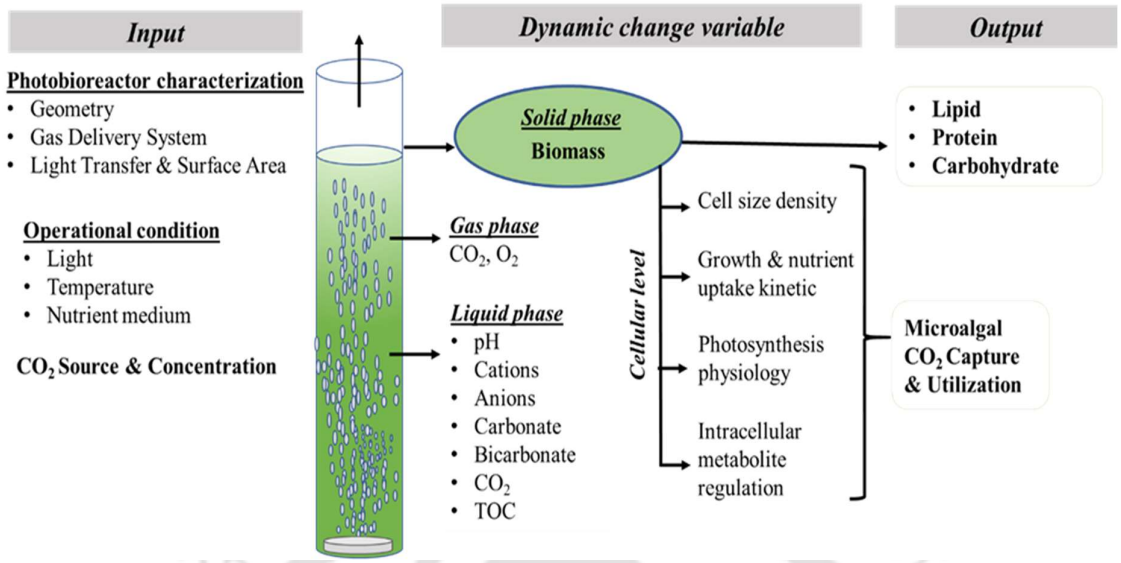

Fig. 1.9. Physiochemical parameter controlling Microalgal CO_2 fixations and biochemical regulation (Adapted and modified from Kroumov et al., 2016; Kumar et al., 2010)

All of these features are interrelated. Studies must do a thorough examination of the intricate relationships between regulated physiochemical components and uncontrolled environmental factors, such as fluctuations in external light and temperature. Comprehensive comprehension of these relationships is essential for optimizing culture conditions. Elements such as the design of the photobioreactor, which affects the distribution of light and exchange of gases, the availability of nutrients, and the rates of flow that affect mixing and delivery of nutrients, are all crucial for this optimization process [21,65].

Researchers can enhance growth conditions throughout the cultivation process by using sensor technologies and automated control systems to dynamically adjust parameters in real-time [66,67]. This approach enhances both the effectiveness and output of microalgal cultures, while also supporting the creation of biofuels in a manner that is environmentally friendly and can be expanded on a large scale. However, the implementation of such systems leads to an increase in both expenses and complexity, presenting obstacles for economically viable and commercially feasible applications [68].

1.6.3 Challenge in CO_2 utilization and stability maintain

Attaining equilibrium between CO_2 utilization and stability in microalgal culture is a significant obstacle, especially during the dynamic growth phase. The major goal is to enhance the efficiency of the supply and assimilation of CO_2, facilitating its effective conversion into

biomass and important biochemical compounds. The typical range for CO_2 utilization by microalgae is 0.2-1%. However, by sophisticated process engineering, this may be improved to 3-5% (Tripathi et al., 2023; Xu et al., 2024). It is important to note that this improvement comes at the expense of increased system cost and complexity in scaling up for industrial applications. To achieve a balance between carbon fixation and availability from gaseous phase to liquid phase, it is necessary to address disruptions in the media buffer and ensure that the pH levels are maintained at the optimum ranges [74]. This entails using an advanced method to improve the rates at which CO_2 propagates, optimizing the flow of CO_2, and controlling cellular metabolism to maximize the conversion of CO_2 into organic carbon molecules. Nevertheless, this undertaking is difficult since microalgae exhibit dynamic reactions to fluctuating CO_2 levels, requiring adaptable approaches to maintain optimum rates of carbon fixation [75]. Furthermore, there are other obstacles associated with attaining stability in CO_2 use. Changes in CO_2 concentrations, pH levels, and other environmental elements such as nutrients and light may disturb cellular equilibrium, impede growth and production, and cause instability during the process of carbon fixation in biomass [76]. Effective carbon capture relies heavily on the use of robust culture techniques and photobioreactor engineering. This requires meticulous strategizing and implementation of components such as spargers, baffles, and geometrical arrangements to regulate hydrodynamics and enhance mass transfer mechanisms [77].

An important challenge in achieving constant utilization of CO_2 is comprehending the fluctuations in environmental light and temperature, as well as their interplay with CO_2. To tackle these issues, it is crucial to modify cultivation conditions, including nutrient levels and the flow rate and concentration of CO_2 [62,78–81]. Achieving efficient carbon dioxide utilization and stability in microalgal production necessitates the implementation of a complete engineering plan that incorporates an interdisciplinary approach. It is essential to overcome these challenges in order to fully use the potential of microalgae as environmentally benign systems for capturing carbon, which will help us advance towards carbon-negative biomanufacturing of bioproducts.

1.6.4 Attaining high biomass production

Improving the productivity of biomass and biochemical synthesis in microalgal development is a significant obstacle, particularly when only depending on CO_2 as the carbon source [82]. The biomass concentration in photoautotrophic mode, where CO_2 is used as the carbon source, normally varies between 1 and 3 g/L at its highest level. However, it may

decrease under circumstances of higher CO_2. The flue gas, containing 15-25% CO_2, had a biomass content that dropped below 2 g/L [82–85]. When exposed to flue gas that is directly polluted, the concentration drops to less than 1 g/L [83,86–90]. This decrease in concentration makes it economically unfeasible and less efficient for the downstream process development of biofuel and biochemical synthesis. The primary goal is to optimize the growth environment and metabolic pathways to enable substantial biomass buildup and the synthesis of important biochemicals. However, accomplishing this ambitious goal requires overcoming a variety of obstacles. In order to enhance biomass production, it is important to optimize the culture factors, such as light intensity, temperature, nutrient availability, and CO_2 concentration [74,76]. This will provide a conducive environment for the rapid development of microalgae. This entails attaining a delicate balance between providing sufficient resources to sustain cellular metabolism and avoiding nutritional insufficiency or excess, which might impede growth and productivity. Furthermore, attaining optimal biochemical synthesis requires a comprehensive understanding of metabolic pathways and regulatory mechanisms that govern the production of macromolecules such as lipids, carbohydrates, proteins, and pigments [93,94]. In order to do this, it is necessary to examine the intricate biochemical networks found inside microalgal cells, identify vital enzymes and regulatory variables, and devise strategies to enhance the rate of metabolic processes [95].

Furthermore, achieving high levels of biomass productivity and biochemical synthesis in large-scale industrial settings has additional challenges. In order to go from small-scale laboratory research to large-scale production facilities, it is imperative to tackle technological constraints, enhance reactor design, and establish economically viable methods for cultivating microalgae. To ensure the economic viability and long-term sustainability of large-scale microalgal biorefineries, it is essential to devise innovative techniques for biomass collection, processing, and downstream processing, while safeguarding the integrity of the biomass.

1.6.5 Cost-Effective harvesting and processing techniques

Harvesting microalgae entails the extraction of microalgae particles from their culture suspension. The cost of biomass harvesting is a major obstacle in the large-scale implication of microalgae-based process in terms of carbon capture or biochemical production, representing about 20%–30% of the entire cost of producing biomass [96]. The collection and treatment of microalgae biomass present significant difficulties because of the minuscule dimensions of the cells (ranging from 2 μm to 10 μm), low sedimentation rates, and high-water

content [97]. When selecting a harvesting approach, it is crucial to consider the intended final products and the extraction of biochemical processes. The method should also be non-toxic to allow for the use of leftover biomass in different applications. Additionally, efficient dewatering is necessary to enable the reuse of nutrients and water [98]. Optimal harvesting methods should be economically efficient and have reduced energy demands, while yet achieving high rates of recovery. Microalgae harvesting normally in bulk scale comprises two primary methods: pre-harvesting and post-harvesting [99]. Pre-harvesting is the process of extracting the microalgal biomass from a diluted growth medium in order to create an algal slurry containing 2%–7% total suspended solids (TSS). Typically, post-harvesting procedures, such as thickening, dewatering, and drying, mostly use physical methods such as flotation, filtration, centrifugation, and convection drying [100]. These procedures may provide microalgae paste containing 15-25% total solids or microalgae powder with a solids content exceeding 90%, hence enhancing the resilience of the biomass by minimizing spoiling [101]. The primary method used for large-scale commercial harvesting is the bulk harvesting methodology. Coagulation and flocculation techniques are often used for the purpose of microalgae harvesting. These methods facilitate the aggregation of microalgae, hence simplifying their separation by sedimentation [102]. The use of cationic polyelectrolytes, such as metallic salts and polyacrylamide-based polymers, for chemical flocculation is a common practice, despite the potential for contamination. Chitosan and cationic starch, while safer alternatives, are not feasible for large-scale operations owing to their exorbitant costs [103]. Each approach has its own advantages and disadvantages in terms of its economic potential as discuss in Table 1.

Table 1.1: The advantages and disadvantages of different algae harvesting methods (Kumar et al., 2023; Singh and Patidar, 2018)

Harvesting Method	Cost ($) per kg of dry biomass	Advantage	Disadvantage
Centrifugation	1.00–3.00	High efficiency in separating microalgae from the growth medium, producing high-purity biomass	High operational costs make it less suitable for large-scale operations unless high-value products are produced

Filtration	0.20–0.50	Effective for larger microalgae species; scalability is feasible	Filter fouling and maintenance can increase costs, and efficiency drops with smaller microalgae species
Sedimentation	0.10-0.20	Simple and cost-effective for initial biomass concentration	Low efficiency due to the small size and low density of microalgae cells, making it unsuitable as a standalone method for fine biomass recovery
Flocculation /Coagulation	0.15–0.30	Can significantly increase the size of microalgal aggregates, improving separation efficiency	Potential contamination from chemical flocculants; safer, more expensive alternatives like chitosan are required for food-grade applications
Auto-flocculation	0.05–0.15	Environmentally friendly and cost-effective	Requires careful control of pH and may not be suitable for all microalgal species

Auto-flocculation is a procedure that involves the introduction of calcium or magnesium into an alkaline setting. It is environmentally harmless and commercially effective as a natural phenomenon [106]. Nevertheless, this method requires meticulous evaluation of the morphology, dimensions, and cellular concentration, as well as the optimization of processes such as the composition of the medium, growth conditions, and the induction of pH adjustment [107].

It is essential to develop sustainable harvesting systems that are energy-efficient, scalable, and commercially feasible. It is crucial to achieve maximum density of microalgal biomass and efficient separation from contaminants, while minimizing biomass loss, in order to achieve the highest possible productivity and purity. In addition, it is crucial to preserve the collected water for its ability to be reused in order to decrease the amount of water used in the cultivation of microalgae, thus improving sustainability. To ensure the desired quality and quantity of the end product, it is essential to employ gentle harvesting techniques that safeguard the delicate microalgae cells from damage.

1.6.6 Water Demand and Reuse in Microalgal Cultivation Systems

The findings demonstrate that the overall water use for growing microalgae varies between 2.4 and 6.8 m^3 /Kg of dry biomass [108]. The stage of operating the photobioreactor (PBR) is responsible for more than 60% of this water consumption. Microalgae need roughly 3726 kg of water to make 1.0 Kg of biodiesel. According to Yang et al., 2011 the act of reusing water has the potential to decrease the need for freshwater by 84% and reduce nutrient consumption by 55%. Efficient management is necessary to address the essential difficulties of water reuse and nutrient delivery in sustainable microalgal culture [110]. This is important in order to decrease operating costs and minimize the environmental effect. Due to the release of extracellular organic matter, which may include toxins and humic compounds that hinder water recyclability, efficient water reuse solutions are required in microalgal systems to meet the high demand for water [98]. To tackle these problems, it is necessary to use sophisticated water treatment techniques such filtration, membrane technology, and advanced oxidation [111]. However, these techniques might escalate operational expenses. Recycled water may include undesirable microorganisms, such as bacteria, fungus, and protozoa. Therefore, it is necessary to implement strong sterilization or disinfection procedures, such as UV irradiation or chemical treatments, to guarantee the absence of these contamination [112]. Another obstacle is the possible nutritional imbalances that occur due to ongoing water reuse, necessitating regular monitoring and adjustment of nutrient concentrations to maintain ideal growth circumstances. The introduction of extracellular organic load into reused medium leads to alterations in water chemistry and parameters, including chemical and biological oxygen demand [113].

Cellular development phase, cell density, availability of nutrients (particularly nitrogen), and stress levels (such as high light intensity and temperature) are important factors that influence the secretion of organic matter and the water recyclability process in microalgal production [114]. The provision of nutrients is equally vital since it has a direct influence on growth rates and the generation of biomass. Conventional nutrient sources, are often expensive and not ecologically sustainable. As a result, researchers are investigating other sources such wastewater and industrial effluents. However, these alternatives may reduce the effectiveness of CO_2 fixation and productivity of process in terms of quantity and quality both [115]. Therefore, to enhance sustainability, it is crucial to maintain the appropriate levels of nutrients, particularly nitrogen and phosphorus, and regulate the release of extracellular organic matter by regulating abiotic stress or process conditions. Additionally, the time of harvesting should

be chosen properly. This technique guarantees efficient productivity, biomass quality, and water reusability while simultaneously ensuring stability in CO_2 fixation and biomass generation in long-term closed-loop systems.

CHAPTER 2

Literature review and Objectives

Chapter 2

Literature review and Objectives

2.1 Microalgal Cultivation System

The use of microalgal culture systems for CO_2 capture encompasses a variety of open ponds and closed cultivation approaches, each with distinct benefits and challenges as shown in Table 2.1. Open pond systems, known for their simplicity and cost-effectiveness, are well-suited for large-scale applications (Figure. 2.1). By using rotatable agitators in circular ponds or paddle wheels in open pond systems, their efficiency and efficacy may be significantly enhanced [116]. The open pond design improves the aeration and CO_2 transfer process, facilitates the even distribution of sunshine and nutrients, and restricts the growth and build-up of microalgae biofilms. In addition, the shallow liquid depth, short retention time, and limited gas exchange interface area greatly restrict the capacity to transfer CO_2 mass in microalgal cell , leading to an efficiency range of only 10% to 30% [117]. On the other hand, closed photobioreactors provide enhanced control of culture factors, such as light intensity, temperature, pH, and nutrient availability [118]. By manipulating these factors that regulate the metabolic pathways and stress physiology of the cell, it becomes possible to enhance the development of microalgae, increase CO_2 fixation rates, and improve the efficiency of converting them into desired biochemicals or bioproducts [119]. Photobioreactors are specifically built to provide CO_2 enrichment, so assuring an enough supply of carbon substrate for microalgae to carry out photosynthesis. This leads to enhanced CO_2 sequestration and reduced CO_2 leakage into the atmosphere compared to an open pond system [120]. However, the substantial initial investment and continuous expenditures associated with photobioreactors may limit their widespread adoption owing to concerns about scalability. The performance and scalability of CO_2 collecting applications are significantly influenced by the design of photobioreactors [121].

Different types of photobioreactors, including as tube, flat-plate, airlift, bubble and annular column layouts (Figure. 2.1), have distinct benefits and disadvantages in terms of how they distribute light, gas and liquid mass transfer, mix efficiently, and their operating complexity [122]. In order to achieve maximum productivity and cost-effectiveness in photobioreactor systems, it is crucial to carefully optimize factors such as reactor geometry, material selection, light source, gas sparging system, and mixing mechanism. This optimization ensures uniform illumination, efficient CO_2 transfer, and minimal energy consumption [77]. Novel reactor shapes, such as helical tubular [123] and panel airlift photobioreactors [124], proved to provide better light dispersion and mixing, resulting in enhanced microalgal growth and productivity.

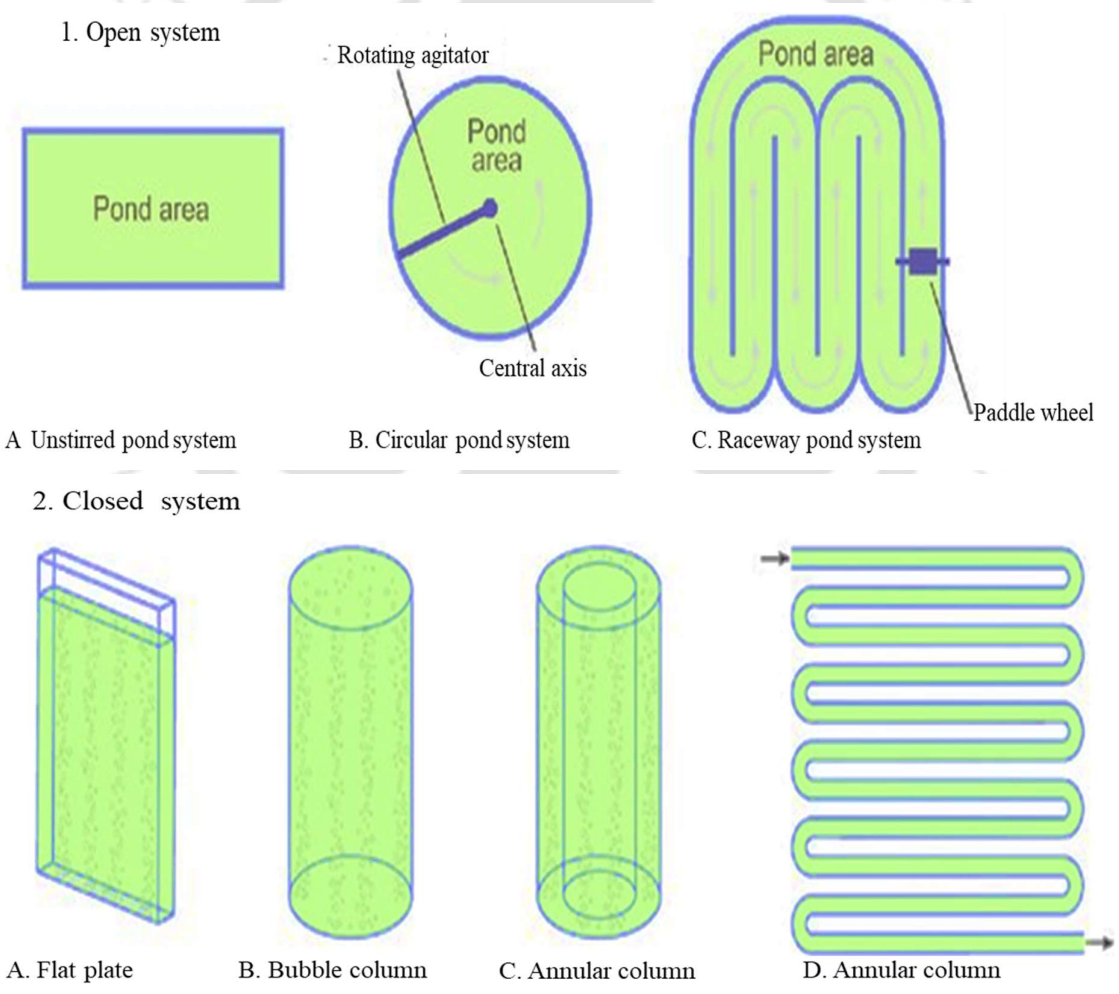

Fig. 2.1: Geometry of open and closed microalgal cultivation systems, illustrating the structural differences and configurations (Source: Satpati and Pal, 2018)

Moreover, advancements in the area of material science have led to the development of transparent and durable materials for reactors, which have enhanced their ability to transmit light [126]. As a consequence, there has been a reduction in energy losses and an improvement in the efficiency of photon capture. In addition, the incorporation of modular components such as a baffle [127], the introduction of membrane sparge [128], and the utilization of advanced nanotechnology and nanobubble technology [129] have been employed to improve the dissolution of CO_2 in the medium.

Table 2.1. Benefits and challenges of open and closed photobioreactor system (modified from Dey et al., 2020; Kim et al., 2022; Sun et al., 2022)

Cultivation system	Benefits	Challenges
Open pond	• Low installation cost and operational cost • Easy operation • Proper distribution of light and nutrient • Proper mixing • Less energy input • Utilize non-agriculture land • Easy scalability for commercial application	• Large area requirement • Large evaporation of media • Risk of contamination • Less CO_2 mass transfer and CO_2 loss to the atmosphere • Less controllable process strategy and difficulty in process optimization • Less biomass productivity and carbon fixation compare to other system • Difficulty in harvesting of biomass
Flat-panel photobioreactor	• Large light surface to volume ratio • High biomass productivity • High CO_2 mas transfer and fixation • Easy operation and sterilization • Easy optimization and control process strategy	• Difficulty in Scale up • Difficulty in controlling temperature • Not suitable for high light condition • Wall growth possibility • Increased hydraulic stress • High installation cost
Tubular photobioreactor	• Large illumination area • Cheap installation and operational cost • Suitable for outdoor condition • High biomass productivity	• Difficulty in control temperature • Oxygen build up problem • Wall growth possibility • Difficulty in sterilization and cleaning • Large land requirement
Bubble-column	• Proper CO_2 mass transfer and carbon fixation • Low energy consumption	• Small illumination area • Poor light penetration depth • Oxygen build up problem

Photobioreactor	• Easy installation • Easy sterilization and manual cleaning

The detailed discussion on the modification and engineering of the photobioreactor will be further discussed in section 2.3.1. However, the essential requirements for a photobioreactor or microalgal culture system include simple installation and operation, economic viability, and the capacity to sustain improved process efficiency. The efficiency shouldn't compromise the output quality and quantity in terms of carbon fixation and biomass production for bioenergy and biochemical synthesis. To achieve the most efficient functioning of photobioreactors for CO_2 capture, it is necessary to carefully adjust the culture settings in order to enhance the development of microalgae and maximize the rates at which CO_2 is fixed. Microalgal physiology and photosynthetic activity are influenced by critical process parameters such as light intensity, photoperiod, temperature, pH, and nutrient concentrations. It is crucial to continuously monitor and adjust these factors in order to maintain optimal development conditions for microalgae and minimize negative consequences such as photoinhibition, nutritional deficiency, and pH variations.

2.2 Process Parameter Effecting Microalgal CO_2 fixation

2.2.1 Influence of microalgal species and Carbon dioxide concentration

The concentration of carbon dioxide (CO_2), as well as the pace at which it flows and the mechanism by which it is delivered, has a considerable impact on the process of photosynthesis CO_2 fixation by microalgae [65]. As discussed in introduction section, optimizing microalgal development requires achieving the optimal equilibrium between CO_2 concentration and pH. Microalgal strains have various degrees of tolerance to different concentration of CO_2. Although certain organisms may flourish in CO_2 concentrations of about 2%, higher levels beyond 5% can impede development by causing acidification of the chloroplast stroma and deactivating enzymes [71]. The studies revealed distinct degrees of CO_2 tolerance across various species of microalgae, emphasizing the differential efficacy of CO_2 fixation and their capacity to flourish under variable CO_2 concentrations. *Chlorella* and *Scenedesmus* species exhibited notable resilience to increased levels of CO_2, as they maintained substantial rates of CO_2 fixation and biomass productivity. The results are shown in Table 2.2,

which displays the comparative performance of various species in detail. For instance, *Desmodesmus sp. , Scenedesmus sp.*, and *Chlorella sp. Nannochloropsis* [133–138] were able to withstand higher levels of CO_2, although they attained their highest output at lower levels. *Chlorella sp.* KR-1 exhibited its maximum growth rate at a CO_2 concentration of 10% and shown resilience up to 70% [139,140]. The impact of CO_2 concentration on the growth of microalgae is complex including both external physiochemical variables internal cellular physiology regulation adaptability that sustain efficient photosynthetic performance and growth [95].

Table 2.2. CO_2 fixation and biomass productivity at different levels of CO_2 concentration in phototrophic mode.

Microalgal strain	CO_2 conc. (%)	CO_2 fixation rate (mg/L/day)	Biomass Productivity (g/L/day)	References
Chlorella minutissima	4	0.26	0.13	[141]
Dunaliella tertiolecta	4	0.16	0.68	[142]
Chlorella vulgaris ISC-23	5	0.44	1.15	[143]
Chlorella sorokiniana GS03	5	0.66	0.37	[82]
Chlorella sorokiniana TH01	5	0.47	0.46	[144]
Scenedesmus obtusiusculus AT-UAM	5	0.13	0.16	[145]
Parachlorella kessleri	5	0.21	0.47	[146]
Chlamydomonas sp. BTA 9032	5	0.04	0.18	[147]
Chlorella sp	10	0.26	0.13	[148]
Chlorella pyrenoidosa	10	0.25	0.35	[144]
Chlorella vulgaris	10	0.12	0.07	
Scenedesmus obliquus	10	0.27	0.14	[149]
Scenedesmus dimorphus	10	0.20	0.12	
Botryococcus braunii	10	0.35	0.03	[150]
Chlorella sp. PY-ZU1	15	1.24	0.68	[142]
Chlorella sp.	15	0.10	0.072	[151]
Scenedesmus sp. ISTGA1	15	0.11	0.1	[152]
Scenedesmus obliquus SA1	15	0.10	0.26	[153]
Nannochloropsis oceanica CCMP1779	15	0.34	0.053	[154]
Botryococcus braunii	20	0.53	0.016	[150]
Scenedesmus sp.	20	2.18	0.18	
Chlorella vulgaris ESP-31	25	0.20	0.61	[155]
Desmodesmus abundans	25	0.42	0.16	[156]
Chlorella vulgaris JSC-6	40	0.14	0.17	[157]
Chlorella sp. LAMB 31	40	0.14	0.12	[158]

Table 2.2 shows that *Scenedesmus* sp. had the greatest rate of CO_2 fixation at a concentration of 20%, with a rate of 2.18 mg/L day^{-1}. These findings reveal that *Scenedesmus* sp. has a strong ability to tolerate and efficiently use CO_2 at high levels [150]. Therefore, it is likely to be very successful in situations with significant CO_2 emissions, such as industrial effluent gases. *Chlorella sorokiniana* GS03 [82] and *Chlorella sorokiniana* TH01 [144] exhibited significant rates of CO_2 fixation, specifically 0.66 mg/L day^{-1} and 0.47 mg/L day^{-1}, respectively, when exposed to a 5% concentration of CO_2. These strains possess a combination of moderate tolerance to CO_2 and high capacities for fixation, rendering them appropriate for use in scenarios where CO_2 concentrations are somewhat higher than the surrounding environment. On the other hand, strains such as *Chlamydomonas sp.* BTA 9032 had a much lower rate of CO_2 fixation, measuring 0.04 mg/L day^{-1} at a 5% CO_2 concentration [147]. This suggests that these strains have limited tolerance and efficiency in using CO_2. This emphasizes the fact that the capacity for CO_2 fixation is particular to certain strains, which means that it is important to choose the right strains for various CO_2 concentrations.

Therefore it clear from Table 2.2 that certain microalgae have the ability to adapt to elevated amounts of CO_2 via gene regulation, whilst others may see a decrease in their efficiency and growth [93,154]. Reducing the rate at which CO_2 is released into the cultivation system may improve the process of carbon fixation, but it may also result in slower rates of growth. According to Hussain et al., 2017 and Jin et al., 2020 the ideal CO_2 content for most microalgae falls between 0.038% to 10%. However, greater levels of CO_2 may actually hinder their development. Excessive aeration of high concentrations of CO_2 (10-20%) leads to acidification of the cultivation medium, which in turn inhibits the growth of algae [41]. Increased levels of CO_2 hinder the growth of microalgae by causing acidification of the chloroplast stroma, reducing the availability of bicarbonate/carbonate ions, and inactivating crucial enzymes in the Calvin-Benson cycle. This hinders the function of carbonic anhydrase, vital for the conversion of bicarbonate to CO_2, and the activity of Rubisco, which is necessary for efficient CO_2 fixation [159]. Ensuring a constant supply of CO_2 is essential for preserving the presence of carbon in microalgal growth systems. This entails the management of both the concentration of CO_2 and the method by which it is delivered. Attaining a state of balance between the demand for CO_2 in photosynthesis and its actual availability is difficult because of the complex interactions between CO_2 with other variables, as well as the growth of microalgae. Sustaining this balance becomes very challenging when CO_2 is continuously

supplied. However, using short-term CO_2 feeding strategies that rely on monitoring pH levels may assist in attaining this equilibrium [53–55]. In order to optimize the supply of CO_2 in the production of microalgae, it is important to have a CO_2 storage facility. Although there are several approaches of supplying CO_2, they frequently do not achieve a state of equilibrium, leading to the acidification of the medium when large amounts of CO_2 (10-15%) are needed for industrial purposes. Therefore, pH-based CO_2 feeding is unsuitable for large-scale industrial operations.

2.2.2 Impact of light intensity on microalgal CO_2 fixation

The key role of light in microalgal CO_2 fixation is essential, since it directly regulates the photosynthetic light-dependent metabolic processes via pigment-photon interaction. These pathways not only provide the necessary ATP and NADPH for CO_2 fixation, but also facilitate the transformation of CO_2 into sugar molecules via the Calvin-Benson cycle. The impact of light on the microalgal CO_2 fixation process is multifaceted, encompassing factors such as light intensity, duration, wavelength, and quality [161]. A study by Rao et al., 2022 using *Nannochloropsis oceanica* revealed that the availability of light controls the CO_2 requirement for microalgal growth and carbon fixation. These factors interact with growth phase factors and photobioreactor conFigureuration, adding to the complexity of the process. Insufficient amounts of light result in reduced biomass concentration and CO_2 fixation, highlighting the requirement to provide a sufficient amount of light, especially as cell density increases [162].

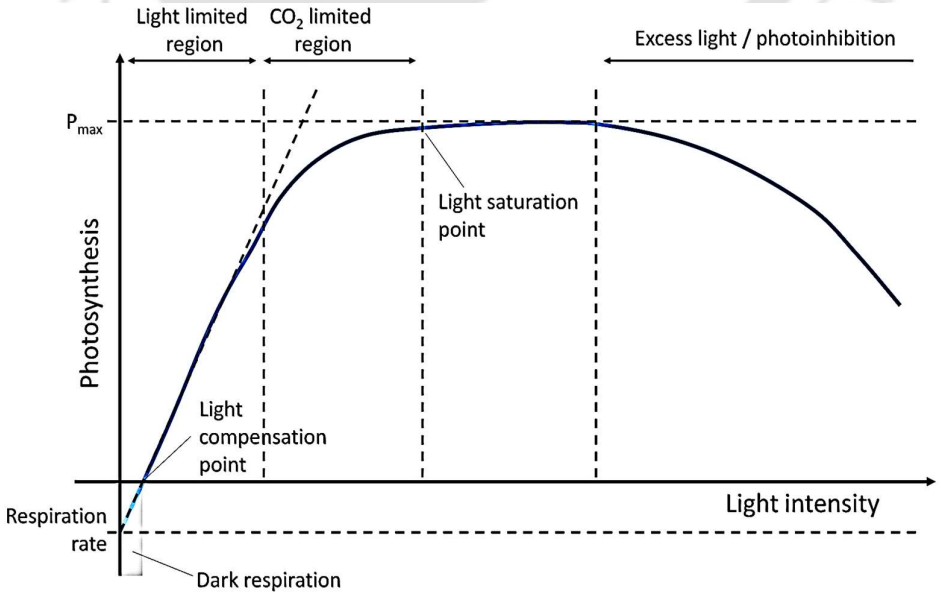

Fig 2.2. Light-responsive photosynthesis graphs showing that carbon fixation begins at the light adjustment point. Net photosynthetic rate increases linearly with light until saturation, where energy quenching reduces efficiency. Extreme light levels can cause photooxidative stress, reducing net photosynthesis (Sourse of data Ramanna et al., 2017).

Photosynthesis-irradiance (P–I) curves are often used to clarify the correlation between irradiance and photosynthesis (Figure. 2.2). The curves represent three clearly defined regions: the zone restricted by photons, the region saturated with light, and the region affected by photoinhibition and directly related to carbon fixation.

As seen in Figure. 2.3, the growth rate of cells in the culture medium fluctuates as the cell density increases. Eventually, it reaches a stationary phase in the dark zone of the culture media. This occurs when the growth time interval increases due to the expansion of the dark zone and the contraction of the light zone. Multiple studies have demonstrated that higher light intensity results in elevated rates of CO_2 removal and increased biomass production in various microalgae species [163–167]. However, excessive light may cause photoinhibition, which is the damage to the photosynthetic machinery caused by the overproduction of reactive oxygen species. Research conducted on *S. obliquus WUST4* shown that higher light intensity initially improved the pace at which CO_2 was removed, but beyond the ideal levels hindered the process of microalgal photosynthesis [168]. The length of time that light is exposed to microalgae is also a critical factor in the conversion of CO_2. Prolonged periods of light exposure are crucial for maintaining metabolic homeostasis, whereas intermittent darkness is necessary to sustain photosynthetic activity [169].

Research has shown that optimizing light-dark cycles, such as using the 12:12 or 18:6 cycles, may enhance the process of CO_2 fixation and ensure the overall health of cells. Research has shown that providing constant light to microalgae such as *Aphanothece microscopica* leads to a significant increase in their ability to capture and use nutrients, highlighting the significance of customized lighting schedules in improving their metabolic processes and facilitating the development of these algae [170]. Additional studies have shown that the intensity of daylight may mitigate the effects of long dark phase time, and vice versa. Short-term periods of intense light may reduce the negative effects of photoinhibition exposure by controlling genes during periods of darkness and improving the ability to adapt to high light [171]. Hence, it is important to maintain the dark phase in outdoor environments to minimize harm caused by excessive sunshine and heat [172]. Studies have shown that microalgae have

the ability to capture a greater amount of CO_2 by optimizing the combination of photoperiod and light intensity [146]. The research done on *Nannochloropsis sp.* and *Chlorella vulgaris* shown a significant variation in growth and CO_2 fixation rate when exposed to different light intensities and photoperiods, as well as their interaction [171,173,174].

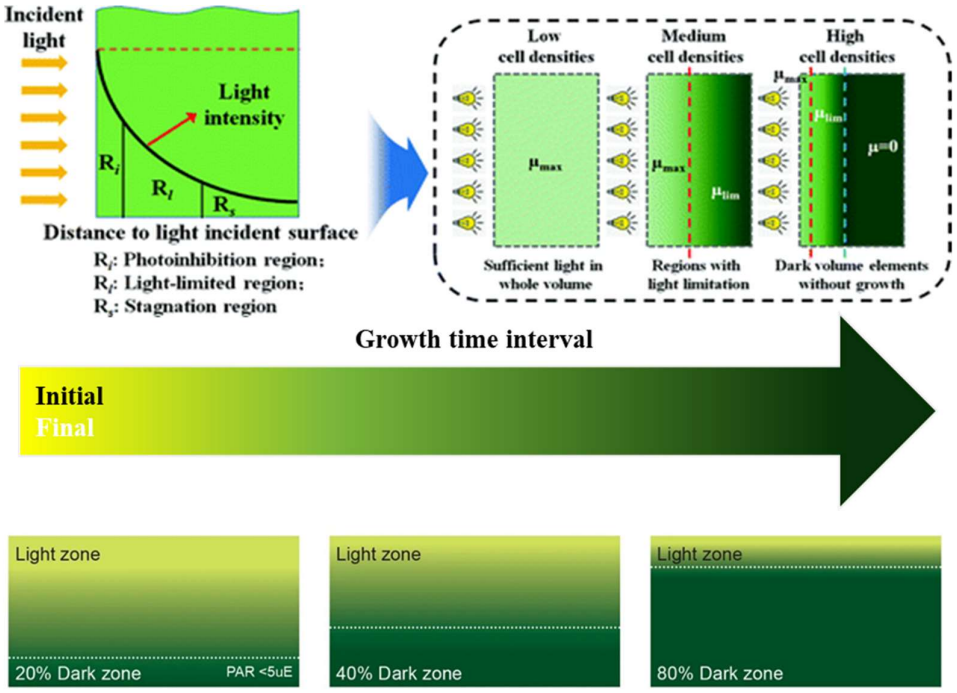

Fig. 2.3. An illustration showcasing the shading effect on microalgal cultivation, highlighting the growth progression over time intervals. It demonstrates the distinction between light and dark zones, as well as the variation in cell growth rates (Source : Modified from Sivakaminathan et al., 2018 & Sun, Y. et al 2018).

2.2.3 Impact of temperature on microalgal CO_2 fixation

The availability of carbon dioxide to cells and the metabolic processes inside the cell are greatly affected by temperature, as shown by Lee et al., 1985; Torzillo et al., 1991. The reduction in CO_2 solubility is well-documented when temperatures was above 20°C [179], and higher temperatures also reduce Rubisco's affinity for carbon dioxide [57]. Therefore, changes in ambient temperature will influence both the metabolism of microalgae and the solubility of CO_2 in culture media. The temperature is crucial in controlling the physiological functions of microalgal cells. Elevated temperatures may enhance microalgal metabolism and hinder biomass formation. Cold temperatures may impede the proliferation of microalgae. However, the effect of temperature on metabolic rates differs across different strains. The experiment

conducted in which *Scenedesmus obliquus* and *Chlorella vulgaris* was grown in outdoor photobioreactors containing constant amounts of nitrogen and CO_2 highlighted the significance of comprehending the influence of temperature on microalgal proliferation as well as carbon and nitrogen fixation mechanisms [180]. Scientific studies have repeatedly shown that the most favorable temperatures for the development of microalgae usually range from 15 °C to 30 °C. Microalgal development may be inhibited by temperatures below 16 °C, while temperatures over 35 °C can frequently be deadly for many species [181]. The solubility of carbon dioxide reduces at higher temperatures, which in turn affects its availability for photosynthesis [44] . Nevertheless, certain species of microalgae have thermal resilience and are capable of acclimating to elevated temperatures. For instance, *Chlorella sp*. KR-1 [182] , *Picochlorum renovo* [183] .exhibited sustained high rates of growth and cell density even when exposed to a temperature of 40 °C. Similarly, it was found that *Chlorella sorokiniana* [184] *Desmodesmus sp*. F2 [185] , and *Micractinium sp.* [186] showed the greatest level of growth at a temperature range of 35 °C - 45 °C. There was no notable variation in growth and the biomass productivity remained stable. A study conducted by Serra-Maia et al., 2016 discovered that the combined impact of rising temperature and CO_2 concentration on stress tolerance is influenced by nutrient availability, particularly nitrogen. The presence of sufficient nitrogen enhances the adaptability of *Thalassiosira pseudonana* to concurrently temperature increase and elevated CO_2 conditions.

In light of these results, the complex link that exists between temperature, the availability of carbon dioxide, and the metabolism of microalgae is put into focus. Optimizing temperature settings is essential for improving the development of microalgae and increasing the effectiveness of carbon dioxide fixation, especially in applications such as the removal of CO_2 from industrial flue emissions by biological means. It is crucial to comprehend the temperature needs particular to each species and their corresponding metabolic reactions in order to advance the efficiency of carbon capture systems using microalgae.

2.2.4 Impact of pH on microalgal CO_2 fixation

The relationship between pH and carbonate chemistry is highly interconnected in the cultural medium of microalgae, and it plays crucial roles in the development and metabolic activities of these microorganisms. Carbonate chemistry refers to the balance between carbon

dioxide (CO_2), bicarbonate ions (HCO_3^-), carbonate ions (CO_3^{2-}), and carbonic acid (H_2CO_3) in water-based systems [179]. And govern by pH as shown in Figure.2.4.

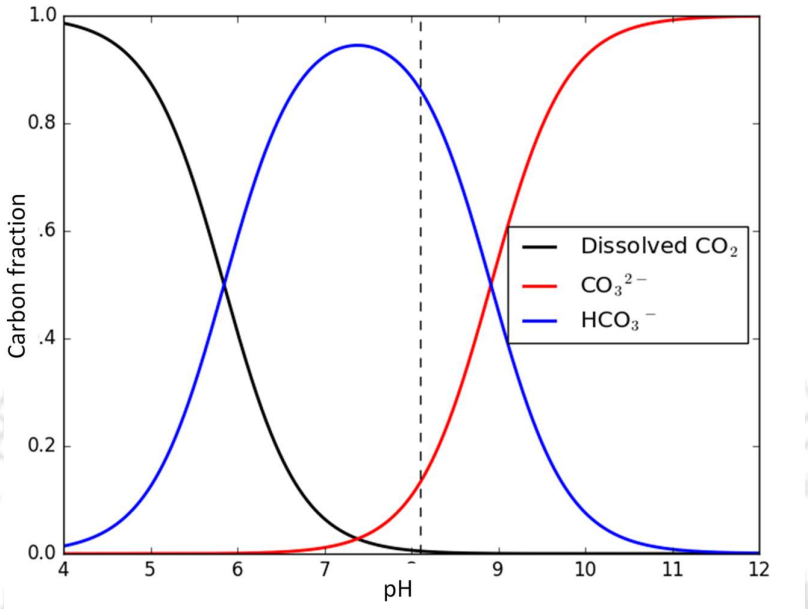

Fig. 2.4. Carbon fraction equilibria in the aqueous phase at a temperature of 25 ◦C, displayed as a function of pH (Source : Hajinajaf et al., 2024).

According to the following equilibria of carbonate chemistry in aqueous phase,

$$H_2O + CO_2 \overset{K_1}{\leftrightarrows} H_2CO_3 \overset{K_2}{\leftrightarrows} H^+ + HCO_3^- \leftrightarrows H^+ + CO_3^{2-} \quad 2.1$$

in which K_1 and K_2 are the first and second acid-dissociation coefficients. CO_2 is an essential carbon source that is used for photosynthesis and the generation of biomass in the culture of microalgae. Upon contact with water, it undergoes dissolution and forms carbonic acid, which then dissociates into bicarbonate and carbonate ions [189]. The pH, temperature, and CO_2 partial pressure have an impact on the proportions of these species [190].

The variation in pH is an intrinsic characteristic of the development of microalgae and the processes of CO_2 fixation. This variation is regulated by the balance between different forms of dissolved inorganic carbon and the dissolution of CO_2. Various microalgae species have different preferences for pH levels in order to achieve optimum development. Studies undertaken by Chen et al., 2015, 2014; Kassim and Meng, 2017; Moghimifam et al., 2019 have shown that most species survive within a pH range of 6 to 8.5, which is slightly alkaline to neutral Extremophile microalgae, namely *Chlorella sorokiniana* str. SLA-04, thrive in very

alkaline settings characterized by pH levels ranging from 9 to 11 [202,203]. These microalgae have shown a high level of efficiency in directly sequestering CO_2 from the atmosphere. However, at increased CO_2 conditions 10% to 25% , a decrease in pH below 4 was found [204]. Modifying pH levels via the use of different alkaline solutions might potentially improve the efficiency of carbon dioxide fixation in microalgae. An effective nutrient modulation approach, which mainly focuses on managing the nitrogen supply and availability, plays a critical role in regulating the pH of the medium by interacting with CO_2 [205].

2.2.5 Impact of nutrient on microalgal CO_2 fixation

Nutrients are essential for the process of microalgal CO_2 fixation, since they have a significant impact on cell development, metabolism, and enzyme activity. They play a crucial role in regulating the conversion of CO_2 into metabolites during photosynthesis. The molecular formula of microalgal biomass, which includes essential components including carbon, nitrogen, phosphorus, magnesium, sulphur, and trace elements, highlights their importance in the cellular structure and function. Carbon, which makes up around 50% of microalgal biomass, highlights the importance of CO_2 fixation for biomass formation [206]. This CO_2 may be obtained from several sources, such as the atmosphere or industrial gaseous streams such as flue gas. After carbon nitrogen is essential for the development and metabolism of microalgae, making up around 6-10% of the cell's dry weight and being the second most abundant nutritional element of microalgae [207]. The nitrogen is mainly used for the synthesis of amino acids, purines, pyrimidines, amino sugars, amines and chlorophyll. Microalgae have the ability to use many nitrogen sources, including nitrate, nitrite, urea and ammonium salts. The availability of nitrogen has a major impact on the process of CO_2 fixation and the total metabolic activity of microalgae. In a study by Ma et al. 2019 and Nguyen and Rittmann 2015 on the microalga *Chlorella vulgaris* and *Nannochloropsis* , it was observed that nitrogen availability significantly control the CO_2 demand and overall growth rate. Many other similarly, research conducted by on other species highlighted the importance of nitrogen sources in regulating CO_2 fixation efficiency and crucial role of carbon and nitrogen fixation and interaction to maintain the stability in growth and metabolite regulation towards biomass production [80,113,209,210]. Nitrogen not only plays a function in biomass formation, but also has an impact on the carbonate chemistry and concentration of CO_2 in the media [62]. The nitrogen and CO_2 interaction are crucial for maintaining stoichiometric equilibrium and

ensuring the availability of carbon for photosynthesis and biomass production [179,211]. Prior research has shown clear patterns in alkalinity when different nitrogen sources, such as ammonia, nitrate, and urea (an organic nitrogen source), are supplied and interact with CO_2 [211]. The selection of the nitrogen source is crucial in controlling the pH of algal cultures on a large scale. A direct relationship was discovered between the concentration of dissolved inorganic carbon and the maintenance of alkalinity in the medium, which is crucial for maintaining CO_2 dilution. Efficiently managing nitrogen sources prevents the acidification of the medium and the loss of CO_2, and maintain the metabolic regulation at elevated CO_2 condition [79,212].

In addition to nitrogen, phosphorus plays a vital role in microalgal metabolism by influencing nucleic acid synthesis and adenosine triphosphate (ATP) generation [213]. A previous study demonstrated that maintaining sufficient phosphorus availability under nitrogen-starvation conditions at 15% CO_2 enhances cellular metabolic activity by redirecting carbon flux towards lipid accumulation in *Chlorella vulgaris* [214]. Numerous studies have investigated the utilization of a two-stage cultivation strategy involving phosphorus supplementation under nitrogen-deficient conditions for enhancing lipid production [215–218]. The availability of phosphorus interacts closely with carbon and nitrogen in microalgal cells, influencing cellular stoichiometry and nutrient uptake kinetics. Imbalances in the phosphorus-to-carbon (P:C) and phosphorus-to-nitrogen (P:N) ratios can affect cellular metabolism, growth rates, and the efficiency of CO_2 fixation, highlighting the importance of maintaining optimal nutrient ratios in microalgal cultures. A study conducted by Kumari et al., 2021 focused on *Chlorella vulgaris*. Under situations when nitrogen is restricted, the presence of phosphorus is crucial for maintaining carbon fixation, preventing substantial loss of biomass, and improving the quality of carbon-neutral compounds such as starch and neutral lipids [216,219]. This ultimately enhances the quality of biomass feedstock for bioenergy generation. In a research conducted by Yao et al., 2018 , it was shown that in *Tetraselmis subcordiformis*, when nitrogen is limited, microalgae tend to prioritize the uptake and utilization of phosphorus in order to maintain cellular homeostasis and metabolic activity. Phosphorus availability may indirectly regulate nitrogen intakes and impact the overall development and productivity of microalgal cultures under nitrogen-limited environments by supplying more ATP for the production of store energy molecules to sustain cellular energy for growth [213].

In addition, oligo and trace elements, such as sodium carbonate and chloride, control the solubility of carbon dioxide and oxygen and influence the development of biomass and the

creation of products. This highlights their significance in the culture of microalgae [220]. Metal ions, such as calcium and magnesium, have a crucial impact on enzyme activation. They specifically help stabilize the transition states of carboxylase and oxygenase activities in enzymes such as Rubisco, which are essential for carbon dioxide assimilation [221]. Additionally, both ions also play a dominant role in the extracellular buffer chemistry of media. They interact with CO_2 and other ions to induce the cell aggregation mechanism in microalgae [222,223].

Therefore, nutrients are essential for the development and CO_2 fixation ability of microalgae. Optimal and well-balanced nutrition availability enhances the growth of microalgal biomass, leading to higher efficiency in CO_2 utilization. Understanding the availability and intake of crucial nutrients, including nitrogen, phosphorus, and trace elements, is necessary for cellular functioning, photosynthesis, and metabolic processes involved in biochemical production. Optimizing nutrient synergy, such as the nitrogen-to-phosphorus ratio with CO_2, and directing carbon towards lipid or starch production can improve the quality of feedstock for bioenergy generation. However, imbalances or deficits in nutrients can result in suboptimal development and reduced CO_2 fixation rates. Additionally, the use of affordable and environmentally-friendly nutrient sources may enhance the economic feasibility and ecological sustainability of microalgal CO_2 capture systems. To fully exploit the potential of microalgae in carbon capture and bioenergy production, it is crucial to understand and optimize nutrient dynamics.

2.2.6 Impact of flue gas compounds NOx and SOx on microalgal CO_2 fixation

Microalgae cultivated utilizing industrial flue gas are exposed to high concentrations of CO_2, varying from 5% to 25%, along with other harmful substances including NOx and SOx. These compounds disrupt the capacity of the growing medium to maintain a stable pH [224]. When these flue gas components are introduced into the liquid phase of a microalgal culture system, they provide additional nitrogen and Sulphur compounds to the cultivation medium as shown in Figure. 2.5. Nitric oxide (NO) moderately dissolves and oxidizes into nitrite (NO_2^-) [225] and, depending on pH, the intermediate product from sulphur dioxide (SO_2), sulphite (SO_3^{2-}) or bisulphite (HSO_3^-) finally converted to sulfate (SO_4^{2-}) [226]. Various microalgal species exhibit varying degrees of tolerance to these pollutants and elevated levels of CO_2.

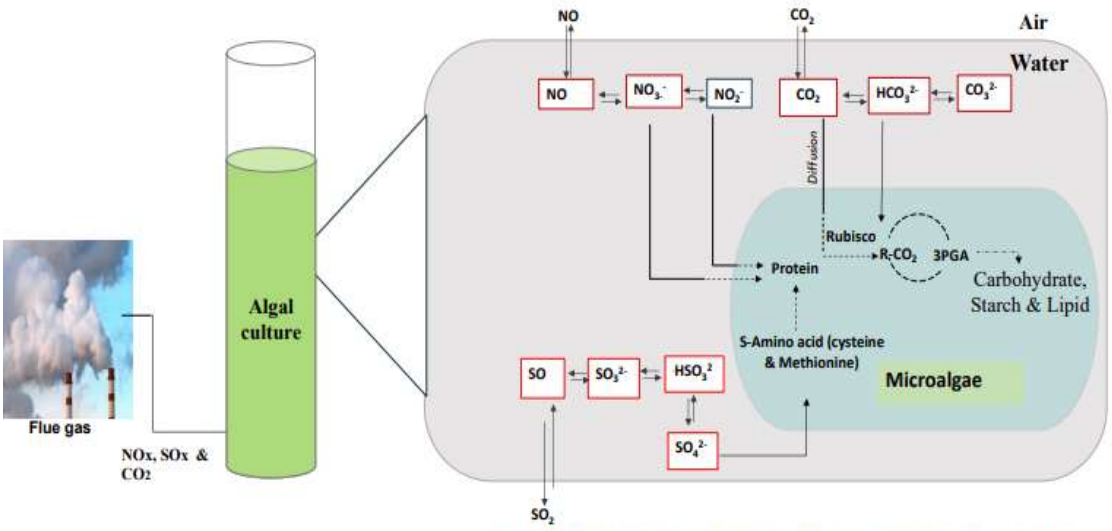

Fig 2.5. Flue gas compounds interaction in cultivation media and utilization in microalgal systems

In this specific context of flue gas compounds dilution and uptake , the nitric oxide (NO) in the exhaust gas slowly dissolves and oxidizes into nitrite (NO_2) [227]. This nitrite may serve as a nitrogenous substrate for microalgae without causing any detrimental effects on their growth. NOx reduction occurs via two mechanisms: direct diffusion into cells, resulting in the conversion to nitrite and nitrate, or dissolving in the suspension, leading to the creation of nitrate and nitrite, which are then absorbed by the cells [228].

Vacuoles function as storage chambers for excess nitrogen, while the remaining nitrogen is converted into ammonium inside the chloroplast and used for the synthesis of essential macromolecules [229]. Meanwhile, sulphur dioxide (SO_2) produces intermediate compounds such as sulphite (SO_3^{2-}) or bisulphite (HSO_3^-) depending on the pH level, finally transforming into sulphate (SO_4^{2-}) [90]. Extended exposure to flue gas leads to the accumulation of these compounds, which in turn produces a rapid decrease in the pH of the substance. Sulphate ions have a significant role in reducing pH, and the high solubility of SO_2 in the liquid phase accelerates the accumulation of SO_4^{2-} [156]. The impact of changes in fuel gas composition on NO_X and SO_X varies depending on the source type and the tolerance capabilities of each species, as seen in Table 2.3. *Chlorella minutissima*, derived from a thermal coal power station, has a high tolerance to NO_X levels of up to 60 ppm and SO_X levels of 0.3%

[230]. *Chlorella vulgaris*, derived from a coal burning boiler, demonstrates resilience to elevated levels of nitrogen oxide (NO_X) at 250 ppm and sulphur oxide (SO_X) at 180 mg/L , while maintaining a productivity rate of 40 mg/L day^{-1} [227].

Scenedesmus abundans, obtained from a coal burning power station, has a moderate level of resistance to NO_X at 207 mg/L and to SO_X at 53 mg/L . However, its production is poor. *Scenedesmus acutus,* a microalgae species found in coal-fired power plants, is capable of tolerating nitrogen oxides (NO_X) concentrations ranging from 50 mg/L to 80 mg/L and sulphur oxides (SO_X) concentrations up to 30 ppm [231]. *Desmodesmus abundans* UTEX 2976, when exposed to flue gas from the cement industry, exhibits significant resistance to NO_X at a concentration of 100 mg/L and SO_X up to 600 mg/L [90]. Additionally, it maintains a biomass productivity of 27 mg/L day^{-1}. This illustrates its capacity to tolerate high levels of SO_X without compromising its growth performance.

The impact of flue gas pollutants NOx and SOx on microalgal CO_2 fixation is intricate, including both beneficial and challenging factors, since some species use these compounds as nutrition. Comprehending these consequences and formulating approaches to reduce negative effects are crucial for maximizing the use of microalgae in CO_2 capture and biofuel generation. By harnessing the adaptive characteristics of microalgae and using specific treatments to mitigate adverse impacts, it is feasible to augment the sustainability and efficiency of this method of treatment, making it a viable resolution for environmental and energy concerns.

Table 2.3. Microalgal Strains Cultivated from Flue Gases of Various Industries

Microalgal Strain	**Flue gas source from different industry**	**Flue gas composition**			**CO_2 fixation rate**	**Biomass productivity**	**References**
		CO_2	SO_X	NO_X			
Chlorella minutissima	Thermal coal power plant	11 %	0.3%	60 mg/L	80 mg/L/day	21 g/m^2 /day	[230]
Chlorella vulgaris	Coal burning boiler	6 %	180 ppm	250 mg/L	-	40 mg/L/day	[227]
Chlorella sorokiniana	Fossil diesel fuel engine	12 %	-	613 mg/L	-	83 mg/L/day	[232]
Scenedesmus abundans	Coal burning power plant	14 %	53 ppm	207 mg/L	-	16 mg/L/day	[231]

Scenedesmus acutus (UTEX B72)	Coal-fired power plant	10-13%,	0-30 ppm,	50–80 mg/L,	200 mg/L/day	110 mg/L/day	[233]
Chlorella vulgaris	Combined heat and power plant	7.4 %	4.4 mg/m^3	38 mg/m^3		27 mg/L/day	[234]
Chlorella sp.	Thermal coal fired power plant	10	30 ppm	61 mg/L	187 mg/l/day	108 mg/L/day	[235]
Scenedesmus obliquus WUST4	Cooking chemical industry	18	200	150 mg/L	-	124 mh/L/day	[168]
Chlorella sp. MTF-15	Coal carbonization industry	22-26 %	15-20 ppm	25-3 mg/L	20-35 g/L/day	342 mg/L/day	[236]
Nannochloropsis oceanica	Coal fired power plant	13 %	30 ppm	139 mg/L	25 mg/L/day	13 mg/L/day	[138]
Chlorella sp. MTF-15	Steel Industry	23 %	87 ppm	78 mg/L	-	360 mg/L/day	[224]
Haematococcus pluvialis NIES-144	Heat and power plant	5 %	-	22 mg/L		31.6 mg/L/day	[237]
Desmodesmus abundans UTEX 2976	Cement industry flue gas	25 %	600 ppm	100 mg/L	0.416	227 mg/L/day	[90]

2.3 Process Strategy for the Enhancement of microalgal CO_2 fixation Efficiency

2.3.1 Light and nutritional management process strategies for improving CO_2 fixation and biochemical production

Efficiently maximizing the process of microalgal CO_2 fixation is crucial for sustained carbon negative biomanufacturing of biochemicals. This requires optimizing both light and nutritional parameters, as stated by Morales et al., 2018 . The phenomenon of light absorption

and transmission in microalgal suspensions is crucial in determining the rates of photosynthesis [238] . Photobioreactors (PBRs), such as tubular and flat panel designs, have been carefully designed to improve the collection and use of light, resulting in the highest possible accumulation of biomass [239]. Nevertheless, there are still obstacles to overcome, particularly the issue of uneven light distribution resulting from the presence of microalgal cells that contain a high concentration of pigments, as well as the light-blocking effects that occur when the cell density is high [240]. In order to tackle this issue, approaches such periodic cell pre-harvesting utilizing recycled media have been developed and result in the improvement of CO2 fixation by 20% [241]. This helps to reduce the impact of light attenuation and allows for better light penetration, which in turn helps to control growth during exponential periods.

In addition, the idea of particular light intake has become more important. This concept involves an increase in light intensity as biomass density increases, which is referred to as the lumostatic enhanced notion. This novel method has shown potential in improving growth and allowing the creation of certain products, as demonstrated in species such as *Haematococcus pluvialis*, *Chlorella zofingiensis*, and *Chlorella minutissima* [241–244]. In addition, Ma et al. 2024 research on dynamic light feeding models has shown significant improvements in rates of CO_2 fixation to 270 mg/L day^{-1}.

Aside from light, the nutrient feeding strategy, namely nitrogen (N) and phosphorus (P), is developed as they are major nutrient source essential for the growth of microalgae and their capacity to convert CO_2 into organic compounds. Research has clarified that nitrogen-based fed-batch methods are effective in improving the growth of biomass and the rate at which carbon dioxide accumulates in species like *Isochrysis galbana* and *Desmodesmus* with 15 to 22 % [245,246] . This leads to higher biomass productivity and enhanced rates of CO_2 fixation. In addition, it is critical to appropriately manage nitrogen sources due to their significant impact on carbonate chemistry and CO_2 dilution, both of which are critical for the preservation of carbon availability and stoichiometric equilibrium. Phosphorus, an essential ingredient for metabolism and cell development, is mainly obtained from phosphates in microalgae production [247]. Previous studies have shown that providing an adequate amount of phosphorus while depriving the cells of nitrogen may boost cellular metabolic activity and promote the accumulation of lipids. This leads to a maximum lipid content of 31.6% of the dry weight of biomass [248]. Furthermore, results that are encouraging in terms of increasing lipid production have been obtained through the investigation of a two-stage cultivation method that incorporates phosphorus supplementation in nitrogen-deficient environments. Studies suggest

that controlling the quality of light and nitrogen levels, together with modifying the carbon supply, may effectively manage microalgae for the synthesis of macromolecules [249]. Nevertheless, the impact of light quality and nitrogen levels on biochemical composition differs considerably among different species.

It is crucial to maintain proper nutrient concentrations since insufficient or excessive quantities might hinder the growth of microalgae and the process of CO_2 fixation. Photobioreactor engineering strategies, such as the use of self-adaptive PBRs with anion exchange membranes, enable the continuous flow of nutrients, which enhances the development of biomass and metabolite regulation [250]. Additionally, the precise adjustment of nutrient amounts and ratios via control and monitoring systems can efficiently meet the evolving metabolic requirements of microalgae and successfully address the physiological challenges faced by microalgae under varying climatic conditions[251,252].

Efforts to improve the way light is distributed inside PBRs have shown potential, since solutions like internal light sources or light-guiding materials have been able to overcome traditional design constraints [253] . Strategies such as arranging LEDs in a hexagonal closest-packed arrangement or vertically inserting transparent tubes into PBRs have shown promise in enhancing the dispersion of light and increasing biomass production from 1.5 to 3.56 g/L [254]. Overall, in order to increase the efficiency of microalgal CO_2 fixation, it is critical to optimize both irradiation and nutritional conditions. Biomanufacturing processes and microalgae-based CO_2 capture systems have a great deal of potential to increase biomass productivity via the use of dynamic nutrient feeding schemes and innovative engineering approaches.

2.3.2 Use of additive for improvement of CO_2 mass transfer in microalgal cultivation system

In order to optimize the transfer of CO_2, it is often necessary to create highly alkaline conditions with a pH level above 10. This allows CO_2 to react with hydroxide ions and form bicarbonate (HCO_3^-). The speed of this process, determined by the reaction's kinetics, is significantly higher than that of CO_2 reacting with water to produce carbonic acid (H_2CO_3). Algae species that thrive in high pH environments, like *Spirulina*, are essential for operations at elevated pH levels due to their remarkable ability to tolerate and flourish in such conditions. Rapid CO_2 dilution occurs when solutions with a very alkaline pH, particularly those beyond pH 10, enhance the presence of dissolved inorganic carbon, even in situations of low CO_2,

directly from the atmosphere. This phenomenon is found in cultures of *Chlorella sorokiniana* SLA-04 [202,203]. An integrated strategy is employed to combine alkali solutions with a microalga growing medium in photobioreactor, leading to the formation of two carbon transportation paths. The first step involves microalgae using CO_2 directly through photosynthesis. Another approach is to utilize alkali solutions, such as Na_2CO_3 [255,256] and K_2CO_3 [257] to absorb CO_2. The salts undergo a transformation into bicarbonate salts within the medium prior to being utilized by microalgae. Exposure to common amine alkali absorbents, such as tertiary amine TEMDA, amine DACH, monoethanolamine (MEA), 2-amino-2-methyl-1-propanol (AMP), diethanolamine (DEA), and triethanolamine (TEA) [71] , resulted in an observed improvement in the metabolic activity of *Scenedesmus* sp. and *Chlorella* sp. [258,259]. The presence of bulky alkyl groups adjacent to amine groups in these absorbents resulted in the instability of the carbamate intermediates, which in turn facilitated their hydrolysis into bicarbonate [258]. This ultimately led to a decrease in cell inhibition. Adding a solution of amines to promote cell development in a regulated way has been shown to be advantageous for enhancing the process of photosynthetic CO_2 fixation. This is achieved by adjusting the ratio of TEA to cell density and counteracting the negative impact of ammonia inhibition [260]. This method ensured a reliable and steady supply of dissolved inorganic carbon (DIC) for algal fixation, without causing any major hindrance to cell development.

2.3.3 Photobioreactor engineering for improvement in CO_2 mass transfer

Considerable study has been carried out to investigate the design of photobioreactors with the aim of optimizing the supply of CO_2 for microalgal fixation, while simultaneously minimizing medium acidification and CO_2 loss. A photobioreactor engineer specializes in improving the design and functionality of photobioreactors (PBRs) to increase their efficiency, user-friendliness, and ability to be scaled up. Primary areas of concentration are altering the surface-to-volume ratio (S/V ratio) and enhancing the processes of mixing and mass transfer[119,132]. These improvements are crucial for optimizing the efficiency of microalgae production in PBRs, by enhancing the rate at which CO_2 is transferred or taken up. The used method improves the transfer of carbon to the surfaces of microalgae by optimizing the rate at which it transitions from the gas phase to the liquid phase. As a result, it boosts the overall effectiveness of the photobioreactor system in capturing carbon and increasing biomass output. The size of bubbles has an adverse effect on sparging efficiency. Larger bubbles enhance gas

transportation, whereas smaller bubbles aid in mixing. The dimensions of bubbles are determined by parameters such as the diameter of the sparger orifice and the velocity of the gas flow. When using aeration holes of a significant size (>1 mm), it results in the formation of bubbles that are at least 5 mm in diameter. Conversely, tiny openings for aeration produce macrobubbles that are larger than 100 μm, [188] microbubbles ranging from 1 μm to 100 μm, and nanobubbles smaller than 1 μm [129]. Regulating the size of bubbles is essential for maintaining efficient gas retention. The traditional approach for delivering CO_2 involves the use of aerators or spargers installed at the bottom of ponds or photobioreactors. These devices influence the dimensions of the bubbles, the surface area of contact, the duration of CO_2 interaction with the liquid, and the process of CO_2 dissolution into the liquid [261]. Sparging, often done using porous stones or air diffusers, is a frequently used technique in microalgae production systems to inject carbon dioxide into the culture media. Micro/nanobubble diffusers enhance gas retention by augmenting the surface area to volume ratio. The current research is mostly focused on innovative aerator designs [262].

Huang et al. 2017 designed circular stomata plate aerators with precisely sized pores and spacing to improve the performance of bubbles, leading to a 83.5% in CO_2 fixation. Y. Song et al. 2020 used 3D printing technology to create microporous fibrous-diaphragm aerators that had a range of gradient micropores, ranging from 6 μm to 126 μm. This resulted in an enhancement of inorganic carbon availability in the surrounding medium, leading to a 15% increase in biomass production. Lim et al. 2023 performed. an evaluation of three gas spargers in a flat-panel photobioreactor. The study revealed surprising results regarding microbubble generation and suggested the use of a dual-mode sparger system. This system consists of normal bubbles ranging from 100 to 120 microns and microbubbles ranging from 60 to 80 microns. The purpose of this system is to improve the mixing of cells and enhance the transfer of CO_2 concurrently. The application of Venturi injector microbubble generators, specifically aimed at CO_2 capture and microalgae cultivation, has led to the development of a novel Venturi-integrated photobioreactor. This innovation results in an 86% to 98% increase in CO_2 capture efficiency [130].

A novel membrane carbonation method has been recently developed to enhance the utilization of CO_2 by microalgae. This method allows for the injection of CO_2 into the liquid solution by diffusion using a non-permeable hollow fiber barrier, therefore preventing the production of visible bubbles [266,267],. This approach offers a carbon mass transfer efficiency that exceeds traditional sparging methods by 30% to 50% in terms of CO_2 mass transfer in a

photobioreactor [41]. Increasing the efficiency of CO_2 mass transfer requires higher pressure and energy consumption compared to conventional bubbles. Conducting a comprehensive assessment of the costs, environmental effect, and economic rewards is essential to establish the practicality of adopting these enhancements in real-world commercial systems.

2.4 Key Challenges and Solutions for sustainable and Cost-effective microalgal CO_2 Capture Development

Microalgae are considered feasible alternatives for capturing CO_2 and sustainably producing biofuels and biochemicals due to their rapid growth rates, abundant lipid content, and ability to flourish in many environmental conditions. However, the implementation of microalgal biomanufacturing processes faces significant challenges related to strict process parameters and environmental conditions. An important concern is on the interaction of flue gas molecules inside the culture medium. As shown in section 2.1, the introduction of flue gas components might lead to acidification of the culture medium, which hampers the carbonate chemistry essential for the dilution of CO_2. This disruption impedes the process of carbon dioxide dissolution, hence restricting the growth of microalgae. The influence of fluctuating environmental circumstances, namely light and temperature, on the process of CO_2 fixation and biochemical synthesis in microalgae is substantial. Therefore, it is crucial to screen, select, and analyze microalgae in order to identify strains that can thrive in these difficult environmental conditions. The presence of acidic compounds such as sulphur oxides (SO_X) and nitrogen oxides (NO_X) in flue gases complicates this process by disturbing the necessary pH balance for optimal microalgal formation. Understanding the capacity of different microalgal strains to adjust to changing environmental circumstances is essential for enhancing the efficiency of CO_2 capture and boosting biomass production. Assessing the adaptation of strain may provide useful information for establishing efficient cultivation methods that maximize biomass production and fixation of CO_2.

Another major challenge is the creation of effective process engineering solutions to improve the utilization of CO_2 and increase the synthesis of biochemicals from biomass. In order to increase biomass production and decrease CO_2 emissions, it is crucial to efficiently control the composition of the growth medium, while continuously supplying CO_2 in its gaseous phase, and comprehending its synergistic interaction with other factors. As mentioned before, the microalgal process of capturing and using CO_2 is influenced by several non-living

elements such as the intensity of light, temperature, pH level, and availability of nutrients. The parameters undergo dynamic changes as microalgae growth progresses. Dynamic fluctuations in pH throughout development, as well as changes in light and nutritional requirements, may significantly impact the activity of enzymes involved in carbon fixation. Therefore, it is crucial to fully understand and assess all of these variables and how they interact with each other in order to improve the efficiency of carbon dioxide fixation and biochemical synthesis.

Moreover, the development of efficient harvesting technology is a significant challenge. Implementing a harvesting technique that balances continuing growth with minimal negative impacts on productivity and biomass quality is crucial. Efficient harvesting procedures should strive to reduce energy and water use, minimize ecological consequences, and sustain high levels of product retrieval. The advancements in technology increase the competitiveness and sustainability of microalgal biomanufacturing as a platform for renewable energy and bioproducts.

To advance the feasibility and scalability of microalgal biomanufacturing technologies, it is essential to address these limitations, particularly in reducing CO_2 emissions. The objective of this thesis is to improve the sustainability and effectiveness of microalgal biomanufacturing for the production of biofuel and biochemicals. This will be achieved by utilizing novel approaches in strain screening, process engineering, media optimization, and harvesting technology development, with a particular emphasis on the utilization of CO_2. This study aims to improve these crucial areas in order to greatly decrease environmental effects and operational expenses, therefore improving the competitiveness of bio-based manufacturing compared to fossil-based alternatives. In essence, this thesis aims to significantly contribute to the continuing shift towards a more sustainable and resilient bio-based economy. This work intends to use the capabilities of microalgae to capture CO_2 and generate valuable bio-products. The goal is to develop cleaner energy sources and efficiently reduce our carbon footprint, resulting in benefits for both society and the environment.

2.5 Objectives

1. Screening, selection, and evaluation of microalgae under harsh environmental conditions:
2. Evaluation of acclimation capacity of microalgal strains in different light and temperature condition and its impact on CO_2 fixation and biomass production:

3. Process engineering strategy for enhancing CO_2 utilization and biomass-derived biochemical production:
4. Development of microalgal harvesting process in continuous growth phase with minimal impact on productivity and biomass quality

.

CHAPTER 3

Screening, Selection, and Performance Evaluation of Resilient Microalgae in Extreme Environmental Conditions

Chapter 3

Screening, Selection, and Performance Evaluation of Resilient Microalgae in Extreme Environmental Conditions

3.1 Background and motivation

The systematic screening, selection, and evaluation of microalgae under harsh environmental conditions in bench scale are crucial for the development of an efficient and resilient strategy for scaling up microalgal strains to achieve commercial and industrial viability. Identifying dominant microalgal strains that can thrive in environments with high concentrations of CO_2 and contaminants such as nitrite, sulfate, and bisulfite byproducts of SOx and NOx in aqueous media presents both a challenge and an opportunity. This chapter presents a systematic approach for screening, acclimating, and evaluating the performance of microalgal strains that are resilient and well-suited for the purpose of CO_2 sequestration and biofuel generation. This is accomplished by utilizing acidic and toxic chemicals found in flue gas emissions, shown in the schematic work plan diagram Figure. 3.1. It begins with a thorough screening of 13 microalgal strains to evaluate their tolerance to the complex composition of industrial flue gas, which includes elevated levels of CO_2, SOx, and NOx dissolve compounds when interact with aqueous phase, serving as the sole sources of carbon, nitrogen, and sulfur. Growth rate metrics, such as specific growth rate (μ) measured in day^{-1} and photosynthetic performance indicators, including maximum quantum yield (*Fv/Fm*), are used to assess the initial screening. Strains showing promising growth and adaptation to these conditions are then subjected to further acclimatization through a two-stage cultivation strategy. Initially, selected strains are cultivated with all dissolved components of flue gas and bicarbonate as the carbon source. This is followed by exposure to 15% CO_2 as the sole carbon source in the same medium. The acclimatization process involves gradually increasing the concentrations of flue gas components to facilitate adaptation to higher levels of CO_2 and pollutants. Throughout this process, continuous monitoring of growth rates and photosynthetic efficiency (*Fv/Fm*) ensures the robustness of the acclimatization.

Subsequently, the strains undergo evaluation in a semi-continuous growth phase under continuous industrial flue gas conditions to assess their stability in CO_2 fixation and lipid production. Metrics such as CO_2 fixation rate (mg CO_2 L^{-1} day^{-1}) and lipid productivity (mg L^{-1} day^{-1}) are used to quantify their performance. The systematic approach includes eight bench-scale experiments, each with specific objectives outlined in Table 3.1. These experiments aim to establish crucial initial bench scale study for developing robust microalgal solutions for carbon capture and renewable energy production.

The main outcomes of this study, among the thirteen microalgal strains, six exhibited significant growth on flue gas salt medium when sodium bicarbonate was the only carbon source. Further evaluation was conducted on 6 strains to assess their growth and photosynthetic ability in 15% CO_2 condition. Strains NCIM5584 and KMC8 exhibited the greatest resistance to flue gas chemicals, while still retaining substantial biomass yield and photosynthetic efficiency. KMC8 had the greatest rate of biomass production in the treatment medium, with a value of 52.5 mg $L^{-1}day^{-1}$, while NCIM5584 revealed a biomass productivity of 48.4 mg L^{-1} day^{-1}. Both strains had favorable *Fv/Fm* ratios of 0.55 and 0.58, respectively, suggesting that photosynthesis was actively occurring and potential of utilizing the flue gas compounds in their photosynthesis process. The cells' development was enhanced through a gradual acclimation to dissolved SOx and NOx molecules. This acclimation led to an increase in photosynthesis performance, with *Fv/Fm* 0.63 from 0.58, similar to the control value observed in normal BG-11 media. As a result, the cell density increased by 1.5 times and the specific growth rate for KMC8 reached 0.214 d^{-1}. The rates of CO_2 fixation and the efficiency of utilization were enhanced by more than 2.5 times in both strains. KMC8 demonstrated exceptional performance in neutral lipid accumulation (up to 20%) and CO_2 fixation (346.43 mg L^{-1} day^{-1}), which renders it a viable candidate for biofuel production. The stability of KMC8 in semi-continuous CO_2 bio-mitigation processes was validated by scale-up tests in photobioreactors. In a mode of 5 cycles, the CO_2 fixation rate varied between 313 and 363 mg L^{-1} day^{-1}, whereas the efficiency varied between 7.66% and 8.57%. The average biomass and lipid productivity were 3.15 mg L^{-1} day^{-1} and 45.34 mg L^{-1} day^{-1}, respectively.

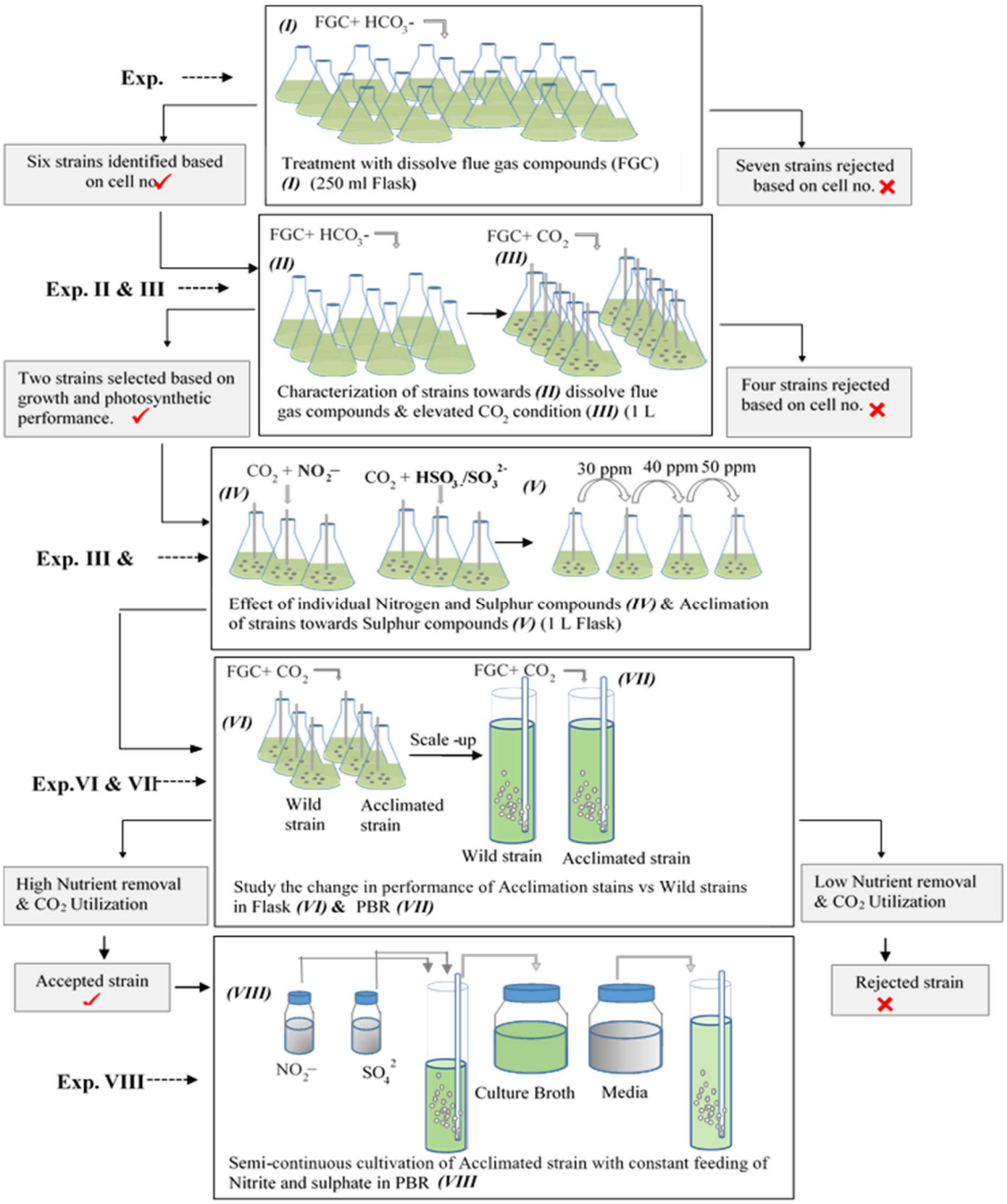

Fig. 3.1. A systematic approach to screening, acclimation, and assessing microalgal strains for the aim of CO_2 sequestration using acidic and toxic flue gas compounds

Table 3.1: Number of Experiments performed with their cultivation condition and objectives

Exp.	Treatment media	Control media	Strains used	Culture vessel & Volume	Biotic variable measured	Objective
Exp.1	Flue gas salt media with bicarbonate as carbon source	-	13	100 ml (50 ml W.V*)	Cell density on the basis of cell number	Adoptability
Exp.2	Flue gas salt media with bicarbonate as carbon source	BG-11 media	6	1L (500 ml W.V)	*Fv/Fm,* P_{max}*, µ*, Photosynthetic pigment	Tolerance capability to flue gas salt
Exp.3	Flue gas salt media with 15% CO_2 as carbon source	Carbon free BG-11 media with 15 % CO_2	6	1L (500 ml W.V)	*Fv/Fm*, P_{max} , μ, Photosynthetic pigment	Tolerance capability to flue gas salt at elevated CO_2 condition
Exp.4	Flue gas salt media only with nitrite and Sulphite /bisulphite separately	Carbon free BG-11 media with 15 % CO_2	KMC-8, NCIM-5584	250 ml (100 ml W.V)	Biomass growth dynamic profile	Understanding the effect of individual dissolve FGC on Growth
Exp.5	Gradient phase addition of sulphite /bisulphite with 15% CO_2 carbon source	Carbon free BG-11 media with 15 % CO_2	KMC-8 NCIM-5584	250 ml (100 ml W.V)	Biomass growth	Acclimation of strains towards dissolve flue gas compounds
Exp.6	Flue gas salt media with 15% CO_2 as carbon source	-	KMC-8 (Wild, Acclimated) NCIM-5584 (Wild, Acclimated)	1L (500 ml W.V)	Dynamic growth profile, *Fv/Fm* , P_{max} µ, C_F* ,C_U*, NRR* , Photosynthetic pigment and Biochemical composition	Study the change in growth, Nutrient, CO_2 uptake and biomass composition after acclamation of strain

Exp.7	Flue gas salt media with 15% CO_2 as carbon source	Carbon free BG-11 media with 15 % CO_2	KMC-8 (Wild, Acclimated) NCIM-5584 (Wild, Acclimated)	2 L Bubble column PBR (1.8 L W.V)	Dynamic profile of Biomass growth and NRR	Performance of acclimated strain in terms of growth and nutrient uptake in PBR
Exp.8	Continuous supply of Nitrate and sulphate with 15% CO_2 as carbon source	-	KMC-8 Acclimated strain	2 L Bubble column PBR (1.8 L W.V)	Dynamic profile of Biomass growth, C_F and C_U	To check the performance in continuous availability of dissolve FGC

*Note – W.V (working volume), P_{max} (Biomass productivity), μ(specific growth rate), NRR (Nutrient removal rate) , FGC (flue gas compounds), C_F and C_U (CO_2 fixation rate and utilization efficiency).

3.2 Materials and methods

3.2.1 Microalgal strains and culture medium

Thirteen green alga (Chlorophyceae) strains used in this study were either consisted of our own isolations from domestic sewage wastewater or procured from national culture facility, NCIM (National Collection of Industrial Microorganisms, National Chemical Laboratory, Pune, India). The five strains included in the Chlorellaceae family are *Chlorella pyrenoidosa* (NCIM2738), *Chlorella sorokiniana* (KMC5), *Chlorella thermophile* (MF179624), *Micractinium pusillum* (KMC8) , *Chlorella* FC-2. The five strains from the Scenedesmaceae family are *Scenedesmus abundans* (NCIM2897), *Scenedesmus acutus* (NCIM5584), *Desmodesmus armatus* (NCIM5583), *Desmodesmus abundans* (KMC3), and *Acutodesmus deserticolal* (KMC6). The three strains from the Selenastraceae family are *Monoraphidium convolutum* (KMC2), *Monoraphidium sp*. (KMC4), and *Monoraphidium contortum* (KMC7). The strains mentioned have a recognized capacity to adapt to wastewater conditions and to mitigate CO_2 [268–271]. The strains were cultivated on a regular basis, once a week, in Erlenmeyer flasks with a capacity of 250 mL. Each flask contained 100 mL of BG-11 media [272]. The pH of the medium before to autoclaving was 7.8, and it was not regulated throughout the growth process. The cultures were placed in an illuminated orbital incubator shaker (Scigenics (India) Pvt Ltd, India) and kept at a temperature of 25 °C. The cultures were exposed to a continuous light intensity of 150 µmol photons m^{-2} s^{-1} and were agitated at a speed of 150 rpm.

In order to assess the level of tolerance and the pace at which NO_X and SO_X are removed as a nutritional source, the strains were cultivated in flue gas salt medium (FGS). This was achieved by removing the carbon, nitrogen, and sulphur sources from the BG-11 media (Camargo and Lombardi, 2017). In the BG-11 medium, sodium nitrate ($NaNO_2$) was substituted with sodium nitrite ($NaNO_3$) at a concentration of 17 mmol L^{-1}, and magnesium sulphate was replaced with $MgCl_2 \cdot 6H_2O$ at a concentration of 0.3 mmol L^{-1}. In order to induce the presence of SO_X compounds in the culture medium, Sodium sulphite and bisulphite were used as supplementary components. This was done to obtain a concentration of sulphite (SO_3^{2-}) and bisulphite (HSO_3^-) at 0.625 and 0.617 mmol L^{-1} respectively in the modified BG-11 media. The purpose of maintaining this concentration was to ensure that each compound remained at a level of 50 mg L^{-1}. The control for the experiment consisted of using native BG-11 media, unless otherwise specified. In the preliminary screening experiment, the culture

media initially contained 100 mmol L^{-1} sodium bicarbonate ($NaHCO_3$) to maintain a high carbon level. Later on, in the modified BG-11 media (FGS), sodium carbonate was replaced with a mixture of 15% CO_2 and compressed air as the carbon source.

3.2.2 Culture condition and Selection of strains

Microalgal growth was evaluated on the basis of counting cell number in a Neubauer Hemocytometer under an inverted microscope (Axio Scope.A1, Zeiss, US). For this, the microalgal strains were cultivated in FGS media with bicarbonate as carbon source (described in section 3.2.1) in 100 mL Erlenmeyer flasks (50 mL culture). These were incubated with cell density (OD_{680} = 0.1), in an orbital incubator shaker with condition as described previously, for 20 days in batch mode, in order to adapt the cells to dissolved flue gas compounds.

Out of the thirteen strains screened, six were selected for further experiments on the basis of their adaptation to FGS media based on higher cell count. They were scaled up to 500 mL in 1 L Erlenmeyer flasks in same conditions described above for their growth and photosynthetic performance analysis. In the second phase of screening experiments, selected strains were exposed to 15% CO_2 mixed with compressed air as sole carbon source at a flow rate of 50 mL^{-1} min^{-1} (0.1 vvm).

Two of these strains showing better performance in terms of higher growth and enhanced photosynthesis rate, were selected for further experiments. The two selected strains were evaluated in a 2 L laboratory-scale photobioreactor (PBR) with a custom-made bubble column for conducting dynamic experiments on growth, pH, and utilisation of nutrients. Figure 3.2a and b provide comprehensive illustrations and actual experimental conFigureurations, including the lighting, temperature, and aeration systems. The reactor was constructed using borosilicate glass owing of its exceptional durability and ability to transmit light. A 15% concentration of CO_2 was introduced into the reactor via the bottom at a flow rate of 500 mL min^{-1}. This was achieved by using a specially built double ring sparger made of perforated silicone rubber tubing with an outer diameter of 60.2 mm and a thickness of 2 mm. The purpose of this design was to aid aeration by generating small bubbles. The PBR temperature was maintained at 25 °C with the help of chiller/water bath. The system was illuminated by cool white LED panels (3 x 50 W per reactor, 6500 K color temperature) installed perpendicular to the surface of the reactor on one side, providing 200 µmol m^{-2} s^{-1} light intensity. The height to diameter ratio (H/D ratio) of reactor was 4.5 (H = 0.54 m, D = 0.08 m), with culture volume of

1.8 L, height of media culture (or culture depth) was of 0.365 m and 0.17 m space was left as head space which is required to remove the surplus oxygen from the reactor. Light intensity was controlled with voltage and current regulation by a DC regulator. The most potential strain was identified on the basis of better specific growth rate, enhanced nutrient removal efficiency and CO_2 kinetics and finally tested in a semi-continuous batch mode by pulse feeding flue gas compounds. The flask experiments were carried out in triplicate the data thus obtained was represented as mean ± std. dev. The scale up experiment in PBR was performed once however with control light and temperature conditions.

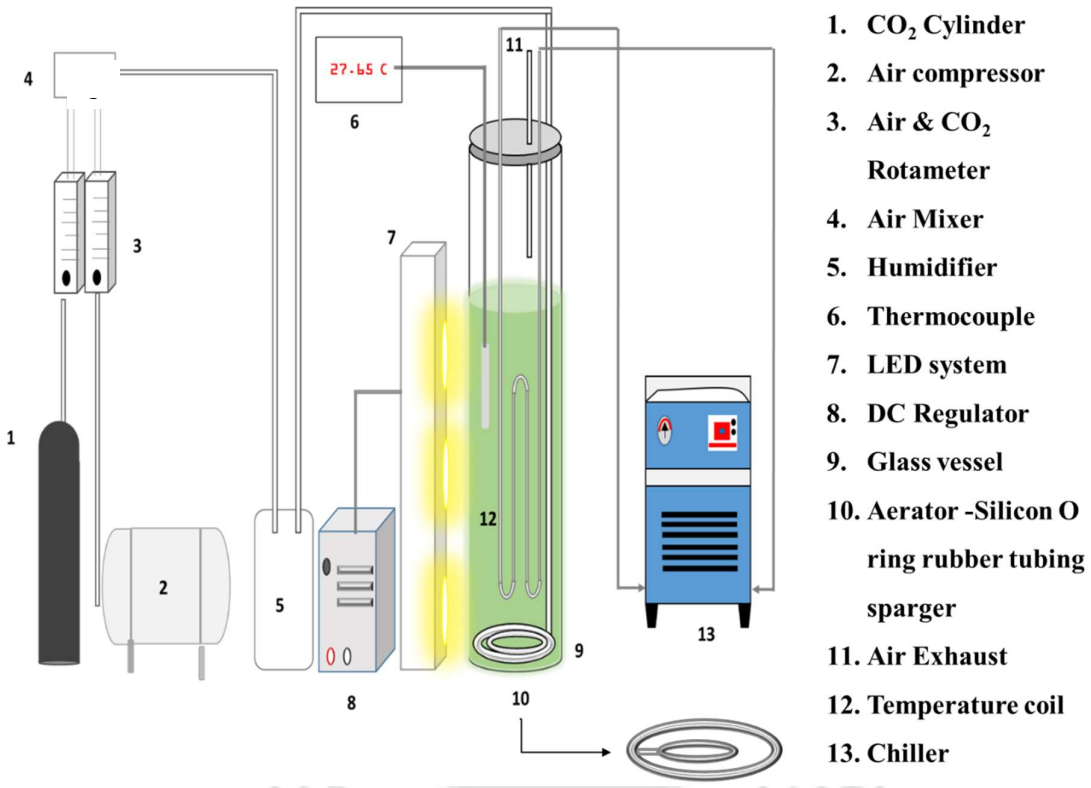

(a)

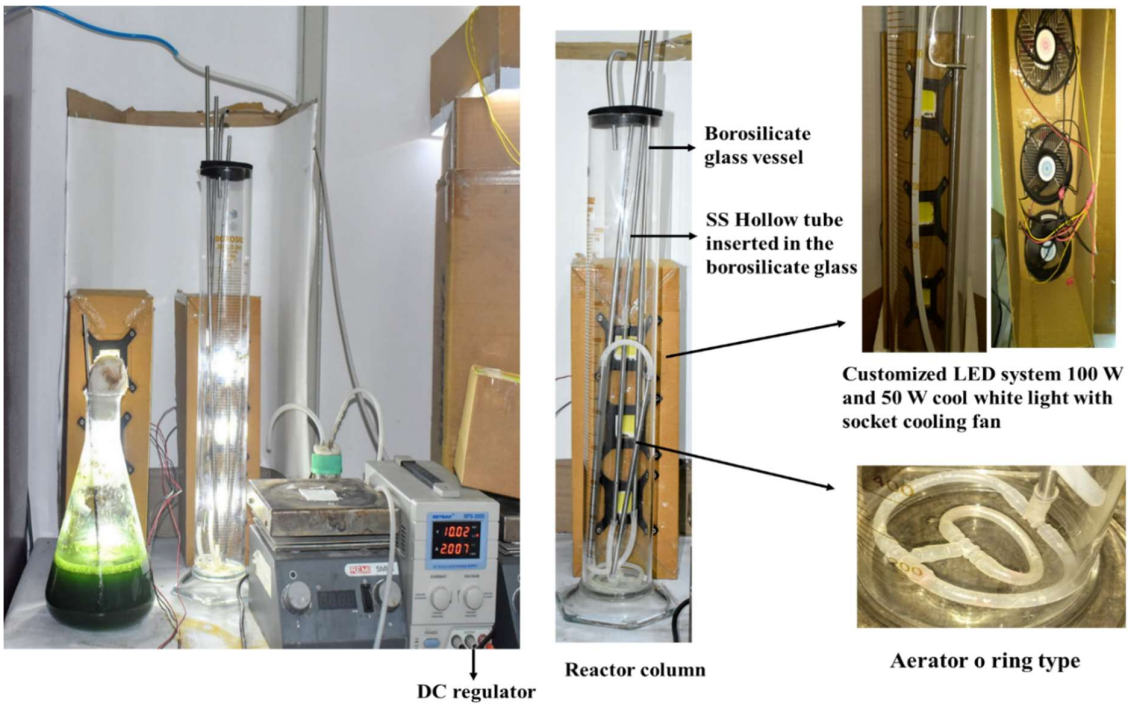

(b)

Fig. 3.2. Comprehensive **(a)** sketch illustrations and **(b)** actual experimental setups of the 2 L custom-made bubble column laboratory-scale photobioreactor (PBR), detailing the lighting, temperature, and aeration systems

3.2.3 Evaluation of the impact of nitrite and sulphite/bisulphite on growth

An experiment was conducted to assess the specific impact of NOx or SOx chemicals on the growth performance of chosen strains. In the process of NOx treatment, the nitrogen source nitrate was substituted with nitrite, maintaining an equal concentration of nitrogen in the standard BG-11 medium. For the treatment of SOx, a concentration of 50 mg L^{-1} of both sulphite and bisulphite was used as the source of sulphur in a sulphur-free BG-11 medium, as detailed in Table 3.1. The cells were cultured in a 1 L Erlenmeyer flask, with a working capacity of 500 mL. The initial inoculum density was measured using an optical density of 0.1 at a wavelength of 680 nm. The cells were cultured for a duration of 20 days. The studies were conducted three times, and the cultures were cultured on BG-11 medium, which served as the control. During both control and treatment trials, a process was carried out to remove 15% of CO_2 from the bottom of the flask, as explained in section 3.2.2.

3.2.4 Acclimation of strains towards sulphur compounds

In this experiment, the impact of sulphur compounds on the suppression of microalgal development was observed over a period of 20 days. The growth of biomass was compared to a control group at regular intervals. The strains' ability to tolerate increasing concentrations of sulphur ion (SO_3^{2-}/HSO_3^-) during their growth was assessed by exposing the cultures to varying concentrations of SO_3^{2-} and HSO_3^-. The concentrations ranged from 10 mg L^{-1} to 50 mg L^{-1}, with increments of 10 mg L^{-1}. Nitrite and 15% CO_2 were used as the nitrogen and carbon sources, respectively, during the whole experiment. The BG-11 medium containing 15% CO_2 was used as the control.

A gradient adaptation approach was used to enhance the strain's resistance to sulphur compounds (SO_3^{2-}/HSO_3^-). Sulphur compounds, namely SO_3^{2-} and HSO_3^-, were introduced into sulphur-free BG-11 medium. The concentration of each compound ranged from 20 to 50 mg L^{-1}, with an increase of 10 mg L^{-1}. The media included 15% CO_2 as the only source of carbon. The incremental rise occurred only when the strain achieved comparable cell growth to that of the control. The number of cycles required to achieve cell tolerance to a certain concentration of sulphur compounds at each incremental increase was measured. The acclimated strain was evaluated in contrast to the wild strain in terms of growth, photosynthesis, biochemical composition, nutrient elimination, and CO_2 utilisation efficiency after being exposed to sulphur compounds.

3.2.5 Scale up culture in Photobioreactor

The growth, pH, nitrite consumption, and sulphate consumption of both wild type and acclimated strains were observed and compared in a 2 L bubble column photobioreactor (with a working volume of 1.8 L) during a 20-day batch culture. The cultivation conditions stated in section 3.2 were used. An experiment consisting of 5 cycles, each lasting 11 days, was conducted to assess the impact of hazardous chemicals on growth and CO_2 bio-mitigation in a constant supply of nitrite and sulphate. The levels of nitrite and sulphate were continuously checked and maintained at 95% to 100% of the original content in the medium by periodically adding small amounts from their respective stock solutions.

3.2.6 Analytical measurement

3.2.6.1 Growth monitoring and Kinetics

In the initial phase, cultures of all the strains were harvested by centrifuging at 5000 rpm for 15 min, the cell pellet oven dried at 80°C for 24 h [272](Basu et al., 2014). For the selected two strains, dry cell weight (DCW) was monitored by measuring the optical density at wavelength T680 nm (OD_{680}) using UV/Vis spectrophotometer (Evolution 201, Thermo Scientific, USA). The linear relationship between the absorbance at OD_{680} and DCW (g L^{-1}) of two selected strains, *Scenedesmus acutus* and *Micractinium pusillum* were determined in normal and modified BG-11 media (Eqs.1 to 4).

$$Y(Micractinium\ pusillum) = 0.1995x + 0.0192\ (R^2 = 0.9935)\ \text{(BG-11 media)} \quad (3.1)$$

$$Y(Micractinium\ pusillum) = 0.3241x - 0.1349\ (R^2 = 0.9898)\ \text{(FGS media)} \quad (3.2)$$

$$Y(Scenedesmus\ acutus) = 0.4280x - 0.0352\ (R^2 = 0.9907)\ \text{(BG-11 media)} \quad (3.3)$$

$$Y(Scenedesmus\ acutus) = 0.3885x - 0.0168\ (R^2 = 0.9889)\ \text{(FGS media)} \quad (3.4)$$

The specific growth rate (μ, day^{-1}) and Productivity (P_{max}, g L^{-1}) was calculated using the equations (Eq. 5 and 6),

$$\mu = \frac{ln\,X_f - ln\,X_i}{t_f - t_i} \quad (3.5)$$

$$P_{max} = \frac{X_f - X_i}{t_f - t_i} \quad (3.6)$$

where, X_f and X_i (mg L^{-1}) represent the finial and initial cell concentration at time of harvesting t_f and initial day of inoculation t_i.

3.2.6.2 Nitrite and sulphate estimation

The concentrations of nitrite and sulphate was determined using the standard method of wastewater analysis as outlined in the protocol procedures established by the American Water Works Association [273] . A 6 ml aliquot of the clear supernatant was collected following centrifugation of the harvested sample at 5000 rpm for 15 min. The method used for nitrite estimation requires the use of 1 ml of collected sample for nitrite and 5 ml for sulphate

estimate in order to maintain a steady magnetic stirring action in the beaker. The color reagent was formulated by dissolving 10 g of sulphanilamide and 1 g of N-(1-naphthyl)-ethylenediamine dihydrochloride in 100 ml of ortho-phosphoric acid. The resulting solution was then diluted with deionized water to a final volume of 1 L. Forty microliters of the color reagent that had been created were combined with a 1 ml sample of the supernatant. The combination was then incubated at room temperature for a duration between 10 min, while being shielded from light to avoid the deterioration of the reagent due to exposure to light. After the sample was incubated, the spectrophotometer was used to determine the optical density (OD) of the sample at a wavelength of 543 nm.

To estimate the amount of sulphate, a 5 mL portion of the water sample (after filtration) was put into an Erlenmeyer flask. 2 mL of a buffer solution was added. The buffer solution was prepared by dissolving 30 g of magnesium chloride hexahydrate ($MgCl_2 \cdot 6H_2O$), 5 g of sodium acetate trihydrate ($CH_3COONa \cdot 3H_2O$), 1.0 g of potassium nitrate (KNO_3), and 20 mL of acetic acid (CH_3COOH, 99%) in 500 mL of distilled water. The volume was then adjusted to 1000 mL. The solution was agitated using a magnetic stirrer, and while maintaining continuous agitation, 0.15 g of barium chloride was added to the flask. The stirring process was maintained for a duration of one hour in order to guarantee the achievement of a thorough reaction and a consistent distribution of the $BaSO_4$ precipitate. Afterwards, the spectrophotometer was used to measure the absorbance of the sample at a wavelength of 420 nm. For standard analysis, sodium salt of nitrite and sulphate were used. For chemical analysis, whenever required sample were appropriately diluted to measurable range of standard concentration. The concentration was measured in mg mL^{-1}.

3.2.6.3 CO_2 utilization and Nutrient removal

CO_2 fixation rate ($mgL^{-1}day^{-1}$) was determined by the method [274]

$$C_F = \frac{(AFD_f \times C_f - AFD_i \times C_i) \times M_{CO2}}{t \times M_c} \quad (3.7)$$

AFD_f and AFDi represent the ash free biomass concentration (mg) at the time of harvesting and inoculation. Ash-free DCW was calculated by subtracting the ash weight from the DCW of biomass, ash weight measured by burning harvested dried biomass in a muffle furnace at 560 °C for 8 h [275]. C_i and C_f are the mass of Carbon in initial and final ash-free

dry biomass. Carbon content in dry biomass was determined by CHNS analyzer (Perkin-Elmer elemental analyzer) and M_{CO2} (g mol^{-1}) and M_C (g mol^{-1}) are the molecular mass of CO_2 and Carbon and t represents the total time of cultivation (days).

CO_2 Utilization efficiency (%) was determined by the method [274],

$$C_U = \frac{CO_2 \text{ fixation rate}}{CO_2 \text{ input rate}} X\ 100 \tag{3.8}$$

CO_2 fixation rate (mg $L^{-1}day^{-1}$) C_F was determined by Eq. 8 and CO_2 input rate (mg L^{-1} day^{-1}) was CO_2 supplied per day (mg day^{-1}) in unit volume (L) of media.

Nitrite and Sulphate removal efficiency (R.E, %) and removal rate (R.R, $mgL^{-1}day^{-1}$) are calculated as,

$$R.E = \frac{S_i - S_f}{S_i} \times 100 \tag{3.9}$$

$$R.R = \frac{S_i - S_f}{t_i - t_f} \tag{3.10}$$

where S_i and S_f represent the initial and final concentration of nutrient ions at the time of inoculation t_i and the time of harvesting t_f. For sulphate ion, the initial time and concentration depend on the conversion of sulphite and bisulphite ions into sulphate.

3.2.6.4 Estimation of photosynthetic pigment and efficiency

The pigments were quantified by the spectrophotometric method taking the OD at 470 nm, 663 nm, 646 nm, and 750 nm for extract pigments by using HPLC grade 100% methanol. To extract pigments from the cells, pellet was kept in dark condition for 12 h at 4 °C and was quantified by the equations described below [276]. The pigments were measured (µg mL^{-1}) at OD_{680} to quantify the change in pigment level, neglecting the cell density achieved in different experiments [277]

$$Chl._a = (1.672 \times OD_{665.2} - 9.16 \times OD_{652.4})/OD_{680} \tag{3.11}$$

$$\text{Chl.}_{b} = (34.09 \times OD_{652.4} - 15.28 \times OD_{665.2})/OD_{680} \quad (3.12)$$

$$\text{Chl.}_{a+b} = (1.44 \times OD_{665.2} + 24.93 \times OD_{652.4})/OD_{680} \quad (3.13)$$

$$\text{Car.} = [(1000 \times OD_{470} - 1.63 \times \text{Chl.}_{a} - 104.96 \times \text{Chl.}_{b})]/OD_{680} \quad (3.14)$$

For photosynthetic performance analysis, the maximum photochemical efficiency of Photosystem II (*Fv/Fm*) was determined using pulse amplitude-modulated fluorometer (PAM; JUNIOR-PAM, Walz, Effeltrich, Germany). For this 1 mL cell was kept in dark for 15 min at room temperature (25±4). The ratio *Fv/Fm* was measured as described by Schreiber et al. (1986) where *Fv* denotes the difference between maximal fluorescence (*Fm*) from saturating light intensity and minimum fluorescence (*Fo*) of dark adopted cell.

3.2.6.5 Estimation of protein, carbohydrate and intracellular neutral lipid

The total carbohydrate was determined by phenol sulphuric acid method with glucose as the standard [279]. For protein estimation, first the cell pellet was hydrolysed in alkaline solution (0.2 N NaOH) at 100 ℃ for 15 min and then the pH was neutralized to 7.5 and the hydrolyzing pellet was thus used for protein estimation by Lowry method by using Bovine Serum Albumin (BSA) as the standard [280].

For intracellular neutral lipid estimation, Nile Red-based fluorescence intensity with excitation of 480 nm and emission in range 550 nm-650 nm was performed in a spectrophotometer (Fluoromax 3, Horiba, USA) with Triolein as standard as described in our previous study with some modification [281]. For Nile red analysis, initially the cell concentration of absorbance at OD_{680} 0.9 was harvested and resuspended in 1 mL of pure DMSO solution and the resuspended pellet was spun down for 5 min in a vortex. Nile red dye 10 µL (4 µg mL^{-1} in 100% acetone) added to the suspended pellet and incubated at 50 °C in a water bath for 1 min. The auto-fluorescence of algal cells and the intrinsic fluorescence of Nile red were subtracted from the fluorescence of Nile red neutral lipid complex obtained at 580 nm.

3.3 Results and discussion

3.3.1 Microalgal Strain Selection

Microscopic analysis of cell density of cultures showed that six of the microalgal strains were able to grow in FGS media with sodium bicarbonate as the sole carbon source (Table 3.2). For the subsequent steps, microalgal strains showing substantial growth were considered for acclimation. Out of thirteen strains, only six strains including *Scenedesmus abundan* NCIM2897, *Scenedesmus acutus* NCIM5584, *Desmodesmus abundans* KMC3, *Chlorella sorokiniana* KMC5, *Acutodesmus deserticola* KMC6, and *Micractinium pusillum* KMC8 were selected for further evaluation of their growth and photosynthetic performance. Both *Scenedesmus* strains NCIM2897 and NCIM5584 showed a reduction of 16.13 and 23.22 mg L^{-1} day^{-1} biomass productivity, about ~ 20-25 % reduction in biomass growth in comparison with control, the other two strains NCIM5583 and KMC8 showed a reduction of 40.64 and 56.39 mg L^{-1} day^{-1} with ~ 40%-55 % reduction in biomass growth. Both KMC 5 and 6 strains showed the lowest productivity in treatment media (Figure. 3.3a).

In the second phase of screening experiments (Figure. 3.4), all six strains demonstrated strong adaptation to a 15% CO_2 environment. The observed biomass productivity ranged from 71.8 to 88.4 mg L^{-1} day^{-1}, with all strains exhibiting a desirable photosynthetic quantum yield value of 0.5 to 0.7 strains [282] (Figure. 3.4a). During the control experiment at the end of the batch, KMC6 exhibited the highest biomass productivity of 88.47 mg L^{-1} day^{-1}. KMC3, KMC8, and NCIM5584 had similar productivity levels ranging from 83 to 85 mg L^{-1} day^{-1}. The remaining two strains, NCIM5583 and KMC5, had lower productivity levels of 74.5 mg L^{-1} day^{-1} and 71 mg L^{-1} day^{-1}, respectively. When exposed to flue gas compounds, specifically treatment medium, the KMC8 strain exhibited the highest biomass production, reaching a value of 52.5 mg L^{-1} day^{-1}. However, when treated with flue gas compounds, there was a drop of 38% in biomass productivity. The Scenedesmus strains, NCIM5584 and NCIM5583, exhibited comparable biomass production, with values of 48.4 and 46.5 mg L^{-1} day^{-1}, respectively. This represents a drop of 41.7% and 37.2% compared to their respective control. The strains KMC6, KMC3, and KMC5 exhibited impaired performance on FGS medium, leading to a decrease in biomass productivity of almost 50%, with values of 36.5, 32.2, and 27.8 mg L^{-1} day^{-1}, respectively. The strains NCIM5584 and KMC8 were able to maintain a desirable *Fv/Fm* value of 0.58 and 0.55 in the treatment media (Figure. 3.4b). However, there was a slight decrease in value compared to the control, indicating that both strains were actively photosynthesizing and able to tolerate elevated CO_2 levels and toxic flue gas compounds. In the remaining four strains (NCIM2738, KMC3, KMC5, and KMC6), a significant decrease in *Fv/Fm* values was

observed, with a reduction of 1.5 to 2 times compared to their respective controls. Additionally, strains with values below 0.5 indicated a disruption in photosynthesis when exposed to flue gas compounds.

Among the 13 strains, two strains, respectively KMC8 and NCIM5584, were chosen for further investigation because to their superior growth performance and photosynthetic efficiency under different culture conditions. Photosystem II in strains KMC8 and NCIM5584 exhibited a desired value, indicating that both strains are capable of using flue gas components as a nutritional source without encountering stress. Furthermore, their biomass production remained unaffected. The screening process of bicarbonate and CO_2 as carbon sources in flue gas media, as depicted in Figure 3.3d and 3.4d, demonstrates that the accumulation of carotenoids and minimal degradation of chlorophyll pigment, as shown in Figure 3.3c and 3.4c, compared to the other four strains, suggests that the cells are developing a protective mechanism against oxidative stress induced by harmful components present in flue gas [283]. The findings indicated that the two strains, KMC8 and NCIM5584, exhibited increased tolerance to flue gas toxic compounds after acclimatisation.

Table 3.2 Quantitative evaluation under a light microscope, using a Neubauer haemocytometer of microalgae growth in FGM + $NaHCO_3$. Cells mL^{-1} were calculated as the difference between final concentration (cells mL^{-1}) and initial concentration (cells mL^{-1})

Microalgae	**(Cell mL^{-1})**
Acutodesmus deserticolal (KMC6)	1.19E+08
Scendesmus acutus (NCIM5584)	1.76E+08
Scedesmus abundans (NCIM2897)	1.43E+08
Desmodesmus armatus (NCIM 5583)	-
Desmodesmus abundans (KMC 3)	1.25E+08
Chlorella sorokiniana (KMC 5)	1.21E+08
Chlorella thermophilaa (MF179624)	-
Chlorella pyrenoidosa (NCIM2738)	1.64 E+07
Chlorella FC-2	-
Monoraphidium convolutum (KMC2)	-
Monoraphidium sp. (KMC4)	-
Monoraphidium contortum (KMC7)	9.5E+07
Micractinium pusillum (KMC8)	1.28E+08

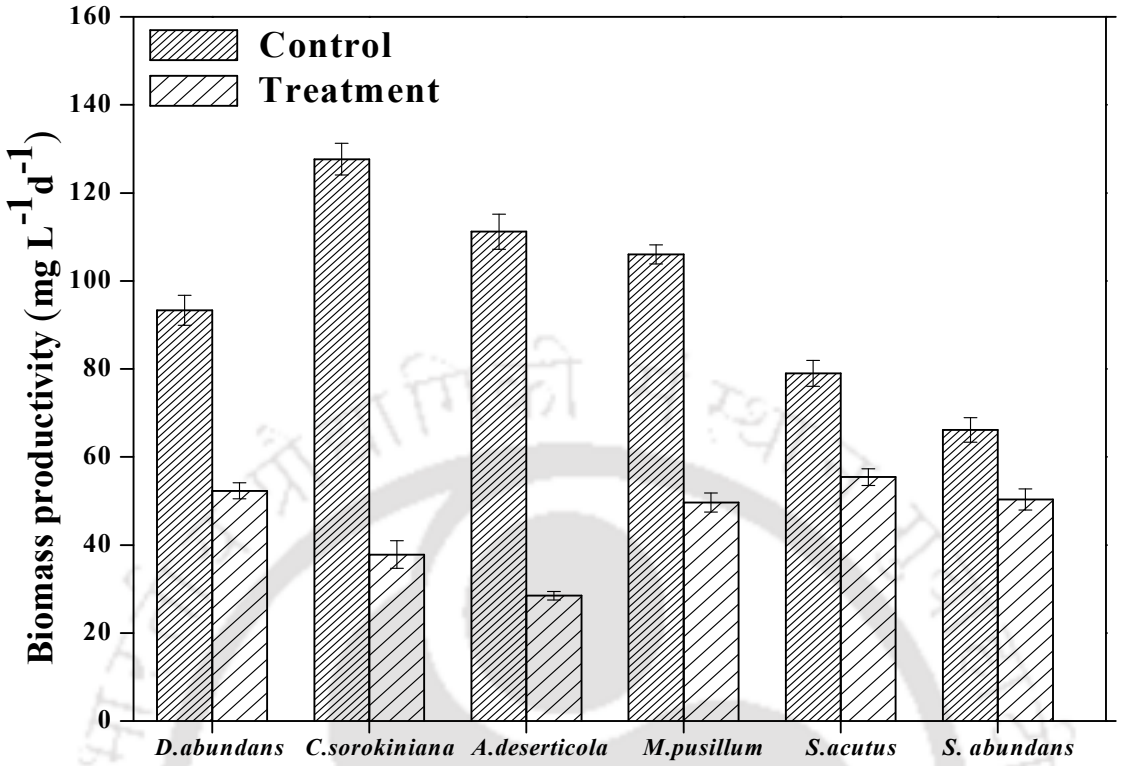
Control
Treatment
Biomass productivity (mg L-1d-1)
160
140
120
100
80
60
40
20
0
D.abundans
C.sorokiniana
A.deserticola
M.pusillum
S.acutus
S. abundans

(a)

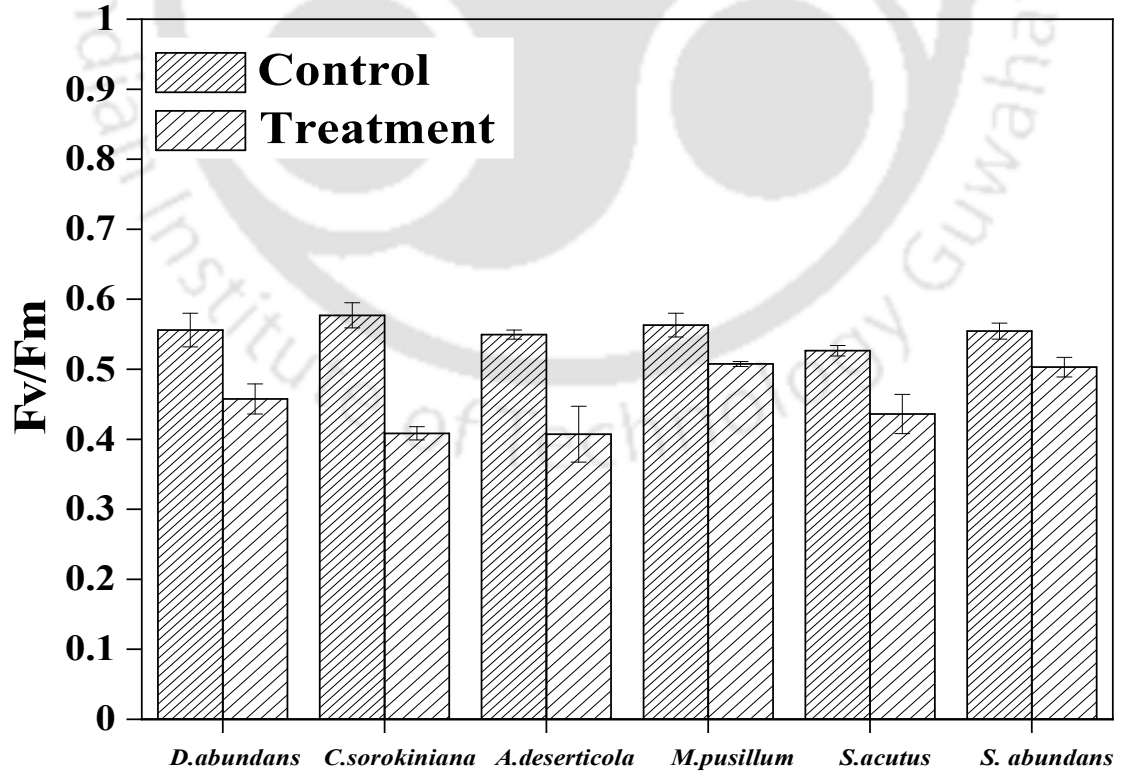
Control
Treatment
Fv/Fm
1
0.9
0.8
0.7
0.6
0.5
0.4
0.3
0.2
0.1
0
D.abundans
C.sorokiniana
A.deserticola
M.pusillum
S.acutus
S. abundans

(b)

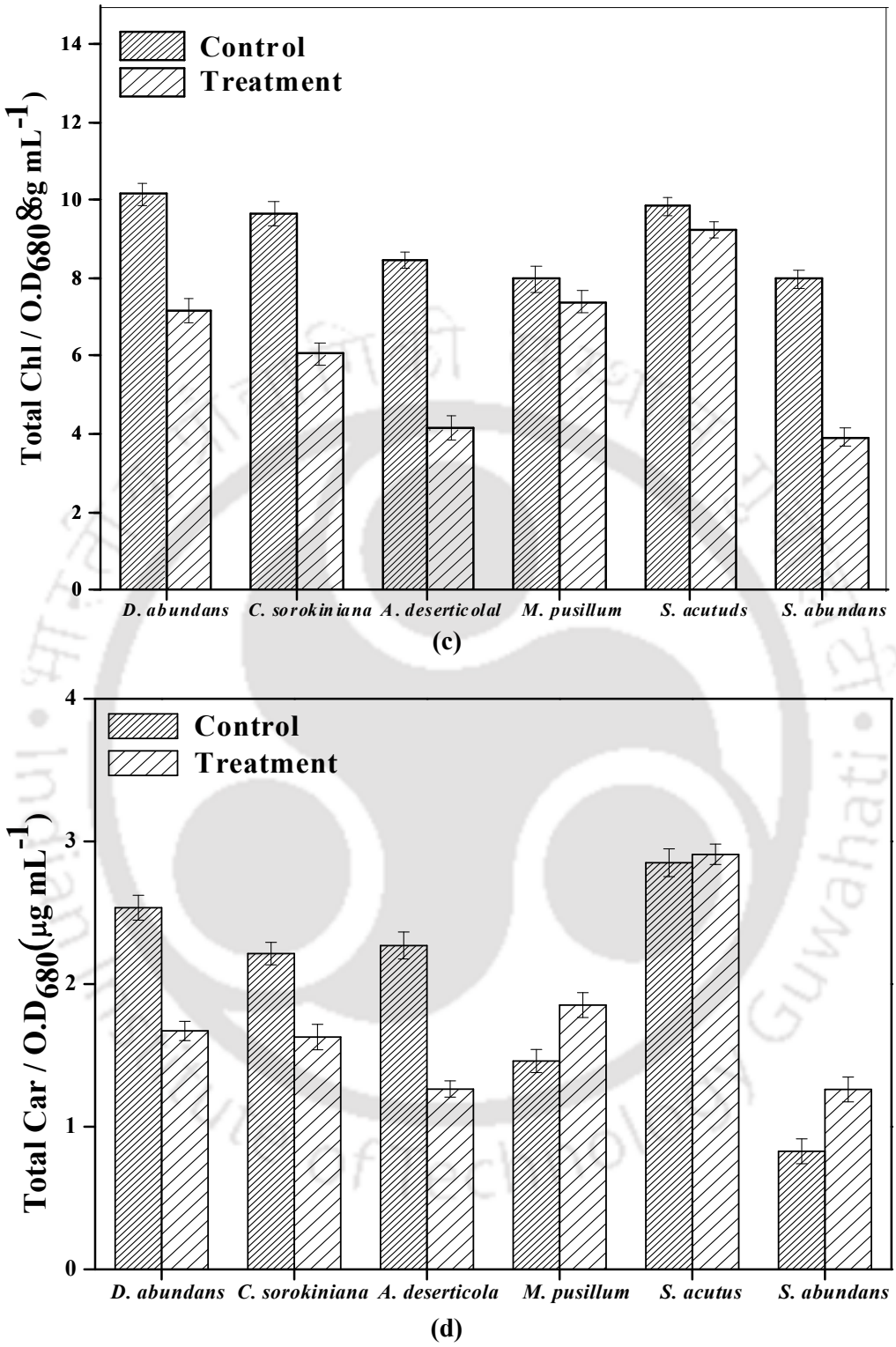

Fig. 3.3. Growth and photosynthetic performance of five microalgae comparison with control (BG-11 media) and Treatment (FGM + $NAHCO_3$) on the basis of **(a)** Biomass productivity **(b)** Photosynthetic efficiency (F_v/F_m) **(c)** Total Chlorophyll (a+b) and **(d)** Total Carotenoids

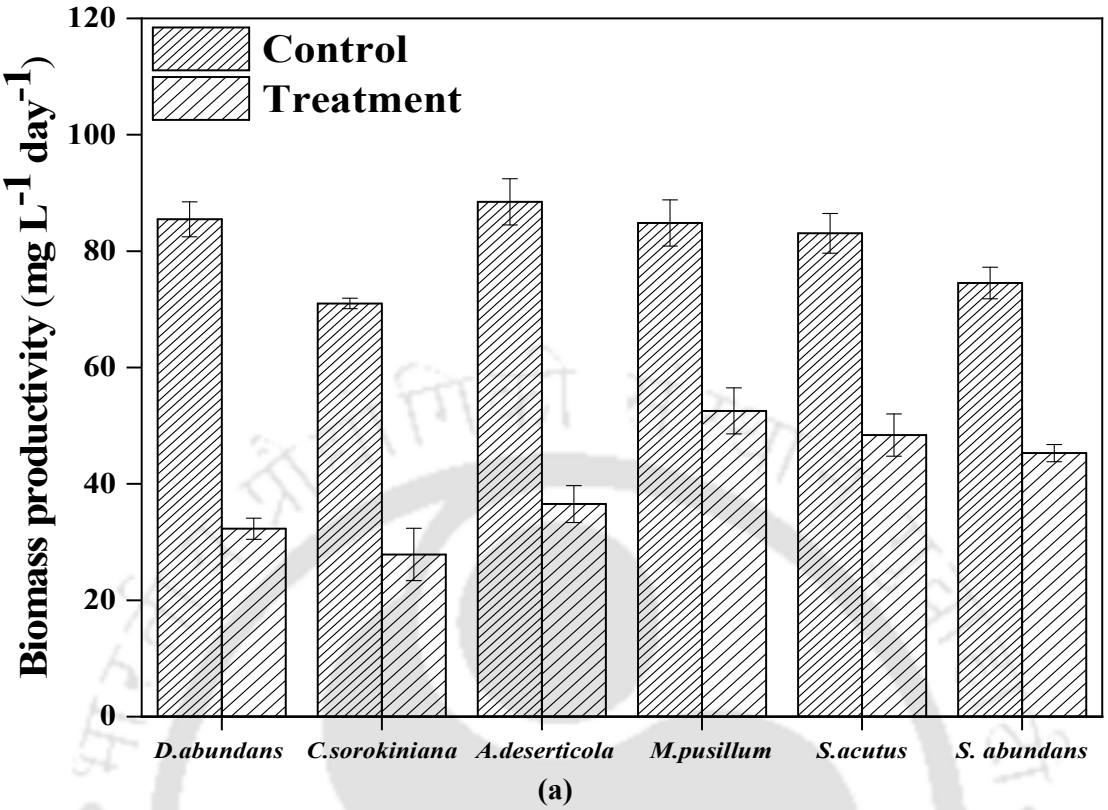
Control
Treatment
Biomass productivity (mg L-1 day-1)
120
100
80
60
40
20
0
D.abundans
C.sorokiniana
A.deserticola
M.pusillum
S.acutus
S. abundans

(a)

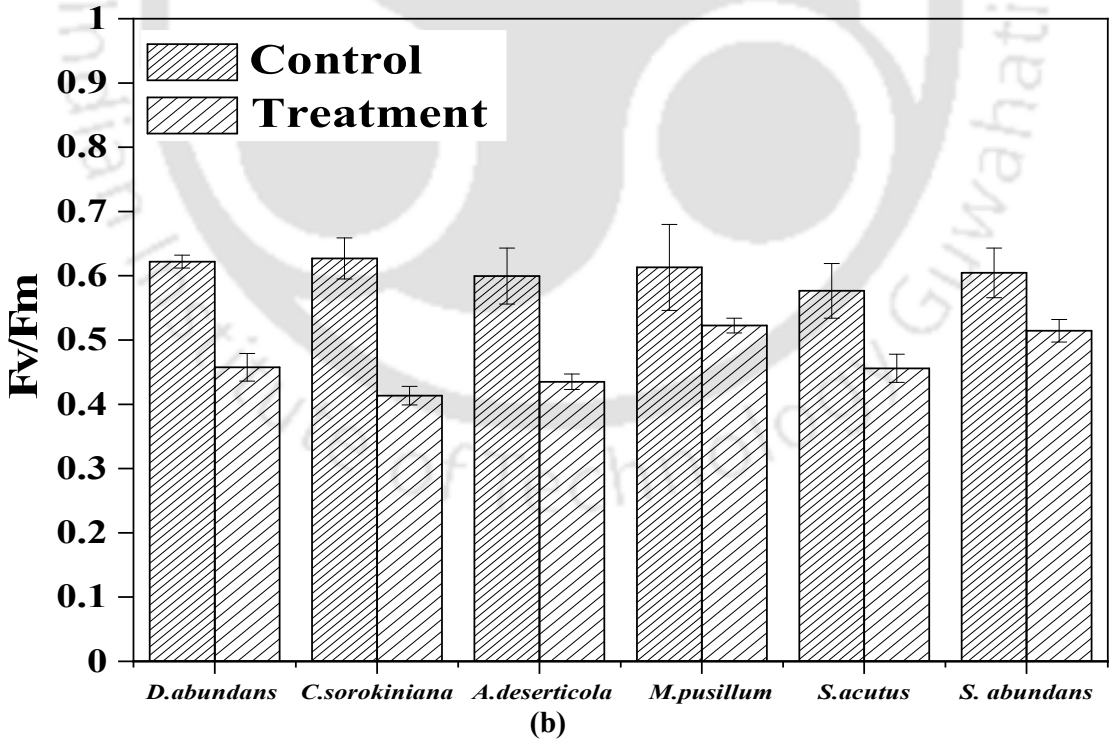
Control
Treatment
Fv/Fm
1
0.9
0.8
0.7
0.6
0.5
0.4
0.3
0.2
0.1
0
D.abundans
C.sorokiniana
A.deserticola
M.pusillum
S.acutus
S. abundans

(b)

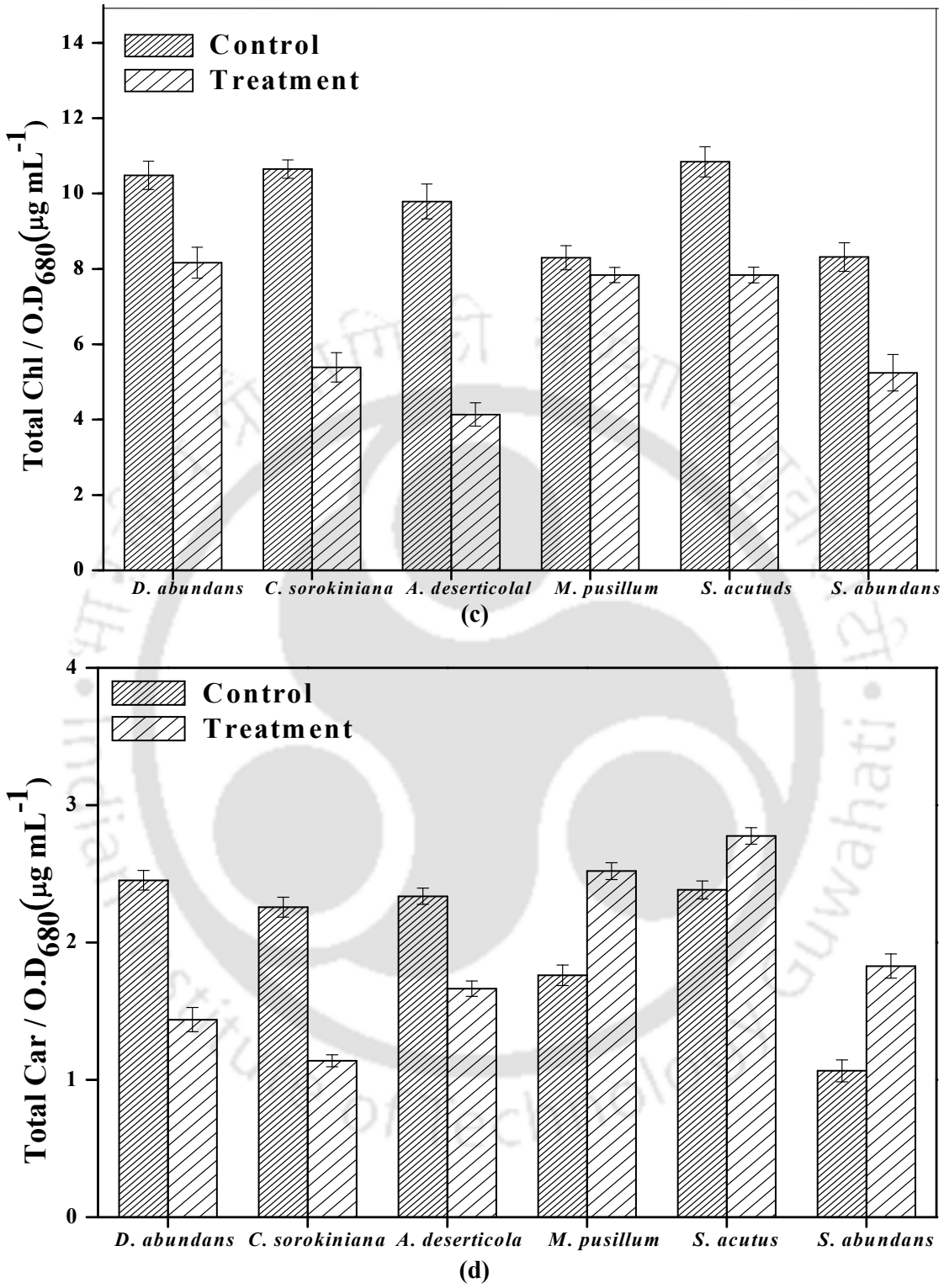

Fig. 3.4. Growth and photosynthetic performance of five microalgae comparison with control (BG-11 media) and Treatment (FGM + 15 % CO_2) on the basis of **(a)** Biomass productivity **(b)** Photosynthetic efficiency (F_v/F_m) **(c)** Total Chlorophyll (a+b) and **(d)** Total Carotenoids

3.3.2 Tolerance and acclimation of strains to flue gas compound

The strains NCIM5584 and KMC8 exhibited a low tolerance for particular flue gas chemicals. Specifically, dissolved SOx compounds, such as sulphite and bisulphite, significantly hindered the development dynamics of the cells, leading to a prolonged adaptive phase. The development of both strains was hardly affected by nitrite, suggesting their capacity to use nitrite as a nitrogen source. NCIM 5584 exhibited greater suppression of particular flue gas components compared to KMC8, as seen in Figure 3.5a and 3.5b.

No inhibition of biomass growth was seen in strains acclimated to sulphite and bisulphite at concentrations of 10 mg L^{-1} and 20 mg L^{-1}, respectively. Increasing the concentration of gradient phase adaptation from 30 mg L^{-1} to 100 mg L^{-1} resulted in an approximately 1.5 times increase in cell density for KMC8 (from 0.45 to 1.12 g L^{-1}) and an approximately 1.65 times increase for NCIM5584 (from 0.36 to 0.97 g L^{-1}). The specific growth rate in FGS media was 0.214 day^{-1} for KMC8 and 0.2 day^{-1} for NCIM5584 (Table 3.3). A marginal reduction (9% and 13% respectively) in biomass growth was reported with KMC8 and NCIM5584 in comparison to the prior control experiment (BG-11-C + 15% CO_2). The acclimation of both strains to sulphite and bisulphite showed a high correlation with their enhancement in maximal photosynthetic quantum yield (*Fv/Fm*). The *Fv/Fm* yield, which initially measured 0.56 in wild KMC8, was enhanced by a factor of 1.13 in acclimated KMC8, resulting in a yield of 0.63. Nevertheless, the *Fv/Fm* yield for NCIM5584 exhibited a modest rise from 0.51 to 0.53, as seen in Table 3.3. The *Fv/Fm* ratio serves as a diagnostic parameter for assessing photosynthetic performance and indicating environmental stress. The *Fv/Fm* ratio exhibited a substantial drop in response to environmental stressors, including nutrition availability, light intensity, pH levels, and temperature fluctuations [284].. The maximal quantum efficiency *Fv/Fm* varied between 0.5 and 0.8, suggesting that the algal cells were in a metabolically active condition with effective water splitting and carbon fixation at PSII, which enhanced the transit of photosynthetic electrons [282]. Both strains KMC8 and NCIM5584 exhibited a decrease in total chlorophyll and carotenoids ratio, with a fold fall of 1.7 and 1.9 respectively, attributed to an increase in carotenoids accumulation (Table 1). An elevation in carotenoids concentration serves as an indicator of cellular photosynthetic stress, however it may also occur as a result of the cell's tolerance mechanism to unfavourable circumstances. The research proposed that carotenoids were not a signal of photosynthetic stress, but rather were created as part of the cells' tolerance mechanism during acclimation to sulphur compounds [285].

The acclimated strains KMC8 and NCIM5584 exhibited enhanced growth performance (Figure. 3.5c). The significant increase in photosynthetic quantum yield in KMC8 indicates that the cells were very active, similar to the cells in the Control BG-11 medium. Furthermore, there was no negative impact seen on the photosynthetic performance of the cells due to the presence of harmful flue gas compounds.

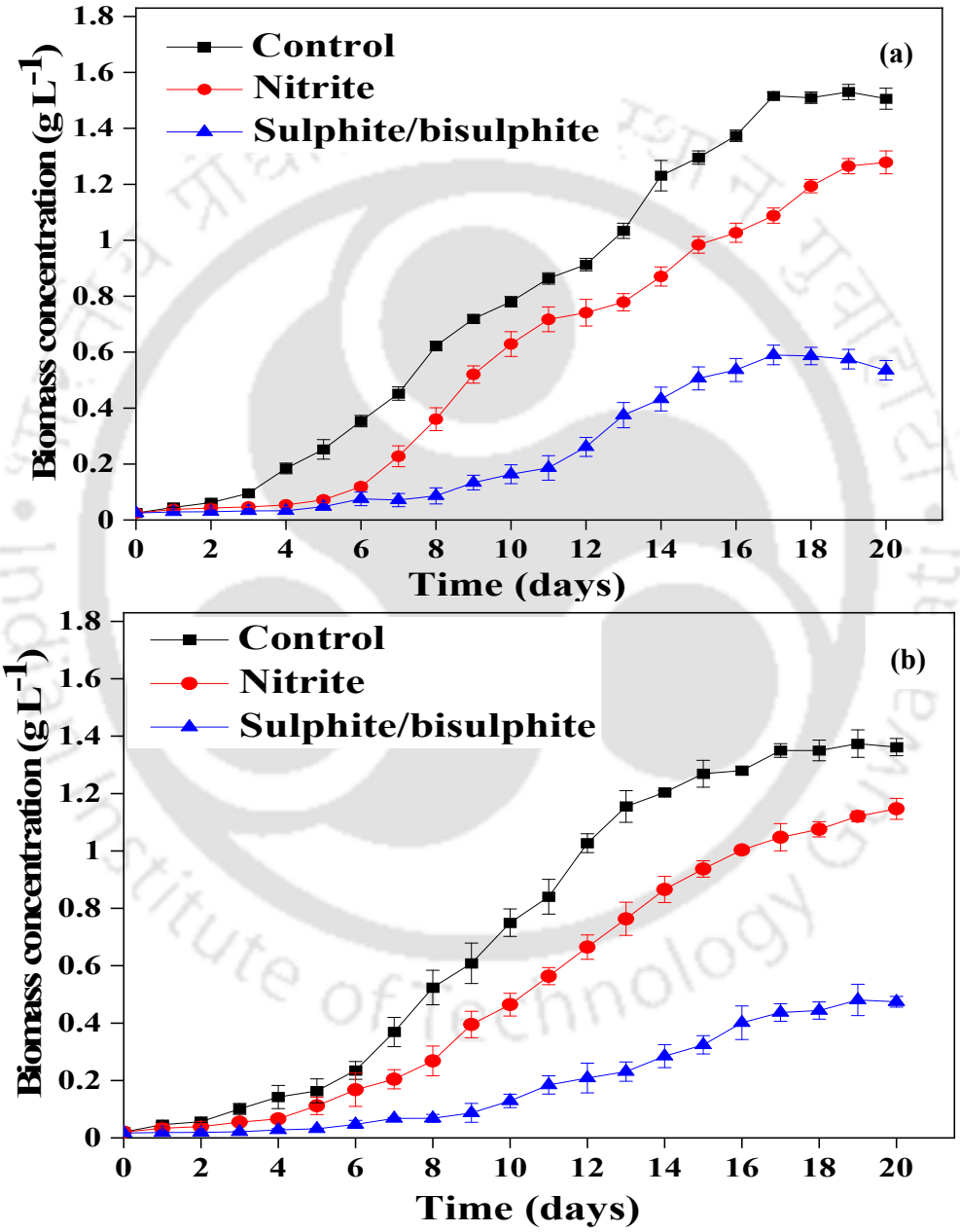

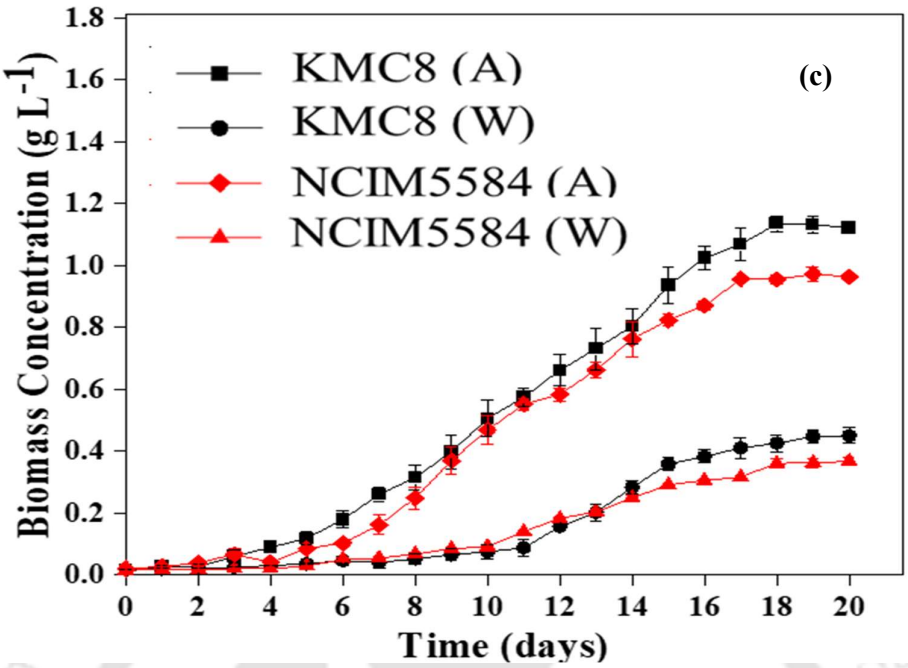

Fig. 3.5. Growth curve of **(a)** *Scendesmus acutus* NCIM5584 **(b)** *Micractinium pusillum* KMC8 in the presence of BG-11 media , Nitrite and Sulphite/bisulphite (1:1) with 15% CO_2 as carbon source **(c)** Growth curve of wild and acclimated strains of *Scedesmus acutus* NCIM5584 and *Micractinum pusillum* KMC8 in Flue gas salt media with 15% CO_2 as carbon source

3.3.3 Removal of flue gas compounds and CO_2 utilization efficiency by acclimated strains

The employing of gradient phase adaptation greatly improved the efficiency of removing sulphate (produced by sulphite and bisulphite) in the acclimated state, compared to the control condition. Additionally, the cells demonstrated higher nitrite consumption. Following the process of acclimation, KMC8 shown the capability to eliminate 96.65% of nitrite and 94.1% of sulphate. Compared to the wild strain, the removal efficiency of nitrite and sulphate improved by 1.15 and 1.12 times, respectively. However, the acclimated NCIM5584 strain was able to remove 88.84% of nitrite and 90% of sulphate with almost 1.5 times faster efficiency (Table 3.3).

As the cells adapted to nitrite and sulphate, both strains, KMC8 and NCIM 5584, saw a notable increase in their rate of CO_2 fixation and their efficiency in using CO_2. The CO_2 fixation rate and CO_2 utilisation efficiency were increased by more than 2.5 times (2.5~2.9). The CO_2 utilisation efficiency increased from 0.37% to 0.86% in KMC8 and from 0.25% to

0.73% in NCIM5584. However, in terms of the level of adaptation, NCIM5584 demonstrated superior performance overall, whereas the rate of removal of nitrite and bisulphite, as well as the rate of CO_2 fixation and utilisation, were generally greater in the KMC8 strain (Table 3.3).

3.3.4 Comparison of biochemical composition in acclimated strains

The intracellular composition of microalgae and its alterations during stress or acclimatisation vary depending on the species[286]. Table 3.3 displays the alterations in biochemical changes seen in the wild and acclimated cells of KMC8 and NCIM584 when exposed to flue gas salt medium. A decrease in the concentration of protein and carbohydrate was found in both acclimated strains. The protein level in KMC8 declined from 24.5% to 22.8% of dry cell weight (DCW), whereas in NCIM5584 it decreased from 21.12% to 17.67%. In KMC8, the carbohydrate content decreased from 37.23% to 35.67% of the dry cell weight (DCW). In NCIM5584, the carbohydrate content decreased from 41.12% to 39.89% of the DCW. The adapted strain KMC8 had a higher capacity for accumulating neutral lipid, with 36.7% of the dry cell weight (DCW) compared to 29.4% in NCIM5584. Both strains demonstrated an increase in neutral lipid content, with KMC8 showing almost 16% and NCIM5584 showing less than 11% compared to the wild strains. The potential cause for the rise in lipid accumulation and decrease in intracellular protein and carbohydrate levels may be attributed to the cell's response to stress, wherein it begins to accumulate energy-rich molecules, specifically triacylglycerol (TAGs), by upregulating the metabolic pathway towards TAGs and utilising carbohydrate and protein intermediates as metabolites [283,287].

Carotenoids and lipid molecules provide protection to cells against various biotic and abiotic stresses. They play a crucial part in the cell's defence system and facilitate adaptation to harsh conditions [285,288]. Based on this, it can be inferred that both the KMC8 and NCIM5584 strains underwent acclimatisation driven by the collaboration of lipids and carotenoids in response to hazardous flue gas compounds. Carotenoids in microalgae serve dual purposes as pigments and antioxidants. They enhance the uptake of light and provide protection against reactive oxygen species (ROS) that are generated during oxidative stress induced by excessive light or nutrient imbalances. Lipids, specifically triacylglycerols (TAGs), play a vital role in both the structure of membranes and the storage of energy. During periods of stress, microalgae store triglycerides (TAGs) in order to preserve the structure and stability of their cells, demonstrating their ability to adapt and withstand challenging conditions.

Table 3.3 Maximum biomass concentration (Xmax), maximum biomass productivity (Pmax), specific growth rate (μ), photosystem II quantum yield *(Fv/Fm)*, ratio of total chlorophyll (a+b) and carotenoids (Chl./Carot.); biochemical composition changes; elemental carbon, hydrogen, nitrogen, sulphur and oxygen; Nitrite and sulphate removal efficiency, CO_2 fixation rate and utilization efficiency after 20 days of inoculation in comparison to wild cell and acclimated cell (A.C) in flask experiment.

Parameter	Variable measured	*M.pusillum*		*S.acutus*	
		Wild	Acclimated	Wild	Acclimated
Growth & Photosynthesis	X_{max} (g L^{-1})	0.45 ± 0.03[a]	1.12 ± 0.024[b]	0.36 ± 0.017[a]	0.97 ± 0.024[c]
	P_{max} (mg L^{-1} day^{-1})	23.72 ± 1.85[a]	59.1 ± 1.30[b]	19.23 ± 1.30[c]	51.13 ± 0.90[d]
	μ (day^{-1})	0.20 ± 0.004[a]	0.25 ± 0.001[b]	0.18 ± 0.002[a]	0.23 ± 0.001[b]
	Fv/Fm	0.56 ± 0.042[a]	0.63 ± 0.078[b]	0.51 ± 0.035[c]	0.53 ± 0.02[ac]
	Chl./Carot.	4.28 ± 0.986[a]	2.45 ± 0.472[b]	4.34 ± 0.326[a]	2.27 ± 0.275[b]
Biochemical composition	Lipid (%w/w)	31.6 ± 0.37[a]	36.7 ± 0.56[b]	26.4 ± 0.45[c]	29.43 ± 0.41[d]
	Protein (%w/w)	24.45 ± 1.76[a]	22.8 ± 0.34[a]	21.17 ± 1.56[a]	17.6 ± 1.32[b]
	Carb. (%w/w)	37.23 ± 0.7[ac]	35.67 ± 1.42[a]	41.12 ± 1.26[b]	39.89 ± 0.8[bc]
	Ash (%w/w)	1.56 ± 1.7[a]	3.32 ±1.24[b]	2.56 ±1.53[c]	3.45 ±1.62[b]
Elemental composition	C (%w/w)	47.86	50.43	46.51	49.21
	H (%w/w)	7.01	7.24	5.74	6.64
	N (%w/w)	5.87	7.1	5.41	6.23
	S (%w/w)	0.23	0.47	0.13	0.52
	O(%w/w)	39.03	34.76	42.21	37.4
Nutrient removal & CO_2 fixation & utilization	NO_2^- R.E (%)	82.38 ± 2.54[a]	94.10 ± 1.87[b]	76.03 ± 2.98[c]	88.84 ± 2.21[d]
	SO_4^{2-} RE (%)	79.19 ± 1.98[a]	96.65 ± 2.07[b]	77.54 ± 2.31[a]	89.94 ± 2.16[c]
	CO_2 fixation rate (mg L^{-1} day^{-1})	47.98	110.38	32.77	92.64
	CO_2 utilization efficiency (%)	0.37	0.86	0.25	0.73

Note: All the experiments were conducted in triplicate and the data were expressed as mean ± standard dev. Values with the same letter in the same row showed insignificant differences analysed using one-way analysis of variance based on Tukey's method.

3.3.5 Growth, CO_2 utilization and lipid productivity in photobioreactor experiment and scale up

The cells of both strains were cultured in two separate 2 L bubble column photobioreactors (PBR) to assess their performance. We monitored the changes in biomass growth, pH, and nutrient consumption throughout time (Figure. 3.6a & b). Both strains exhibited little variation in growth when cultivated in a photobioreactor (PBR) and were capable of maintaining consistent performance comparable to that seen in the flask experiment. The performance of the system is summarised in detail in terms of biomass production, nutrient removal, CO_2 utilisation, and neutral lipid production (refer to table 3.4). Both strains exhibited a significant decrease in pH, ranging from 4.5 to 4.8, in the culture medium on the first day. This reduction in pH was caused by the build-up of sulphate ions resulting from the oxidation of sulphite and bisulphite ions. The conversion rate of SO_3^{2-} and HSO_3^{2-} ranges from 97% to 98%, resulting in the production of 1.16 to 1.19 mmol L^{-1} of SO_4^{2-} on the second day. This concentration gradually reduced as the algae population increased [289,290]. The pH increased as the acclimated strains showed higher rates of NO^{2-} and SO_4^{2-} utilisation compared to the wild strain, resulting in increased growth. Based on this outcome, it may be inferred that the toxicity of SOx was caused by a rapid decrease in pH resulting from the oxidation of intermediate molecules, such as SO_3^{2-} and HSO_3^{2-}, producing SO_4^{2-}. To address this toxicity, it is possible to use microalgae that have a high capacity to utilise sulphate and choose species that can tolerate a wide range of pH levels, particularly acidic pH. This toxicity is caused by the oxidation of compounds in flue gas. Both strains exhibited varying changes in neutral lipid content throughout their scale-up in PBR. Additionally, a simultaneous drop in neutral lipid content was also detected. The slight decrease in nutrient removal efficiency and the improvement in both CO_2 utilisation efficiency and CO_2 fixation rate may be attributed to the longer duration that the CO_2 mixture remains in contact with the medium in the PBR, compared to the flask tests.

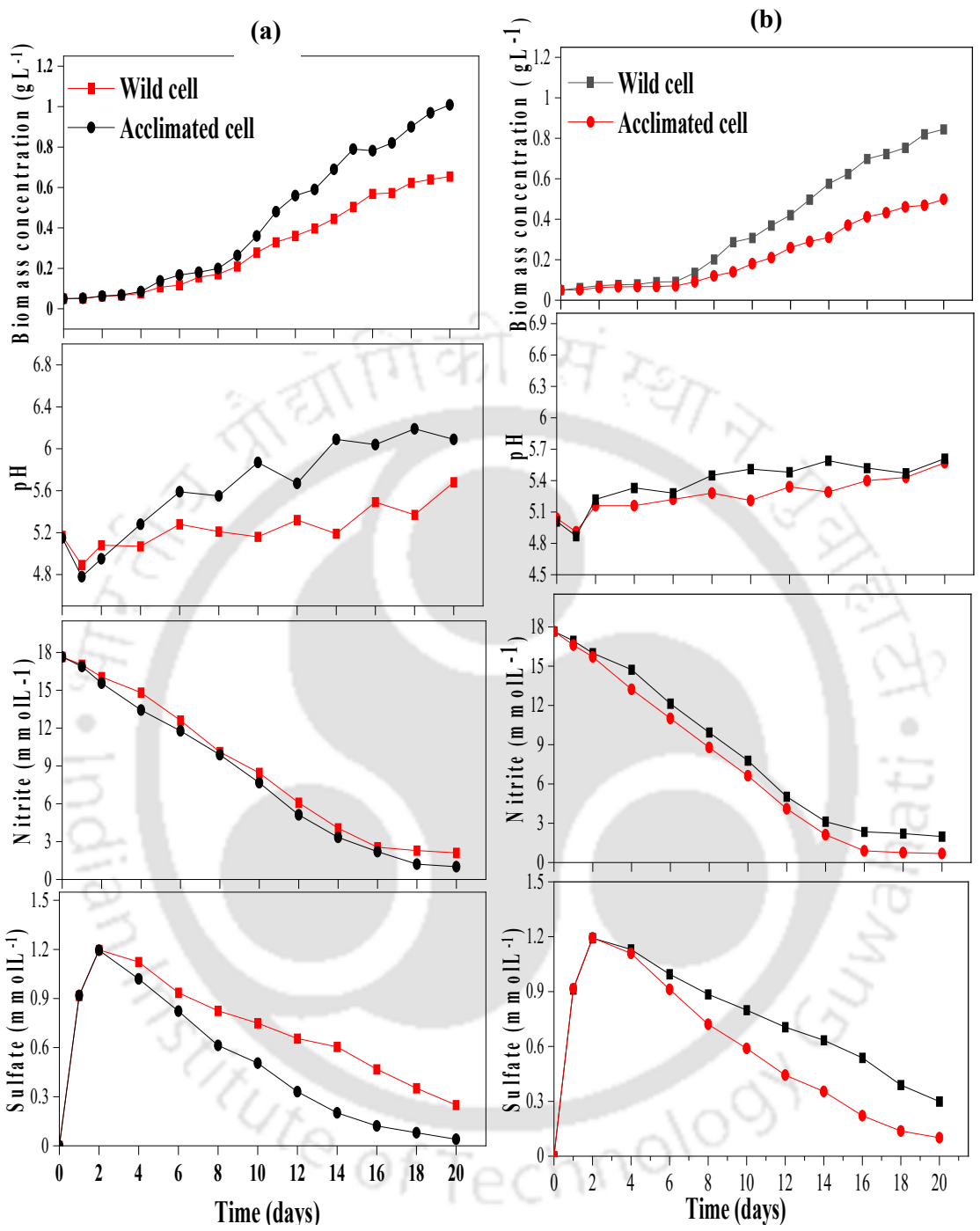

Fig. 3.6. (a) Growth profile of **(a)** *Micractinum pusillum* KMC8 and **(b)** *Scedesmus acutus* NCIM5584 in 2 L bubble column PBR with change in pH, nitrite and sulphate removal in FGM with 15 % CO_2 as carbon source

.

3.3.6 Evaluation of stability in growth performance, lipid productivity and CO_2 utilization under semi-continuous mode

Based on its greater tolerance and adaptability to dissolved flue gas components (NOx and SOx), ability to use CO_2, and capacity for neutral lipid accumulation, KMC8 was shown to be more efficient than NCIM5584. The strain KMC8 was evaluated under semi-continuous conditions and exhibited constant increase of biomass, as seen in Figure 3.7a. The biomass concentration ranged from 2.19 to 3.75 g L^{-1}, with an average of 2.68 g L^{-1}. The biomass productivity varied between 0.19 and 0.24 g L^{-1} day^{-1}, with an average of 0.22 g L^{-1} day^{-1}. In addition, the precise growth rate varied between 0.11 and 0.17 day^{-1}. During the preceding 20-day period, the cells had a biomass concentration of 3.25 and a specific growth rate of 0.106 day^{-1}. Figure 3.7b illustrates that the rate of CO_2 fixation and the efficiency of CO_2 utilization remained constant over the first four cycles of semi-continuous mode culture. The rate varied between 313 and 363 mg L^{-1} day^{-1}, whereas the efficiency varied between 7.66% and 8.57%. The average rate was 346.43 g L^{-1} day^{-1} and the efficiency was 8.17 percent. During the fifth cycle, the rates of CO_2 fixation and CO_2 utilization efficiency reached their minimum levels. This may be attributed to the prolonged period of the culture, which lasted for 20 days. As a consequence, the values obtained were 277.28 mg L^{-1} day^{-1} and 6.54% respectively. The performance linked to nutrient utilization and elemental content is shown in Table 3.4, demonstrating an improvement in the parameter. The neutral lipid content varied between 18% and 20%, with a productivity ranging from 40.95 to 50.6 mg L^{-1} day^{-1}. A decrease in lipid content was seen when comparing the findings of previous studies done in both flask and photobioreactor (PBR) in batch mode. The decrease in lipid content was most likely a result of the ongoing administration of nitrite, which prompted a shift in cell metabolism towards the synthesis of proteins instead of the formation of neutral lipids. This shift in metabolism is commonly seen under situations of nitrogen deficiency and famine [277].

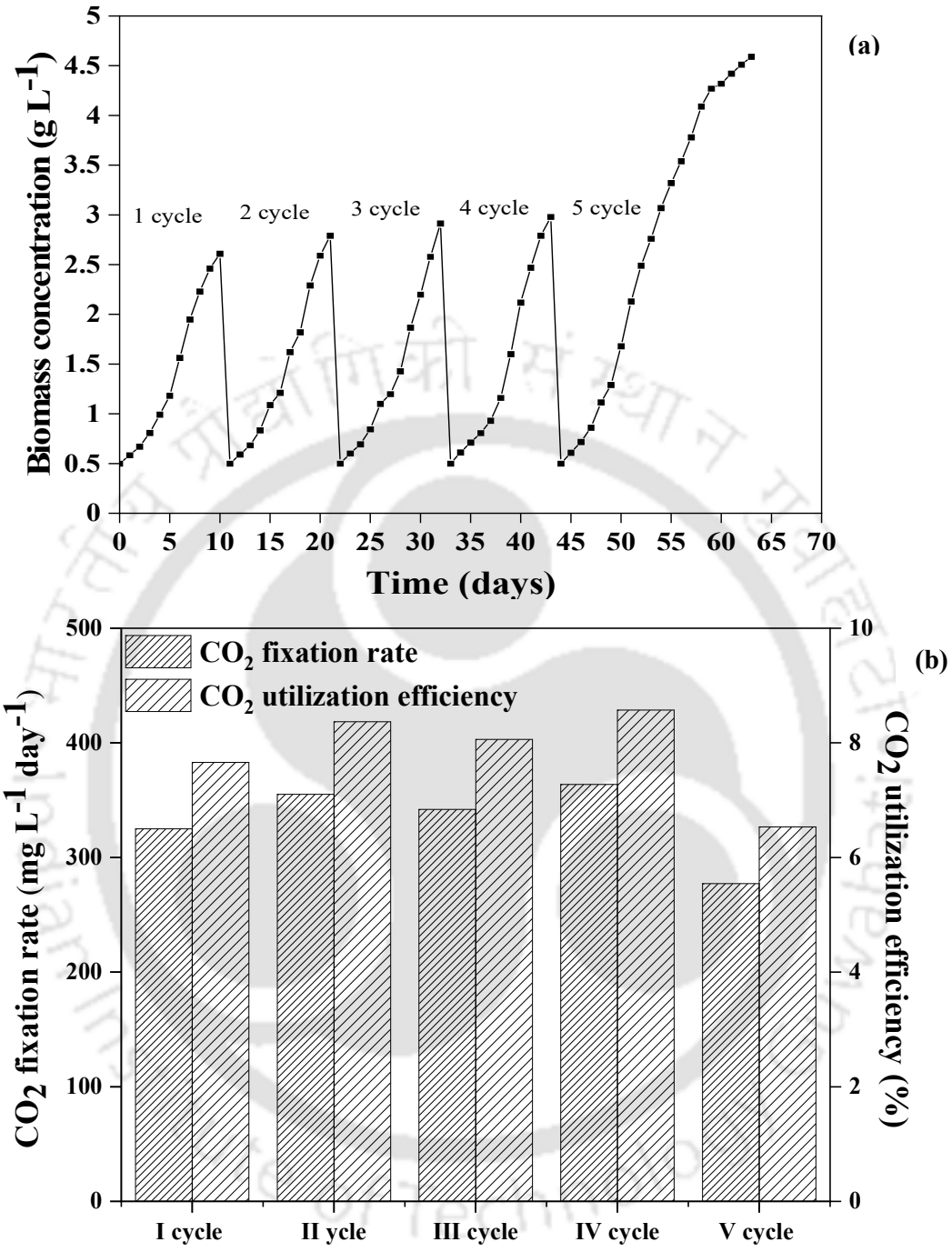

Fig. 3.1. (a) Growth profile of *Micractinum pusillum* KMC8 in 2 L bubble column PBR in semi-continuous mode of 4 cycle with 11 days each and last 5 cycle in batch mode of 20 days **(b)** CO_2 fixation rate and CO_2 utilization efficiency at the end of each cycle.

Table 3.4. Summary of growth parameter (X_{max}, μ, P_{max}), photosynthetic efficiency (F_v/Fm) , nutrient removal (nitrite, sulphate), CO_2 fixation efficiency and utilization rate, lipid production, and elemental analysis in 20 days of inoculation in comparison to wild (W.C) and acclimated cell (A.C) in Photobioreactor

Parameter	*M. pusillum*		*S. acutus*	
	Wild	Acclimated	Wild	Acclimated
Xmax (g L^{-1})	0.58	1.32	0.49	1.15
μ (day^{-1})	0.21	0.25	0.20	0.24
Pmax (mg L^{-1} day^{-1})	30.52	69.47	25.74	58.94
F_v/Fm	0.57	0.68	0.52	0.58
NO_2^- R.E (%)	84.21	96.45	79.32	72.12
SO_4^{2-} R.E (%)	78.34	90.76	75.43	87.34
C_F (mg L^{-1} day^{-1})	55.34	136.79	44.51	110.8
C_U (%)	1.35	3.07	1.14	2.67
Neutral Lipid (% wt/wt DCW)	27.32	32.14	22.52	24.78
Neutral Lipid productivity (mg L^{-1} day^{-1})	8.34	22.33	5.81	14.61
C (% wt/wt)	49.46	53.56	47.17	51.34
H (% wt/wt)	6.45	7.87	6.89	7.89
N (% wt/wt)	4.43	3.65	5.65	3.23
S (% wt/wt)	0.21	0.53	-	0.58
O (% wt/wt)	39.24	35.4	40.3	36.96

3.4 Conclusion

Out of the 13 microalgal strains that were examined, two strains, *Micractinium pusillum* KMC8 and *Scenedesmus acutus* NCIM5584, were identified as being appropriate for using CO_2 bio-mitigation to reduce emissions from flue gas. The gradual adaptation of cells from these two strains to dissolved sulphur compounds greatly enhanced cell proliferation, nutrient clearance, and CO_2 utilization efficiency. Out of these two strains, KMC8 exhibited superiority over NCIM5584 in terms of CO_2 utilization, efficiency in removing flue gas compounds, and buildup of neutral lipids. The successful adjustment and enhanced productivity of KMC8, while maintaining stability in CO_2 utilization and biomass quality, demonstrate the viability of using microalgae for large-scale commercial purposes.

In order to demonstrate the strength of microalgal strains in large-scale commercial applications, it is essential to assess their ability to adapt to different light and temperature

conditions and how this impacts photosynthesis and their capacity to fix CO_2 and generate biomass. Understanding the precise effects of these environmental parameters on the performance of microalgae in the local climatic conditions is crucial. Therefore, it is necessary to conduct more bench-scale tests to confirm the reliability of microalgae strains that can consistently achieve high productivity, efficiently capture CO_2, and remain stable under particular local weather circumstances. By identifying the optimal light and temperature conditions for adapted strains, we may enhance their adaptability for certain local geographical locations. This will guarantee the robustness and feasibility of microalgal strains for microalgal-based biotechnological applications, making them efficient for both CO_2 accumulation and bioenergy generation.

CHAPTER 4

Acclimation capacity of microalgal strains in different light and temperature condition and its impact on CO_2 fixation and biochemical production

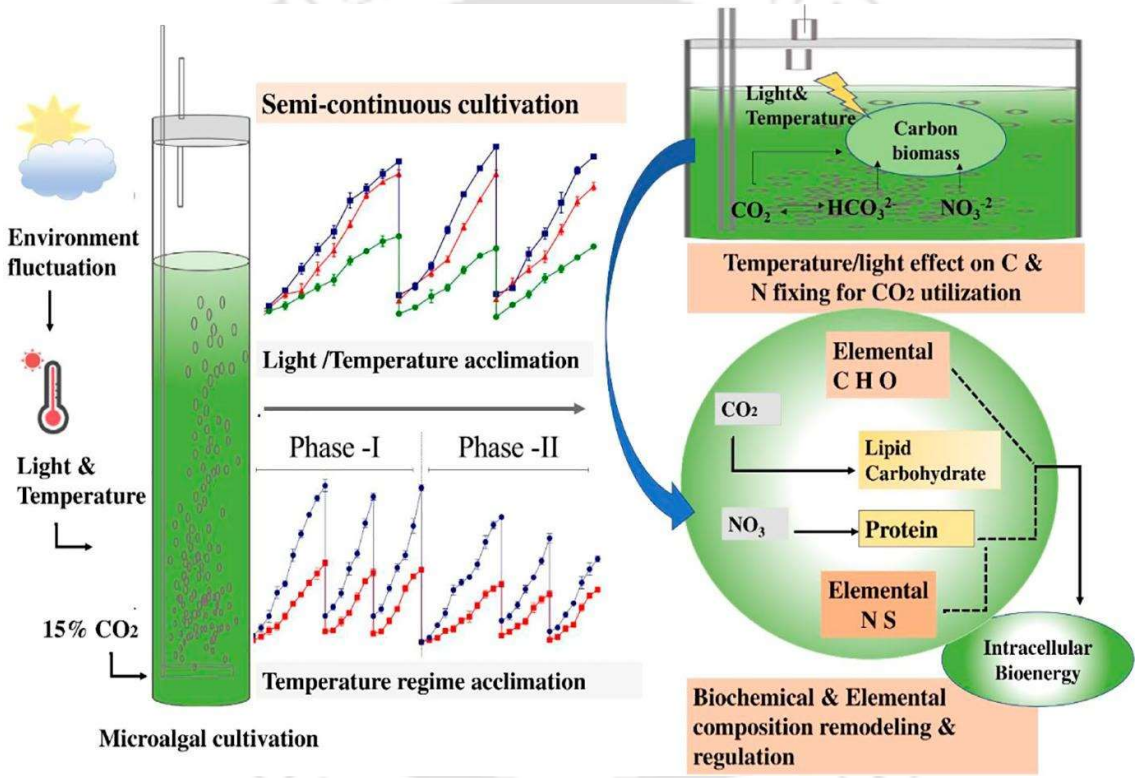

Chapter 4

Acclimation capacity of microalgal strains in different light and temperature condition and its impact on CO_2 fixation and biochemical production

4.1 Background and motivation

Chapter 3 of this thesis investigates the adaptive mechanisms of *Micractinium pusillum* KMC8 in response to changes in light and temperature during semi-continuous culture. The objective is to reveal its capacity for photosynthesis, CO_2 fixation, and adaptation in different environmental situations. For commercial scale-up in outdoor local climatic conditions, it is crucial to evaluate growth parameters, ensure stability in CO_2 fixation rates, and monitor metabolite changes to maintain stability in biomass quality and quantity for bioenergy production. The semi-continuous culture method offers a complete framework for comprehending and enhancing the development and stability of microalgae under different environmental situations. Acquiring this information is essential for expanding the use of microalgae to capture CO_2 and produce bioenergy in outdoor environments, while guaranteeing a constant level of biomass in terms of both quality and quantity.

The study examined the impact of temperature and light conditions on the appropriateness of *M. pusillum* for CO_2 bio-mitigation and bioenergy production. It simulated severe summer and winter temperatures over a 24-hour period, considering fluctuations between day and night. The experiment involved growing cells in a semi-continuous way at three fixed temperatures (15 °C, 25 °C, and 35 °C) and light intensities (50, 350, and 650 µmol m^{-2} s^{-1}). Additionally, two different variations in temperature were used: one with temperatures alternating between 35 °C and 25 °C, and another with temperatures alternating between 21 °C and 12 °C. Both temperature patterns followed a 16-hour light and 8-hour dark cycle. The experiment was conducted under two light intensity conditions: moderate light intensity of 150 µmol m^{-2} s^{-1} and high light intensity of 750 µmol m^{-2} s^{-1}.

The study conducted a detailed analysis of growth productivity, changes in metabolites, compositions of fatty acids, carbon fixation, and bioenergy content. *M. pusillum* had a peak specific growth rate of 0.26 day^{-1} at 25 °C, with no notable disparity at 35 °C at light intensities of 350 and 650 µmol m^{-2} s^{-1}. However, it exhibited a lower average growth rate of 0.17 day^{-1} at both 15 °C and 50 µmol m^{-2} s^{-1}. The growth rate was enhanced in both temperature regimes (35/25 °C and 21/12 °C) because to the high light intensity. The CO_2 utilization efficiency ranges from 0.32% to 2.03%, while the lipid content ranges between 23% and 34%. These lipids are rich in C-18 and C-16 fatty acids, making them excellent for biodiesel production.

Despite the presence of high temperature and light intensity, there was no decrease in the photosystem II quantum yield *Fv/Fm*), indicating that the cells were able to effectively adapt to the increased photon and thermal conditions. This adaptation was achieved through changes in pigments, intracellular macromolecules, and fatty acid profiles, which helped protect the cells from damage caused by excessive light and heat.

There is a clear correlation between temperature increases and the processes of carbon and nitrogen fixation, as well as CO_2 fixation. Furthermore, there was a direct correlation between temperature rises and a significant carbon build-up of over 50% in biomass. Nevertheless, no substantial link was seen between light intensity and these characteristics. Increased light intensity had a positive impact on experiments conducted in both low and high-temperature environments. This led to improved utilization of nutrients and CO_2, as well as increased accumulation of biomass carbon in storage molecules such as lipids and carbohydrates. Therefore, there was a significant increase in bioenergy accumulation in the biomass.

This research explores the ability of *M. pusillum* to adjust to changes in its environment, with a focus on its potential for effectively capturing CO_2, generating bioenergy, and maintaining constant biomass quality for biodiesel production under different cultivation settings. This study demonstrates the capability to sustain carbon fixation and acclimation ability in long-term cultivation systems, while simultaneously enhancing the quality of biomass throughout the acclimatization process, without any negative impact on carbon capture and biomass yield.

4.2 Materials and methods

4.2.1 Microalgal strain and culture conditions

The strain of the microalgae *M. pussillum* (KMC8) maintained on complete BG-11 medium as described in section 3.2.1. The initial inoculum was prepared for the experiment in a 1 L Erlenmeyer flask with a 500 mL culture volume in a photo incubator shaker at 25 °C, under 100 µmol m^{-2} s^{-1} light intensity with a 24:0 (light/dark) cycle at 150 rpm. The inoculum culture was cultivated for one week to achieve a biomass concentration of 0.78 g DCW L^{-1}, which was quantified by measuring the optical density at 680 nm using a UV-2450 spectrophotometer (1 OD_{680} equals 0.22 g DCW L^{-1}). The cells were collected by centrifugation, resuspended in 50 mL of freshly prepared autoclave carbon free BG-11 media, and used as an inoculum for further experiments.

4.2.2 Experimental setup and procedure

To evaluate the influence of light intensity and temperature in a semi-continuous mode, experiments were conducted in a 2 L custom-made bubble column photobioreactor (PBR), as detailed in our previous study as described in section 3.2.2. For each experiment, 23 mL of each seed culture (7.8 g L^{-1}) was centrifuged, the cell pellet was re-suspended in both the reactor and the culture volume was adjusted to 1.8 L with an initial cell density of 0.1 g L^{-1} (0.5 at 680 nm) for each treatment.

4.2.3 Semi-continuous cultivation with multi temperature and light intensity conditions

The research entailed the semi-continuous cultivation of cells over the course of twenty-four days. Initial cell density was 0.1 g L^{-1}, and the cultivation consisted of three cycles. The experiment consisted of three cycles: a 10-day cycle in the late exponential phase, followed by two 7-day cycles in the mid-exponential phase. Approximately 50-60% of the initial culture volume was replaced with fresh medium based on the cell density. If the cell density did not reach 0.3 g L^{-1}, a smaller amount of media was taken out. The goal was to sustain a blend concentration of at least 0.1 g L^{-1} at the outset of each cycle in order to assure a constant initial cell concentration across all experiments. Under varying light and temperature conditions, semi-continuous cultivation was carried out. The experimental conditions included three constant temperatures (15 °C, 25 °C, and 35 °C), a 24-hour light/dark cycle ratio, and 150 µmol

m^{-2} s^{-1} of light intensity. Three light intensities (50, 350, and 650 µmol m^{-2} s^{-1}) were administered at a light/dark cycle of 24:0 and a temperature of 25 °C. With a diurnal cycle of 16:8 light/dark and a constant temperature of 38 °C during the light phase and 25 °C during the dark phase, one condition simulated extreme summer temperatures. Experiments were conducted in two phases: the first phase utilized a light intensity of 150 µmol m^{-2} s^{-1} for 24 days, while the second phase utilized a light intensity of 750 µmol m^{-2} s^{-1} for another 24-day cycle. Similar to the prior procedure, the experimental protocol for extreme winter conditions involved a light/dark cycle temperature of 21/12 °C.

4.2.4 Analytical of growth, photosynthesis performance and cellular component

The optical density at 680 nm (OD_{680}) was measured using a UV–visible spectrophotometer (Cary 50, Varian, Australia) and converted into dry cell weight using a linear equation as described in section 3.2.6.1. Biomass concentration was measured daily after 24 h from both reactors using a UV–visible spectrophotometer. At the completion of each cycle of semi-continuous batch, the specific growth rate (day^{-1}), maximum productivity (P_{max}, g L^{-1}) were estimated using the equations described in section 3.2.6.1 by equation 3.1.

The pigment was quantified using a spectrophotometric approach that assessed the optical density, as outlined in our prior methodology section 3.2.6.4, utilizing four equations specified in sections 3.11 to 3.14. For photosynthetic performance study, the maximal photochemical efficiency of Photosystem II (*Fv/Fm*) culture was evaluated using a pulse amplitude-modulated fluorometer as described in section 3.2.6.4. Proteins were measured using Lowry's method Carbohydrates were calculated using the phenol sulphuric acid method with glucose as the standard. For lipid analysis, the Nile red fluorescence neutral lipid staining method as described in previous section methodology section 3.2.6.5.

4.2.5 Determination of CO_2 utilization and nutrient fixation

CO_2 utilization efficiency and fixation rate were calculated by the previous equation by carbon elemental analysis at the end of semi-continuous cycle by equation 3.7 and 3.8 in previous ection 3.2.6.3. For the calculation of CO_2 utilization and fixation for each individual 3 cycle in every treatment by using typical microalgal formula $CO_{0.48}H_{1.83}$ $N_{0.11}P_{0.01}$ considering 51.39% of carbon in the dry biomass [153].

Nitrogen and carbon fixation were estimated using Eq.10, where U_i and U_f represent the nitrogen and carbon content at the beginning and end of the III cycle of the semi-continuous batch and t_i and t_f represents the stating and harvesting time of end cycle (III)

$$N_f = \frac{AFD_f \times U_f - AFD_i \times U_i}{t_f - t_i} \quad (4.1)$$

4.2.6 Estimation of cellar bioenergy and energy content of microalgae

Using the primary metabolites lipid, protein, and carbohydrate, biomass energy was determined by estimating the amount of energy released during the full oxidation of macromolecules, i.e. 15.7 kJ g^{-1} for carbohydrate, 37.6 kJ g^{-1} for lipid, and 16.7 kJ g^{-1} for protein. (Yang et al., 2022). Thus, the biomass energy or bioenergy (kJ) of microalgae was derived from the following equation.

$$Bioenergy = \Delta X\ (g) \times [Carbohydrate\ (dcw\%) \times 16.7 + Lipid\ (dcw\%) \times 36.7 + Protein(dcw\%) \times 16.7] \quad (4.2)$$

Based on their elemental and ash content , the higher heating value (HHV) of biomass was calculated using a method developed by Channiwala and Parikh [291].

$$HHV = 0.3491 \times C + 1.1783 \times H + 0.1005 \times S - 0.1034 \times O - 0.0151 \times N - 0.0211 \times A \quad (4.3)$$

4.3 Result and discussion

4.3.1 Semi-continuous growth and photosynthetic performance under varying light and temperature conditions

4.3.1.1 Growth and photosynthetic performance three different continuous temperature experiments

In three different temperature treatments, as shown in Figure. 4.1A and 4.1D, the fastest growth was observed at 25 °C with high chlorophyll and low carotenoids content (23.18 µg

mL^{-1} and 2.1 µg mL^{-1}, respectively). The photosystem quantum yield (*Fv/Fm*) was 0.72 in the semi-continuous batch final III cycle. The growth curve accelerates without a lag phase and reaches the exponential phase promptly in all three cycles, with an average biomass productivity of 174.36 mg L^{-1} day^{-1} and a consistent specific growth rate more than 0.26 day^{-1} with no significant difference throughout the cycle. The preponderance of chlorophyte species are most productive and have the greatest carbon mitigation potential between 25 °C and 28 °C; thus, this temperature range was determined to be optimal by our study also [181]. Both increase and decrease in temperature by 10 ℃ inhibit growth in the first cycle of semi-continuous culture, with a one-day lag phase at 35 °C and a four-day adaptation time at 15 °C (Figure. 4.1A). In contrast, no lag phase was found in the II and III growth cycles of both the 15 °C and 35 °C constant temperature treatment studies, but the stagnation exponential phase was observed at 15 °C (Figure. 4.1A), which may be a result of poor photosynthesis and metabolic activity of the cell [292].

As shown in Figure. 4.1A, when exposing KMC8 to high temperature range 35 °C, stability in growth and adaptability were observed, as evidenced by a similar growth profile at optimal temperature with an average biomass productivity of 162.6 mg L^{-1} day^{-1}. Also, no significant difference in biomass productivity between the II and III cycles was observed. Consistent specific growth of more than 0.25 in all three cycles were observed, almost similar to at control temperature 25 ℃. Photosystem quantum yield (*Fv/Fm*) of 0.68 was noted, which was slightly lower than the normal temperature range value of 25 ℃ (Figure. 4.1B). By constantly exposing microalgae to extreme temperatures and CO_2 condition , a few strains were able to undergo physiological changes to counteract the impact of increased temperature by increasing the heat stability of the photosystem and lowering the cell size in order to preserve the cell's low metabolic activity to enhance it carbon fixation capability [293–295]. Some species acquire antioxidants such as carotenoids at high temperatures [296]. In this work, the accumulation of carotenoids increased by two-fold, from 2.1 µg mL^{-1} to 4.04 µg mL^{-1}, whereas the amount of chlorophyll got declined by 1.5-fold when the temperature was varied from 25 ℃ to 35 ℃. The average cell density reduced by almost 54% from 25 °C (174.36 mg L^{-1} day^{-1}) to 15 °C (79.7 mg L^{-1} day^{-1}) and the specific growth rate was 0.18-0.20 day^{-1} with a significant decrease compared to that obtained at 25 °C and 35 °C. Chlorophyll and carotenoid concentrations also decreased with recoded value of 11.18 µg mL^{-1} and 1.2 µg mL^{-1}, along with a decrease in Photosystem II quantum yield *Fv/Fm* from 0.72 (at 25 °C) to 0.51 (at 15 °C) (Figure. 4.1D). This was a clear indicator of insufficient carbon fixation and slow electron

transport in photosynthesis, both of which retarded cell development and CO_2 utilization potential [297]. The superior ability to acclimatize to high temperatures and elevated CO_2 levels demonstrated by this strain indicates its enhanced aptitude for CO_2 bio-mitigation from hot industrial flue gas.

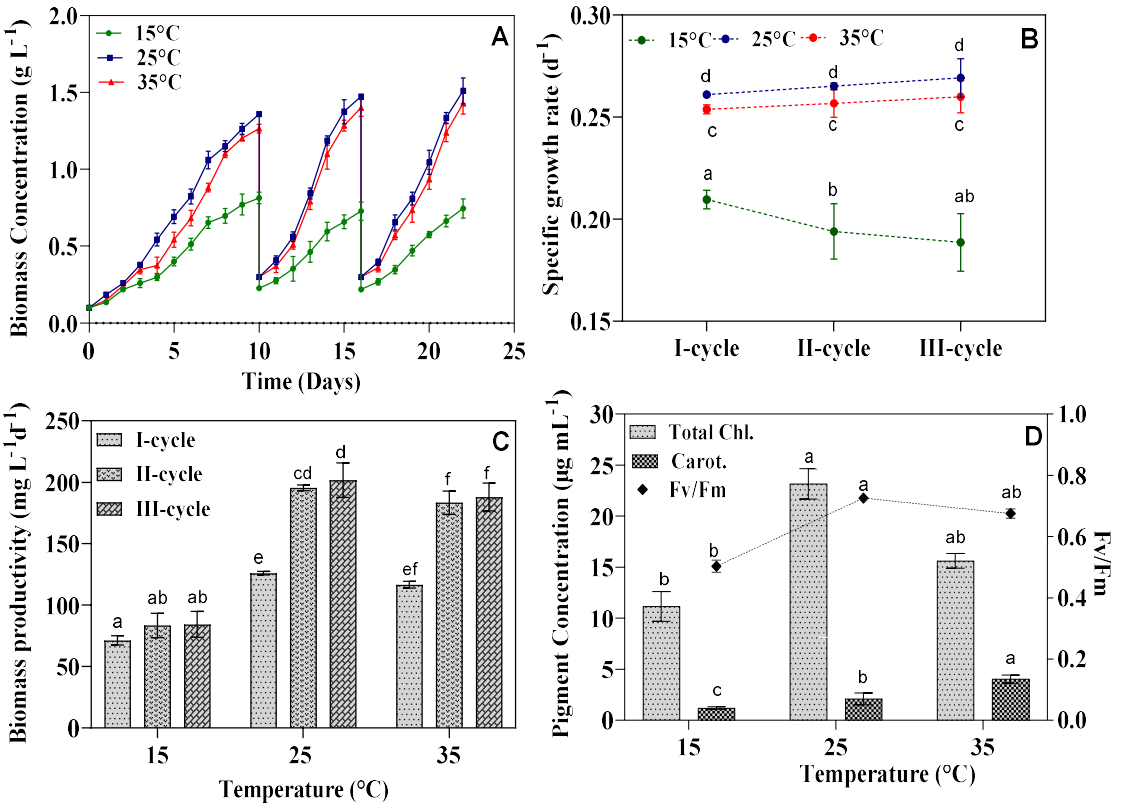

Fig. 4.1: Semi-continuous growth and photosynthesis of *M. pusillum* at 15, 25, and 35°C **(A)** dynamic growth profile **(B)** Growth rate of every cycle **(C)** productivity of biomass. **(D)** *Fv/Fm* and photosynthetic pigments (III cycle). Data presented as mean ± SD, n = 2. The identical letters imply statistical insignificance ($p< 0.05$) using one-way ANOVA (Tukey's technique)

4.3.1.2 Growth and photosynthetic performance under three different continuous light experiments

As previously discussed, at 25 °C and 150 µmol m^{-2} s^{-1}, no lag phase was observed, but increasing light intensity extended the adoptable phase by 2 days at 350 µmol m^{-2} s^{-1} and 3 days at 650 µmol m^{-2} s^{-1}. The longest adoptable phase of about 4 days with a shorter exponential phase was observed at 50 µmol m^{-2} s^{-1} in the first cycle. Furthermore, as shown in

Figure. 4.2A, at both 650 and 50 µmol m^{-2} s^{-1} light intensity, the lag phase continued in II cycle and slightly declined in III cycle at 650 µmol m^{-2} s^{-1}. At 350 µmol m^{-2} s^{-1}, cells directly progressed to the exponential phase in both II and III cycles (Figure. 4.2A). At light intensity of 350 µmol m^{-2} s^{-1} yielded an average biomass productivity of 154 mg L^{-1} day^{-1} and a specific growth rate of 0.23-0.25 day^{-1}. Similarly, a light intensity of 650 µmol m^{-2} s^{-1} resulted in an average biomass productivity of 132 mg L^{-1} day^{-1} and a specific growth rate of 0.22-0.24 day^{-1}, with a marginal reduction of only 14% from the values observed at 350 µmol m^{-2} s^{-1}. The lowest biomass productivity of 69 mg L^{-1} day^{-1} along with specific growth rate 0.16-0.19 day^{-1} was reached under low light treatment of 50 µmol m^{-2} s^{-1}. Compared to all three batch semi-continuous cycles, a significant increase in biomass productivity was observed in the II cycle at 350 µmol m^{-2} s^{-1} and 650 µmol m^{-2} s^{-1}, and this productivity was maintained in the III cycle, indicating that the strain had adapted to both light intensities by maintaining a stable growth rate of more than 0.24 day^{-1}. As shown in Figure. 4.2A and B, for the three-cycle experiment with low light intensity, a drop-in growth rate did not reveal any significant changes or improvements in growth. In light treatment experiment, highest total chlorophyll content was observed in 350 µmol m^{-2} s^{-1} which reached a value of 21.8 µg mL^{-1}. Higher light intensity of 650 and low light intensity of 50 µmol m^{-2} s^{-1} resulted in 17.9 µg mL^{-1} and 13.47 µg mL^{-1} total chlorophyll content (Figure. 4.2D). However as shown in Figure. 4.2B, carotenoids production increase with escalation in light intensity (1.03, 2.36, 4.25 µg mL^{-1} for 50, 350, 650 µmol m^{-2} s^{-1}) *M. pusillum* growth and adaptability to low light intensity were limited, possibly due to self-shading effects that impeded photosynthesis. Insufficient light for photosynthesis inhibited cell productivity [298]. The quantum yield (*Fv/Fm*) of Photosystem II was 0.51, indicating that it was below the desirable range [297]. Reduced chlorophyll levels suggest a hindrance in photosynthesis. Under high light intensity (650 µmol m^{-2} s^{-1}) in a semi-continuous mode, the *Fv/Fm* ratio increased to 0.64 (Figure. 4.2D), indicating physiological acclimation despite limited enhancements in growth parameters. Elevated light and temperature conditions stimulated a rise in carotenoid levels, serving as a defense mechanism against oxidative stress [286]. *M. pusillum* growth patterns were influenced by light intensity and exhibited adaptive phases similar to temperature experiments. Carotenoids played a vital role in protecting the cells.

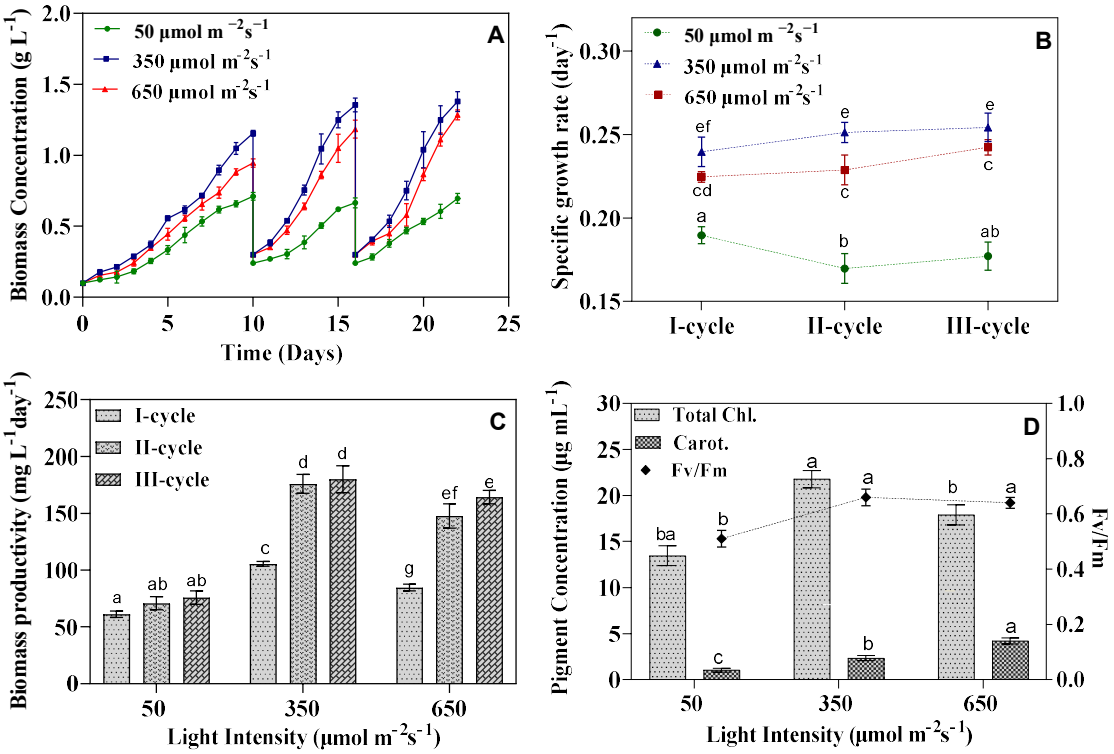

Fig. 4.2. Growth and photosynthetic performance of *M.pusillum* at three different light intensity treatment 50, 350 and 650 µmol m^{-2} s^{-1} **(A)** dynamic growth profile **(B)** growth rate of every cycle **(C)** productivity of biomass. **(D)** *Fv/Fm* and photosynthetic pigments (III cycle).

4.3.1.3 Growth and photosynthetic performance in high temperature regime

As depicted in Figure. 4.3A, under 38 °C/25 °C culture conditions, a 3 days lag phase was observed when the culture was initiated in Phase-I with a light intensity of 150 µmol m^{-2} s^{-1}. The lag phase was reduced in Phases II and III with an average biomass productivity of 88.54 mg L^{-1} day^{-1} and a specific growth rate of 0.20-0.21 day^{-1}. By switching the culture conditions to high light intensity (750 µmol m^{-2} s^{-1}), the adaptability of *M. pusillum* to an increased temperature regime was boosted, resulting in a 1.6-fold increase in average biomass output from 0.74 g L^{-1} to 1.2 g L^{-1}. As seen in Figure. 4.3B, the value of growth rate increased significantly from 0.21 day^{-1} to 0.28 day^{-1} when the culture was shifted to high light intensity, while productivity remained stable in the range of 150 mg L^{-1} day^{-1} to 158 mg L^{-1} day^{-1} in the II and III cycles, resulting in a productivity increase of more than 40% in comparison to 150 µmol m^{-2} s^{-1}. The photosystem II quantum yield (*Fv/Fm*) increased from 0.62 to 0.68, with a 2-fold rise in carotenoids (1.67 to 3.23 µg mL^{-1}) and a 1.4-fold decrease in chlorophyll content

(21.65 to 15.9 µg mL^{-1}) (Figure. 4.3D). The enhancement of *Fv/Fm* and carotenoids value directly indicated the improvement in photosynthesis adaptation of the cell, as described in section 3.1.2. It has been reported that the acclimation of microalgae to high light intensity resulted in increased thermal tolerance of PSII [65]. A night-time temperature of 25 ℃ promotes respiration and maintains a balance between catabolic and anabolic processes, supporting the ATP demand required for cellular metabolic energy [286]. The experiment's findings indicate that strain acclimation was superior and led to enhanced development compared to the continuous photon and thermal stress treatment in terms of temperature regime. High light intensity played a significant role in the thermal acclimatization of the strain to high temperature conditions by regulating the pigment and biochemical composition, specifically the fatty acid profile (further discussed below in sections 4.3.2 and 4.3.3).

4.3.1.4 Growth and photosynthetic performance in low temperature regime

When culture was exposed to a low temperature environment, a five-day long adaptation phase formed with sluggish growth in Phase I of the first cycle, and this phase persisted in the II and III cycles with an average productivity of 42.25 mg L^{-1} day^{-1} and a specific growth rate of 0.15 to 0.18 day^{-1}. Intriguingly, changing the culture to high light resulted in a 1.86-fold increase in average cell density, with a value of 0.58 g L^{-1} and a specific growth of 0.18-0.24 day^{-1} (Figure. 4.3A &B). By altering the growth conditions from low to high light intensity the average biomass productivity enhanced nearly by 1.5-fold with value 62.4 mg L^{-1} day^{-1}, the photosystem quantum yield (*Fv/Fm*) rose from 0.54 to 0.63, confirming its photo adaptability to high light intensity (Singh et al., 2022). Carotenoids concentration increased by a factor of 2.25, from 1.04 µg mL^{-1} (150 µmol m^{-2} s^{-1}) to 2.34 µg mL^{-1} (750 µmol m^{-2} s^{-1}). As indicated in Figure. 4.3D, there was no significant variation in chlorophyll concentration between the two different light intensity experiments. Certain microalgae were shown to be able to adapt to low temperature stress in the presence of high light intensity, and this adaptation was achieved by the accumulation of high carotenoid levels [299]. High light intensities during the day time led to higher concentrations of carbohydrates accumulation in cell which provided more energy for maintenance purposes during cold stress for the synthesis of proteins for cell division [292]. Apart from the general finding that the respiration rate depends on the temperature, the amount of light received over the day also seems to affect the respiration losses during the night [292].

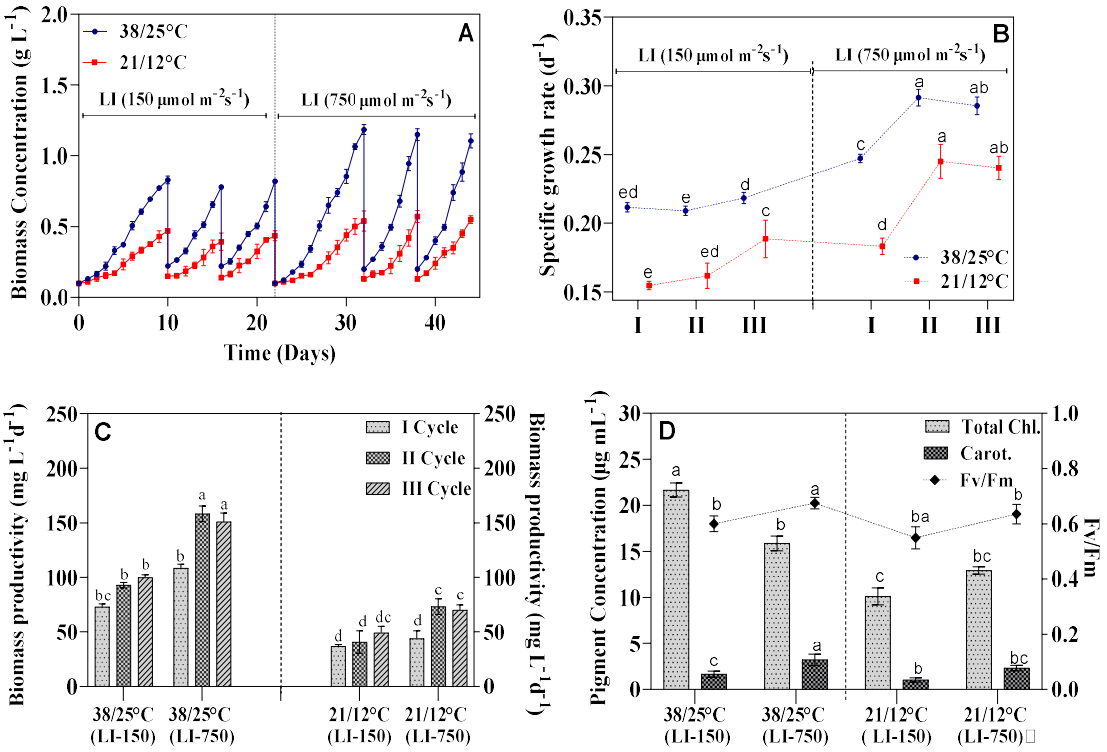

Fig. 4.3. Growth and photosynthesis of *M. pusillum* throughout a daily light/dark temperature cycle at LI 150 and 750 mol m^{-2} s^{-1} and 38/25°C and 21/12°C, respectively. **(A)** growth profile with two temperature regimes and two phases of light. **(B)** growth rate indicating the shift to high LI along a vertical dotted line. **(C)** biomass productivity per cycle. **(D)** *Fv/Fm* and photosynthetic pigments

4.3.2 Differential regulation of cellular components under varying continuous light and temperature condition

Significant changes in cellular components were observed under varying light and temperature conditions. (Figure. 4.4A). Lipid accumulation increased with temperature for both heat and cold stress. The lowest level was observed at 25 °C (7.63% of DCW), with higher levels at 15 °C (14.45%) and a significant increase at 35°C (26.78%). Lipid content was measured at light intensities of 50, 350, and 650 µmol m^{-2} s^{-1} with their value of 15.7%, 12.9%, and 23.85%, respectively. The lipid content increased 2-fold when exposed to a high light intensity of 650 µmol m^{-2} s^{-1} compared to 350 µmol m^{-2} s^{-1}. This demonstrates the role of microalgae in the sequestration of carbon dioxide through the production of lipids rather than carbohydrates. The carbohydrate content exhibited a decreasing trend with an increase in temperature 15 °C (44.6%) > 25 °C (40.7%) > 35 °C (34.5%), suggesting a shift in carbon

allocation towards lipid production for CO_2 mitigation, while no distinct trend was observed with varying light intensity (Figure. 4.4A). Carbohydrate concentration was highest at 350 µmol m^{-2} s^{-1} (45%), followed by 50 µmol m^{-2} s^{-1} (41.26%) and 650 µmol m^{-2} s^{-1} (35.4%). Protein content remained stable during light treatment, but decreased slightly at higher intensities (50-650 µmol m^{-2} s^{-1}), reaching values of 35.8%, 33.4%, and 28.9%. Protein concentrations were measured at 15, 25, and 35 °C, yielding values of 33.6%, 38.6%, and 30.3%, respectively. Protein content declined by 8% and 3% under high (35 °C) and low temperature (15 °C) stress, respectively.

Prolonged exposure to high temperatures resulted in elevated lipid levels and decreased carbohydrate concentrations. It is significant that the extended exposure to elevated temperatures resulted in an increase in lipid levels and a decrease in carbohydrate concentrations. This indicates that under stressful conditions, there is a preference for utilizing carbohydrates for energy production and lipid synthesis. The metabolic transition observed in microalgae allows for the redirection of surplus CO_2 towards the synthesis of energy-reserving compounds, such as lipids and carbohydrates, thereby promoting CO_2 sequestration and bioremediation [300]. Lipid productivity peaked at 46.95 mg L^{-1} day^{-1} when the temperature was 35 °C. Carbohydrate productivity peaked at 25 °C, with a maximum value of 81.32 mg L^{-1} day^{-1}. Under three distinct lighting conditions. The maximum lipid productivity of 39.3 mg L^{-1} day^{-1} was attained at a high light intensity of 650 µmol m^{-2} s^{-1} (Figure. 4.4B). Comprehending the metabolic reactions is of utmost importance in order to enhance the efficiency of carbon dioxide capture and storage through employment of microalgae. The variability of light and temperature, as well as the acclimation process, induce remodeling of microalgae to facilitate the utilization of CO_2 for diverse metabolic pathways [301].

Regarding fatty acid regulation, the study revealed that increased light intensities and temperatures led to higher levels of saturated and monounsaturated fatty acids, while polyunsaturated fatty acid levels decreased (Figure. 4.4D). The most significant changes were observed in palmitic and stearic acids, with stearic acid showing the most prominent modulation, as illustrated in Figure. 4.4C. These findings indicate that prolonged exposure to high light and temperature can lead to oxidative damage to PUFAs and stimulate the production of SFAs through de novo fatty acid synthesis. [302]. This process alleviates photoinhibition and photodamage while enhancing the quality of biodiesel.

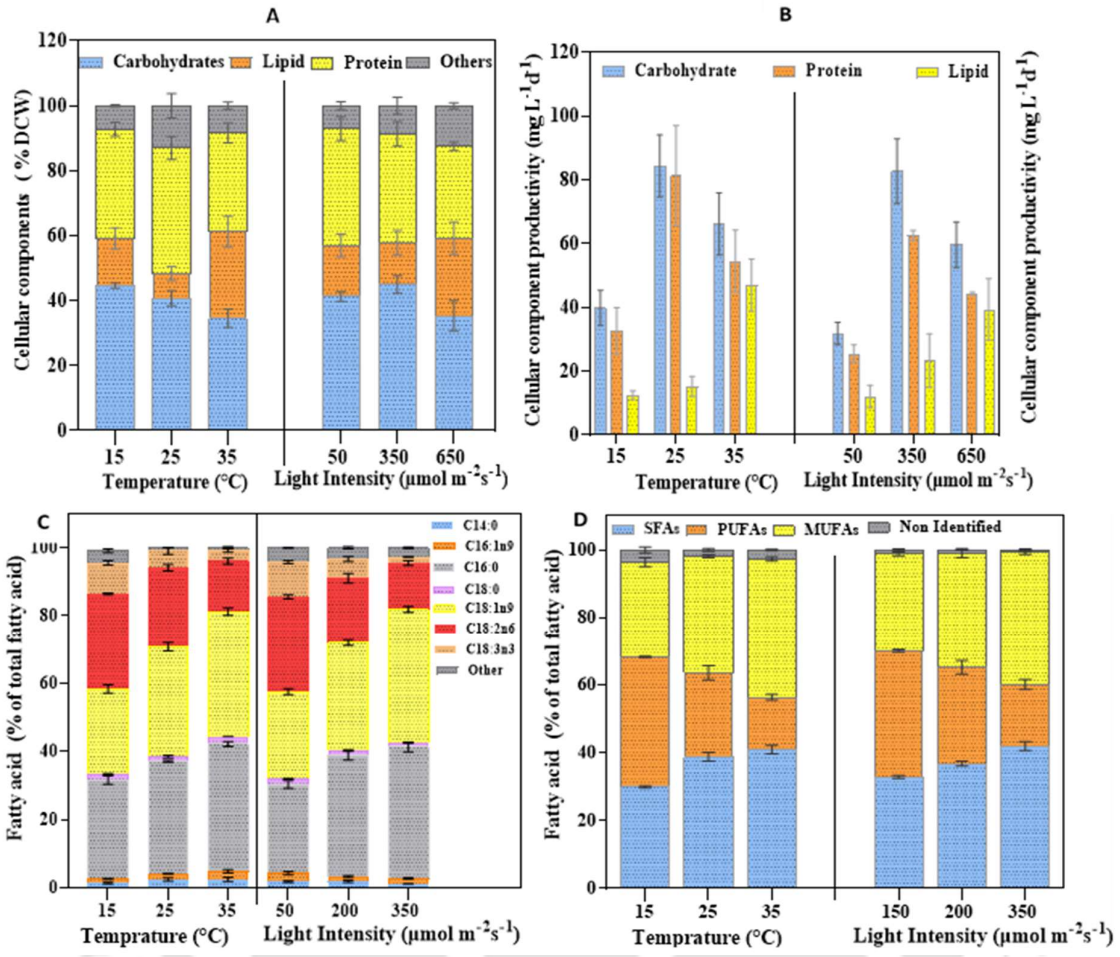

Fig. 4.4. In response to three different light and temperature conditions. **(A)** Percentages and **(B)** productivity of lipids, protein, carbohydrates, and other types of biomass **(C)** fatty acid composition and **(D)** % of saturated, Mono and polyunsaturated fatty acid.

4.3.3 Differential Regulation of cellular component in light and dark temperature regime in low and high light intensity

The lipid content was 23.7% at 38/25°C and a light intensity of 150 µmol m^{-2} s^{-1}. After switching the culture to high light intensity (750 µmol m^{-2} s^{-1}), lipid content increased by 22% and carbohydrate content decreased from 34.22 to 30.24% (Figure. 4.5A). The results suggest that microalgae demonstrate a significant level of effectiveness in the allocation of carbon derived from CO_2 towards the synthesis of lipids when exposed to high temperature and light conditions during the acclimation experiment. However, protein content remained stable between light phases, ranging from 29.38% to 27.76%. Under low temperatures (21°C/12°C)

and a light intensity of 150 μmol m^{-2} s^{-1}, the lipid and carbohydrate contents were 14.5% and 30.8%, respectively. During the second phase, increasing the light intensity from 150 to 750 μmol m^{-2} s^{-1} resulted in a 16.2% increase in carbohydrates and a 32.2% increase in lipids, while protein content decreased from 34.35% to 28.9%.

Figure.4.5A and 4.5B demonstrate that the lipid content and productivity were greater in the high temperature regime during both light intensity phases, in comparison to the low temperature regime. The concurrent presence of elevated temperature and intense light led to the attainment of the maximum lipid content (29%) and productivity (42.3 mg L^{-1} day^{-1}). Enhanced lighting conditions improved the ability of photosystems to adjust to changes in light, resulting in an increase in the energy needed for converting CO_2 into carbohydrate [303]. Prolonged exposure to elevated light and temperature conditions leads to a progressive substitution of carbohydrates with neutral lipids, which function as an alternate strategy for storing energy[303]. Extended exposure to light increases the amount of light available and prolongs the time during which photosynthesis occurs. This leads to an increased uptake of CO_2 via the Calvin cycle, which allows for the buildup of more carbohydrate molecules. The investigation revealed disparities in protein accumulation and glucose concentration between the studies conducted under the light-dark regime and those carried out under continuous light conditions. Protein buildup was found to be greater and carbohydrate content lower under the light-dark regime. This was attributed to the use of stored carbs in photorespiration during the dark phase [304]. The research shown that manipulating the light and dark temperature regime and photon intensity duration helps to elucidate the rapid metabolic adaptations and acclimation responses of microalgae in response to changes in light availability[305]. This facilitates the examination of the shift from photoautotrophic metabolism to heterotrophic respiration and the interdependence of these mechanisms in CO_2 assimilation.

The findings also indicated that the temperature regime has an impact on the restructuring of fatty acid chains (Figure.4.5C and D). More precisely, a rise in the amount of unsaturated fatty acids was seen at lower temperatures, whereas a rise in the amount of saturated fatty acids was noticed at higher temperatures. The current study found that polyunsaturated fatty acids (PUFAs) had the highest concentration of fatty acids at low temperature settings. Nevertheless, when subjected to intense light, polyunsaturated fatty acids (PUFAs) experienced a reduction of 3.1%, but saturated fatty acids (SFAs) exhibited a rise of 5.1% (Figure.4.5D). The shift observed may be attributed to the oxidative deterioration of PUFAs in response to the higher light intensity, as explained in section 4.3.2. The growing

conditions consistently yielded the greatest levels of palmitic and stearic acid, suggesting their suitability as desirable fuel characteristics for biodiesel generation. The primary observations were the separation of unsaturation and the alteration of fatty acid composition in both light and temperature conditions for C-16 and C-18 specifically in both low temperature condition towards unsaturation of fatty acid. Low Temperature affects enzymatic activities and membrane fluidity, with optimal temperatures boosting metabolic rates and lipid biosynthesis, and higher temperatures increasing saturated and monounsaturated fatty acids to stabilize membranes. Low temperatures slow metabolic processes, leading to a rise in polyunsaturated fatty acids to maintain membrane fluidity [306].

Microalgae KMC8 have remarkable adaptability in response to changes in light and temperature, which have a substantial impact on their cellular composition and fatty acid profiles. The interaction between light and temperature forms an intricate regulatory system that increases the generation of lipids and the productivity of biomass under ideal circumstances. However, when conditions are less than perfect, stress responses and metabolic changes are activated to support growth. Gaining a comprehensive understanding of these regulatory systems is essential for optimizing the production of microalgae, with the goal of maximizing both the quantity and quality of biofuels for commercial bioenergy applications. Therefore, instead of the biochemical composition, the fatty acid has a significant influence on the cell's ability to adapt to various culture techniques.

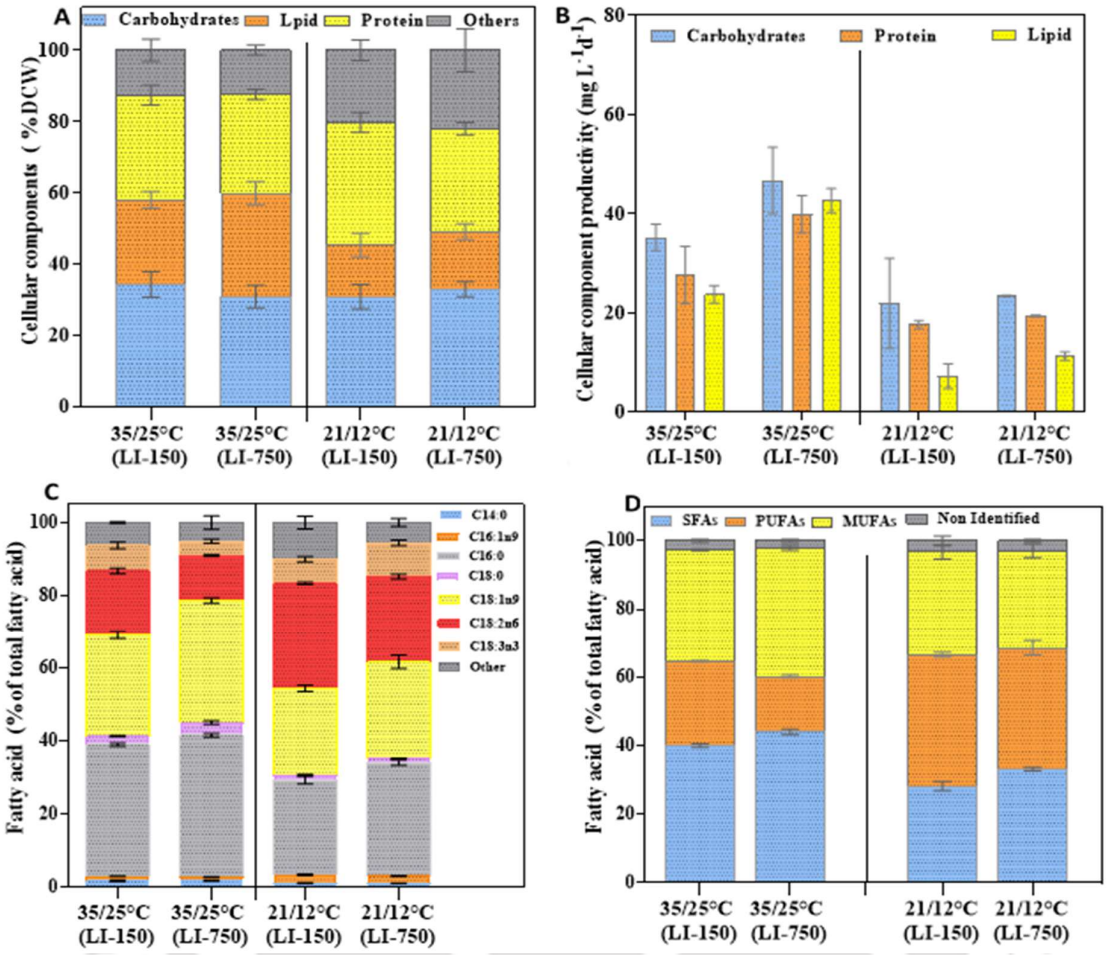

Fig. 4.5. In response to two different temperature regimes continue in low to high light intensity cultivation condition **(A)** Percentages and **(B)** productivity of lipids, protein, carbohydrates, and other types of biomass **(C)** fatty acid composition and **(D)** % of saturated, Mono and polyunsaturated fatty acid

4.3.4 Assessment of the CO_2 utilization efficiency in different light and temperature conditions

CO_2 utilization was most efficient at 25 ℃, averaging 1.2 ± 0.23% over three cycles. No significant difference was observed at 35 ℃, with an average of 0.98 ± 0.24% being maintained. The efficiency was lowest at 15 ℃, with a value of 0.47 ± 0.04% (Figure. 4.6A). The CO_2 utilization efficiency were measured at light intensities of 50, 350 and 650 µmol m^{-2} s^{-1}, resulting in average values of 0.4 ± 0.04%, 0.92 ± 0.22%, and 0.75 ± 0.21%, respectively (Figure. 4.6B). In experiments with low temperature (15 ℃) and low light (50 µmol m^{-2} s^{-1}),

CO_2 utilization efficiency decreased, whereas there was no discernible difference in experiments with high temperature and light Figure. 4.6B and C. A marginal improvement in CO_2 utilization efficiency was noted in the II and III cycles as compared to the I cycle, when the experiment was conducted at 25 ℃ and 35 ℃, and with light intensity of 350 and 650 µmol m^{-2} s^{-1}. The observed outcome can be attributed to the high initial inoculum density, while no notable variation was detected in the low light and low temperature treatment. According to section 4.3.1, the performance of the cells' photosystems was a factor in the connection between biomass output and CO_2 utilization. High temperature and light treatments resulted in enhanced photosystem quantum yield and no growth inhibition. Rising temperature reduces CO_2 solubility, which may restrict microalgae's access to this substrate. The effect of temperature on CO_2 availability can be reduced by introducing high concentration CO_2 into appropriate systems. Sustaining CO_2 fixation through photosynthesis is vital for the adaptation of microalgae to elevated temperatures [44]. The average CO_2 utilization efficiency was 0.78 ± 0.12% in outdoor simulation experiments conducted at a temperature of 38 ℃/25 ℃ and light intensity of 150 µmol m^{-2} s^{-1}. Increasing the light intensity to 750 µmol m^{-2} s^{-1} resulted in a 1.5-fold increase in efficiency, with an average value of 1.23 ± 0.23%. At a temperature of 21 ℃/12 ℃, CO_2 utilization efficiency was lower but increased by 1.4 times to 0.56 ± 0.149% at a light intensity of 750 µmol m^{-2} s^{-1}. The growth rate and photosystem quantum yield were enhanced by exposing the culture to high light intensity at different temperature regimes. The findings of the study suggest that microalgae exhibit enhanced CO_2 utilizations under light and dark temperature cycles, and that their utilizations of photochemical energy and photosynthesis is further improved by recurrent periods of darkness [65]. Sufficient levels of light intensity during the daytime are crucial for promoting growth and facilitating acclimation to thermal and cold stress, while also promoting optimal utilizations of CO_2 [307].

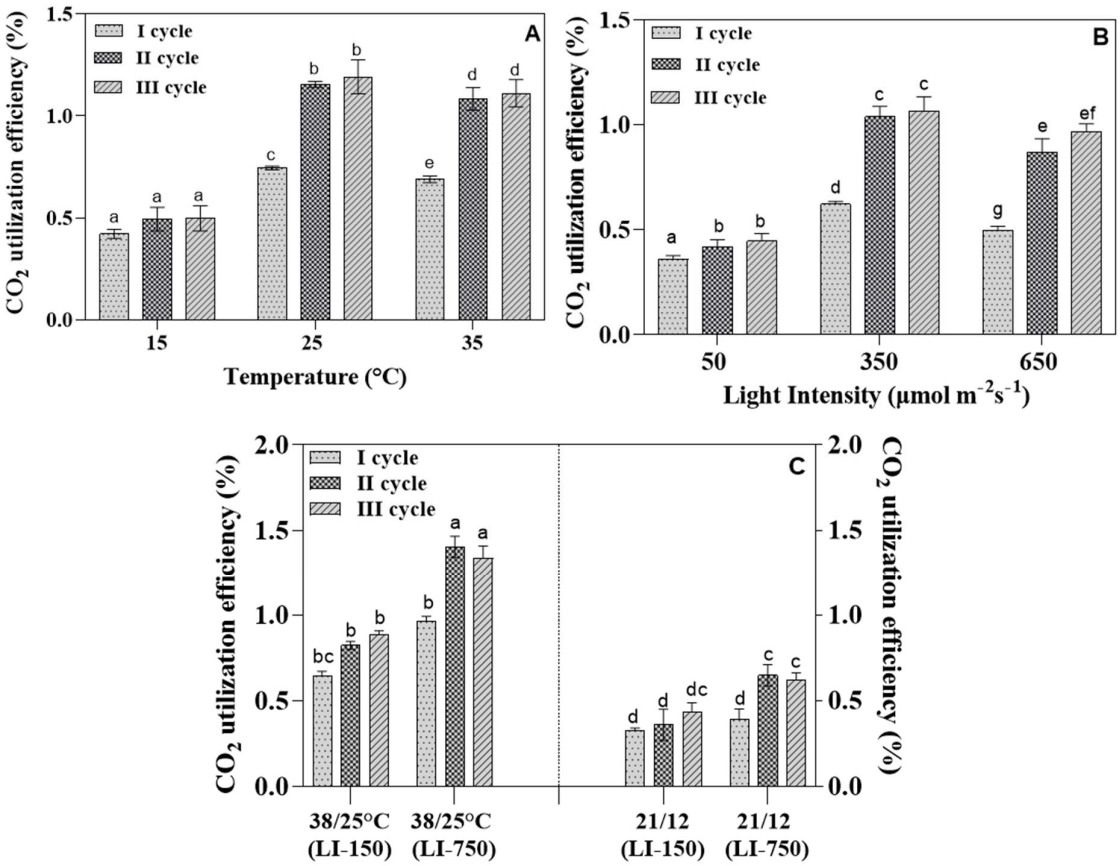

Fig. 4.6. CO_2 utilization efficiency in three distinct **(A)** temperature and **(B)** light treatments and **(C)** two distinct temperature regimes in response to two distinct light intensities at the end of semi-continuous mode. All data points represent the mean of n=2 biological replicates; error bars represent the replicates standard deviation**.**

4.3.5 Assessment the interaction of carbon and nitrogen assimilation for bioenergy generation and CO_2 sequestration potential

4.3.5.1 Light and temperature treatment

***Constant temperature*:** Table 4.2 shows that increasing the temperature from 15 °C to 25 °C resulted in a two-fold increase in carbon and nitrogen fixation rates. Carbon and nitrogen fixation rates showed a significant increase from 43.5 ± 0.02 to 97 ± 0.02 mg L^{-1} day^{-1} and from 4.65 ± 0.51 to 10.03 ± 0.43 mg L^{-1} day^{-1}, respectively. Increased temperature led to improved CO_2 utilization efficiency (0.5 ± 0.07 to 1.12 ± 0.1%) and a 2.3-fold rise in CO_2 fixation rate (160 ± 0.05 to 355 ± 0.03 mg L^{-1} day^{-1}). Nitrogen and carbon fixation rates slightly increased at 35 °C compared to 25 °C. Increased temperature (35 °C) improved the ability of

CO_2 bioremediation by promoting nitrogen and carbon fixation rates. CO_2 utilization efficiency was 1.15 ± 0.06% and fixation was 370 ± 0.02 mg L^{-1} day^{-1}. Carbon and nitrogen fixation are important for energy buildup in biomass, highlighting their role in CO_2 assimilation and sustainable bioenergy production. Cellular metabolite-based bioenergy reached maximum at 35°C, with 58.82 ± 0.35 kJ and HHV of 25.97 kJ g^{-1}. The phenomenon was associated with increased lipid concentration, leading to greater carbon biomass accumulation (50.08 ± 1.92 mmol C L^{-1}). At 25 °C, bioenergy stored was 48.51 ± 2.31 kJ and HHV was 22.40 kJ g^{-1}, with carbon assimilation at 48.26 ± 2.73 mmol C L^{-1} [76]. Reduced temperatures decreased C and N fixation rates, leading to lower productivity, energy content, and carbon assimilation in biomass. Bioenergy and carbon assimilation were measured at 15 °C (27.34 ± 1.25 kJ and 21.86 ± 1.25 mmol C L^{-1}) and compared to 25 °C and 35 °C (Table 4.1). Fixation of carbon and nitrogen is vital for sustaining photosynthesis and enhancing metabolite productivity for biomass formation [308]. The growth-related metabolism of microalgae is subject to modulation by both temperature and CO_2 conditions, which in turn affect the demand for and limitation of nitrogen. An increase in the supply of carbon and nitrogen is linked to a rise in the rate of this metabolic pathway for the production of high-energy carbon storage molecules within cells [287]. Therefore, maintaining a suitable balance between carbon and nitrogen is crucial to ensure efficient utilization of CO_2 and assimilation of biomass with high carbon content for bioenergy production, while considering fixation rate and cellular stoichiometry under different temperature conditions [309,310].

***Constant light*:** Distinct trends in nutrient and CO_2 fixation were observed in experiments comparing temperature and light intensity. At 50 µmol m^{-2} s^{-1} light intensity, C and N fixation rates were 38.21 ± 0.02 and 4.39 ± 0.23 mg L^{-1} day^{-1}, respectively. At 350 µmol m^{-2} s^{-1}, C and N fixation rate rates increased by 2.7 and 1.93-fold. CO_2 utilization efficiency and fixing rate increased significantly from 0.44% to 1.18% and 140 to 370 mg L^{-1} day^{-1}, respectively**.** The carbon output increased by 2.68 times, from 19.11 ± 1.12 to 51.06 ± 1.96 mmol C L^{-1}. At a light intensity of 650 µmol m^{-2} s^{-1}, both carbon and nitrogen fixation rates decreased compared to 350 µmol m^{-2} s^{-1}. Specifically, carbon fixation decreased from 102 ± 0.01 to 82.8 ± 0.02 mg L^{-1} day^{-1}, and nitrogen fixation decreased from 8.48 ± 0.27 to 6.58 ± 0.02 mg L^{-1} day^{-1}. Additionally, there was a 20% reduction in carbon yield, which was measured at 41.02± 0.94 mmol C L^{-1}. Increasing light intensity from 50 to 350 µmol m^{-2} s^{-1} enhanced photosynthesis, indicated by higher photosystem II quantum yield (*Fv/Fm*) from 0.53 to 0.64 and increased chlorophyll content. The changes facilitated faster carbon and nitrogen

intake and increased carbon biomass by utilizing CO_2. At 650 µmol m^{-2} s^{-1} light intensity, no photoinhibition was observed based on *Fv/Fm* ratio and chlorophyll content [303,311]. Evidence of photoacclimation to light intensity was observed [303]. Biomass bioenergy and heating value were similar at 350 and 650 µmol m^{-2} s^{-1} light intensity. Elevated light intensity (650 µmol m^{-2} s^{-1}) increased lipid content and reduced carbohydrate content, but had no significant impact on bioenergy or high heating value. Bioenergy content was lowest at 25.97 ± 1.83 kJ with 50 µmol m^{-2} s^{-1} light intensity. At 350 µmol m^{-2} s^{-1} light intensity, the experiment showed moderate lipid content, no growth inhibition, and higher carbohydrate accumulation. A positive correlation exists between the intensity of light and the rate of photosynthesis, which consequently leads to an augmentation in the levels of CO_2 fixation. The underlying cause of this phenomenon is that an elevation in luminous intensity 50 to 350 µmol m^{-2} s^{-1} yields a heightened supply of energy for the light-dependent reactions involved in the process of photosynthesis. The aforementioned reactions entail the assimilation of light and the synthesis of ATP and NADPH, which are fundamental for the sequestration of CO_2 [312]. Under conditions of optimal light intensity 350 µmol m^{-2} s^{-1}, microalgae utilize CO_2 to primarily synthesize carbohydrates, which supports their growth, reproduction, and metabolic functions. This process enables microalgae to maintain a harmonious equilibrium between energy availability and metabolic demands [313]. High light intensities can result in photoinhibition, a state in which an overabundance of light energy causes harm to the photosynthetic apparatus. This can decrease the assimilation capacity and alter the pathway towards energy storage molecules, primarily lipids, instead of metabolite productivity for growth [244]. The results indicate that at a light intensity of 650 µmol m^{-2} s^{-1}, lipid productivity is significantly elevated while maintaining the bioenergy value of the biomass.

Correlation of carbon and nitrogen to light and temperature: Based on Figure. 4.7A, both nitrogen and carbon fixation increased linearly with temperature. Nitrogen fixation was shown to have a stronger link (r^2 = 0.9, p = 0.003) than carbon fixation (r^2 = 0.77, p = 0.02), even though both carbon and nitrogen fixation seem to have a high correlation impact on the temperature treatment experiment. The present findings unambiguously demonstrate that the process of thermal acclimation in the strain under investigation has led to a notable increase in the metabolic activity of the cell, thereby strengthening its potential for CO_2 fixation [186]. As indicated in Figure. 4.7B, there is no significant linear association between light intensity and the fixation of carbon and nitrogen, as was found for temperature. However, it has been

observed that photo acclimatization of cells has a positive correlation with elevated rates of photosynthesis and CO_2 fixation, resulting in a subsequent increase in carbon assimilation.

However, based on the overall results of the continuous light and temperature treatment experiments, we conclude that the semi-continuous derived acclimation of the strain led to an enhancement in its photon and thermotolerance, which was attributed to an elevation in the assimilation rate of both carbon and nitrogen. Consequently, there was a rise in the need for carbon and nitrogen to sustain the process of CO_2 assimilation and the conversion into of organic carbon-rich biomass, which facilitated the accumulation of high levels of intracellular bioenergy in the biomass [185].

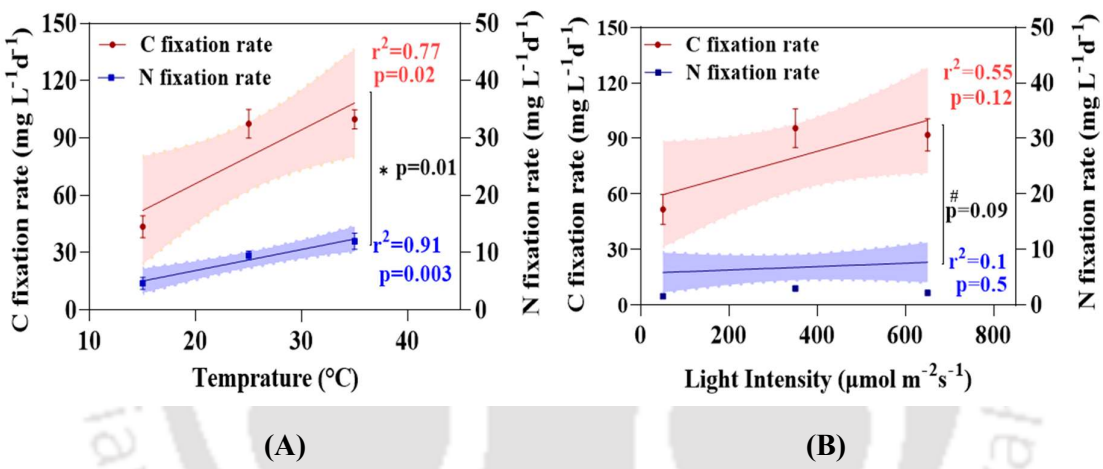

Fig. 4.7: Effect of different (**A)** continues light and (**B**) temperature condition on carbon and nitrogen fixation. All data points represent the mean of n=2 biological replicates; error bars represent the replicates' standard deviation. Light pink and blue area represent 95% of confidence interval. The graph displays the Pearson correlation *(p*) derived from a multiple linear regression analysis of carbon and nitrogen fixation under various light and temperature conditions.

4.3.5.2 Light and dark temperature regime in low and high light intensity

High temperature regime (38 °C/25 °C)*:* The nitrogen and carbon fixation in the high temperature regime studies were 4.25 ± 0.05 mg L^{-1} $day^{-1}$and 51.16 ± 0.01 mg L^{-1} day^{-1} at a light intensity of 150 µmol m^{-2} s^{-1}, respectively, with a CO_2 utilisation efficiency of 1.33% and CO_2 fixation of 190 ± 0.01 mg L^{-1} day^{-1}. The transition to high-light cultivation 750 µmol m^{-2} s^{-1} increased carbon and nitrogen fixation rates by 1.5 and 1.3 times, respectively, with a CO_2 utilisation efficiency of 2.03% and a 1.5-fold increase in CO_2 fixation rate of 280 ± 0.02 mg L^{-}

^{1} day^{-1} (Table 4.2). Carbon and nitrogen fixation enhancements increase cellular bioenergy accumulation by 1.6 times, from 31.71± 0.77 kJ to 45.51 ± 0.79 kJ, while carbon production output increases from 25.58 ± 0.32 to 38.40 ± 1.26 mmol C L^{-1} (Table 4.1). High daylight and temperature have a positive effect on biomass productivity to maintain the proper balance between photosynthesis and respiration and can overcome the high photon and thermal stress received during the day [177,314]. Whereas, the low temperature at night provides an opportunity for cells to temporarily recover cell function in response to high light and temperature treatment by secreting more protein to maintain cell metabolic function [315]. As shown by this work, thermal or photon acclimatisation may be increased by varying temperature and light conditions as opposed to continuous thermal and photon stress.

Low temperature regime (21 °C/12 °C). Carbon and nitrogen fixation are slower in the low temperature experiment than in the high temperature experiment, but continuing the culture at high light intensity 750 µmol m^{-2} s^{-1} improved nutrient fixation (carbon fixation from 23.43 to 33.92 mg L^{-1} day^{-1} and nitrogen fixation from 2.64 to 3.03 mg L^{-1} day^{-1}). Also, the CO_2 utilization efficiency and CO_2 fixation increased from 0.59 ±0.06% to 0.88 ±0.03% and 80 ± 0.01 to 120 ± 0.01 mg L^{-1} day^{-1} respectively. The accumulation yield of carbon biomass increased from 11.45± 1.21 to 16.96± 0.82 mmol C L^{-1} (Table 4.2). In the low temperature regime of 21°C/12 °C, a considerable loss of cellular bioenergy accumulation in biomass was detected, but the high light intensity increased bioenergy accumulation from 14.1±0.92 kJ to 17.85 ± 0.50 kJ (Table 4.1). Adaptation of strains to both high and low temperature regimes is dominated by the intensity of light. This is performed by enhancing the capacity to ingest nitrogen and carbon, which enables the storage of a greater quantity of carbon biomass. Microalgae maintain their cellular energy level by undergoing metabolic changes, balancing stoichiometric elements, and acquiring nutrients in response to environmental variations.

Correlation of carbon and nitrogen to light and temperature regime: In temperature regime experiments, both carbon and nitrogen fixation were observed to increase linearly with light intensity (Figure. 4.8A & B). Nitrogen fixation follows the same linear relationship in both high and low temperature regimes (r^2 = 0.58); however, as discussed, the nitrogen fixation rate was greater in the high temperature regime experiment. Studies conducted at both high and low temperatures revealed a linear relationship between the rate of carbon fixation and temperature, with r^2 = 0.94, p = 0.02 at high temperatures and r^2 = 0.89, p = 0.01 at low temperatures. However, the link between carbon fixation and temperature was stronger in experiments done at higher temperatures. Carbon and nitrogen fixation are extremely

significant and therefore are corelated to each other; however, the correlation is greater at higher temperatures (p = 0.007) in contrast to the low temperature regime (p = 0.01). The balance between carbon and nitrogen fixing is crucial for sustaining carbon accumulation in biomass at increased CO_2 levels (Figure. 4.8B).

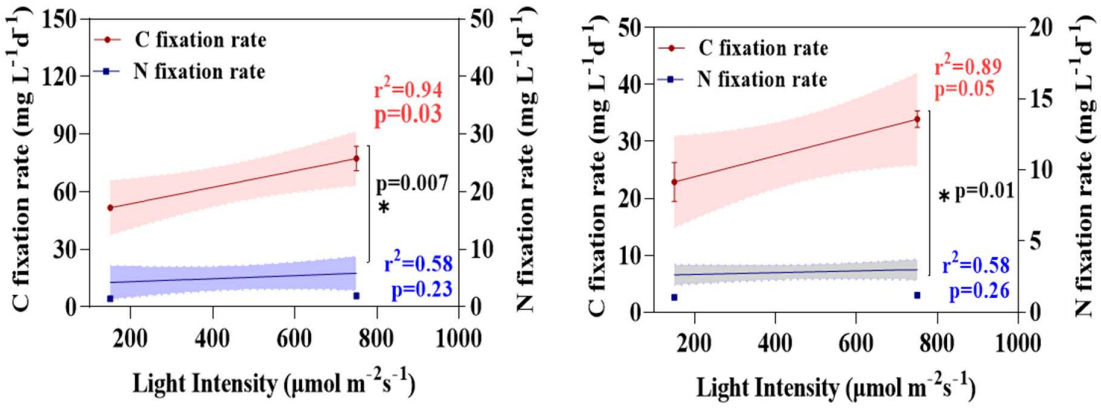

Fig. 4.8. Effect of different (**A**) high temperature regime and (**B**) low temperature regime condition on carbon and nitrogen fixation. All data points represent the mean of n=2 biological replicates; error bars represent the replicates' standard deviation. Light pink and blue area represent 95% of confidence interval. The graph displays the Pearson correlation *(p)* derived from a multiple linear regression analysis of carbon and nitrogen fixation under various light and temperature conditions.

Table 4.1 Elemental stichometry bioenergy and carbon yield of *M.pusillum* in different treatment conditions

Culture Condition	Elementary composition (%)				HHV KJ g^{-1}	C: N mol:mol	Biomass yield (mmol C L^{-1})	Bioenergy (KJ)	Bioenergy productivity (KJ $L^{-1}d^{-1}$)
Temperature	C	H	N	S					
15℃	49.82	4.34	5.27	0.55	21.56	11.04 ± 0.75	21.86 ± 2.14	27.34 ± 1.25	1.39 ± 0.03
25℃	48.17	5.53	5.93	0.61	22.40	9.57 ± 1.06	48.26 ± 2.73	48.51 ± 2.31	2.89 ± 0.15
35℃	52.87	7.12	4.78	0.26	25.97	13.08 ± 1.09	50.08± 1.92	58.82 ± 0.35	3.39 ± 0.01
Light (µmol $m^{-2}s^{-1}$)									
50	50.25	6.17	5.82	0.50	23.87	10.22 ± 1.13	19.11±1.12	25.97 ± 1.83	1.58 ± 0.19
200	51.34	6.70	4.72	0.42	26.02	14.04 ± 0.60	51.06± 1.96	49.25 ± 2.12	3.60 ± 0.35
750	52.27	6.75	4.05	0.35	26.59	14.71 ± 0.41	41.02± 0.94	49.82 ± 2.52	3.65 ± 0.27
Dural temperature									
38/25℃ (LL)[a]	50.92	6.86	4.26	0.37	25.18	14.03 ± 0.12	25.58 ± 0.32	31.71 ± 0.77	1.93 ± 0.03
38/25℃ (HL)[b]	51.96	6.84	3.79	0.17	25.62	16.22 ± 1.15	38.65 ± 1.26	45.15 ± 0.79	3.08 ± 0.06
21/12℃ (LL)	46.64	5.28	5.39	0.47	21.63	10.09 ± 0.54	11.45 ± 1.21	14.1 ± 0.92	0.80 ± 0.07
21/12℃ (HL)	48.93	5.70	4.28	0.39	23.01	13.21 ± 0.48	16.96 ± 0.82	17.85 ± 0.48	1.16 ± 0.52

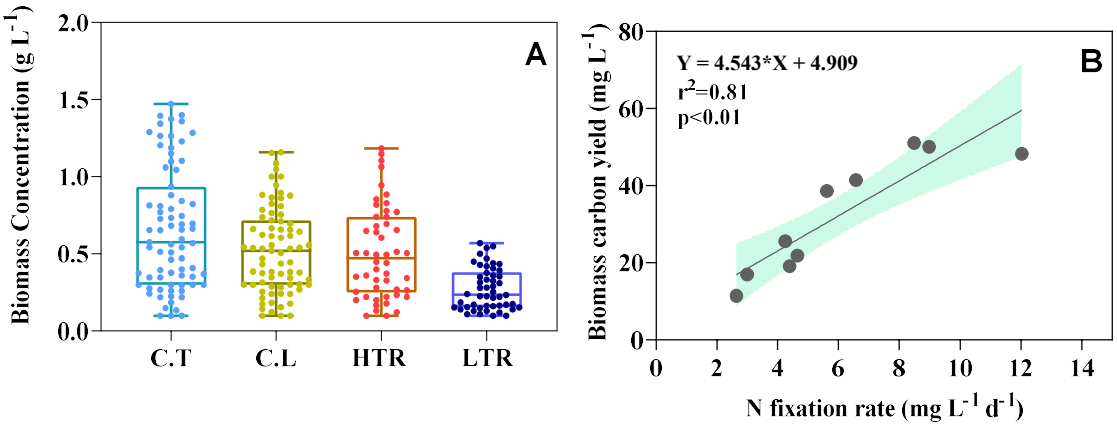

Fig. 4.9. (A) Box-whisker plot illustrating changes in the overall range of biomass growth in three different temperature (C.T.) and light treatment (C.L.) of three semi-continuous batch cycles and with high temperature (HTR, 38°C/25°C) and low temperature (LTR, 21°C/12°C) regimes of six cycles, three cycles each in two light intensities. **(B)** Overall nitrogen fixation-carbon yield correlation. Points show the average light and temperature conditions.

Table 4.2 Evaluation of CO_2 bio-mitigation with carbon and nitrogen fixation rate of *M.pusillum* in different treatment conditions

Temperature (°C)	**CO_2 fixation rate (mg L^{-1} d^{-1})**	**CO_2 utilization efficiency (%)**	**Carbon fixation rate (mg L^{-1} d^{-1})**	**Nitrogen fixation rate (mg L^{-1} d^{-1})**
15	160 ± 0.05	0.5 ± 0.07	43.5 ± 0.02	4.65 ± 0.51
25	355± 0.03	1.12 ± 0.1	97 ± 0.01	10.03 ± 0.43
35	370 ± 0.02	1.15 ± 0.06	99.3 ± 0.01	12.97 ± 1.03
Light intensity (µmol $m^{-2}s^{-1}$)	**CO_2 fixation rate (mg L^{-1} d^{-1})**	**CO_2 utilization efficiency (%)**	**Carbon fixation rate (mg L^{-1} d^{-1})**	**Nitrogen fixation rate (mg L^{-1} d^{-1})**
50	140 ± 0.02	0.44 ± 0.04	38.21 ± 0.02	4.39 ± 0.23
200	370 ± 0.01	1.18 ± 0.06	102 ± 0.01	8.48 ± 0.27
750	310 ± 0.02	0.96 ± 0.05	82.8 ± 0.02	6.58 ± 0.02
Diurnal temperature	**CO_2 fixation rate (mg L^{-1} d^{-1})**	**CO_2 utilization efficiency (%)**	**Carbon fixation rate (mg L^{-1} d^{-1})**	**Nitrogen fixation rate (mg L^{-1} d^{-1})**
38/25°C (LL)	190 ± 0.01	1.33 ± 0.01	51.16 ± 0.01	4.25 ± 0.05
38/25°C (HL)	280 ± 0.02	2.03 ± 0.14	78.25 ± 0.01	5.62 ± 0.12
21/12°C(LL)	80 ± 0.01	0.59 ± 0.06	23.43 ± 0.01	2.64 ± 0.14
21/12°C (HL)	120 ± 0.01	0.88 ± 0.03	33.92 ± 0.01	3.03 ± 0.18

4.4 Conclusion

Overall, this research showed that the growth rate, lipid and carbohydrate levels, efficiency of CO_2 utilization, and bioenergy production of *M. pusillum* are greatly affected by temperature, light intensity, and daily temperature patterns. *M. pusillum* has shown its promise as a bioenergy source with carbon capture and storage, especially in tropical areas such as Assam, by achieving the maximum biomass productivity and bioenergy output under high light and temperature conditions. Nevertheless, the occurrence of poor production was noted at very cold winter temperatures, which may be alleviated by increased light intensity. The range of CO_2 utilization efficiency varied from 0.32% to 2.03%, with values above 1.5% under ideal circumstances. The lipid content ranged from 23% to 34%, consisting of C-18 and C-16 fatty acids that are ideal for the generation of biodiesel. By exposing the strain to high light and temperature conditions, the quality of the biomass was improved by controlling and restructuring metabolites with a carbon content above 50%, while maintaining normal levels of photosynthesis and growth. The rapid metabolic adjustments and acclimation responses of *M. pusillum*, together with its exceptional ability to mitigate CO_2, demonstrate its ability to thrive in outdoor settings with diverse light and temperature conditions. The availability of nitrogen played a vital role in influencing the process of carbon utilization in biomass under all circumstances. This was evident from the positive linear connection ($r^2 = 0.81$) observed between the rate of nitrogen fixation and the yield of carbon. Optimizing nitrogen levels is crucial under varying CO_2, light, and temperature circumstances. Semi-continuous operation improves the efficiency of microalgae-based carbon dioxide reduction and bioenergy production, hence increasing its economic viability. These results provide crucial insights for the development of a sustainable 'Microalgae Bioenergy with Carbon Capture and Storage System' for future large-scale production.

CHAPTER 5

Process engineering strategy for enhancing CO_2 utilization and biomass-derived biochemical production

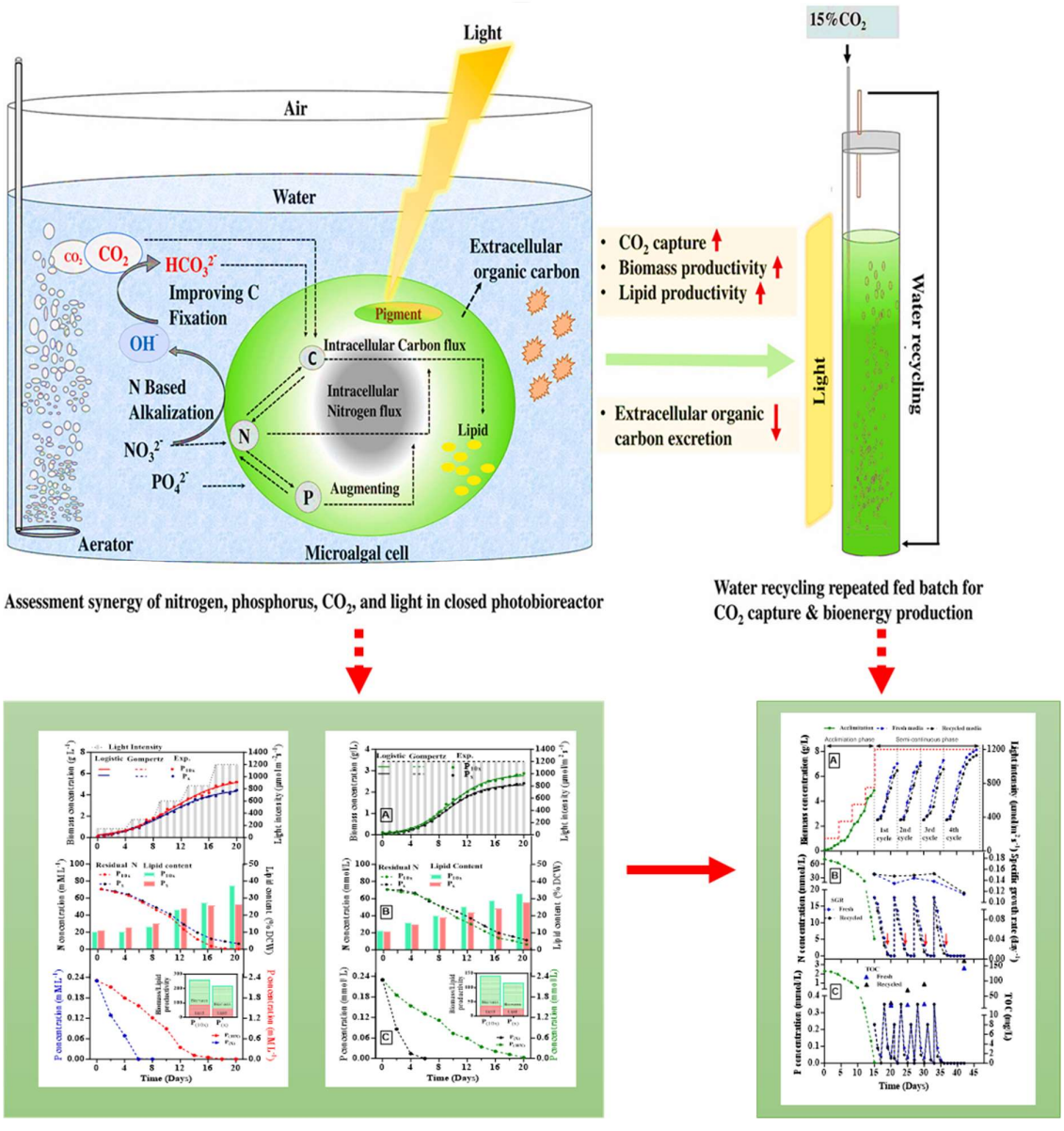

Chapter 5

Process engineering strategy for enhancing CO_2 utilization and biomass-derived biochemical production

5.1 Background and motivation

The pursuit of sustainable and scalable processes for microalgal-based CO2 capture and bioenergy production hinges upon strategic process engineering. This approach aims not only to enhance CO_2 utilization but also to optimize the assimilation of carbon energy molecules, specifically lipids, thereby improving economic viability and sustainability. A significant challenge in microalgal cultivation is the substantial water requirement exacerbated by the release of dissolved organic carbon (DOC), which impedes the recycling and reusability of cultivation media and nutrients. The interplay between nitrogen, phosphorus, and light profoundly influences key biological processes in microalgae, including photosynthesis, CO_2 fixation, and the regulation of DOC release crucial for water recyclability. Understanding these dynamics is essential for enhancing microalgal biomass production towards CO_2 reduction and lipid synthesis. This understanding becomes particularly critical in mitigating the effects of CO_2 saturation and ensuring efficient carbon fixation under elevated CO_2 conditions. This study focuses on *Micractinium pusillum* KMC8 and investigates the impact of initial nitrogen levels on growth dynamics, CO_2 utilization, organic carbon excretion, and their interactions with carbon and nitrogen assimilation, emphasizing biomass production. Furthermore, it explores the relationship between phosphate availability, light conditions, and two photobioreactor strategies, offering insights into microalgae adaptability, carbon and nitrogen assimilation, and lipid production.

.

Long-term productivity and CO_2 mitigation strategies are evaluated in a semi-continuous cultivation system incorporating media recycling. The study assesses biomass productivity and carbon utilization across multiple cycles, emphasizing optimal nitrogen concentrations for growth and nitrogen utilization under a 15% CO_2 environment. Kinetic models such as Logistic and Gompertz are employed to analyze KMC8 cell growth dynamics, revealing that varying nitrogen concentrations impact biomass growth and lipid productivity differently. Moreover, the study investigates the effects of phosphorus availability and light intensity on microalgal performance. Incremental increases in light intensity coupled with sufficient phosphorus significantly enhance biomass and lipid productivity, demonstrating improved CO_2 utilization efficiency compared to constant high light conditions. Finally, this study proposes a water recycling-fed batch cycle with gradual light feeding, resulting in substantial CO_2 fixation, enhanced biomass and lipid productivity, and efficient lipid synthesis.

The key results indicate a robust connection between nitrate levels and the development of microalgae. Higher concentrations of nitrogen have a considerable positive impact on biomass production and prolong the period of exponential growth. An increase of four times in nitrogen concentration (70.6 mmol/L) led to a 28.78% increase in biomass (2.06 g L^{-1}) and a 30.34% enhancement in productivity (140 mg $L^{-1}day^{-1}$) compared to the control. In contrast, the lack of nitrogen significantly hindered growth, resulting in a substantial 67% decline in output when exposed to nitrogen levels of 0.25 times the normal concentration (4.42 mmol/L). Furthermore, the availability of nitrogen significantly influenced both the efficiency of photosynthesis and the accumulation of lipids. Increased nitrogen levels at 70.6 mmol/L enhanced photosynthetic efficiency and decreased lipid content. Conversely, nitrogen deprivation greatly boosted lipid output. Significantly, the lipid content increased to 26% when the nitrogen level was low (4.42 mmol/L), however the development of biomass was impeded. Nitrogen has a dual function in regulating pH and assimilating CO_2, since higher nitrogen levels improve the ability to buffer pH and enhance the efficacy of CO_2 mitigation.

Phosphorus and light conditions further influenced growth and lipid productivity, with higher phosphorus (2.3 mmol/L) and initial high light intensity (1200 µmol/m^2 s^{-1}) leading to improved biomass (2.87 g L^{-1}) and lipid productivity (34.34 mg L^{-1} day^{-1}). A gradual increase in light intensity also positively affected growth, with a 17.49% rise in biomass productivity (255 mg L^{-1} day^{-1}) under high phosphorus. Finally, an acclimatized high cell density repeated fed-batch strategy using reused media demonstrated stable performance in biomass and lipid productivity. Reused media showed periodic fluctuations in productivity, with a notable 23%

increase in average lipid productivity compared to fresh media. CO_2 fixation rates and organic carbon excretion patterns indicated metabolic adaptations to nutrient availability and cycling conditions. Overall, this study underscores the critical role of nitrogen in optimizing microalgal growth, photosynthesis, lipid productivity, and CO_2 mitigation, providing insights for enhancing biofuel production and carbon sequestration using *M. pusillum*.

5.2 Materials and methods

5.2.1 Microalgal strain and culture conditions

For this study the culture was maintained in a 500 mL reagent bottle (Borosil 1501024) containing carbon-free BG11 medium as described in section 3.2.1, 15% CO_2 mixed with compressed air was used as sole carbon source by replacing sodium carbonate as carbon source in normal BG11 media. The bottle featured two perforations in the screw cap to facilitate air exchange as shown in Figure.5.1A. The culture volume was 400 mL, and air with carbon dioxide (15%) was supplied through one cap opening, at a rate of 50 ml min^{-1} regulated by a calibrated rotameter (section 3.2.2). A stone aerator was used at the base of the reactor to facilitate aeration. The culture was subjected to a light intensity of 150 µmol m^{-2} s^{-1} using three cool white tube lights (Philips 20-watt 6500k), with a 16:8 (light/dark) cycle at a room temperature of 25±3 ℃. The inoculum was cultured weekly under consistent conditions to enhance its adaptability to the elevated CO_2 conditions. On the 7^{th} day of the mid-logarithmic growth phase, cells were obtained from the culture by subjecting the culture broth to centrifugation at a force of 5000 g for a duration of 5 min. In all experiments, the resulting pellet was resuspended to maintain an initial cell density of 0.1 g L^{-1}. This density was monitored and controlled by measuring optical density (OD_{680}), with 1 OD_{680} corresponding to 0.22 g DCW L^{-1} [297]. In all experiments, the pH was not controlled, including the preparation of the inoculum.

5.2.2 Culture in different nitrogen concentration

The experiments utilized different nitrogen levels to examine the impact of nitrogen concentration in 500 mL reagent bottle (Figure.5.1A). The nitrogen concentrations used in this study were as follows: a standard BG11 media concentration of 17.65 mmol L^{-1} (1x) of nitrate nitrogen, which stayed as the control, and four additional levels: 4.42 and 8.83 mmol L^{-1} (0.25x

and 0.5x, representing nitrogen limitation), as well as 35.3 and 70.6 mmol L^{-1} (2x and 4x, representing nitrogen sufficiency) and one with without nitrogen. All experiments were conducted in duplicate for 15 days using a reagent bottle under identical culture conditions as previously described for inoculum preparation (section 5.2.1).

Fig. 5.1. (A) Schematic diagram of Reagent bottle experiment **(B)** Real experimental setup picture **(C)** Attached air and CO_2 rotameter

5.2.3 Culture in different light and phosphorus condition

This study utilized a previously described custom photobioreactor with controlled and adjustable light conditions as described in section 3.2.2 to assess the impact of different phosphorus concentrations and light conditions. In a 20-day batch process, two phosphorus levels were examined: a standard concentration of 0.23 mmol L^{-1} (1x) representing BG11 media, and a high concentration of 2.3 mmol L^{-1} (10x), under two distinct light conditions. A light intensity of 1200 µmol m^{-2} s^{-1} with 16:8 (light: dark) cycle was consistently maintained for 20 days. The second condition entailed a progressive augmentation in light intensity. The experiment began with an initial light intensity of 150 µmol /m^2 s^{-1} for four days. This was then increased to 300, 600, and 850 µmol m^{-2} s^{-1} for four days each, before reaching a final intensity of 1200 µmol m^{-2} s^{-1}. The light intensity in the photobioreactor was regulated by adjusting the power output using a DC regulator (Metravi RPS-3005 DC India) and the distance

of the light source. The intensity was measured using a quantum meter (MQ-200, Apogee Instruments, Logan, UT). Aeration in the reactor was accomplished by utilizing a customized silicone fine bubble, double ring sparger positioned at the bottom (Figure.5.1B), with a flow rate of 200 mL min^{-1} (0.1 vvm, volume of gas per volume of culture per min). Four distinct batch runs were carried out to investigate the growth, nutrient fixation, and CO_2 mitigation processes within specific time intervals (0-4, 5-12, and 12-20 days), with a focus on understanding the adaptable exponential phase and nutrient requirements.

5.2.4 Process of operation procedure for repeated fed-batch culturing with water recycling

The cultivation process began with a 15-day batch culture phase, during which the light intensity progressively escalated in accordance with the prescribed gradual light feeding strategy as mentioned in above section 5.2.3, thereafter maintaining a consistent level of 1200 µmol m^{-2} s^{-1}. After this stage, around 45-50% of the culture broth volume was collected and then centrifuged at 3000 rpm for 3 min to separate the microalgal biomass. The harvested medium was recycled as the culture medium for subsequent microalgae cultivations, transitioning to a fed-batch cultivation mode. The recycled medium was supplemented with nitrate, phosphorus, sulphur, and trace metals to match the standard concentration of BG11 media. The phosphate pulse-feeding was carefully timed to coincide with a specific fourth-day interval, when nitrate concentrations in the medium consistently stayed below 4 mmol L^{-1}. The cultivation process was repeated for four cycles, each lasting 7 days, except for the final cycle which lasted 10 days to ensure optimal nutrient utilization.

5.2.5 Microalgal Growth, lipid production and Photosynthesis Performance

The microalgal growth study is conducted using an equation that relates optical density to dry cell weight by equation 3.2 mentioned in previous chapter 3 n. Additionally, the parameters of biomass production and specific growth are assessed using an equation provided in the methodology part of chapter 3 by equation 3.5 and 3.6.

Microalgal growth data were subjected to modelling using GraphPad Prism 10 software. The Monad kinetic model was employed to simulate the effect of nitrogen concertation on growth rate by Eqs. 5.1. The Logistic or Gompertz models were employed for

the analysis of growth parameter. The equations for the general form of the Logistic and Gompertz equations were presented in Eqs. 5.2 and 5.3 respectively. The parameters of the kinetic equation were defined as follows: the growth rate (μ, day^{-1}), maximum growth rate (μ_{max} day^{-1}), initial nitrogen concentration (S_i, mmol/L), half saturation constant (K_m, mmol/L). The starting biomass (X_i, g/L), maximum biomass ($X_{max.}$, g/L), growth rate constant (μ, day^{-1}), time (t, day), and the biomass (X, g/L).

$$\mu = \frac{\mu_{max.} \times [S_i]}{k_m + [S_i]} \tag{5.1}$$

$$X = \frac{X_{max.} \times X_i}{(X_{max.} - X_i) \times exp^{(-\mu \times t)} \times X_i} \tag{5.2}$$

$$X = X_{max,} \times \left(\frac{X_i}{X_{max.}}\right)^{exp(-\mu \times t)} \tag{5.3}$$

Photosynthesis performance was analyzed by quantification of pigment using a spectrophotometric method and, the maximal photochemical efficiency of Photosystem II (F_v/F_m) using a pulse amplitude-modulated fluorometer as described in previous chapter 3 methodology section 3.2.6.4.

The estimation of lipid content was conducted by the use of the Nile red fluorescent technique, as described in previous chapter 3 methodology section 3.2.6.5.

5.2.6 Nutrient and CO_2 fixation and utilization

To analyses the nitrate and phosphate, 1 mL volume of the sample was centrifuged at 10,000 rpm for 10 minutes. The resulting supernatant containing the cells was collected and used for chemical assays. Nitrate estimation was conducted using the salicylic acid method with sodium nitrate as the standard [316]. Phosphate quantification was performed using the ascorbic acid method with dipotassium phosphate as the standard [317]. Michaelis-Menten kinetics model employed to evaluate the impact of initial nitrogen concentration on the rate of nitrogen consumption by Eq. 5.4. Nutrient removal and fixation rate (mmol/L day^{-1}) were determined by Eqs.5.5 and 5.6 [318]. Carbon and nitrogen fixation rate (mmol/L day^{-1}) measured on the basis of elemental basis of carbon and nitrogen content in biomass (% w/w).

The carbon and nitrogen content in dry biomass were measured using a CHNS analyzer, by the Perkin Elmer elementary analyzer, PE-2400, series.

$$V = \frac{V_{max} \times [S_i]}{K_m + [S_i]} \tag{5.4}$$

$$Nutrient\ utilizatation\ rate = \frac{S_i - S_f}{t_f - t_i} \tag{5.5}$$

$$Nutrient\ fixitation\ rate\ = \frac{(X_f \times E_f\ -\ X_i \times E_i)}{t \times M_E} \times 1000 \tag{5.6}$$

where, V and V_{max} represent specific rate consumption rate and maximum specific rate consumption of nitrogen (mmol/g DCW day^{-1}), S_f and S_i (mg/L) represent the finial and initial cell concentration of nitrogen and phosphorus at time of harvesting t_f and initial day of inoculation t_i.; E_f, Ei, and M_E represents the final and initial carbon and nitrogen content (%w/w) and their respective molecular weight .

The CO_2 capture capability was assessed by measuring the rate of CO_2 fixation (mg/L day^{-1}) and the efficiency of utilization (%) using elemental carbon analysis of biomass, as explained in the previous part of chapter 3 methodology section 3.7 and 3.8. The cellular C/N ratio indicates the ratio of carbon to nitrogen in the biomass (mol/mol).

$$Cellular\ \ C/N\ ratio = \frac{C/M_C}{N/M_N} \tag{5.7}$$

Eq.5.7 defines the C and N as the concentrations (g) of total carbon and nitrogen biomass growth (g/L), respectively. The variable M_C and M_N represents the molecular mass of carbon and nitrogen.

5.3 Results and Discussion

5.3.1 Influence of initial nitrogen concentration on growth

The study demonstrates a strong association between nitrate concentration and the growth of microalgae *M. pusillum*. Figure. 5.2A depicts the influence of nitrogen levels, specifically in the presence of 15% CO_2. Linear cell growth patterns in KMC8 cultures indicate

nitrogen limitation, particularly when initial nitrate concentrations are restricted. During the phase of mid-exponential development, the nitrogen concentrations of 2x (35.3 mmol/L) and 4x (70.6 mmol/L) were found to be comparable to those of the control BG-11 medium (1x=17.65 mmol/L). The control group achieved a biomass of 1.6 g L^{-1}. Doubling the nitrogen concentration led to a 12.5% rise in biomass growth, reaching a concentration of 1.8 g L^{-1}. A fourfold increase in nitrogen extended the exponential growth phase by three days, resulting in a 28.78% increase in growth to reach 2.06 g L^{-1}. The biomass productivity showed an increase from 107 mg L^{-1} day^{-1} under x conditions to 128 mg L^{-1} day^{-1} in 2x. It further reached 140 mg L^{-1} day^{-1} under 4x conditions, with enhancements of 19.25% (2x) and 30.34% (4x) compared to the control (x) (Figure. 5.3B). The specific growth rates showed a consistent pattern of increase, ranging from 0.19 day^{-1} to 0.23 day^{-1}, in relation to nitrogen concentration. Growth performance declined under nitrogen-deprived conditions of 8.83 mmol L^{-1} (0.5x) and 4.42 mmol L^{-1} (0.25x). The biomass productivity decreased by 18% to 88 mg L^{-1} day^{-1} when exposed to 0.5x nitrogen concentration.

The growth rate was measured at 0.18 day^{-1} and the biomass concentration reached 1.34 g L^{-1}. Under the 0.25x nitrogen condition, the productivity of microalgae decreased by around 67% to 35 mg L^{-1} day^{-1}. The growth rate was 0.12 day^{-1} and the biomass reached 0.6 g L^{-1}. The microalgae showed a truncated exponential phase and a prolonged stationary phase under nitrogen deprivation conditions (0.5x and 0.25x). However, a significant decline in productivity and growth performance was observed specifically in the 0.25x nitrogen condition.

Figure 5.2A shows parameters for *M. pusillum* derived from Logistic and Gompertz models. Table 5.1 shows data of KMC8 maximum growth (X_m) and specific growth rate (μ). Nitrogen 4x condition had significant growth, while nitrogen 2x condition had highest growth rate. R^2 values were consistently high (0.962-0.991) across all experiments, regardless of the equation used (Logistic or Gompertz). Highly significant Monod kinetic model with R^2 =0.99 also proves the significant effect of nitrogen on growth rate (Figure. 5.3C). The culture with no nitrogen did not show any growth and the culture become pale yellow in color so no further analysis was study further by normal observation culture. Upon general observation, the culture appeared to be nonviable.

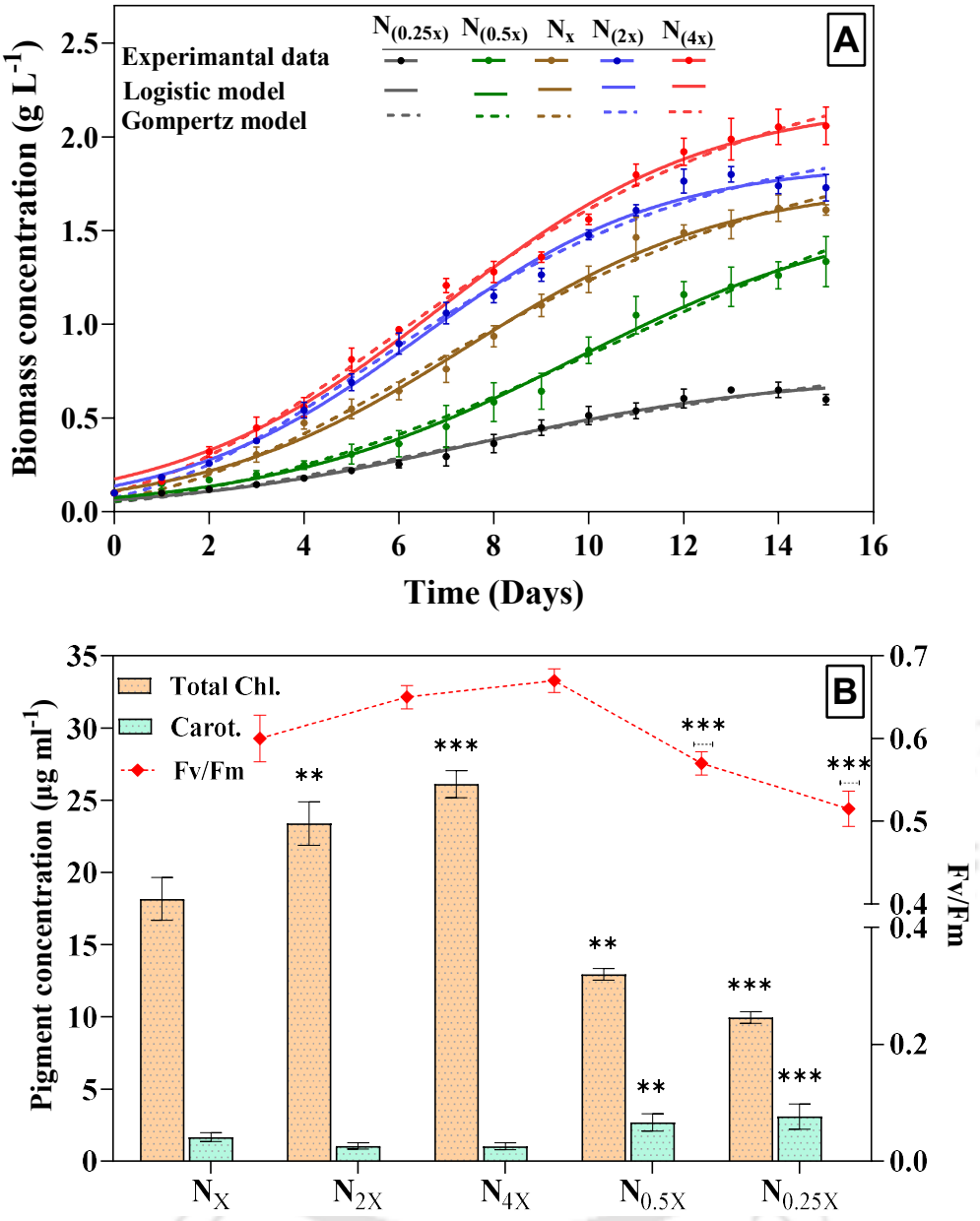

Fig. 5.2. Growth and photosynthetic performance of *M. pusillum* at five nitrogen concentrations. **(A)** Dynamic growth profile modelled applying Logistic and Gompertz models. **(B)** Fv/Fm and photosynthetic pigment data. Error bars depict the standard deviation of n=2 biological replicates. Asterisks indicate significant differences between the control (Nx = 1.76 mmol/L) and the other concentrations, as determined by one-way ANOVA (Tukey's method). Significance in growth conditions is denoted by different symbols: no asterisk ($p = 0$), single asterisk *(* $p < 0.05$)*, double asterisk *(** $0.05 < p < 0.5$)*, and triple asterisk *(*** $0.5 < p < 1.0$)*

Table 5.1. Model of *M.pusillum's* kinetic growth at five different nitrogen concentrations in a 500 ml reagent bottle.

Experimental condition	Model	X*i* (g/L)	X*max* (g/L)	μ (day^{-1})	R^2
N concentration (x=17.3mmol/L)					
$N_{(0.25x)}$	Logistic	0.06	0.72	0.308	0.971
	Gompertz	0.05	0.91	0.149	0.962
$N_{(0.5x)}$	Logistic	0.07	1.62	0.312	0.975
	Gompertz	0.05	2.56	0.122	0.969
$N_{(x)}$	Logistic	0.12	1.75	0.360	0.989
	Gompertz	0.06	2.04	0.192	0.987
$N_{(2x)}$	Logistic	0.13	1.86	0.392	0.990
	Gompertz	0.07	2.04	0.228	0.989
$N_{(4x)}$	Logistic	0.17	2.19	0.354	0.988
	Gompertz	0.10	2.47	0.200	0.991

5.3.2 Photosynthetic nitrogen deprivation and lipid productivity

The initial availability of nitrogen has a significant impact on photosynthesis, nitrogen assimilation, and lipid accumulation. This has been shown through various experimental and model-based studies. As seen clearly from Figure. 5.3C and Figure. 5.3D both the Michaelis-Menten and Monod kinetics models highlight the significance of adequate nitrogen supply both on growth and nitrogen consumption with R^2 value of 0.99. The Monod model specifically indicates a half-saturation value (K_m) of 3.35 mmol L^{-1} (Figure. 5.3D). The Michaelis-Menten equation (Figure. 5.3C) illustrates the impact of nitrogen on the specific nitrogen consumption rate, with a K_m value of 45.45 mmol L^{-1}. Nitrogen deficiency was observed in the control and low nitrogen conditions, with concentrations of 17.65 mmol L^{-1}, 8.83 mmol L^{-1}, and 4.42 mmol L^{-1} on different days. This deficiency had an impact on cellular processes. The quantum yield of photosystem II was reduced under extended nitrogen deprivation, as indicated by quantum values of 0.51 and 0.57 at low nitrogen levels 8.83 and 4.42 mmol L^{-1} (Figure. 5.2B). Higher nitrogen concentrations (17.6, 35.3, and 70.6 mmol/L) resulted in improved photosynthetic performance, as evidenced by increased chlorophyll content and a peak quantum value of 0.67, especially at 70.6 mmol L^{-1}. Increased nitrogen levels resulted in a decrease in carotenoid and lipid concentrations, as shown in Figure. 5.2B and 5.3B. The lipid content was found to be 9.84% and 7.87% (w/w of DCW) in the 2x and 4x conditions, respectively. The lipid

productivity rates observed were 12.68 mg L^{-1} day^{-1} and 11.52 mg L^{-1} day^{-1}, which were not significantly different from the control conditions (12.14% lipid content and 12.48 mg/L day^{-1} lipid productivity). Nitrogen deprivation at concentrations of 8.83 and 4.42 mmol L^{-1} resulted in a significant increase in lipid productivity. Specifically, at 8.83 mmol L^{-1}, lipid content reached 22.4% and productivity reached 18.62 mg L^{-1} day^{-1}. At a concentration of 4.42 mmol L^{-1}, the lipid content reached 26%, but the growth of biomass was reduced, resulting in a 50% decrease in lipid productivity. This reduction was caused by a shortened exponential growth phase, as shown in Figure. 5.2A. The study indicates that lipid productivity can be increased by combining nitrogen limitation and short-term starvation conditions. Insufficient nitrogen levels 4.42 mmol L^{-1} can impede biomass growth and subsequently impact lipid productivity.

The nitrogen supply has a critical role in maintaining the buffering capacity of a microalgal culture, which is essential for increasing the accessibility of inorganic carbon [62]. The results of our study are consistent with prior research, indicating that a continuous supply of nitrogen is crucial for achieving the best buffering capacity, which in turn enhances the growth of microalgae and their effectiveness in photosynthesis [79]. On the other hand, if nitrogen deprivation is protracted, it will have a detrimental effect on the culture's ability to resist changes in acidity, leading to a decrease in growth and efficiency of photosynthesis. This state results in the buildup of carbon-rich reserve compounds, deterioration of the photosynthetic system, and the development of pyrenoid structures. These observations emphasize the intricate equilibrium necessary to provide a continuous supply of nitrogen that can meet the metabolic needs of microalgae, affecting crucial physiological processes and cellular architecture [277].

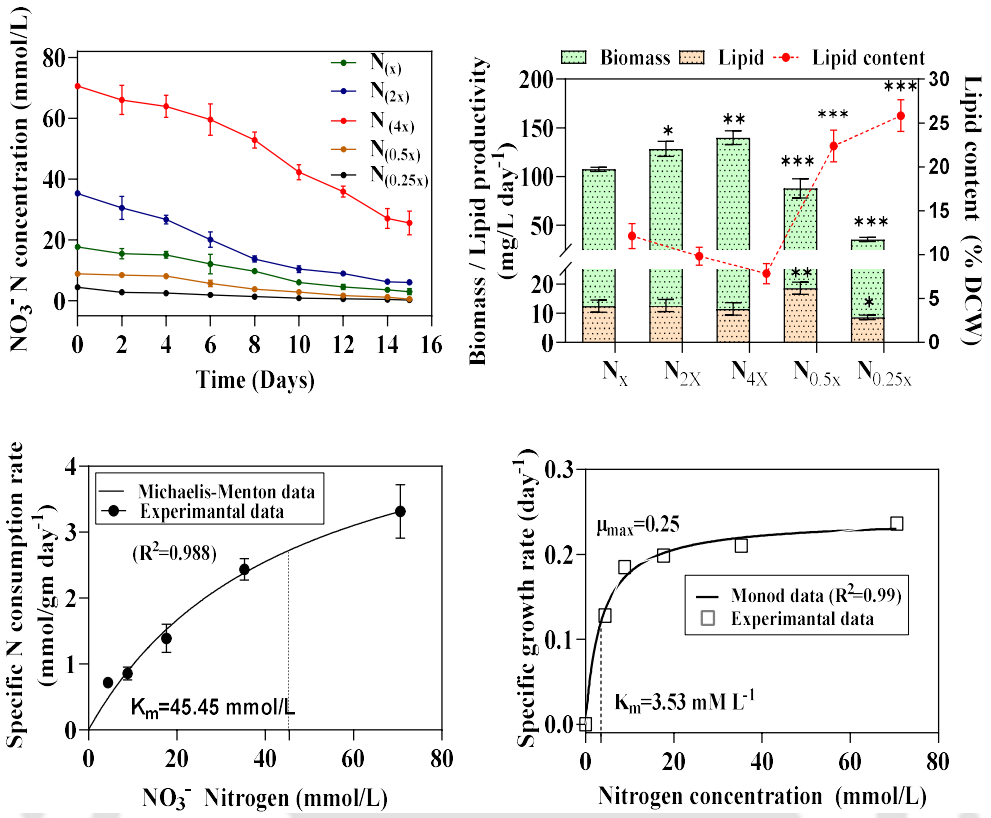

Fig. 5.3. **(A)** Residual nitrogen concentration under five nitrogen levels with Nx as the control. **(B)** Biomass and lipid productivity, with lipid content. Asterisks denote significant differences from the control (Nx = 1.76 mmol/L) using one-way ANOVA (Tukey's method) for biomass and lipid productivity. Comparison of experimental and simulated data for **(C)** Michaelis-Menton and **(D)** Monod model, displaying *Km* values.

5.3.3 Nitrogen dual role in pH regulation and CO_2 assimilation

The box and whisker plot in Figure. 5.4B illustrate pH fluctuations in microalgae cultivation at varying nitrogen concentrations. Significant pH variations are observed in the control, 2x, and 4x conditions, with a larger range between the first and third quartiles suggesting alkaline tendencies (pH > 6.8). The role of nitrate in pH regulation is consistent with previous studies (Cabello et al., 2015; Solovchenko et al., 2016a; Young and Beardall, 2005). Nitrate-based nitrogen alkalization involves the incorporation of hydrogen through proton exchange during nitrogen assimilation, achieving charge neutrality by substituting cations [205]. The average pH levels consistently surpass 6.8 in all three nitrogen conditions, with a slight elevation above 7 in the 4x condition. The condition of 0.5x maintains a stable pH

level between 6 and 5.2. In contrast, the condition with a 0.25x concentration shows a small range between the first and third quartiles and a high degree of variability in pH, indicating a tendency towards acidity. The decrease in pH (below 6) observed in the 0.5x and 0.25x conditions can be attributed to a depletion of nitrogen. Nitrogen availability and fixation are important factors in regulating CO_2 dissolution and the availability of inorganic carbon for microalgae growth [62]. Resilience could be associated with nitrogen depletion, which temporarily interrupts buffering mechanisms involved in nitrogen assimilation, as discuss in above section 5.3.2.

This study evaluates the ability of microalgae to utilize CO_2 by measuring the amount of carbon fixed in biomass and the rate at which CO_2 is incorporated. The carbon dioxide utilization efficiency *of M. pusillum* increased over a 15-day maturation period with increased nitrogen concentration from 4.42 to 70.6 mmol L^{-1}. The values showed a rise from 0.65% to 2.27%, along with CO_2 fixation rates ranging from 70.6 to 250.4 mg L^{-1} day^{-1} (Figure. 5.4A). Elevated nitrate levels are expected to enhance the pH buffering capacity of the medium, leading to a more neutral or alkaline pH. The impact of nitrogen addition on pH levels offers valuable information on the dissolution of CO_2 and the reduction of accumulation of carbonic acid in culture media [42].

The study demonstrates an increase in nitrogen concentration, as indicated by Figure. 5.4A and Figure. 5.4B, which show a rise in pH. The notable rise in nitrogen content is strongly linked to a substantial improvement in the ability to mitigate CO_2, primarily due to the nitrogen-based buffering mechanism. This is because the assimilation of nitrogen by microalgae directly affects the dynamics of CO_2 [62]. The impact is particularly notable at 2x and 4x levels, resulting in a 1.8 and 2-fold increase in CO_2 mitigation potential, specifically in terms of fixation and utilization value, compared to the control.

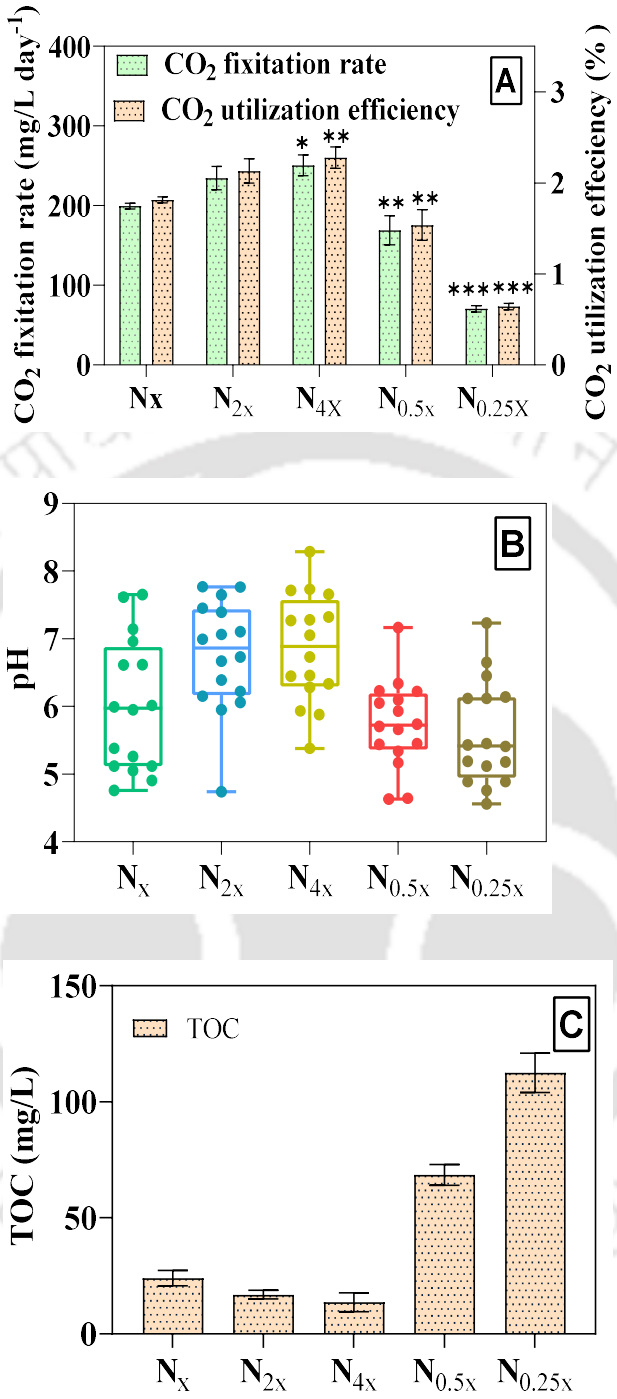

Fig. 5.4. (A) CO_2 fixation rate and utilization efficiency under five nitrogen concentrations, with Nx as the control. **(B)** Box and whisker plot illustrating the distribution of pH values. The central box represents the interquartile range (IQR), with the median indicated by the line inside. Whiskers extend to the minimum and maximum values, while data points beyond the whiskers are considered outliers. **(C)** Total organic carbon concentration in the media.

5.3.4 Relationship between photosynthetic carbon and nitrogen fixation with initial nitrogen availability

This study explores the impact of nitrogen treatment on carbon and nitrogen fixation rates and the elemental content of carbon and nitrogen in KMC8 biomass. It sheds light on the intricate relationship between nitrogen availability and the balance of carbon and nitrogen dynamics in biomass. Increasing nitrogen concentration from 4.42 to 70.6 mmol L^{-1} in the medium reduced carbon content in the biomass from 53.34% to 48.89% DCW with a negative linear relationship (R^2=0.78, p=0.023). Conversely, nitrogen content increased from 4.12% to 7.25% DCW with a positive relationship (R^2=0.80, p=0.03) (Figure. 5.5A and Figure. 5.5C). These findings align with previous studies emphasizing nitrogen's role in microalgae proliferation and CO_2 sequestration via photosynthesis [80,113,209,210]. The augmentation of nitrogen content in the medium resulted in a significant increase in the rates of both carbon and nitrogen fixation. The observed augmentation had a hyperbolic trajectory, specifically linked to the phase of stationary, when nitrogen contents were elevated. The correlation between nitrogen concentration (mmol/L) and carbon fixation rate (mmol/L day^{-1}) had an R^2 value of 0.92, while the nitrogen fixation rate exhibited a very significant association with an R^2 value of 0.96 (see Figure. 5.5B and Figure. 5.5D). This suggests an optimal nitrogen concentration range for efficient assimilation of both nitrogen and carbon, promoting biomass growth. Increasing nitrogen concentrations from 4.42 to 8.85, and 17.65 mmol L^{-1} corresponded to increased nitrogen and carbon biomass fixation, with carbon fixation rates of 5.05, 11.79, and 15.4 mmol L^{-1} day^{-1}, respectively. In contrast, elevated nitrogen concentrations (35.3 and 70.6 mmol/L) did not result in significant increases, with rates of 16.5 and 17.65 mmol L^{-1} day^{-1}, showing only a 7.12% and 18% rise compared to the control (17.65 mmol/L nitrogen). However, under nitrogen-limiting conditions (0.25x and 0.5x), carbon fixation rate decreased significantly by 67.15% and 23.52%, respectively. Assimilation of nitrogen followed a predictable pattern, with a higher correlation between nitrogen availability and fixation in biomass than with carbon. Increasing nitrogen from 4.42 to 8.85 mmol L^{-1} led to a threefold increase in nitrogen fixation rate, rising from 0.08 to 0.24 mmol L^{-1} day^{-1}. At 17.65 mmol L^{-1}, the rate doubled to 0.45 mmol L^{-1} day^{-1}. Slight increase of 1.12-fold and 1.18-fold occurred at 35.3 and 70.6 mmol L^{-1}, corresponding to 0.55 and 0.64 mmol L^{-1} day^{-1}, respectively. The study highlights the delicate balance between cellular nitrogen levels, primarily through protein breakdown, and carbon biomass accumulation, particularly lipid synthesis. The complex interaction between nitrogen availability has a substantial impact on important biological

processes in microalgae, which is assisted by mechanisms that fix nitrogen [319,320]. The observations made indicate that microalgae may have limitations in their ability to absorb excessive amounts of nitrogen, showing a subtle feature. Significantly, residual nitrogen levels of 40% and 20% remain in the growth medium when nitrogen concentrations are four times and two times higher than the standard, respectively. This suggests that variables other than the availability of nitrogen, such as the availability of light or interactions with other nutrients, may play a role in restricting the efficient conversion of carbon and nitrogen into biomass [321].

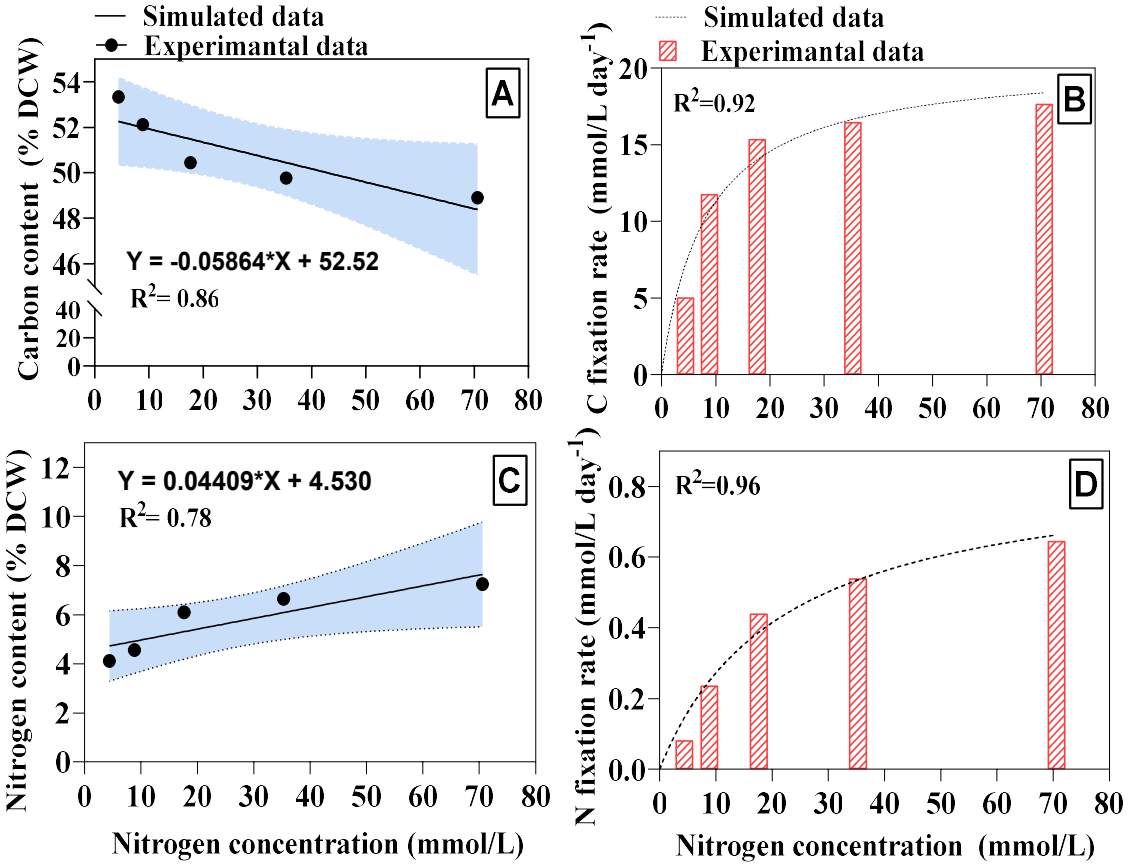

Fig. 5.5. (A) Carbon content & **(B)** carbon fixation rate as a function of five nitrogen concentrations. The light blue area shows the 95% confidence interval. **(C)** Nitrogen content & **(D)** nitrogen fixation rates as a function of nitrogen concentration. The graph shows the results of linear and nonlinear regression analyses (R^2) of carbon and nitrogen content and fixation rates.

5.3.5 Influence of initial nitrogen on organic carbon excretion

An increase in the initial nitrogen concentration resulted in a decrease in the levels of total organic carbon (TOC) with value of 13.67 < 16.9 < 24.12 < 68.55 < 112.5 mg L^{-1} at the concentrations 70.6, 35.3, 17.65, 8.85 and 4.42 mmol L^{-1}. This observation implies that the availability of nitrogen is crucial in controlling the excretion of organic carbon by microalgae. The levels of total organic carbon (TOC) exhibited an increase under low nitrogen conditions during a 15-day incubation period. This finding suggests a prolonged response to nitrogen limitation and depletion, wherein carbon assimilation through photosynthesis surpasses nitrogen assimilation. This imbalance leads to the accumulation of carbon compounds, such as lipids, as indicated in the aforementioned results, resulting in an excess of organic carbon [322]. During a cultivation period of 15 days, the microalgae experienced nitrogen starvation conditions on the fifth and eighth days, with concentrations of 8.85 and 4.42 mmol L^{-1}, respectively as discussed in section 5.3.2. When the microalgae were subjected to higher nitrogen concentrations (35.3 and 70.6 mmol/L), the total organic carbon levels dropped, since there was no nitrogen restriction condition in the 15-day batch. Ample nitrogen likely decreased the requirement for excessive organic carbon release, resulting in a more controlled carbon-nitrogen balance and fixation in response to elevated CO_2 levels.

Our next study will examine the impact of light intensity, phosphorus levels (control and high), and optimized nitrogen content (70.6 mmol/L) on the growth of microalgae. The used methodology employed a strategy of beginning with an elevated level of luminosity initially (Strategy I), while the other choice Strategy II included gradually increasing it. The research examined differences in the reduction of CO_2, the generation of biomass and lipids, and the release of organic carbon over three specific time intervals: 0-4 days (lag phase), 4-12 days (middle log phase), and 12-20 days (late log to stationary phase). The intervals were derived from nitrogen batch tests, as outlined in Section 5.3.1 and from Figure 5.2.

5.3.6 Strategy I - Initial high light condition

5.3.6.1. Initial high light intensity effect on biomass and lipid productivity

The simulation data of the Logistic and Gompertz models, showed a high degree of correlation (R^2 = 0.99) between phosphate concentrations and the proliferation of cells (Figure. 5.6A). The findings of the experiment indicate that the final biomass is greater in the presence of a phosphorus concentration of 2.3 mmol L^{-1}, with recorded values of 2.87 and 2.42 g L^{-1} in

the 0.23 mmol L^{-1} phosphorus condition. Additionally, both the Logistic and Gompertz models demonstrate maximum growth (X_m) and specific growth rate (μ) in high phosphorus, as shown in Table 5.2. The higher phosphorus concentration ($P_{10x,}$ 2.3 mmol/l) led to significant enhancements in biomass and lipid productivity, in comparison to the lower or control phosphorus concentration (0.23 mmol/L). Increasing the phosphorus concentration from 0.23 to 2.3 mmol L^{-1} leads to a 20.15% increase in biomass productivity. The biomass productivity values change from 115 to 138 mg L^{-1} day^{-1}. This increase highlights the importance of adequate phosphorus availability in promoting greater biomass production, with enhancement of nitrogen utilization (Figure. 5.6B). The lipid productivity demonstrates a notable rise of around 30.6% with an increase in phosphorus concentration from 0.23 mmol L^{-1} to 2.3 mmol L^{-1}. The lipid productivity values increase from 26.3 to 34.34 mg L^{-1} day^{-1}. Phosphorus is essential for regulating growth and guiding carbon allocation towards lipid synthesis. It serves as a limiting nutrient, particularly in situations with insufficient nitrogen [216]. This is demonstrated in Figure. 5.6 A, 5.6B, and 5.6C, where increased growth and lipid production were observed when phosphorus was present in the P_{10x} condition during the 16-20-time interval of nitrogen limitation. As shown by the data presented in Table 5.3, there was a notable rise in the utilization of phosphorus throughout the specified period. The observed increase in phosphorus utilization, as outlined in Table 5.3, signifies a well-known phenomenon in microalgae—luxury uptake of phosphorus. This adaptive technique is most evident in situations where nutrient availability fluctuates, with a specific emphasis on nitrogen. Under such circumstances, microalgae demonstrate their ability to maintain growth and reproduction even in the presence of nitrogen concentrations that are below ideal levels. Phosphorus availability is crucial for promoting growth by helping to use nitrogen biomass inside cells, mainly in the form of proteins, to store more energy in vital biomolecules like lipids and carbohydrates. Multiple studies confirm the essential interaction between phosphorus and nitrogen in the dynamics of microalgal development. An example is the study conducted on *Chlorella vulgaris*, which shows that when there is a deficiency of nitrogen, an increase in phosphorus availability results in a significant improvement in lipid accumulation, increasing it from 3 to 4.2 [216,323]. Similarly, an additional study on *Tetraselmis subcordiformis* reveals a notable 57% surge in starch accumulation when phosphorus becomes available during nitrogen deprivation circumstances.

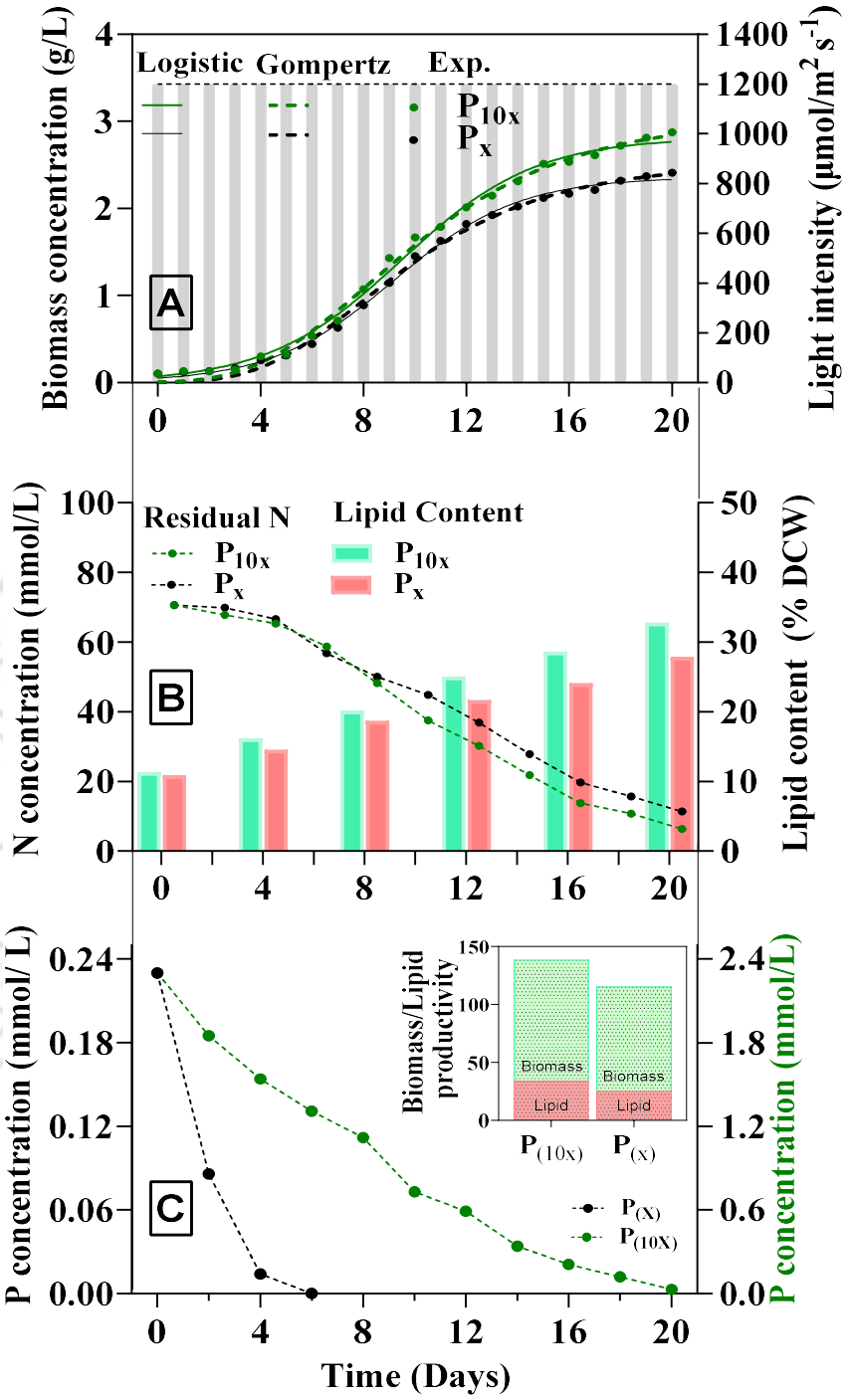

Fig. 5.6. High light intensity of 1200 µmol/m² s⁻¹ in a photobioreactor under two phosphate concentrations: 0.23 mmol/L (Px) and 2.3 mmol/L (P_{10x}). **(A)** Dynamic growth profile modelled using Logistic and Gompertz model. **(B)** Residual nitrogen concentration and lipid content. **(C)** Residual phosphate concentration, biomass, and lipid productivity

5.3.6.2. Nutrient fixation, utilization rate and CO_2 assimilation

Under conditions of high light intensity (1200 µmol/m^2 s^{-1}) and controlled phosphorus concentration (0.23 mmol/L), microalgae exhibited moderate rates of CO_2 fixation (70.03 mg/L day^{-1}) and utilization efficiency (0.48%). The nitrogen and utilization rate were 0.98 and 0.04 mmol L^{-1} day^{-1}. The C/N ratio was 2.63 mol/mol and the photosynthetic efficiency was 0.51. Under high phosphorus conditions (23.3 mmol/L), the rate of CO_2 fixation increased to 93.1 mg L^{-1} day^{-1}, with a CO_2 utilization efficiency of 0.64%. The utilizations of nitrogen and phosphorus increased to 1.31 and 0.13 mmol L^{-1} day^{-1}, respectively. The C/N ratio was 3.23 mol/mol, and the photosynthetic efficiency was 0.56. During the mid-exponential phase (4-12 days) period, both conditions showed a significant increase in CO_2 fixation and improved CO_2 utilization efficiency by 5.2-fold increment under phosphorus control. The rate of nitrogen utilizations rose to 4.1 mmol L^{-1} day^{-1}. Under conditions of elevated phosphorus levels, the rate of carbon dioxide fixation was measured 393.16 mg L^{-1} day^{-1}, with an CO_2 utilizations efficiency of 2.68%. The rate of nitrogen utilizations was 4.3 mmol L^{-1} day^{-1}, while phosphorus utilizations was 0.18 mmol L^{-1} day^{-1}. During the 12-20 days period, there was a decrease in CO_2 fixation, specifically in the control phosphorus condition, with a reduced utilization efficiency of 0.96%. The nitrogen utilization rate rose to 3.18 mmol L^{-1} day^{-1}, while high light and phosphorus levels resulted in a CO_2 fixation rate of 215.34 mg L^{-1} day^{-1}, with an efficiency of 1.67%. Nitrogen utilizations remained high at a rate of 3 mmol L^{-1} day^{-1}, whereas phosphorus utilizations decreased to 0.04 mmol L^{-1} day^{-1}.

Over the course of the first four-day period, microalgae displayed diverse and distinct reactions. The experimental manipulation of phosphorus levels resulted in a modest degree of carbon dioxide fixation and an inadequate efficiency of utilization, which may be attributed to potential limitations in both carbon and nitrogen fixation processes (Figure.5.8B[i] and [ii]). Nevertheless, the heightened accessibility of phosphorus, in conjunction with optimal light circumstances, resulted in an augmentation of carbon dioxide fixation and utilization, ultimately resulting to an enhancement in the efficiency of carbon and nitrogen fixation in biomass. The combined presence of these factors contributed to the enhanced efficacy of carbon dioxide (CO_2) mitigation within the designated time frame of 4-12 days, hence facilitating growth. Over the course of the last 12-20 days, there has been a decrease in the efficiency of CO_2 fixation and utilization as a result of nutritional depletion. However, the loss was counteracted by the presence of elevated phosphorus levels, which served to continue the processes of carbon and nitrogen fixation. It is worth noting that there was a rise in nitrogen

utilization, although phosphorus utilization remained restricted, thus highlighting the importance of nitrogen in the processes of photosynthesis and carbon assimilation. The presence of an excess of phosphorus was seen to contribute to the continuing keeping of a balanced carbon-to-nitrogen ratio and little loss of photosynthetic efficiency (Figure. 5.8B[ii]).

Table 5.2. Model of the kinetic growth of *M.pusillum* under four distinct cultivation concentrations in a 2L photobioreactor.

High light intensity (1200 µmol m^{-2} s^{-1})					
P concentration (x=0.23mmol/L)	Model	X*i* (g/L)	X*max* (g/L)	µ (day^{-1})	R^2
$P_{(x)}$	Logistic	0.05	2.36	0.415	0.997
	Gompertz	0.001	2.51	0.250	0.996
$P_{(10X)}$	Logistic	0.07	2.82	0.384	0.995
	Gompertz	0.01	3.03	0.228	0.996
Gradual light intensity (from150 to 1200 µmol m^{-2} s^{-1})					
$P_{(x)}$	Logistic	0.22	4.56	0.298	0.994
	Gompertz	0.08	5.25	0.160	0.994
$P_{(10x)}$	Logistic	0.25	5.57	0.281	0.992
	Gompertz	0.09	6.59	0.147	0.995

5.3.7 Strategy II - Gradual intensification of light

5.3.7.1. Gradual intensification of light effect on biomass and lipid productivity

Cell growth is significantly higher at higher phosphorus concentrations (2.3 mmol/L) compared to lower concentrations (0.23 mmol/L). Under the condition of 2.3 mmol L^{-1} phosphorus, the cell population showed substantial growth, reaching 5.21 g L^{-1} in 20 days. In contrast, cell growth was significantly lower under the 0.23 mmol L^{-1} phosphorus condition, reaching a maximum of 4.46 g L^{-1}. Increasing the phosphorus concentration from 0.23 mmol L^{-1} to 2.3 mmol L^{-1} results in a 17.49% increase in biomass productivity, rising from 217 mg L^{-1} day^{-1} to 255 mg L^{-1} day^{-1}. Additionally, there has been a substantial 38.44% increase in lipid productivity, rising from 61.18 mg L^{-1} day^{-1} to 84.76 mg L^{-1} day^{-1} (Figure. 5.7 A & C).

The progressive increase in light intensity observed significantly contributed to the enhancement of both biomass and lipid productivity. Previous research corroborates the idea that a deliberate increase in the intensity of light has a positive impact on microalgae by enhancing their photosynthetic activity. This optimization method facilitates the adaptation of

microalgae to different light conditions, hence minimizing photoinhibition and optimizing the use of light energy for photosynthesis [243,324]. Furthermore, the combination of high phosphate feeding and the steady increase in light intensity in this study resulted in a synergistic impact on both biomass and lipid output. The implementation of this co-interaction technique resulted in a simultaneous increase in production, highlighting the significance of considering several elements such as light availability and nutrient feeding in the culture of microalgae. The data in Table 5.2 supports the correlation between growth and phosphorus availability. Both the Logistic and Gompertz models highlighted the influence of phosphorus availability on maximum growth (X_m) and specific growth rate (μ) for cellular growth. The R^2 value consistently exhibited a robust correlation of 0.99 throughout all four experimental circumstances, including Strategy I (as described in Section 5.3.6.1) and Strategy II at both high and low phosphorus concentrations.

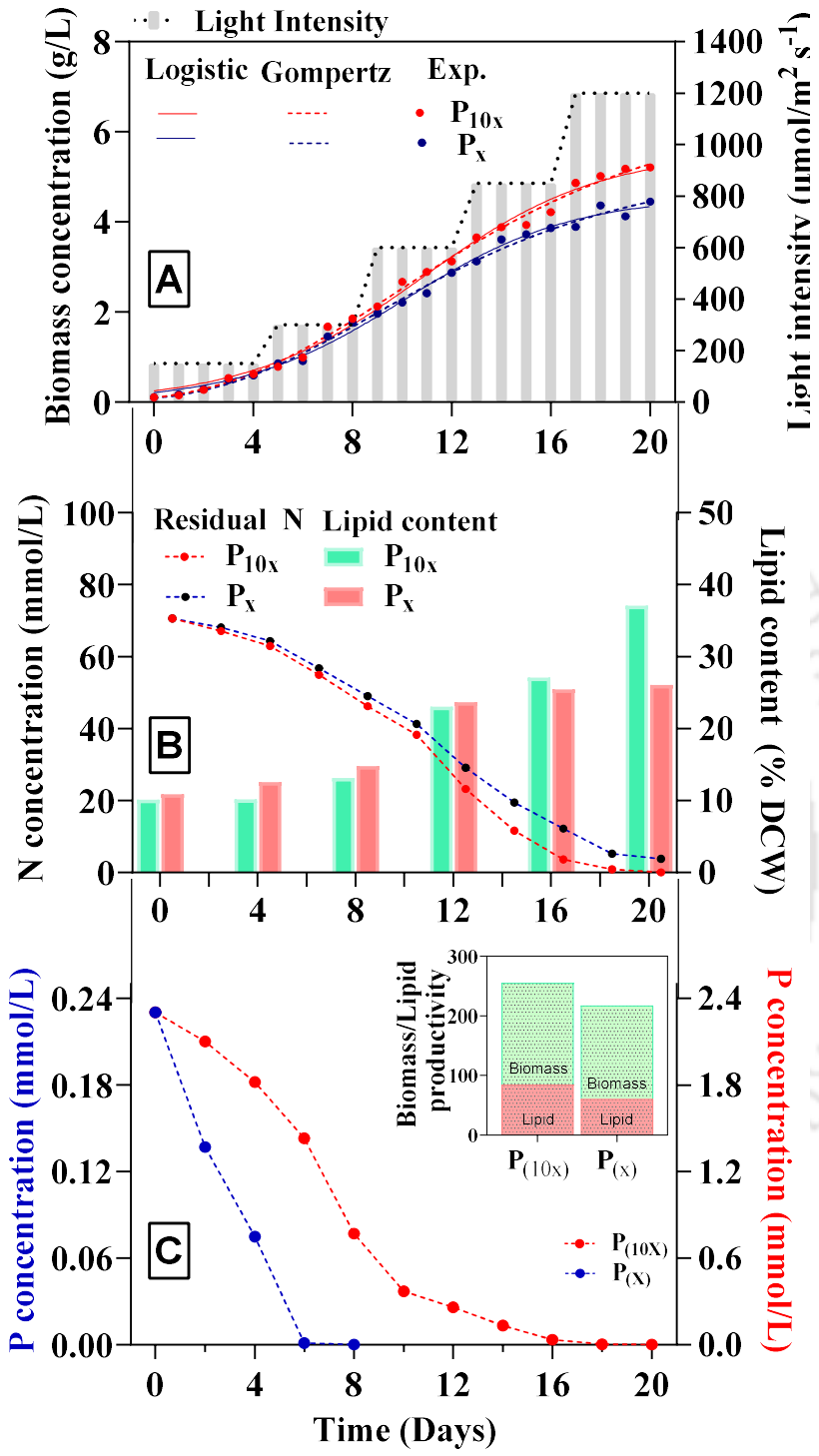

Fig. 5.7. Gradual intensification of light from 150 to 1200 µmol/m² s⁻¹ in a photobioreactor under two phosphate concentrations: 0.23 mmol/L (Px) and 2.3 mmol/L (P_{10x}). **(A)** Dynamic growth profile modelled using Logistic and Gompertz model **(B)** Residual nitrogen concentration and lipid content. **(C)** Residual phosphate concentration, biomass, and lipid productivity

5.3.7.2. Nutrient fixation, utilization rate and CO_2 assimilation

During the first 0-4 days, microalgae exhibited distinct responses to different phosphorus conditions and increasing light intensity. Under conditions of low phosphorus concentration (0.23 mmol/L), displayed a moderate rate of CO_2 fixation (220.56 mg/L day^{-1}) and a CO_2 utilization efficiency of 1.5%. The rates of nitrogen and phosphorus utilizations were 1.56 and 0.04 mmol L^{-1} day^{-1}, respectively. High phosphorus conditions resulted in a higher CO_2 fixation rate of 239.58 mg L^{-1} day^{-1} and 3.25% utilization efficiency, with nitrogen and phosphorus utilization rates of 1.90 and 0.12 mmol L^{-1} day^{-1}, respectively. Microalgae exhibited increased CO_2 fixation rate (526.4 mg/L day^{-1}) and utilizations efficiency (3.6%) under controlled phosphorus conditions within 4-12 days. They also showed elevated nitrogen utilization (3.83 mmol/L day^{-1}) but limited phosphorus utilization, suggesting phosphorus starvation. Under high phosphorus conditions, there was a significant increase in the rate of CO_2 fixation (582.33 mg/L day^{-1}) and a utilization efficiency of 3.97%. Nitrogen utilization was observed at a rate of 4.2 mmol L^{-1} day^{-1}, while phosphorus utilization occurred at a rate of 0.20 mmol L^{-1} day^{-1}. During the last 12-20 days, microalgae grown under controlled phosphorus conditions showed a decrease in CO_2 fixation (368.08 mg/L day^{-1}) and a decrease in utilization efficiency (2.51%), while nitrogen utilization increased (3.16 mmol/L day^{-1}). Under high phosphorus conditions, there was a decrease in nutrient and CO_2 uptake performance, but not a significant loss compared to the control phosphorus condition. The rate of CO_2 fixation was 503.67 mg L^{-1} d^{-1}, with a utilization efficiency of 3.43%. Nitrogen utilization decreased to 2.9 mmol L^{-1} day^{-1}, while phosphorus utilization remained stable at 0.03 mmol L^{-1} day^{-1}. Furthermore, the C/N ratios increased significantly from 3.24 to 20.47 mol/mol, primarily as a result of the substantial buildup of carbon biomass and the degradation of nitrogenous biomass. In conditions of low phosphorus, the C/N ratio reached 9.67 mol/mol.

Microalgae utilize nutrient conservation strategies to adapt to phosphorus scarcity. High phosphorus levels stimulate the growth and increase carbon dioxide fixation. The 4-12-day period has the highest CO_2 fixation efficiency because of increased growth and greater nitrogen demands caused by highly efficient nitrogen fixation in biomass (Figure. 5.8A). Low phosphorus concentrations are associated with reduced carbon fixation, showing a connection between the availability of phosphorus for growth and nitrogen fixation, which in turn affect CO_2 mitigation (Figure. 5.8A[i]). CO_2 fixation patterns change during late exponential and stationary phases, indicating sustained growth. A notable improvement in carbon and nitrogen fixation occurs with the gradual increase in light feeding, especially in high phosphate

conditions. This is supported by a rise in the C/N ratio and the capacity to sustain efficient CO_2 fixation even when nitrogen is limited (Figure. 5.8A[ii]). The results of the research underscore the significant impact of light availability and phosphorus levels on carbon fixation and its allocation towards lipid formation. This, in turn, enhances the quality of biomass for bioenergy generation. As demonstrated in Figure. 5.8A and B, a gradual increase in light intensity enhances the acclimation capacity of the microalgal culture by facilitating carbon and nitrogen fixation in the biomass. This effect is observed in comparison to the application of high light intensity from the outset. Maintaining a proper carbon-to-nitrogen (C/N) balance is particularly crucial in conditions of high phosphorus concentration. This indicates that both phosphorus availability and light intensity are critical factors under nitrogen-limited conditions, as they modulate the intracellular C/N balance. This modulation supports photosynthesis and enhances the accumulation of carbon energy molecules in the biomass.

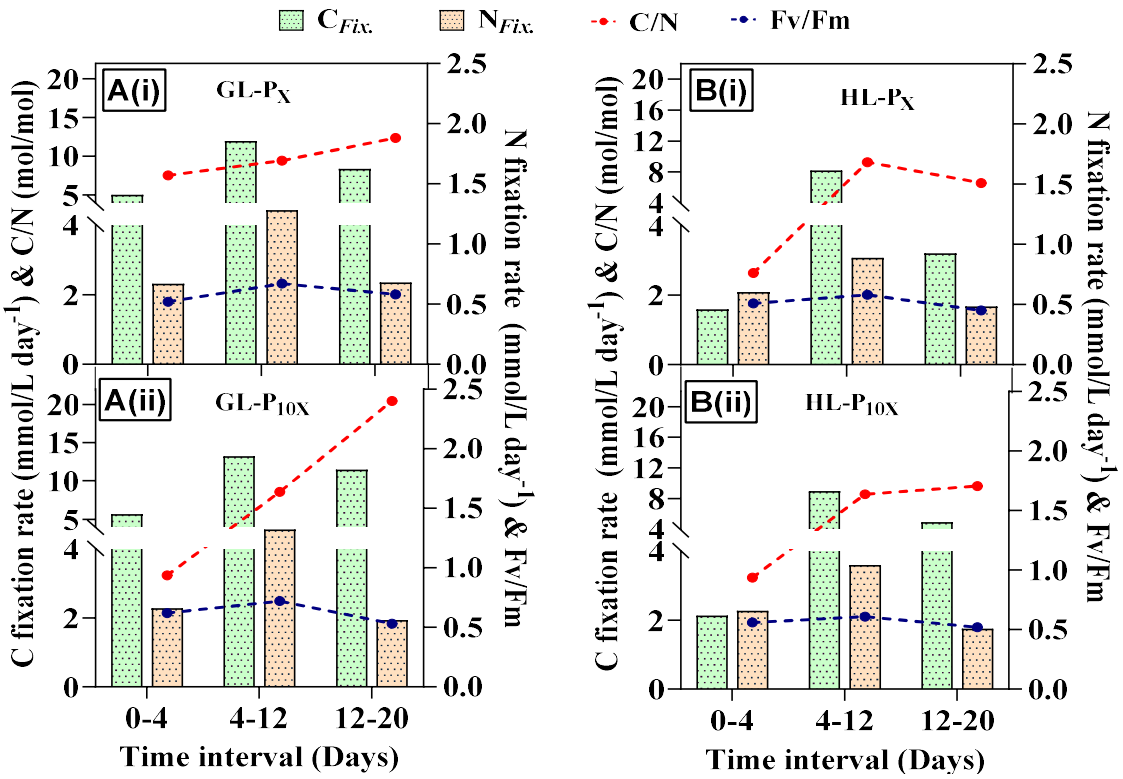

Fig. 5.8. (A) Gradual intensification of light (GL) in two phosphate concentration carbon and Nitrogen fixation with C/N ratio in a photobioreactor **(i)** GL-P_x (0.23mmol/L) & **(ii)** GL-P_{10x} (2.3 mmol/L) **(B)** High light intensity (HL) in two phosphate concentration carbon and Nitrogen fixation with C/N ratio **(i)** HL-P_x **(ii)** HL-P_{10x}

5.3.8 Phosphorus and light conditions impact on organic carbon secretion in media

In Strategy I, with a high initial light intensity of 1200 µmol m^{-2} s^{-1}, the total organic carbon (TOC) content increased significantly. It ranged from 21.32 to 138.63 mg L^{-1}, with a consistent secretion rate of 7 mg L^{-1} day^{-1} in the final 16 days. In the group that had phosphorus control (0.23 mmol/L), the TOC values were higher, ranging from 26.67 to 162.34 mg L^{-1}. The secretion rate reached 9.24 mg L^{-1} day^{-1} in the last 8 days. Increased light exposure was observed to promote the production of organic compounds, which may act as a protective response to external stressors.

Strategy II resulted in a small decrease in organic carbon secretion. Organic carbon secretion showed a significant increase from 14.23 to 70.6 mg L^{-1} under controlled phosphorus conditions (0.23 mmol/L). However, under excess phosphorus (2.3 mmol/L), the range of organic carbon secretion was narrower, ranging from 12.13 to 54.45 mg L^{-1}. The secretion rate declined during the exponential phase, dropping to 3.56 to 2.91 mg L^{-1} day^{-1} in the control phosphorus condition and 3.05 to 1.43 mg L^{-1} day^{-1} in the excess phosphorus condition. Excess phosphorus significantly influenced the secretion rate, with a value of 3.86 mg L^{-1} day^{-1}. In contrast, under low phosphorus conditions, the secretion rate increased to 4.13 mg L^{-1} day^{-1} between days 12 and 20.

These findings highlight the impact of phosphorus and light intensity on the release of extracellular organic carbon. Phosphorus is essential for cellular energy transfer and storage, as well as for nutrient uptake, storage, and utilization [325]. This phenomenon has the potential to disturb the equilibrium between organic carbon excretion and intracellular nitrogen metabolism, which may result in a decrease in the outward flow of carbon from the cell [326]. Nitrogen remobilization, or recycling, is a significant phenomenon in which microalgae break down proteins to release nitrogen for metabolic pathways that result in carbon-neutral storage compounds [213]. Phosphorus and light intensity have significant effects on the excretion of extracellular organic carbon, indicating their importance in microalgal metabolism and adaptation.

Table 5.3: Evaluation of CO_2 bio-mitigation, nitrogen and phosphate utilization rate and dissolve organic carbon concentration and secretion rate of *M.pusillum* in different cultivation condition

High light intensity (1200 µmol m^{-2} s^{-1})	Px			P_{10x}		
	Time interval (days)			Time intervals (days)		
	0-4	4-12	12-20	0-4	4-12	12-20
CO_2 fixation rate (mg/L day^{-1})	70.03	361.5	140.5	93.1	393.16	215.34
CO_2 utilization efficiency (%)	0.48	2.46	0.96	0.64	2.68	1.67
N utilization rate (mmol/L day^{-1})	0.98	4.13	3.18	1.31	4.29	2.99
P utilization rate (mmol/L day^{-1})	0.04	0	0	0.13	0.18	0.04
DOC concertation (mg/L)	26.67	88.47	162.34	21.32	78.12	138.63
DOC secretion rate (mg/L day^{-1})	6.67	7.73	9.24	5.33	7.1	7.56
Gradual light intensity (150-1200 µmol m^{-2} s^{-1})						
CO_2 fixation rate (mg L^{-1}/day)	220.56	526.4	368.08	239.58	582.33	503.67
CO_2 utilization efficiency (%)	1.5	3.59	2.51	1.63	3.97	3.43
N utilization rate (mmol/L day^{-1})	1.56	3.83	3.16	1.90	4.20	2.90
P utilization rate (mmol/L day^{-1})	0.04	0	0	0.12	0.20	0.03
DOC concertation (mg/L)	14.23	37.45	70.45	12.13	23.51	54.45
DOC secretion rate (mg/L day^{-1})	3.56	2.91	4.13	3.05	1.43	3.86

5.3.9 Acclimatized high cell density repeated fed batch strategy for CO_2 bio-mitigation and lipid productivity in reused media performance study

5.3.9.1 Performance and stability in biomass and lipid productivity

A noticeable pattern was observed in biomass productivity (Figure. 5.9A). In Cycle 1, it was found that fresh media had higher biomass productivity compared to reused media. The difference was approximately 13.6%, with biomass productivity decreasing from 0.65 to 0.56

g L^{-1} day^{-1}. This decrease corresponded to a decrease in specific growth rate from 0.147 to 0.134 day^{-1}. The advantage of fresh media lies in its provision of optimal nutrients and conducive growth conditions. The biomass productivity between fresh and recycled media showed periodic fluctuations as the cycles progressed. The disparity decreased in Cycle 2, going from 0.66 to 0.62 g L^{-1} day^{-1} (specific growth rate of 0.150 and 0.144 day^{-1}), resulting in a reduction of about 6.1%. In Cycle 3, the gap observed a rise, reaching around 14.5%. The disparity between the values of 0.56 and 0.54 g L^{-1} day^{-1} decreased to approximately 2.8% by the end of Cycle 4. Additionally, both conditions exhibited a similar specific growth rate of 0.11 day^{-1}. This decrease in growth performance can be attributed to the longer cultivation period of 10 days instead of 7. Observed variations suggest that microalgae may adapt or change in response to the conditions of using media repeatedly.

Regarding lipid productivity, the utilization of recycled media presented a benefit, showing an approximate 23% enhancement in average lipid productivity compared to the utilization of new media, with respective values of 0.13 and 0.16 g L^{-1} day^{-1} in fresh and reused media. The observed enhancement may be attributed to the heightened accumulation of lipid content inside the microalgae, (Figure. 5.10A). This accumulation ranged from 25% to 31% in reused media and from 20% to 22% in fresh media. The observed rise in lipid content can be ascribed to multiple factors, such as the potential activation of stress responses or the microalgae's ability to efficiently utilize external organic carbon nutrients.

5.3.9.2 Performance and stability in CO_2 capture

In the initial cycle, it was found that the fresh and reused media had similar rates of CO_2 fixation of 1.23 and 1.2 g L^{-1} day^{-1} and utilization efficiency (7.2% and 8.3%) (Figure.5.10B). This indicates a consistent level of metabolic activity. Nevertheless, as the cycles advanced, it became apparent that there was a divergence in the rates of CO_2 fixation and the efficiency of its utilization. The findings from cycles 2 and 3 showed that fresh media had higher rates of CO_2 fixation and utilization efficiency compared to reused media. There was a 5% decrease in CO_2 fixation rate in reused media, from 1.28 to 1.17 g L^{-1} day^{-1}, and CO_2 utilization efficiency from 8.71% to 8.2% in cycle 2. In cycle 3, there was a 13% decrease in CO_2 fixation rate, from 1.28 to 1.03 g L^{-1} day^{-1}, and a decrease in utilization efficiency from 8.73% to 7.45%. During Cycle 4, a convergence occurred where both fresh and reused media showed a decrease in CO_2 fixation rates. The rates were 1.1 g L^{-1} day^{-1} in fresh media and 0.98

g L^{-1} day^{-1} in reused media. The utilization efficiency was 7.5% in fresh media and 7.12% in reused media. This decline may suggest the establishment of an equilibrium between metabolic demands and nutrient availability, potentially influenced by extending the duration of the last cycle from 7 to 10 days.

5.3.9.3 Organic carbon exertion

The TOC levels in reused media showed interesting and informative patterns during the cycling process (Figure. 5.9C). During the initial cycle, there was a noticeable increase in total organic carbon (TOC) levels in the reused media, suggesting a possible buildup of organic carbon. The increase was significant, with a percentage increment of 41%, as values changed from 19.23 to 27.12 mg L^{-1} in fresh and reused media. This disparity became more pronounced in subsequent cycles. During the 2 and 3 cycles, the levels of TOC increased significantly in the reused media. In contrast, the TOC levels in fresh media remained relatively stable, with values of 21.12 and 23.63 mg L^{-1} respectively. The increase in TOC levels for recycled media in these cycles was significant, with increases of 233% and 279%, corresponding to values of 70.6 and 89.67 mg L^{-1}, respectively. The last cycle exhibited a modest 17% rise in reused media, with the TOC levels reaching 143.16 mg L^{-1} in fresh media and 167.40 mg L^{-1} in reused media. The higher excretion of organic carbon can be explained by longer phases in the cycle (7 to 10 days) with restricted nitrogen and phosphorus availability for over five days. The data showed that the TOC did not accumulate excessively, especially in the later stages. This phenomenon suggests that microalgae may use TOC as an additional carbon source for growth and metabolism. This mechanism could be enhanced by optimizing the nitrogen/phosphorus ratio in each cycle and effectively managing organic carbon excretion in the media. This strategic approach shows potential for reducing the negative impact of dissolved organic carbon, allowing it to be used for strong biomass growth and potentially increasing lipid accumulation.

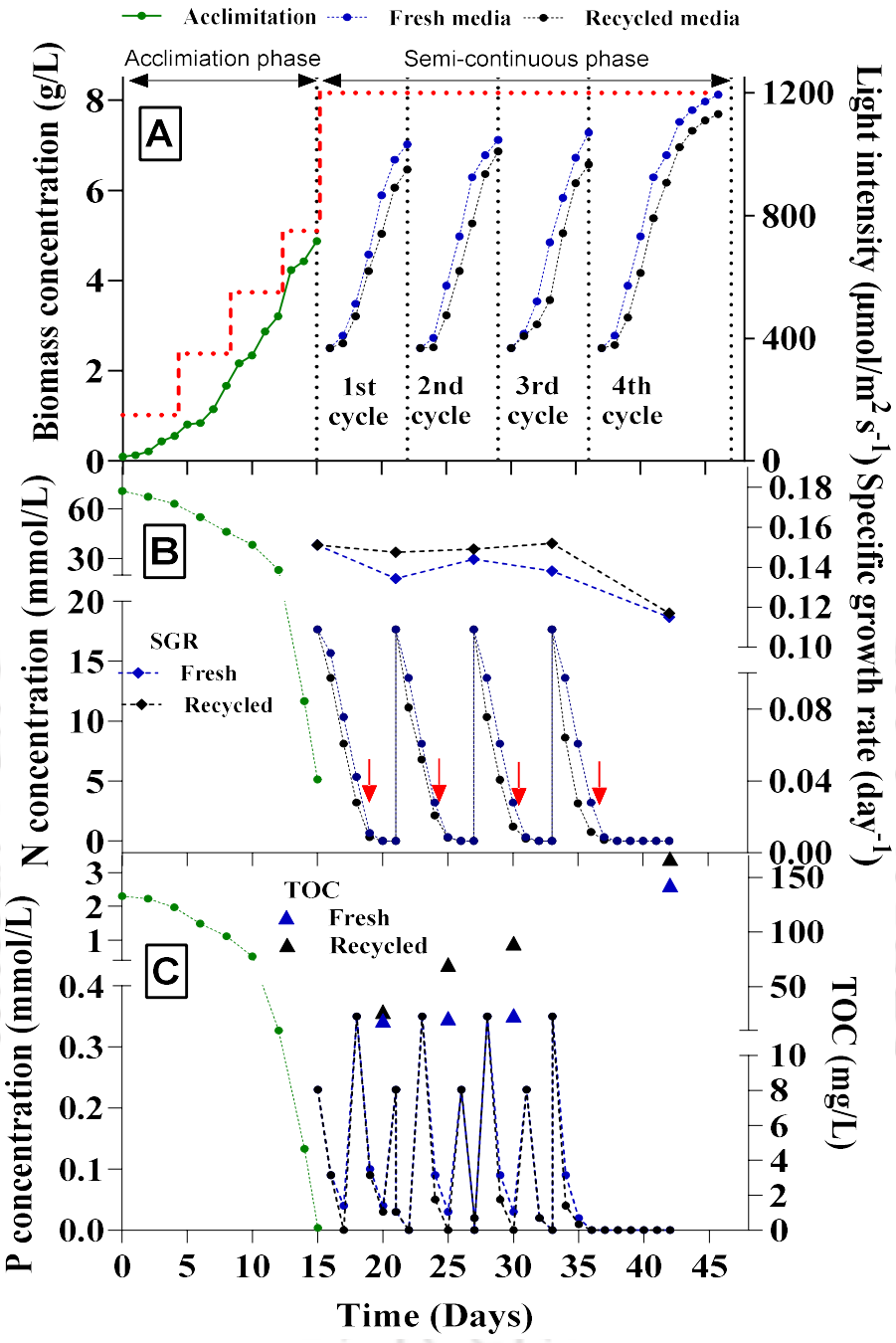

Fig. 5.9. Repeated fed batch cycle in a photobioreactor **(A)** dynamic growth profile of four cycles in fresh and reused media. **(B)** Residual Nitrogen concentration and lipid content of four cycle in fresh and reused media, with the down arrow represent phosphate feeding. **(C)** Residual phosphate concentration and TOC in fresh and reused media in four cycle

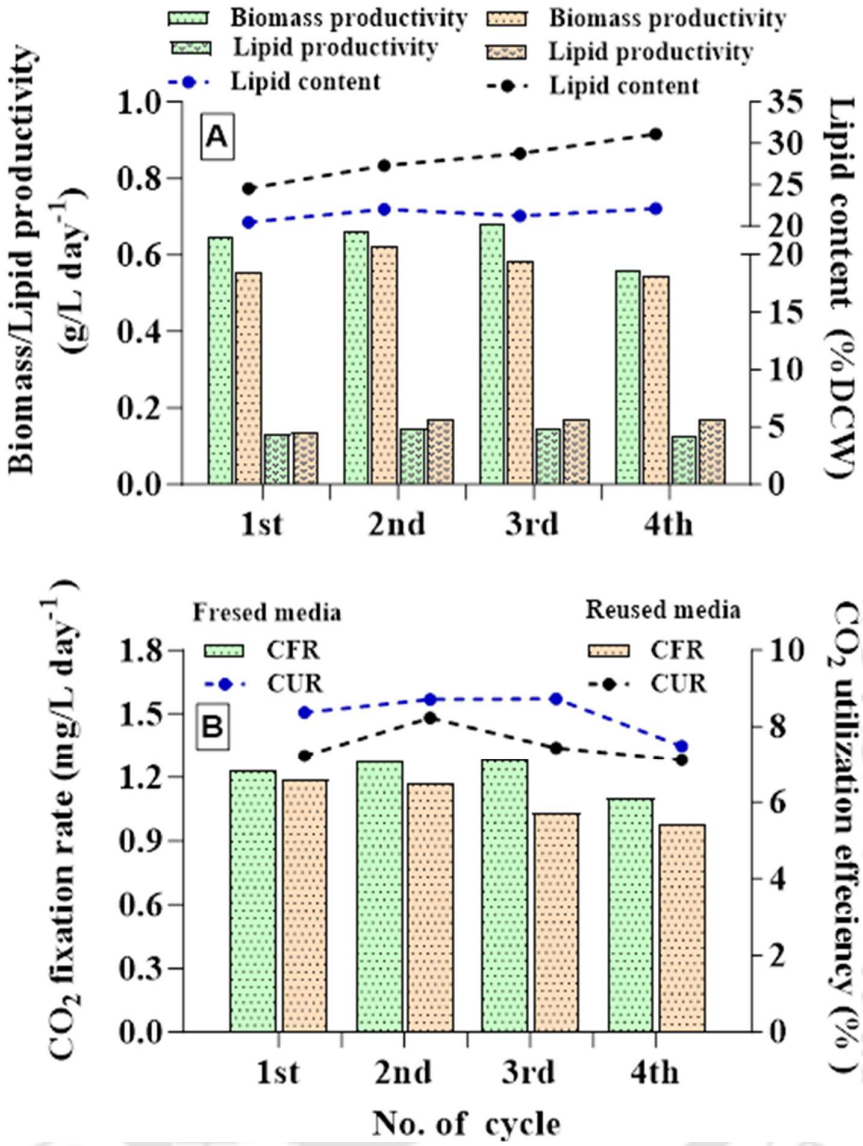

Fig. 5.10. Repeated fed batch cycle in a photobioreactor **(A)** biomass productivity and specific growth rate of each four-cycle. **(B)** CO_2 fixation and utilization efficiency in all four cycle of repeated fed batch

5.4 Conclusion

This study highlights the significant interplay between the effect of light, nitrogen, and phosphate on microalgae growth, offering valuable insights for the development of targeted nutrient management approaches. This breakthrough not only enhances microalgal CO_2 capture and lipid production, but also promotes sustainable water management by effectively

controlling organic carbon excretion. The findings present a promising opportunity to enhance the production of sustainable microalgal biomass. The adoption of microalgal culture in tropical climates, where there is a high light intensity of sunshine and water shortage, promises great potential in the future. This not only allows the effective sequestration of carbon for efficient mitigation of CO_2 emissions from industrial flue gas, but also enables the generation of biofuels within a circular bioeconomic paradigm.

CHAPTER 6

Optimization of Microalgal Harvesting in Continuous Growth Phase with Minimal Impact on Productivity and Biomass Quality

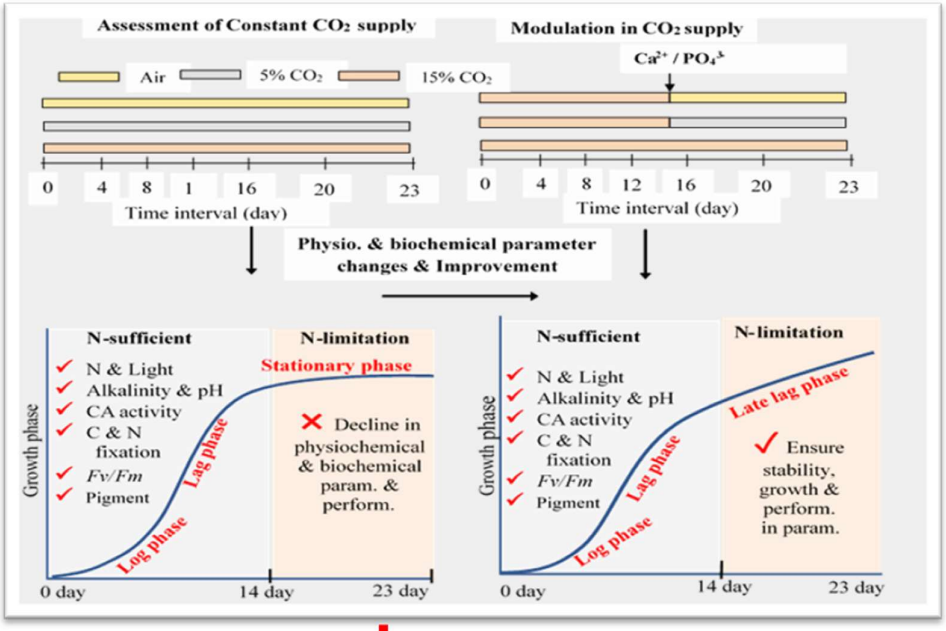

Result

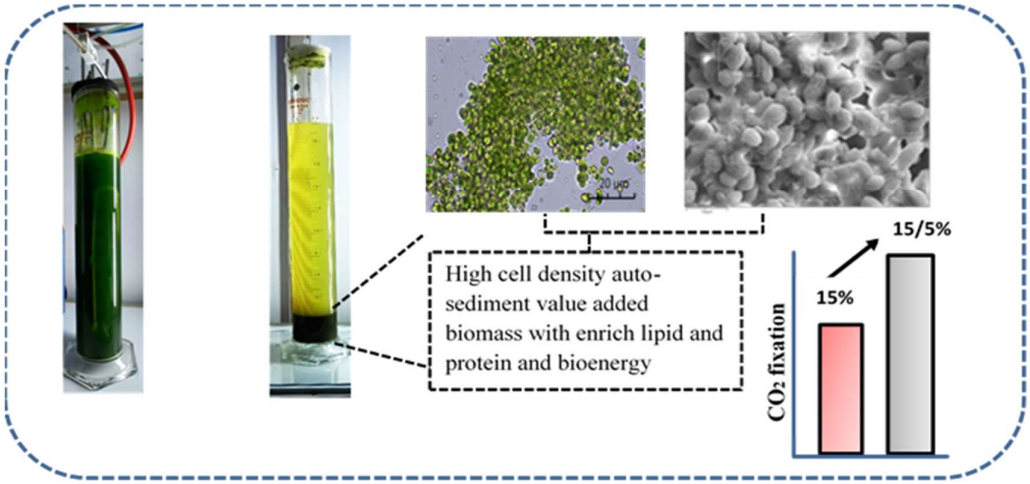

Chapter 6

Optimization of Microalgal Harvesting in Continuous Growth Phase with Minimal Impact on Productivity and Biomass Quality

6.1 Background and motivation

This chapter delves into the critical aspects of enhancing productivity, cost-effectiveness, and sustainability in CO_2 cultivation, with a particular emphasis on optimizing biomass harvesting and CO2 conversion efficiency during the continuous growth phase of microalgae. The study addresses several challenges inherent in the process, such as CO_2 acidification, saturation, and the limited access to flue gas concentrations (5-15%), which often hinder stable carbon fixation and result in suboptimal biomass productivity over periods of 5-15 days. To tackle these challenges, the research investigates various strategies to boost microalgae *Micractinium pusillum* strain growth and CO_2 utilization over a 23-day period, specifically focusing on the. growth and CO_2 utilization over a 23-day period, building upon existing literature and previous assessment of this strain, this research introduces a novel approach to enhancing microalgal growth and CO_2 capture by dynamically adjusting CO_2 levels and providing specific nutrients. The concept, based on the correlation between CO_2 concentration and nitrogen fixation rate, suggests that strategic alterations in CO_2 concentrations, considering nitrogen availability, along with supplemental phosphorus and calcium to induce media alkalinity, will significantly improve photosynthetic efficiency, biomass yield, and metabolic composition. One of the key approaches involves using urea as a cost-effective nitrogen supplement to facilitate growth. The study finds that exposure to 5% CO_2 allows for a longer growth phase, which is later followed by a transition to 15% CO_2. However, this transition to higher CO_2 levels initially leads to increased media acidity and reduced alkalinity due to nitrogen deprivation, resulting in pigment loss and decreased photosynthetic efficiency, ultimately impacting carbon assimilation in the biomass.

To mitigate these issues, the cultivation strategy is adjusted to start with 15% CO_2 and then transition to 5% CO_2 after 15 days. This method incorporates a calcium-induced phosphorus fed-batch approach, effectively reducing media acidification and stabilizing photosynthesis and carbonic anhydrase activity. This adjustment leads to a significant 20% increase in CO_2 fixation and a 15% boost in biomass productivity. Additionally, there is a notable increase in lipid, protein, and carbohydrate content, enhancing both carbon and nitrogen assimilation and their bioenergy potential. Despite these improvements, the study observes performance declines during transitions to air and continuous 15% CO_2 conditions, indicating the need for further optimization. The SEM-EDX analysis highlights auto-sedimentation dynamics and underscores the pivotal roles of calcium and phosphorus in cell aggregation.

Through a comprehensive batch study, the research aims to investigate the intricate relationships between CO_2 concentrations, nutrient interactions, and growth kinetics. The primary objective is to maximize CO_2 fixation while maintaining productivity, thereby laying the foundation for sustainable bioproduction and carbon sequestration initiatives. These findings offer valuable insights into improving algal bioprocessing for effective CO_2 mitigation and biochemical production, demonstrating the potential for scalable and feasible application.

6.2 Materials and method

6.2.1 Microalgal strain and cultivation condition

In this study, microalgae *Micractinium pusillum* (KMC8) was used, with urea replacing nitrate-based nitrogen in a modified BG-11 medium at a concentration of 17.3 mmol L^{-1}. The medium was 121 °C sterilized for 20 min. To prepare the initial inoculum, 500 mL Erlenmeyer flasks were incubated at 25 °C in a photo incubator shaker set to a 16:8 h light/dark cycle at 150 rpm. The light intensity was 150 µmol m^{-2} s^{-1}. The experiments were carried out in triplicate utilizing compounds of analytical grade.

6.2.2 Experiment Photobioreactor set up

The experiment utilized a 500 mL reagent bottle (Borosil 1501024) with two perforations in the screw cap for air exchange as previous described in chapter 5 in section 5.2.1. A culture volume of 400 mL was employed, with aeration introduced at a controlled rate

of 50 mL min^{-1} using a calibrated rotameter and a stone aerator at the reactor's bottom. The setup included subjecting the culture to a light intensity of 150 µmol m^{-2} s^{-1} with three cool white tube lights, maintaining a 16:8 light/dark cycle at a temperature of 25±3 ℃. Inoculum pellet resuspension maintained an initial cell density of 0.1 g L^{-1}, monitored by optical density (OD_{680}). pH remained uncontrolled throughout experiments, including inoculum preparation. Experiments lasted 23 days, followed by further investigation in a 2 L bubble column photobioreactor over a 23-days batch cultivation period, employing optimized conditions for feasibility evaluation. Photobioreactor details designed are reported in section 3.2.2.

6.2.3 Culture in different CO_2 concentration

To investigate the interplay between CO_2 concentration and urea on photosynthesis, growth, and CO_2 fixation, KMC8 cultures were aerated with three constant CO_2 concentrations: 0.04% (air), 5%, and 15%, serving as the sole carbon source. This was achieved by substituting sodium carbonate with CO_2 to create modified BG-11 media. Additionally, the nitrogen source was adjusted to a 70.6 mmol/L urea-based nitrogen concentration, replacing nitrate-based nitrogen. The choice of nitrogen content was determined based on previous optimization tests conducted in chapter 5, which showed that this particular concentration promotes optimum growth and enhances carbon capture efficiency at elevated 15% CO_2 levels. Desired CO_2 levels were attained by mixing air and pure CO_2 (100%), and the flow rate of the gas mixture was controlled using flowmeters.

6.2.4 Schemes of changing CO_2 concentration with calcium induced phosphorus fed-batch

The CO_2 modulation approach was developed based on the performance of microalgae under varying CO_2 concentrations. Calcium-induced phosphorus fed-batch cultivation was employed, achieved through pulse feeding of calcium chloride and potassium phosphate salts to reach concentrations of 0.45 mmol/L for calcium and 2.3 mmol/L for phosphorus over a 23-day cultivation period. The choice of this phosphorus content was based on its beneficial effects on growth and lipid formation, as well as its ability to sustain efficient CO_2 fixation under nitrogen restriction conditions, as seen in our prior experiments in chapter 5 of KMC8. Similarly, calcium concentration plays a role in increasing the alkalinity and inducing auto-flocculation in microalgae. This is achieved by interacting with the natural increase in pH

caused by high CO_2 fixation and growth. Calcium also interacts with binding bridging forces on the microalgal cell surface, leading to the formation of flocculation particles. These particles cause the biomass to settle due to its increased density [327,328] . Three different methodologies were utilized to assess the impact of CO_2 modulation in calcium-induced phosphate fed-batch cultivation as shown in Figure 6.1.

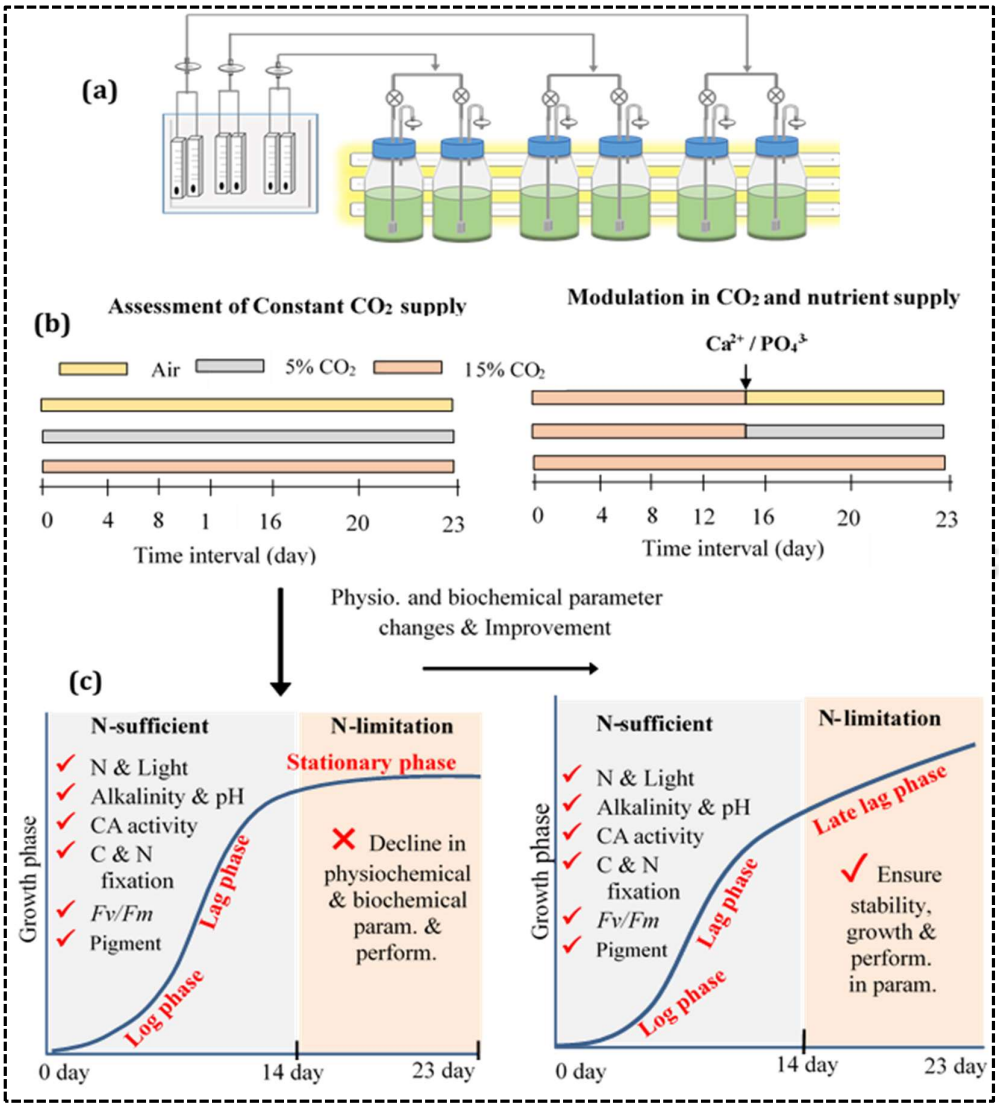

Fig. 6.1. Workflow of process development to enhance CO_2 fixation and biomass production by microalgae. (a) Experimental setup; (b) Evaluation of CO_2 at a constant concentration followed by dilution of CO_2 concentration under nitrogen limitation conditions; (c) Modulation and improvement of physiochemical and biochemical parameters, including nitrogen sufficient and limitation, alkalinity, pH, carbonic anhydrase activity (CA), and carbon (C)and nitrogen (N) fixation, photosystem II quantum yield (*Fv/Fm*) and pigment. The Figure illustrates the modulation of the growth phase curve over a 23-day cultivation period.

6.2.5 Analysis of growth, nitrogen and CO_2 fixation kinetics parameter

The analysis of growth and CO_2 fixation was performed using the protocol described in Section 3.2.6.3 by equation 3.7. This involved applying the kinetic equation and logistic model as detailed in Chapter 3 and Section 3.21.2.

The overall carbon and nitrogen elemental biomass productivity (P_E mg/L day^{-1}) was determined by the following Eq. 6.1

$$P_E = \frac{(X_f \times E_f - X_i \times E_i)}{t_f - t_i} \quad (6.1)$$

where $E_{f\ and}$ E_i, represents the final and initial carbon and nitrogen content (%w/w) in final X_f and initial biomass X_i. Carbon and nitrogen content in dry biomass were measured using a CHNS analyzer (Perkin Elmer elementary analyzer, PE-2400 series).

The carbon growth yield coefficient ($Y_{C/N}$) was determined based on the nitrogen consumed by Eq.6.2

$$Y_{C/N} = \frac{Total\ carbon\ biomass\ produced\ (g)}{Total\ nitrogen\ consumed\ (g)} \quad (6.2)$$

Urea was quantified using the diacetyl monoxime method as described by Wybenga et al.1971 [329]. The method uses 1:1:1 mixture of mixed acid reagent (containing sulfuric acid, ferric chloride and orthophosphoric acid), mixed colour reagent (containing 2% w/v diacetyl monoxime and 0.5 % w/v thiosemicarbazide) and distilled water as coloring reagent which on reaction with urea at 100°C forms a pink color product. The reagents are prepared freshly before the assay and a maximum of 0.1 mL sample was used in the analysis.

6.2.6 Analysis of Photosynthetic performance, pigment, cellular component and bioenergy accumulation in biomass

Photosynthesis performance was analyzed by quantification of pigment using a spectrophotometric method and, the maximal photochemical efficiency of Photosystem II (*Fv/Fm*) using a pulse amplitude-modulated fluorometer as described in previous chapter 3 methodology section 3.2.6.4 by equation 3.11 to 3.14.

The analysis of intracellular components, including carbohydrates, proteins, and lipids, was conducted as described in Section 3.2.6.5 of the methodology chapter 3. The determination of bioenergy content was based on the high heating value (HHV) calculated from the elemental composition of biomass and the accumulation of intracellular components, as outlined in section 4.5 of the methodology chapter 4, using equations 4.2 and 4.3.

6.2.7 Analysis of alkalinity and TOC

The cell suspension obtained was harvested and centrifuged at 6000 rpm for 10 minutes to pellet down the microalgal cells. The resulting supernatant was used for estimating alkalinity and total organic carbon (TOC). Alkalinity was determined as described by Sun et al., 2005 [330] via the titration method by mixing the supernatant with excess 0.1N NaOH solution, followed by the addition of 10 mL of 20% $BaCl_2$ solution to precipitate $BaCO_3$. Phenolphthalein indicator was added, and the solution was titrated with 0.1 N HCl until the pink color disappeared, then with methyl orange indicator until a pink color appeared, with the quantity of HCl consumed recorded for alkalinity calculation. TOC analysis of the supernatant was conducted using a TOC analyzer (model no. 1030, O-I-Analytical, Aurora, USA).

6.2.8 Analysis of carbonic anhydrase activity

CA activity was assayed electrometrically using a modified procedure of Basu et al., 2014 [331]. The sample was assayed at 3 °C by adding cells (equivalent to 200 µg Chlorophyll a) to 3 ml of HEPES buffer (pH 8.0) and sonicated for 10 min. The reaction was initiated by addition of 2 ml ice-cold CO_2 water. The time required for the pH to decrease from 8.0 to 7.0 was measured using digital pH meter (model Orion 3 Star pH Benchtop, Thermo Scientific, USA). The enzyme activity in the test sample was calculated using the equation: $EU = 10(T_0/T_1)$, where EU is the enzyme unit, T_0 is the time required for pH change when sample is present, and T_1 is the time required for pH change when sterilized distilled water was used in place of the algal sample. The periplasmic CA activity was measured with whole intact cells, and the total activity was determined on the cell homogenate. The intracellular CA activity was calculated by subtracting periplasmic CA activity from the total CA activity in the cell homogenate.

6.2.9 Analysis of cellular aggregation, flocculation and harvesting performance

Following the experiment's conclusion, aeration ceased, and the culture from the reactor system was transferred to a 500 mL beaker, ensuring proper sampling and clear flocculation visibility. The beaker, left undisturbed, facilitated subsequent sample collection. Algal samples were gently obtained from a 2.5 cm depth without disruption, and absorbance measurements were taken at 680 nm every 2 hours. Microalgae morphology and cell abundance were assessed using an optical microscope (Motic BA210, China), magnifying from 40x to 100x. Additionally, SEM analysis was conducted on fixed samples in 2.5% glutaraldehyde and dehydrated in ethanol. Samples were then coated with gold before SEM imaging. Zeta potential was measured using a Malvern Zetasizer Nano ZS90. Testing involved evenly dispersed microalgae in a cuvette at 25 °C. Harvesting performance was analyzed based on three parameters: flocculation efficiency, pre-concentrated biomass density (i.e., sludge density), and volume reduction.

Where slurry density and volume reduction calculated by the equation 6.3 and 6.4

$$Slurry\ density = \frac{Total\ working\ volume\ \times cell\ density}{pre\text{-}concentrated\ \times Slurry\ Volume} \tag{6.3}$$

$$Volume\ reduction\ = \frac{Total\ working\ volume - Slurry\ volume}{Total\ culture\ volume} \times 100 \tag{6.4}$$

Following the end of reactor operation from Day 0 to Day 23, the process of sparging was totally halted and the culture was transferred to a beaker. Afterwards, a little amount of algal sample was carefully obtained from the beaker without causing any disturbance, namely from the 0.1 L mark volume, which represents one-fourth of the total culture volume. The absorbance was quantified at a wavelength of 680 nm, with measurements taken at regular intervals of 1 hour. The quantification of flocculation efficiency was performed using the previously reported equation [332]

$$Flocculation\ efficiency = 100 \times [1 - \frac{C_t}{C_0}] \tag{6.5}$$

where Ct represents the absorbance of the algal culture at 750 nm at time 't', and C_0 represents the absorbance at the start of the experiment (0 hour). In the 2L photobioreactor experiment, the same process was followed, but there was no transfer of culture. Instead, the

procedure was carried out within the photobioreactor itself. The sample was taken gently using a peristaltic pump from one-fourth of the culture volume, namely from the 0.5 L mark.

6.3 Result and discussion

6.3.1 Impact of CO_2 concentration on growth, nitrogen and CO_2 fixation

The results indicate that microalgae consistently exhibited increased biomass production under varied CO_2 conditions (Figure. 6.2a). Specifically, exposure to 15% CO_2 led to a biomass concentration of 2.5 g/L by day 23, with a growth rate of 0.145 day^{-1}. In contrast, when exposed to 5% CO_2, the biomass concentration increased to 2.73 g/L and the growth rate reached 0.155 day^{-1}. This surpassed the growth recorded under 15% CO_2 and ambient air conditions, which resulted in a biomass concentration of 1.78 g/L and a growth rate of 0.128 day^{-1}, respectively. These findings underscore the critical role of CO_2 enrichment in enhancing microalgae productivity. The microalgae exposed to 15% CO_2 entered the saturation phase at a faster rate in comparison to the microalgae exposed to a concentration of 5% CO_2. According to Figure. 6.2a, the growth continued in the late log phase until day 23 when exposed to 5% CO_2. However, under 15% CO_2 conditions, saturation was reached by day 15. Therefore, increasing the CO_2 concentration from 5% to 15% resulted in a 10% decrease in biomass productivity, with the lowest productivity observed under ambient air conditions (Table 6.1). Analysis of the logistic growth curve further validated these findings, revealing the highest growth rate at 5% CO_2, followed by 15% CO_2, while growth significantly decreased under ambient air conditions. Figure. 6.2a-d demonstrates that species adaptation to varying CO_2 concentrations has an impact on growth kinetics, photosynthetic efficacy, and nitrogen utilization. Previous research found nitrate-based nitrogen fixation yielded similar growth rates as urea in KMC8 [333]. However, urea usage boosted biomass productivity by 3%. Previous study by Rosa et al., 2023 [334] have shown urea's dual role as a source of both carbon and nitrogen, enhancing biomass productivity by effectively fixing C/N without interfering with other nutrients in the media . Thus, under nitrogen limitation, urea promote adjustment in C/N metabolism increased biomass productivity [335]. Hence, substituting nitrate with urea proves to be a sustainable and efficient option for nitrogen in this situation, given that the elevated CO_2 concentration increases the need for nitrogen to support optimal carbon fixation and production.

The optimum CO_2 concentration for microalgae growth was found to be 5%, resulting in remarkable biomass production and CO_2 fixation rates, followed by 15% CO_2 and the least in ambient air (Table 6.1). The majority of microalgae species exhibited optimal growth and productivity in 15-20% CO_2. However, their growth performance decreased when CO_2 concentrations exceeded 10%, whereas enhanced growth and productivity were found when CO_2 levels were reduced to 5% [336]. In KMC8, the introduction of urea-based nitrogen initially resulted in rapid development under 15% CO_2 circumstances with high nitrogen fixation. However, the growth phase was afterwards impacted by nitrogen limitation.

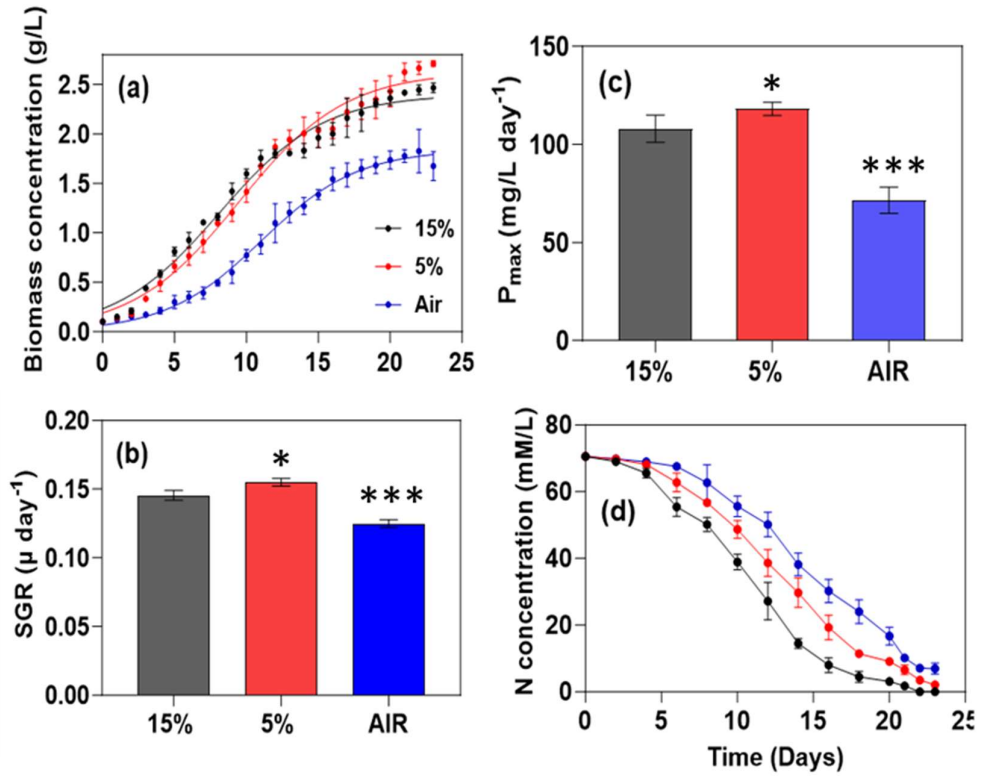

Fig. 6.2. Effects of different air/CO_2 mixtures (air, 5%, 15%) on various parameters: (a) dynamic biomass growth profile modeled using Logistic models, (b) specific growth rate, (c) biomass productivity. Error bars depict the standard deviation of n = 2 biological replicates. Asterisks indicate significant differences between the !5% the other concentrations, as determined by one-way ANOVA (Tukey's method). Significance in growth conditions is denoted by different symbols: hash symbol ($^{\#}p = 0$), single asterisk *($^{*}p < 0.05$)*, double asterisk *($^{**}\ 0.05 < p < 0.5$)*, and triple asterisk *($^{***}\ 0.5 < p < 1.0$)*.

6.3.2 Impact of CO_2 concentration on biomass composition and C/N Stoichiometry

The investigation explored the impact of varied CO_2 concentrations on microalgal biomass composition and productivity, revealing distinct patterns (Table 6.1). Under 5% CO_2 conditions, lipid, carbohydrate, and protein productivity enhanced notably at 23.14 mg/L day^{-1}, 48.33 mg/L $day^{-1,}$ and 39.06 mg/L day^{-1}, respectively. Interestingly, lipid production increased to 25.2 mg/L day^{-1} with 15% CO_2, possibly due to a 4-day period of nitrogen starvation (Figure. 6.2d). In contrast, biochemical productivity decreased significantly in ambient air conditions, with protein and carbohydrate productivity at around 30 mg/L day^{-1} and lipid productivity at 10.7 mg/L day^{-1}. These findings highlighted the complex relationship between CO_2 levels, microalgae growth, and metabolite accumulation, with 5% CO_2 emerging as the most optimal concentration. The metabolite ratio is balanced at this level, and cellular carbon and nitrogen production has gone up by 60.47 mg/L day^{-1} and 6.28 mg/L day^{-1} in proper ratio, respectively. Inadequate carbon availability in the air hinders growth and CO_2 capture, resulting in decreased productivity. Surprisingly, despite the presence of 15% CO_2, carbon productivity is lower compared to 5% CO_2 (56.15 mg/L day^{-1}), while nitrogen productivity stands at 5.08 mg/L day^{-1}.

This disparity in productivity is attributed to a change in the carbon-to-nitrogen ratio induced by nitrogen deficiency at 15% CO_2. Urea supplementation emerges as an effective strategy for maintaining the proper C/N balance by providing more carbon and nitrogen compared to other nitrogen sources, as supported by Rosa et al., 2023 [334].

This approach balances carbon and nitrogen metabolism, increasing lipid and metabolite production without reducing productivity [198]. An optimum growth requires a balanced nutritional composition, with particular attention to the C/N ratio, both externally and internally. The metrics $Y_{C/N}$ (specific carbon yield on a nitrogen basis) and intracellular C/N ratio increased with an increase on CO_2 level as shown in Table 6.1. This highlights the significant influence of CO_2 on the utilization of urea-based nitrogen and the synergistic relationship between CO_2 and nitrogen in regulating metabolites for biomass production by maintaining the intracellular C/N balance.

Table 6.1 Comparison of growth parameters, nutrient fixation, total organic carbon in media and biochemical productivity performance after 23 days of inoculation in air, 5%, and 15% CO_2 conditions for microalgae *M. pusillum* KMC8 (data represents mean ± standard deviation, n=3)

Parameter	Unit	Air	5% CO_2	15% CO_2
Biomass productivity	mg L^{-1} day^{-1}	71.6 ± 2.2	118.7 ± 1.3	107.5±1.8
Specific growth rate	day^{-1}	0.128 ± 0.01	0.155 ± 0.01	0.145 ± 0.01
CO_2 fixation	mg L^{-1} day^{-1}	129.80 ± 5.37	221.45 ± 3.80	200.8 3± 3.10
Total organic carbon	mg/L	17.12 ± 0.87	26.54 ± 1.09	83.34 ± 0.65
Nitrogen utilization rate	mg L^{-1} day^{-1}	33.83 ± 1.97	38.95 ± 2.48	45.97 ± 2.30
Lipid productivity	mg L^{-1} day^{-1}	10.67 ± 0.24	23.14 ± 1.83	25.2 ± 1.05
Carbohydrate productivity	mg L^{-1} day^{-1}	30.15 ± 1.87	48.33 ± 1.45	40.28 ± 1.57
Crude protein productivity	mg L^{-1} day^{-1}	29.48 ± 1.52	39.06±0.50	31.57±1.92
Carbon productivity	mg L^{-1} day^{-1}	56.15 ± 0.23	60.47 ±1.04	35.24 ±1.23
Nitrogen productivity	mg L^{-1} day^{-1}	5.08 ± 0.22	6.28 ± 0.07	4.75 ± 0.32
Cellular C/N quota	(gm/gm)	7.42 ± 0.78	9.63 ± 0.62	11.05 + 0.27
$Y_{C/N}$	-	0.93 ± 0.08	1.42 ± 0.15	1.48 ± 0.12

6.3.3 Impact of CO_2 concentration on photosynthesis and pH dynamics

In a 23-day growth study, the influence of CO_2 levels on KMC8 photosynthesis, pigment production, and pH dynamics was examined (Figure. 6.3a-d). Initially, all CO_2 concentrations resulted in increased photosynthetic quantum yield (*Fv/Fm*) on days 5 and 10, with the most significant improvement observed at 15% CO_2. However, by day 15, a slight decrease in photosynthesis efficiency, particularly pronounced at 15% CO_2, was evident (Figure. 6.3d). On the 23rd day, the *Fv/Fm* values reached their minimum in the ambient air (0.44), were elevated in 5% CO_2 (0.6), and decreased in 15% CO_2 (0.48). This indicates a potential shift towards nitrogen deficiency in the elevated CO_2 environment or carbon limitation in the surrounding air, where the value did not exceed 0.6 from the starting point (Figure. 6.3b). Chlorophyll levels peaked in ambient air, followed by 5% CO_2, while carotenoid secretion peaked at 5% CO_2 but declined after 15 days at 15% CO_2 (Figure. 6.3c & d). Simultaneously, the pH levels significantly dropped to 15% CO_2 by day 15, indicating that acidification and nitrogen deficiency influenced the metabolic adaptation (Figure.6.3a). Previous studies show that chlorophyll and carotenoid synthesis decrease between pH 4 and 7.5, affecting pigment synthesis efficiency in *Dunaliella bardawil*, *Chlorella ellipsoidea* and N*annochloropsis sp.* [78,154,160]. Exposure to 5% CO_2 enhanced the energy conversion

efficiency by synthesis of more pigments [337]. Changes in photosynthetic efficiency have a significant impact on cellular carbon and nitrogen fixation processes, as well as growth and CO_2 assimilation rates by increasing light capturing efficiency [338]. The *Fv/Fm* ratio, a measure of Photosystem II (PSII) photochemistry efficiency, provides insight into microalgae stress and photosynthetic health. A value exceeding 0.6 signifies robust photosynthesis, ample nutrient presence, and efficient utilization [339]. Monitoring and adjusting nutrient modulation conditions using *Fv/Fm as* a proxy can enhance microalgal growth and productivity. Nitrate mitigates acidification but hampers carbon and nitrogen fixation, whereas urea's neutral ionic charge makes it a dependable pH buffer [334].

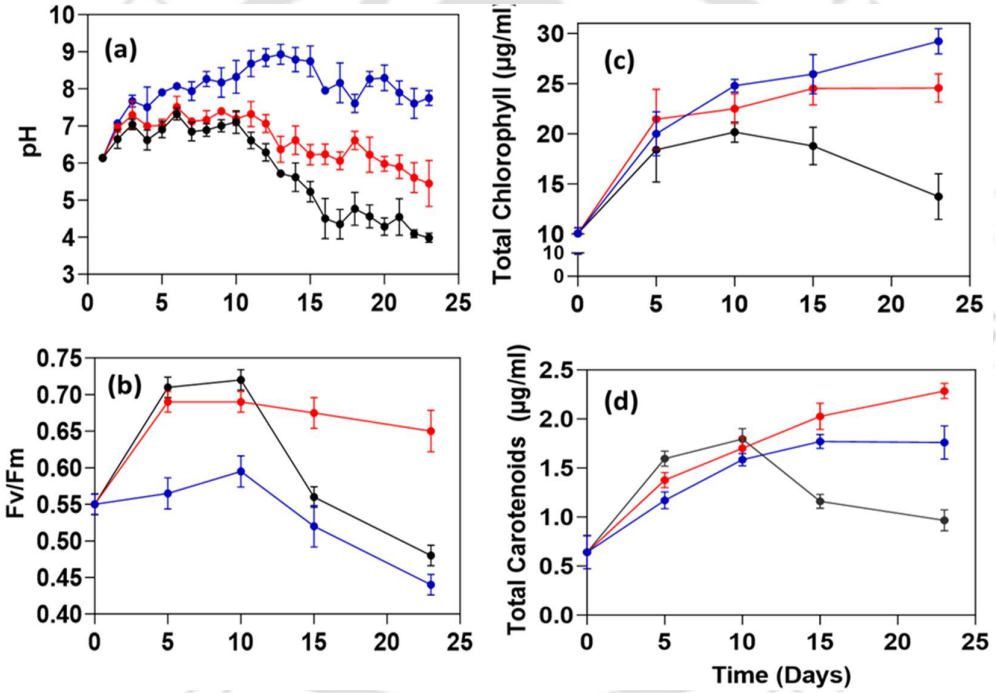

Fig. 6.3. Effects of different air/CO_2 mixtures (air, 5%, 15%) on various parameters: **(a)** dynamic pH profile, **(b)** Fv/Fm, **(c)** total chlorophyll, and **(d)** carotenoids pigment. All data points represent the mean of n = 3 biological replicates; error bars represent the replicates standard deviation

6.3.4 Process Strategies of CO_2 concentration dilution with calcium-induced phosphorus fed-batch

The study observed enhanced microalgae growth in the presence of 15% CO_2 compared to 5% CO_2 and normal air, indicating increased tolerance to high CO_2 levels and improved photosynthetic activity. However, prolonged exposure to 15% CO_2 resulted in rapid culture acidification after 15 days, leading to reduced *Fv/Fm* and pigment loss. In contrast, a prolonged growth phase at 5% CO_2 showed improved growth and production. This work, together with our earlier research, highlights the significant reliance on nitrogen fixation and nitrogen availability when carbon is continuously supplied via CO_2 [333]. Hence, 5% CO_2 level maintaining a carbon flow rate (CFR) of 0.1 g/L day^{-1}, can sustain this balance by interacting with residual nitrogen for a 23-day development period. However, a 15% CO_2 level, which maintains a CFR of 0.3 g/L day^{-1}, disrupts this equilibrium quickly. Higher CO_2 levels, combined with adequate nitrogen supply, control pH and alkalinity by ensuring a balanced C/N ratio in the medium, promoted CO_2 assimilation, and growth [340,341].

From days 0 to 15, a nitrogen concentration of 70–17.67 mmol/L, based on urea, promoted substantial growth in an environment with 15% CO_2. This showed that there was a beneficial interaction between the continuous aeration of 15% CO_2 and the buffer capacity, leading to efficient dilution of CO_2. However, the nitrogen concentration of 14.3 mmol/L after 15 days was insufficient to sustain photosynthesis and pH regulation in KMC8, indicating the presence of nitrogen limitation stress. *Fv/Fm* can be used to evaluate the nitrogen limitation factor, monitor changes in CO_2 modulation conditions, and establish a direct relationship with the buffer capacity of the medium. Supplementing phosphorus in environments lacking nitrogen can enhance the process of CO_2 fixation and increase lipid levels, while also sustaining biomass production. This shows potential for thriving in situations with limited nutrients.

Three novel process strategies were investigated to improve photosynthetic efficiency and CO_2 fixation, especially under nitrogen-deficient conditions. The strategies involved a transition from a 15% to a 5% CO_2 concentration after 14 days, followed by a switch to regular air while maintaining a constant 15% CO_2 level. Additionally, phosphorus feed with calcium induction was utilized, as depicted in Figure. 6.1. Increased nitrogen labelling optimizes photosynthesis by utilizing ample nitrogen and carbon resources, consequently enhancing the efficiency of CO_2 absorption. This effect has been demonstrated in our previous study (Chapter 5) and is further supported by the findings of this current study. Our hypothesis is that by

modulating CO_2 levels to interact with residual nitrogen, we may sustain elevated alkalinity and mitigate acidification resulting from CO_2 under nitrogen-deprived settings. In Chapter 5, it is shown that maintaining a CO_2 concentration of 15% results in a pH level below 4 once nitrogen becomes restricted. The insufficient nitrogen content is unsuitable for maintaining the appropriate pH balance in the microalgal culture medium.

6.3.4.1 Impact of process strategies on improvement of cell growth and biomass productivity

In comparison with previous results obtained at a constant 15% CO_2 concentration (Section 6.3.1), the introduction of phosphorus supplementation on the 14th day, in conjunction with different CO_2 modulation, resulted in substantial changes in the growth dynamics of microalgae (Figure.6.4a). The study documented a notable alteration in the pattern of the logistic growth curve following modifications to the culture conditions on the 14th day. When subjected to a consistent 15% CO_2 environment and provided with additional phosphorus, the biomass quantity increased to 2.6 g/L, confirming the significant influence of phosphorus supplementation, in line with our prior investigation in chapter 5 . The productivity rate was measured at 109.8 mg/L day^{-1}, with growth rate of 0.156 day^{-1} which showed a slight improvement compared to the conditions of continuous 15% CO_2 without phosphorus supplementation. However, a noticeable growth response occurred when the CO_2 concentration diluted from 15% to 5%, revealing a clear lag period as microalgae adapted to lower CO_2 levels. This led to an increase in growth to 3.1 g/L, with a productivity of 130 mg/L day^{-1} and growth rate 0.17 day^{-1}, demonstrating significant improvements in productivity of 122.8% and 11.2% compared to continuous 15% and 5% CO_2 conditions, respectively. Transitioning to ambient air (15/Air) caused a growth delay but resulted in higher biomass growth (1.85 to 2.03 g/L) and productivity (84 mg/L day^{-1}) with growth rate of 0.137 day^{-1} compared to continuous air conditions.

Supplementing with phosphorus enhanced development in habitats with both 15/5% CO_2 and 15/Air settings, emphasizing the significance of nitrogen and growth-dependent CO_2 control in sustaining uninterrupted microalgal growth. In their studies, Chen et al., 2020; Chen and Xu, 2021 [78,160] conducted experiments that demonstrated that elevated CO_2 levels enhanced the growth and biomass yield of microalgae species *Nannochloropsis salina* and *Dunaliella salina.* Nevertheless, this study found that the growth rates increased as the

concentration of CO_2 decreased from high to low levels, as determined by the interpretation of the *Fv/Fm* under nitrogen limitation stress. This underscores the significance of maintaining suitable C/N ratios not only in heterotrophic cultures, as noted by Sun et al., 2020 [287], , but also in phototrophic cultures. Adjusting the concentration levels of carbon flow in response to the presence of nitrogen from urea improves productivity and aids in the conversion of CO_2 into organic biomass. Prior studies done by Rosa et al., 2023; Sheng et al., 2022 [198,334] have shown that urea has the capacity to liberate carbon molecules to support growth, hence possibly mitigating any limitations imposed by carbon availability.

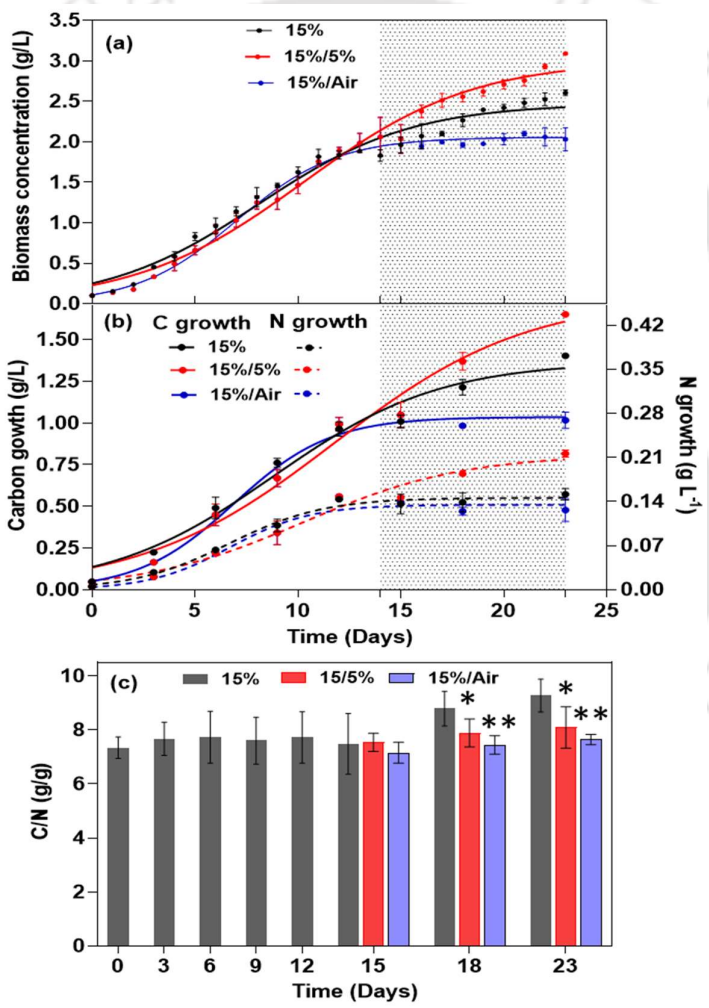

Fig. 6.4. Effect of continuous exposure to 15% CO_2 and dilution CO_2 concentration from 15% to 5% (15%/5%) and 15% to 0.04% (15%/Air) condition in calcium-induced phosphorus fed batch on dynamic **(a)** biomass, **(b)** carbon and nitrogen-based growth profile modelled using Logistic models, and **(c)** cellular C/N ratio. Asterisks denote significant differences from the

continuous 15% CO_2 condition and other two CO_2 modulation condition using one-way ANOVA (Tukey's method) for C/N balance

6.3.4.2 Impact of process strategies on improvement on carbon and nitrogen stoichiometry and CO_2 fixation

The microalgae exhibited strong growth in a 15% CO_2 environment over a period of 14 days. This growth was accompanied by constant absorption of carbon and nitrogen, indicating the microalgae's ability to adapt to high levels of CO_2. This information is shown in Figure 6.4b. This flexibility enabled a more effective utilization of both carbon and nitrogen, leading to improved total growth. Modifying the circumstances on the 14th day by changing the CO_2 ratio from 15% to 5% resulted in a significant rise in both carbon and nitrogen growth, suggesting enhanced intake of nutrients. When exposed to a constant level of 15% CO_2, with a carbon feed rate of 0.3 g/L per day, the growth of carbon biomass significantly rose to 1.4 g/L. Switching to a 5% concentration of CO_2 resulted in a 25% increase in carbon growth, however this growth fell by 23% after transitioning back to a normal air condition. Conversely, growth that relies on nitrogen remained rather stable across various levels of CO_2, emphasizing the need of regulating CO_2 for achieving optimum growth. The growth that relies on nitrogen stayed stable independent of fluctuations in CO_2 levels, highlighting the need of controlling CO_2 levels for achieving the best possible growth. More precisely, when exposed to a consistent level of 15% CO_2, the growth rate decreased to 0.15 g/L. When the environment was changed to normal air on the 14th day, the growth rate stabilized at 0.13 g/L. However, a significant alteration took place when the concentration of CO_2 decreased to 5%, while the levels of nitrogen often reached a maximum of 0.21 g/L. Observations were made on fluctuations in the carbon-to-nitrogen (C/N) ratio, where sustained elevated levels of carbon dioxide (CO_2) resulted in a rise from 7.3 to 9.2. Nevertheless, the act of reducing the concentration of CO_2 to 5% on the 14th day led to the establishment of a consistent ratio ranging from 7.2 to 7.8 (as shown in Figure 6.4c). The described balance is essential for optimizing output and fostering development. Microalgae are capable of performing the simultaneous conversion of nitrogen into protein-based biomass and carbon into energy molecules. This process facilitates the build-up of bioenergy by capturing carbon dioxide and converting it into biomass during the process of photosynthesis [338].

The manipulation of CO_2 levels during cultivation had a substantial impact on the rates of photosynthesis and CO_2 fixation. At the beginning, in a span of 12 days, the microalgae

showed a significant and swift rise in CO_2 fixation, going from 168.45 mg/L day^{-1} to 335.5 mg/L day^{-1} (Figure. 6.5a). Nevertheless, as the cultivation persisted with a consistent 15% CO_2 concentration for more than 15 days, the efficiency of CO_2 fixation decreased. In contrast, maintaining a 5% concentration of CO_2 led to consistent rates of CO_2 fixation, whereas transitioning to regular ambient air resulted in the poorest performance. This observation indicates that cellular stress caused by a lack of nitrogen, extended exposure to a high concentration of 15% CO_2, and limited availability of carbon in normal air conditions led to a decrease in photosynthesis and CO_2 fixation. Nevertheless, the shift to a 5% concentration of carbon dioxide after 14 days seemed to establish advantageous circumstances for facilitating the process of CO_2 fixation.

The stability of carbonic anhydrase (CA) activity is crucial for its successful regulation of carbon dioxide (CO_2) concentrations, as seen in Figure 6.5b of the research. The enzyme's efficiency is maximized when carbon dioxide (CO_2) levels are kept at around 15% with 5%. Any deviations from this particular ratio result in a significant decline in CA activity. Throughout the experiment, scientists noted that the continuous exposure of the culture to a high concentration of CO_2 (particularly 15% CO_2) for a duration of 23 days did not facilitate effective CO_2 fixing. However, it had a negative impact on the system's buffer capacity as discuss in further detail section 6.3.4.3. The consequences of variable levels of CO_2 are substantial: inadequate amounts of CO_2 may result in a shortage of accessible carbon for vital biological activities, while continuous exposure to elevated amounts of CO_2 can result in acidification. The acidification has a direct effect on the amounts of inorganic carbon, namely bicarbonate, which is strongly associated with the functioning of carbonic anhydrase. This stability enables the conversion of bicarbonate to CO_2, which is crucial for the efficient carboxylation of RuBP [337].

This outcome, in conjunction with our prior findings in chapter 5, verifies that the sole augmentation in dynamic growth does not solely ascertain the escalation in CO_2 necessity imperative for sustaining growth. The statement emphasizes the significance of the interaction between CO_2 in the gaseous phase and other nutrients, specifically nitrogen conditions in the media. This interaction plays a crucial role in controlling the carbon demand and aiding the adaptation of microalgae to varying CO_2 concentrations. Phosphorus availability is crucial for maximizing the efficiency of CO_2 fixation, especially in conditions where nitrogen is limited. The adjustment of carbon flow rate under nitrogen-limiting conditions, along with the interaction of phosphorus and calcium-induced alkalinity, significantly enhances and stabilizes

CO_2 fixation. These factors have been thoroughly discussed in previous sections 6.3. 2 and 6.3.4.1, respectively. To achieve the best possible dissolution of CO_2 and facilitate appropriate development, it is crucial to meticulously synchronize the flow of CO_2 concentration in the medium with the remaining nitrogen levels. This alignment guarantees the preservation of the C/N balance and buffer chemistry in the media, establishing optimal conditions for the growth of microalgae.

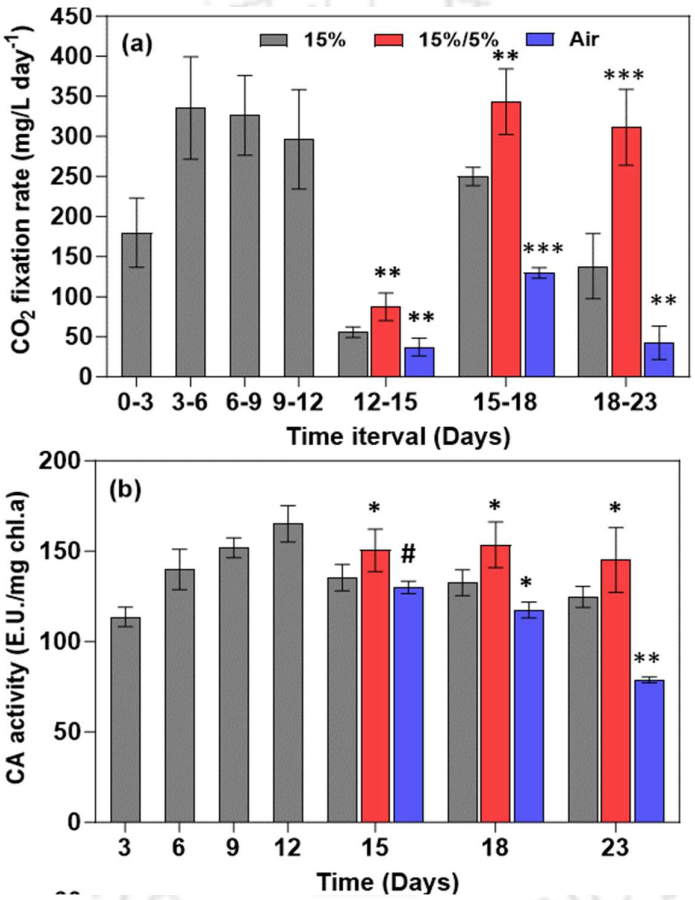

Fig. 6.5. Effect of continuous exposure to 15% CO_2 and dilution of CO_2 concentration from 15% to 5% (15%/5%) and 15% to 0.04% (15%/Air) condition in calcium-induced phosphorus fed batch on **(a)** CO_2 fixation in different time intervals, **(b)** carbonic anhydrase activity. Asterisks denote significant differences from the continuous 15% CO_2 condition and other two CO_2 modulation condition using one-way ANOVA (Tukey's method).

6.3.4.3 Impact of process strategies on improvement of buffer capacity and photosynthesis activity

The manipulation of CO_2 concentrations and the introduction of calcium-induced phosphorus feeding have provided significant insights into buffer capacity (Figure. 6.6b and c) and photosynthesis activity (Figure. 6.6d and f). pH levels exhibited notable fluctuations over the experimental period, with a significant decrease observed from 7.45 to 5.45 in the initial 0-14 days, indicative of a shift towards acidity (Figure. 6.6b). This decline aligns with previous findings suggesting that elevated CO_2 concentrations contribute to increased acidity due to carbonic acid production [32]. Notably, significant changes occurred on the 14th day, particularly in the 15/5% CO_2 condition, where the pH increased from 5.02 to 6.68, underscoring the adaptability of microalgae. Conversely, minimal pH variation was observed in the 15/Air condition, indicating inadequate pH control. Alkalinity mirrored pH trends, starting at 6.17 and rising to 13.78 with 15% CO_2 before stabilizing between 9.57 to 11.62 with the adjustment of CO_2 levels (Figure.6.5c). The observations from Figure. 6.6b and c clearly indicate the importance of accurate carbon management for the development and production of microalgae, particularly under nitrogen-limited stress circumstances. This management is necessary to regulate pH and alkalinity and ensure the stability of carbon fixation [33]. Further details on this topic will be discussed in the section 6.3.4.3. In addition, the incorporation of calcium ions facilitated effective biomineralization, resulting in the creation of calcium carbonate [34]. This compound not only modified the pH of the medium but also promoted the growth of microalgae and brought about alkalescent characteristics CO_2. The proof of concept for developing this strategy is evident in its ability to promote cell growth and mitigate the negative effects of increased CO_2 levels, such as acidity-related losses, during prolonged cultivation periods.

Photosystem quantum yield II (*Fv/Fm*) showed variation in response to changes in CO_2 concentration, as depicted in Figure. 6.6d. The decrease in pH and alkalinity caused by nitrogen deficiency led to a significant decrease in *Fv/Fm* , ratios, even though there was a constant 15% CO_2 supply.. In contrast, the introduction of phosphorus supplemented the nitrogen deficiency, consequently improving the activity of photosynthesis. Through CO_2 reduction and phosphorus adjustment, microalgae were resilient to nitrogen constraint with *Fv/Fm* ratios >0.6. However, both 15/Air and continuous 15% CO_2 exhibited suboptimal *Fv/Fm* ratios below 0.5, indicating unfavorable photosynthetic behavior in KMC8. This observation aligns with findings from our prior investigations, which noted a decline in pigment synthesis and growth

inhibition associated with *Fv/Fm* ratios below 0.5, suggesting stress [2,11]. Reducing the concentration of CO_2 on the 14th day increased pigment synthesis (Figure. 6.6e and f) especially carotenoid synthesis, in nitrogen-deficient conditions, phosphorus increases carotenoids to protect against stress [35]. Overall, changes in pH and alkalinity underscore the significance of keeping CO_2 levels in check to maintain optimal photosynthesis and microalgal growth. Phosphorus helps carbon uptake via intracellular nitrogen utilization pathways, so optimizing CO_2 and phosphorus levels improves physiological process and stabilize carbon fixation in conditions of nitrogen limitation [5].

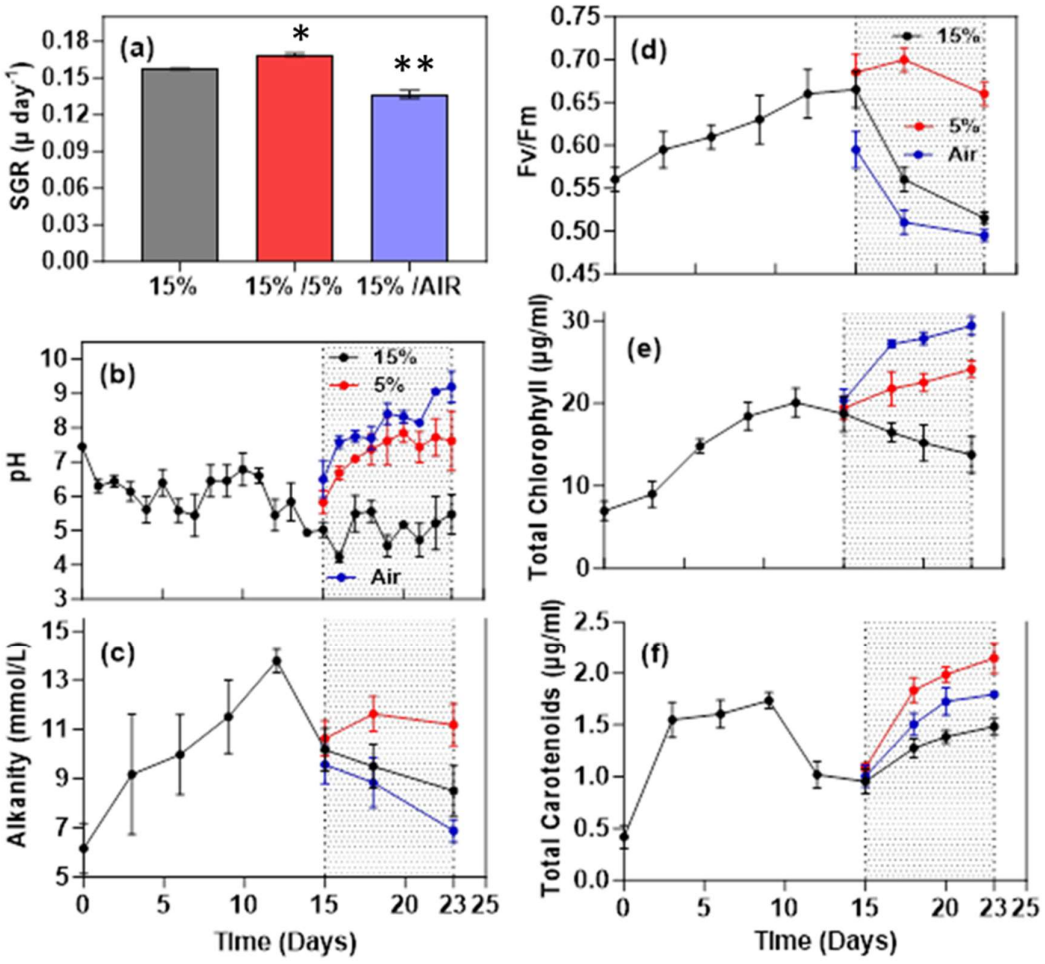

Fig. 6.6. Effect of continuous exposure to 15% CO_2 and dilution of CO_2 concentration from 15% to 5% (15%/5%) and 15% to 0.04% (15%/Air) condition in calcium-induced phosphorus fed batch on **(a)** specific growth rate, **(b)** dynamic pH profile, **(c)** alkalinity, **(d)** Fv/Fm, **(e)** total chlorophyll and **(f)** carotenoids pigment. Asterisks denote significant differences from the

continuous 15% CO_2 condition and other two CO_2 modulation condition using one-way ANOVA (Tukey's method) for specific growth rate.

6.3.4.4 Impact of process strategies on improvement on metabolite productivity of biomass

The fluctuations in lipid productivity and biochemical composition in microalgae are closely linked to the interaction between carbon and nitrogen metabolism under varying CO_2 levels (Figure. 6.7). Under 15% CO_2 conditions, lipid productivity peaked at 29.38 mg/L day^{-1}, with the highest lipid content recorded at 26.24%, illustrating the impact of increased carbon availability and nitrogen limitation on lipid synthesis. Concurrently, carbohydrate and protein content stood at 36.34% and 35.4%, with respective productivities of 39.75 and 38.04 mg/L day^{-1}. Phosphorus addition led to a 17% increase in lipid productivity compared to trials without phosphorus under 15% CO_2, emphasizing its role in sustaining photosynthesis and carbon fixation under nitrogen limitation, vital for cellular growth development. Transitioning from 15% to 5% CO_2 resulted in a significant increase in metabolite productivity, with lipid production reaching 29.845 mg/L day^{-1}, and protein and carbohydrate productivity at 57.30 and 30.24 mg/L day^{-1}, respectively. However, this change coincided with a decrease in lipid content to 22.45%, indicating a shift towards heightened carbohydrate and protein production.

This underscores the necessity of maintaining a balanced C/N ratio throughout cultivation to ensure proper carbon and nitrogen fixation, crucial for CO_2 fixation and biomass production in biorefinery approaches as we observed the result and discussed under section 3.2.2. Under 15/AIR conditions, lipid productivity dropped to 15.87 mg/L day^{-1} due to limited carbon availability, prompting microalgae to allocate resources towards carbohydrate and protein synthesis, evident by higher carbohydrate and protein values at 38.85% and 40.56%, respectively. The shift from a 15% CO_2 concentration to a 5% CO_2 concentration resulted in a significant rise in the production of lipids, carbohydrates, and proteins. This demonstrates the ability of microalgae to adapt to different levels of CO_2 by efficiently utilizing carbon and nitrogen for biomass development, while maintaining a stable C/N ratio, as discussed in section 3.2.3. Phosphorus addition enhances cellular growth by bolstering ATP production through the oxidative phosphorylation pathway [219].

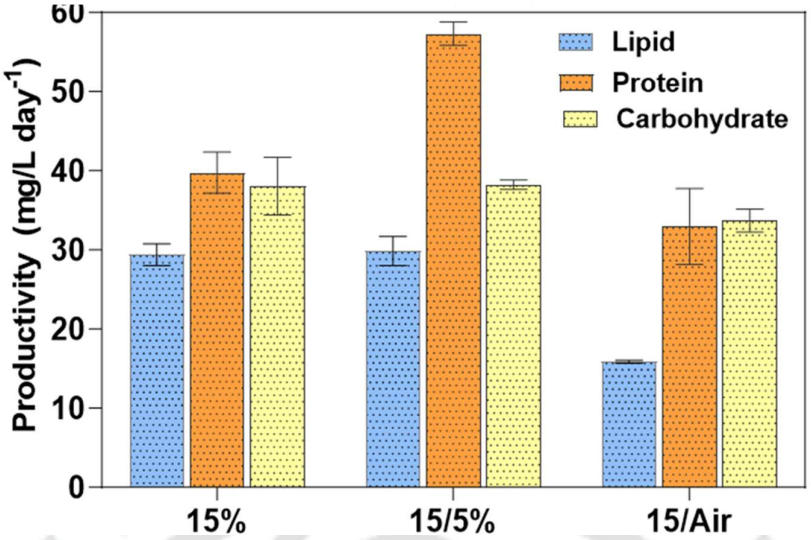

Fig. 6.7. Effect of continuous exposure to 15% CO_2 and dilution of CO_2 concentration from 15% to 5% (15%/5%) and 15% to 0.04% (15%/Air) condition in calcium-induced phosphorus fed batch on biochemical composition productivity

6.3.5 Induced of self -flocculation mechanism in microalgae

The study explored enhancing biomass harvesting efficiency in microalgae by inducing self-flocculation mechanisms through Ca^{2+} ion addition and CO_2 level adjustments (Figure. 6.8 and 6.10). Assessment of flocculation efficacy revealed varied outcomes across modulation conditions (Figure. 6.8a). A 15%/Air modulation achieved 100% success within 100 hours, sustained for an additional 20 hours. Similarly, modulation from 15% to 5% CO_2 showed consistent growth, reaching 96.17% after 100 hours and peaking at 100% after 120 hours. Continuous exposure to 15% CO_2 yielded steady but lower efficiency, stabilizing at 84.45% after 120 hours. Notably, the 15/5% CO_2 experimental condition exhibited the highest 97.6% volume reduction efficiency due to the initial highest cell density (Table 6.2), reducing centrifugation load and power consumption for subsequent harvesting processes the detail from cultivation to dewatering represent in Figure. 6.9b and c. Phosphorus and calcium supplementation alongside CO_2 regulation enhanced buffer capacity, influencing alkalinity and carbonic anhydrase activity, subsequently improving photosynthetic efficiency. Zeta potential analysis indicated maximum values in the 15 to air dilution condition, followed by 15% to 5% CO_2 dilution, and the lowest in continuous 15% CO_2 (Figure.6.8a). Higher zeta potential in air, moving towards neutrality, suggests stronger particle aggregation on cell surfaces, enhancing flocculation efficiency [342]. Under 15% CO_2, increased zeta potential may disperse microalgae cells, reducing flocculation efficiency. SEM-EDX analysis indicates significant

calcium, magnesium, and phosphorus ions on cell surfaces under air and 5% CO_2, favoring flocculation (as shown in Figure. 6.9). Modulating ions and CO_2 levels induces self-flocculation, improving biomass harvesting sustainability. Gradual increase in pH and alkalinity cause ion precipitation, notably calcium, magnesium, and iron, facilitating auto-flocculation and validating effectiveness [332].

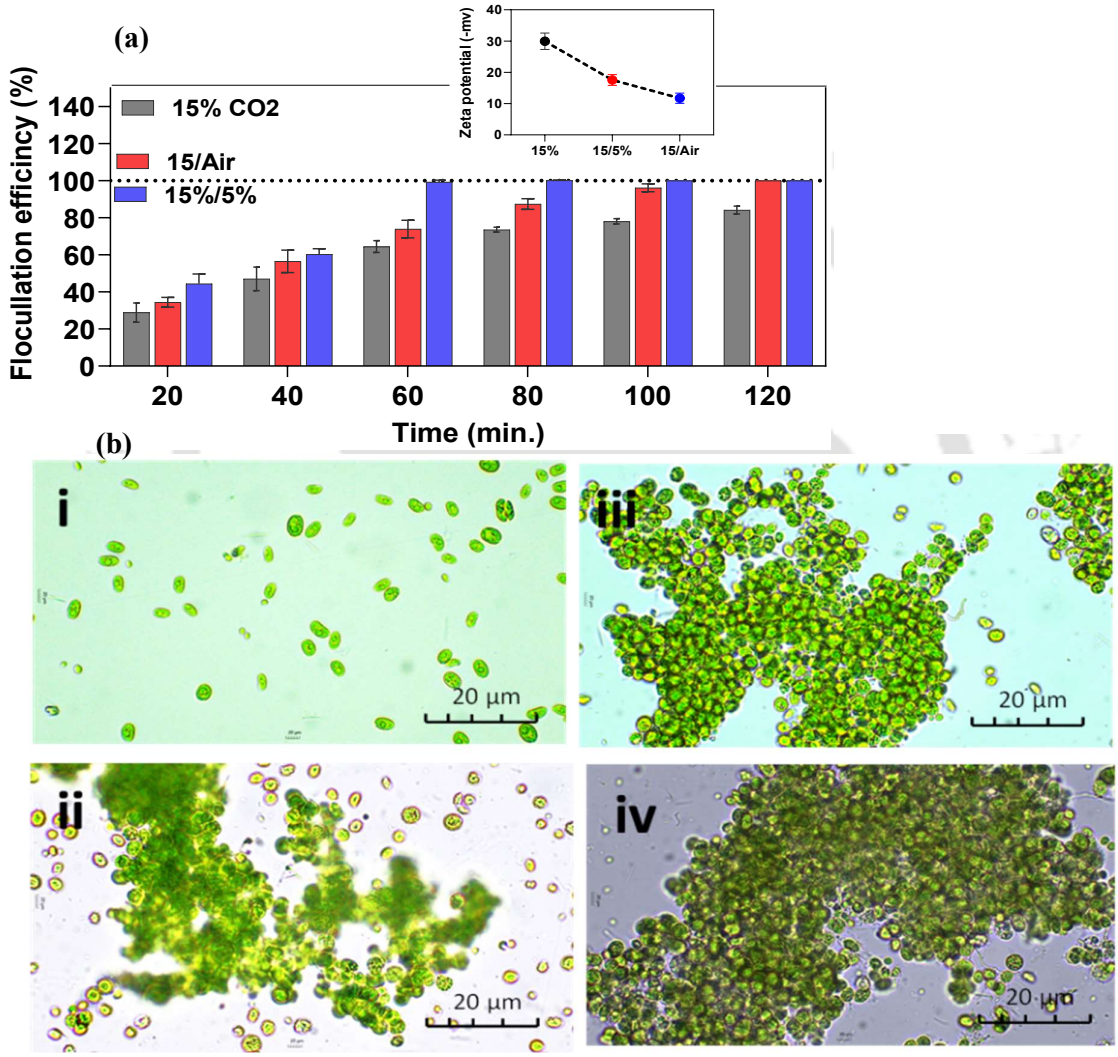

Fig. 6.8. (a) Flocculation efficiency and Zeta potential at 15% CO_2 and 15%/5% and 15%/Air condition in calcium-induced phosphorus fed batch, **(b)** Microscope images of microalgal cell after flocculation at (i) normal BG-11 media (ii) 15% CO_2 (iii)15%/5% (iv) 15%/Air, and (c) dissolve organic carbon in media

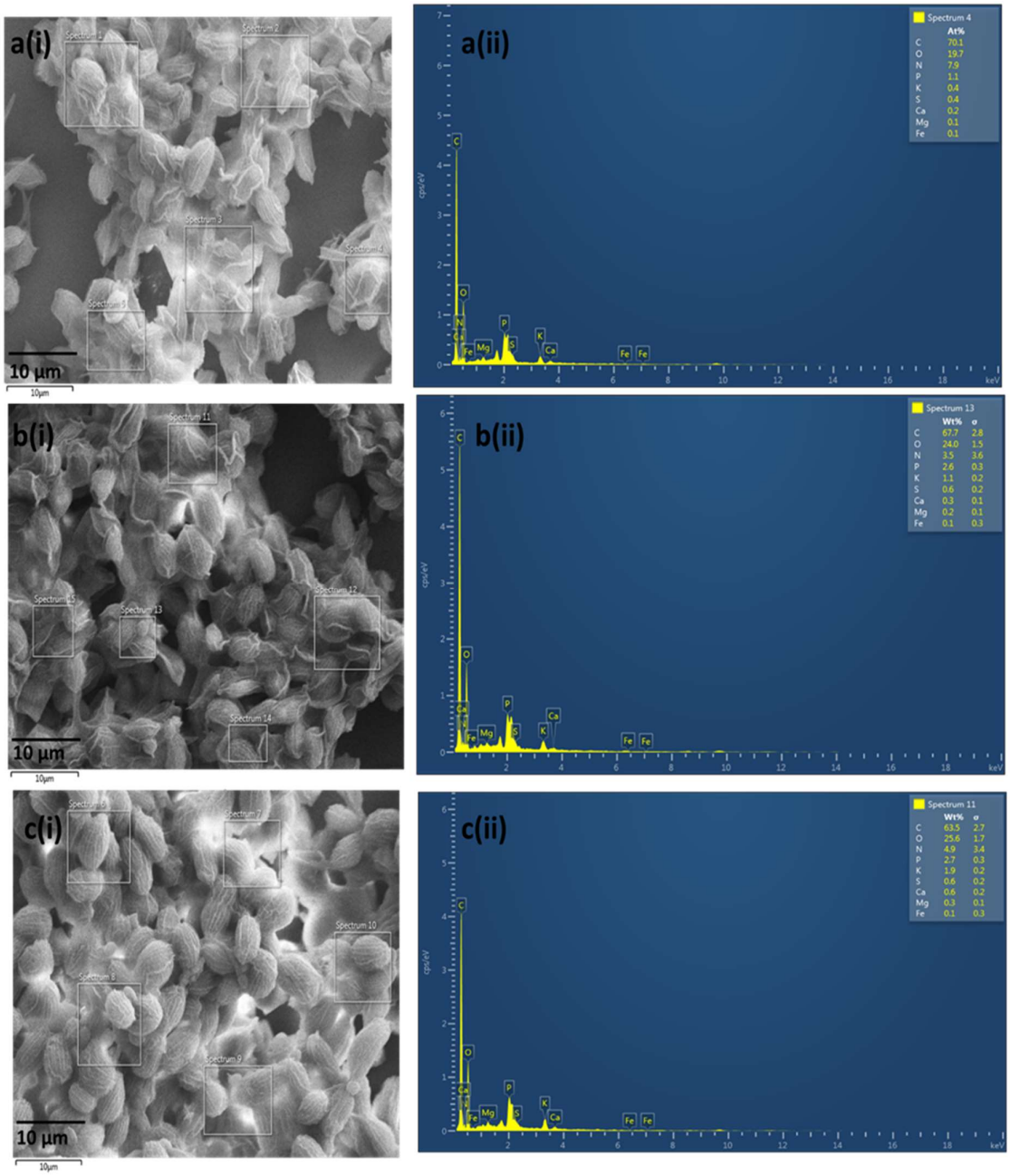

Fig. 6.9. Scanning Electron Microscopy-Energy Dispersive X-ray spectroscopy (SEM-EDX) analysis of microalgal cells under different conditions: **(a) (i) & (ii)** 15% CO_2, **(b) (i) & (ii)** 15%/5% CO_2 concentration, and **(c) (i) & (ii)** 15%/Air condition in calcium-induced phosphorus fed batch.

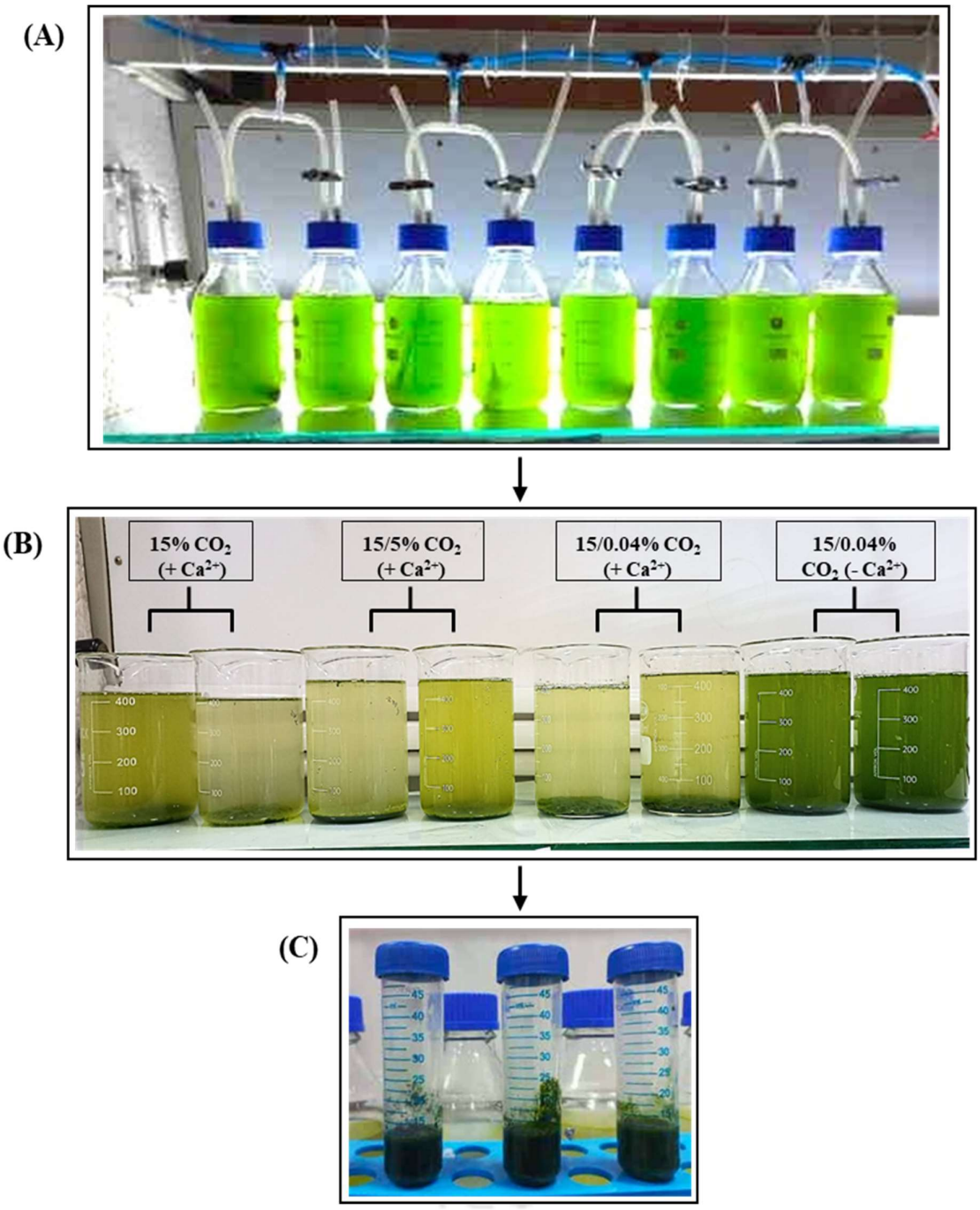

Fig. 6.10. (A) Schematic diagram of the bench-top customized experimental setup. **(B)** Image of the culture broth in beaker used for slurry depth and volume analysis. **(C)** Images showing the slurry volume after removing the culture media

Table 6.2: Harvesting performance in different CO_2 modulation strategies in terms of slurry density and volume reduction

Culture condition	Cell density (g/L)	*Slurry density (g/L)	**Volume reduction (%)
15% (+ Ca2+)	2.63	67.56	96.56
15/5 (+ Ca2+)	3.1	84.23	97.12
15/Air (+ Ca2+)	2.05	61.99	94.12
15/Air (- Ca2+)	1.98	-	-

6.3.6 Photobioreactor study key findings, and future perspectives

The research investigated the use of an optimized CO_2 dilution technique in a photobioreactor. This technique included employing a 15/5% CO_2 calcium-induced phosphorus fed-batch method. The findings obtained were statistically significant and are given in Table 6.3. The rate of CO_2 fixation increased to 264.55 mg L^{-1} day^{-1} mostly due to the bubble column's larger vertical size, which resulted in a longer retention time. The biomass density saw a significant rise to 3.23 g L^{-1} day^{-1}, leading to a notable enhancement in metabolic output. This was shown by the production of high cell density biomass, as seen in Figure. 6.11, which represents the culture density in the experimental setup. The biomass exhibited an impressive settling efficiency of 96% during a span of one hour, accompanied by a decrease of 92.3% in the culture volume relative to the entire culture volume. This led to notable energy conservation After undergoing centrifugation, the total output of wet biomass is 5.25 g. The culture volume is decreased from 2 L to 0.15 L, shown in Figure.6.12. Moreover, there was a reduction in the release of organic carbon, enhancing the potential for reusing the medium in future growing cycles. This optimized approach not only highlights its effectiveness in CO_2 capture and biomass production but also surpasses prior studies employing alternative energy-saving harvesting technologies in continuous culture phases. It underscores the focus on advancing sustainable practices and cost-efficiency within photobioreactor operations, paving the way for more efficient biomass production and resource utilization.

Cellular elemental analysis and metabolite-based bioenergy accumulation demonstrate enhanced energy content, driving sustainable bioprocess engineering. These findings underscore the potential for scalable, environmentally responsible biomanufacturing, aligning with principles of cleaner production, circular economy, and CO_2 capture. This study marks significant progress in leveraging algae for CO_2 capture and biomass generation, promoting cleaner and more sustainable production techniques. Future research should focus on

optimizing carbon capture effectiveness and reducing medium acidity through flue gas utilization and urea addition. Investigating methods to understand nitrogen and CO_2 concentration limitations through air dilution can enhance algae growth stability and carbon assimilation efficiency. Continuous evaluation of carbon capture systems is crucial to ensure long-term stability and adaptability, emphasizing alkalinity preservation, metabolite production maximization, and lipid storage optimization. Exploring sulfur and nitrogen compounds in flue gases offers novel pH regulation strategies in photobioreactors, supported by optimizing the F_v/F_m ratio for efficient carbon and NO_X/SO_X compound fixation. Utilizing cost-effective urea supplementation and pre-cultivation in flue gases can enhance algae's resilience to CO_2 and hazardous chemicals, facilitating large-scale industrial applications. Resource extraction from sulfur and nitrogen oxides in flue gases presents opportunities to address CO_2 excess and media acidification challenges in algae cultivation.

Fig. 6.11. Photobioreactor setup with a high culture cell density of 3.23 ± 0.23, using a 2-liter working volume. This was achieved by applying an optimized calcium-induced fed-batch process with CO_2 modulation over a 23-day cultivation period. Results represent the mean of n = 2 biological replicates; error bars indicate the standard deviation of the replicates.

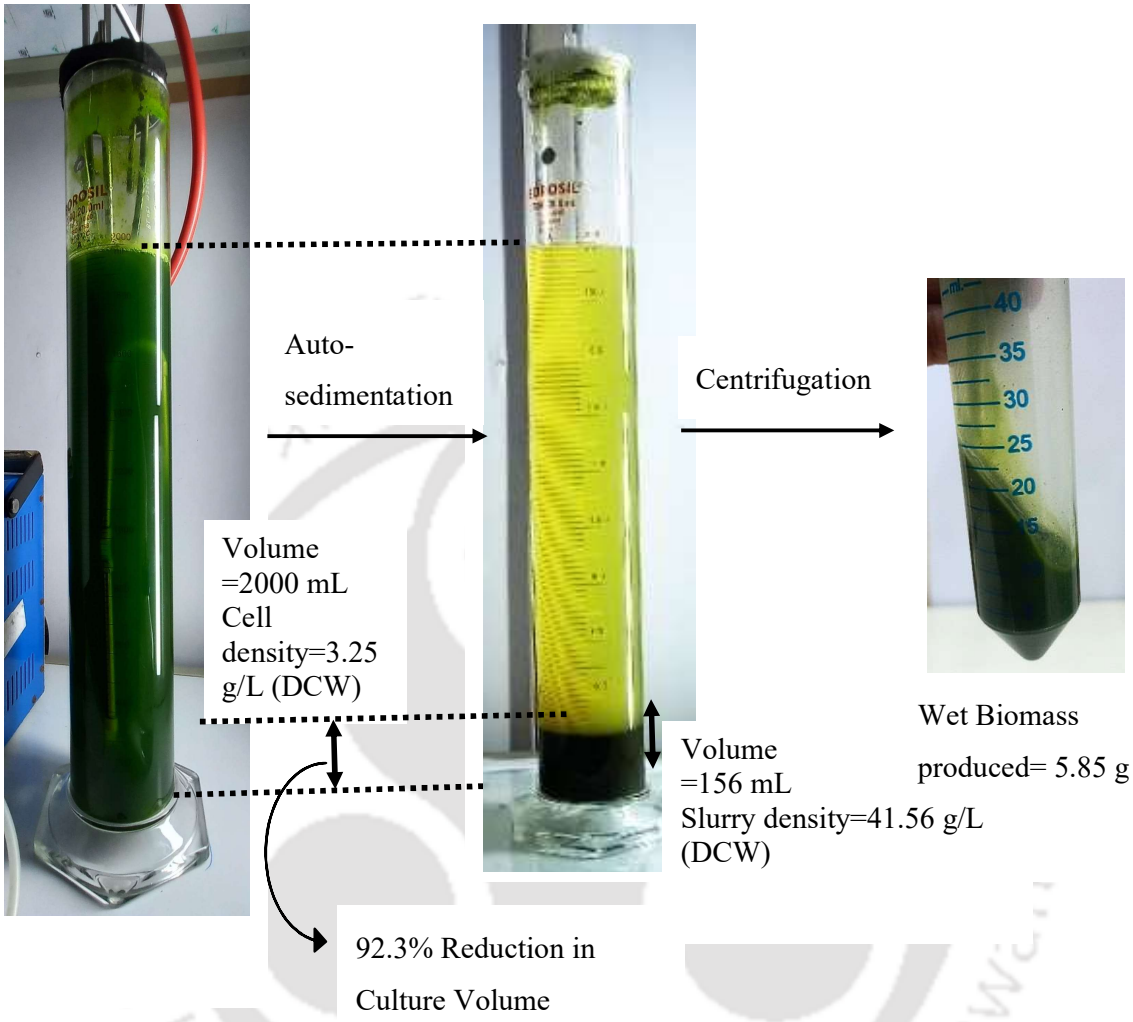

Fig. 6.12. Image displaying the scale and value of volume reduction after the auto-sediment process and the density of wet algal biomass pellets after 60 minutes.

Table 6.3 Summary of growth parameters, CO_2 fixation efficiency, Total organic carbon in media, biochemical productivity, elemental analysis, and energy potential of *M.pusillum* in a 15% to 5% CO_2 dilution within a calcium-induced fed-batch cultivation optimized strategy over 23 days in a closed photobioreactor ((data represents mean ± standard deviation, n=2)

Parameters	Value
Biomass yield	3.23 ± 0.23
Biomass productivity (mg/L day^{-1})	136 ± 1.43
Specific growth rate (day^{-1})	0.172 ± 0.01
CO_2 fixation efficiency (mg/L day^{-1})	264.53 ± 2.56
Total organic carbon (mg/L)	31.45
Lipid productivity (mg/L day^{-1})	41.45 ± 1.03
Carbohydrate productivity (mg/L day^{-1})	52.45 ± 1.23
Crude protein productivity (mg/L day^{-1})	56.57 ± 1.65
Carbon (%DCW)	53.12 ± 1.22
Hydrogen (%DCW)	7.08 ± 1.56
Nitrogen (%DCW)	6.65 ± 0.78
Sulphur (%DCW)	0.216 ± 0.03
HHV (kJ/g)	23.40 ± 1.67
Bioenergy yield (kJ)	65.14 ± 2.12

6.4 Conclusions

This study sheds light on the significant challenges hindering the widespread adoption of microalgal CO_2 cultivation, with a focus on productivity, cost-effectiveness, and environmental sustainability. Addressing issues such as CO_2 acidification and saturation is imperative for achieving stable carbon fixation. The study highlights the crucial role of maintaining high nitrogen availability to support growth and CO_2 fixation, effectively mitigating media acidification in coal-based CO_2 environments. Despite the initial growth benefits associated

with exposure to 15% CO_2, challenges such as nitrogen deprivation and reduced photosynthetic efficiency emerge. To address these challenges, a novel approach is proposed, involving the implementation of calcium-induced phosphorus-fed samples and a gradual reduction of CO_2 concentration through air dilution over a 15-day period. This approach enhances biomass productivity, CO_2 fixation, and induces self-flocculation. Furthermore, the selected strain demonstrates remarkable tolerance to toxic flue gas compounds, enhancing its suitability for real-world applications. These findings, along with previous research, underscore the importance of effectively managing CO_2-based carbon flow, nitrogen availability, and light exposure during the growth phase. By carefully controlling these parameters and leveraging F_v/F_m measurements, promising opportunities emerge for efficiently capturing CO_2 emissions from coal-based industries. This can be achieved through the utilization of cost-effective urea supplements and innovative dilution techniques with air, resulting in a reduction of harmful emissions and facilitating the transformation of flue gas components into valuable biochemicals by microalgae. Aligned with the objectives of the Paris Agreement and UN sustainable development goals, this innovative approach offers a greener and more sustainable pathway for microalgal CO_2-based carbon-negative biomanufacturing processes with long term stability in terms of performance.

CHAPTER 7

Overall Conclusion and Future scope

Chapter 7

Overall Conclusion and Future scope

7.1 Conclusions

This research underscores the potential of microalgae as a sustainable solution for CO_2 sequestration and biofuel production. Despite the significant challenges associated with microalgal cultivation, including low CO_2 capture efficiency, sensitivity to abiotic stresses, high water and nutrient demands, and difficulties in large-scale harvesting, the findings of this thesis provide promising solutions. The screening and acclimatization of 13 microalgal strains, particularly NCIM5584 and KMC8, demonstrated significant resistance to industrial flue gas components, with KMC8 showing exceptional performance in biomass production, CO_2 fixation, and lipid accumulation.

The adaptive mechanisms of *Micractinium pusillum* KMC8 demonstrate its ability to sustain photosynthetic efficiency and bioenergy content in response to changes in light and temperature conditions. The study emphasized the crucial influence of nutrient levels and light intensity on the utilization of CO_2 and the production of lipids, with optimized circumstances greatly improving the amount of biomass and lipids produced. In addition, the implementation of novel techniques to regulate CO_2 levels and provide specific nutrient supplements, such as the use of a calcium-induced phosphorus fed-batch method, effectively prevented media acidification and maintained stable photosynthetic activity. As a result, there were significant enhancements in CO_2 utilization and biomass production.

This thesis clearly illustrates the feasibility and efficiency of using comprehensive methods of screening and strategic process engineering to improve the development of microalgae, promote photosynthesis, decrease CO_2 emissions, and greatly augment bioenergy generation. The findings provide essential knowledge for the widespread and sustainable use of microalgae in capturing CO_2 and generating biofuels. This highlights their potential for effective bioprocessing, carbon capture, efficient biomass collection, and water reuse.

This study enhances microalgal adaptation for efficient carbon fixation, biochemical conversion, and the release of organic carbon for water recyclability by using effective process engineering strategies and tailored culture approaches. These developments are crucial in the development of carbon-negative and circular bioeconomy bioenergy production systems using microalgae. They represent a significant progress in renewable energy and environmental sustainability.

7.2 Future Prospects

1. **Field Trials and Pilot Projects**: Conduct field trials and pilot projects to verify the accuracy of laboratory results in real-life situations, showcasing the practical usability and scalability of the suggested solutions.
2. **Industrial Wastewater and Flue Gas Utilization**: By using actual industrial effluent and flue gas, it is possible to fulfil the significant water and nutrient requirements, so improving the overall sustainability of the process and achieving a more carbon-negative and environmentally friendly bioenergy production system.
3. **Optimized Photobioreactor Designs**: Enhancing photobioreactor designs and cultivation systems via the use of sophisticated sensor technologies and automated control systems may lead to improved physiochemical regulation, increased carbon capture, enhanced conversion yield into biomass, and decreased operating costs.
4. **Co-product Exploration**: Explore the feasibility and benefits of using co-products such as biofertilizers, bioplastics, and high-value chemicals in conjunction with biofuel production to improve the economic viability and sustainability of microalgal biorefineries.
5. **Economic and Life Cycle Analyses**: Perform thorough economic and life cycle assessments to evaluate the practicality and ecological consequences of implementing large-scale microalgal carbon capture and biofuel production. This will provide valuable information for expanding and incorporating these processes into current industrial systems.

References

[1] International Energy Agency, CO2 Emissions in 2023, 2023. https://www.iea.org/reports/co2-emissions-in-2023.

[2] F. Dong, Y. Wang, B. Su, Y. Hua, Y. Zhang, The process of peak CO2 emissions in developed economies: A perspective of industrialization and urbanization, Resour. Conserv. Recycl. 141 (2019) 61–75. https://doi.org/10.1016/j.resconrec.2018.10.010.

[3] H. Adun, J.D. Ampah, O. Bamisile, Y. Hu, The synergistic role of carbon dioxide removal and emission reductions in achieving the Paris Agreement goal, Sustain. Prod. Consum. 45 (2024) 386–407. https://doi.org/10.1016/j.spc.2024.01.004.

[4] V. Chaturvedi, A. Malyan, Implications of a net-zero target for India's sectoral energy transitions and climate policy, Oxford Open Clim. Chang. 2 (2022) 1–15. https://doi.org/10.1093/oxfclm/kgac001.

[5] C.D. Scown, Prospects for carbon-negative biomanufacturing, Trends Biotechnol. 40 (2022) 1415–1424. https://doi.org/10.1016/j.tibtech.2022.09.004.

[6] IEA, CCUS Legal and Regulatory Handbook, (2022) 1–111. www.iea.org/t&c/.

[7] M. Shen, F. Kong, L. Tong, Y. Luo, S. Yin, C. Liu, P. Zhang, L. Wang, P.K. Chu, Y. Ding, Carbon capture and storage (CCS): development path based on carbon neutrality and economic policy, Carbon Neutrality. 1 (2022) 1–21. https://doi.org/10.1007/s43979-022-00039-z.

[8] M. Wang, A. Lawal, P. Stephenson, J. Sidders, C. Ramshaw, Post-combustion CO2capture with chemical absorption: A state-of-the-art review, Chem. Eng. Res. Des. 89 (2011) 1609–1624. https://doi.org/10.1016/j.cherd.2010.11.005.

[9] D.Y.C. Leung, G. Caramanna, M.M. Maroto-Valer, An overview of current status of carbon dioxide capture and storage technologies, Renew. Sustain. Energy Rev. 39 (2014) 426–443. https://doi.org/10.1016/j.rser.2014.07.093.

[10] W.H. Chen, S.M. Chen, C.I. Hung, Carbon dioxide capture by single droplet using Selexol, Rectisol and water as absorbents: A theoretical approach, Appl. Energy. 111 (2013) 731–741. https://doi.org/10.1016/j.apenergy.2013.05.051.

[11] M. Pardakhti, T. Jafari, Z. Tobin, B. Dutta, E. Moharreri, N.S. Shemshaki, S. Suib, R. Srivastava, Trends in Solid Adsorbent Materials Development for CO2 Capture, ACS Appl. Mater. Interfaces. 11 (2019) 34533–34559. https://doi.org/10.1021/acsami.9b08487.

[12] N. Norahim, P. Yaisanga, K. Faungnawakij, T. Charinpanitkul, C. Klaysom, Recent Membrane Developments for CO2 Separation and Capture, Chem. Eng. Technol. 41 (2018) 211–223. https://doi.org/10.1002/ceat.201700406.

[13] R.P. Anugraha, V.D. Pratiwi, R. Renanto, J. Juwari, A.N. Islami, M.Y. Bakhtiar, Techno-economic analysis of CO2 cryogenic distillation from high CO2 content gas field: A case study in Indonesia, Chem. Eng. Res. Des. 202 (2024) 226–234.

https://doi.org/10.1016/j.cherd.2023.12.035.

[14] Y. Lee, S. Lee, D. Seo, S. Moon, Y.H. Ahn, Y. Park, Highly efficient separation and equilibrium recovery of H2/CO2 in hydrate-based pre-combustion CO2 capture, Chem. Eng. J. 481 (2024) 148709. https://doi.org/10.1016/j.cej.2024.148709.

[15] L. Zhang, K. Ye, Y. Wang, W. Han, M. Xie, L. Chen, Performance analysis of a hybrid system combining cryogenic separation carbon capture and liquid air energy storage (CS-LAES), Energy. 290 (2024) 129867. https://doi.org/10.1016/j.energy.2023.129867.

[16] C. Descamps, C. Bouallou, M. Kanniche, Efficiency of an Integrated Gasification Combined Cycle (IGCC) power plant including CO2 removal, Energy. 33 (2008) 874–881. https://doi.org/10.1016/j.energy.2007.07.013.

[17] T. Wilberforce, A. Baroutaji, B. Soudan, A.H. Al-Alami, A.G. Olabi, Outlook of carbon capture technology and challenges, Sci. Total Environ. 657 (2019) 56–72. https://doi.org/10.1016/j.scitotenv.2018.11.424.

[18] A. Dubey, A. Arora, Advancements in carbon capture technologies: A review, J. Clean. Prod. 373 (2022) 133932. https://doi.org/10.1016/j.jclepro.2022.133932.

[19] A. Laude, Bioenergy with carbon capture and storage: are short-term issues set aside?, Mitig. Adapt. Strateg. Glob. Chang. 25 (2020) 185–203. https://doi.org/10.1007/s11027-019-09856-7.

[20] I. Ibrahim, M.N.I. Salehmin, K. Balachandran, M.F. Hil Me, K.S. Loh, M.H. Abu Bakar, B.C. Jong, S.S. Lim, Role of microbial electrosynthesis system in CO2 capture and conversion: a recent advancement toward cathode development, Front. Microbiol. 14 (2023) 1–19. https://doi.org/10.3389/fmicb.2023.1192187.

[21] B. Zhao, Y. Su, Process effect of microalgal-carbon dioxide fixation and biomass production: A review, Renew. Sustain. Energy Rev. 31 (2014) 121–132. https://doi.org/10.1016/j.rser.2013.11.054.

[22] S. Arun, A. Sinharoy, K. Pakshirajan, P.N.L. Lens, Algae based microbial fuel cells for wastewater treatment and recovery of value-added products, Renew. Sustain. Energy Rev. 132 (2020) 110041. https://doi.org/10.1016/j.rser.2020.110041.

[23] J. Singh, D.W. Dhar, Overview of carbon capture technology: Microalgal biorefinery concept and state-of-the-art, Front. Mar. Sci. 6 (2019) 1–9. https://doi.org/10.3389/fmars.2019.00029.

[24] J.E. Coons, D.M. Kalb, T. Dale, B.L. Marrone, Getting to low-cost algal biofuels: A monograph on conventional and cutting-edge harvesting and extraction technologies, Algal Res. 6 (2014) 250–270. https://doi.org/10.1016/j.algal.2014.08.005.

[25] J.R. Seth, P.P. Wangikar, Challenges and opportunities for microalgae-mediated CO 2 capture and biorefinery, Biotechnol. Bioeng. 112 (2015) 1281–1296. https://doi.org/10.1002/bit.25619.

[26] J. Minagawa, R. Tokutsu, Dynamic regulation of photosynthesis in Chlamydomonas reinhardtii, Plant J. 82 (2015) 413–428. https://doi.org/10.1111/tpj.12805.

[27] R.J.G. and B. A., P Hoto- Algal, n.d.

[28] I. Andersson, Catalysis and regulation in Rubisco, in: J. Exp. Bot., 2008: pp. 1555–1568. https://doi.org/10.1093/jxb/ern091.

[29] M.R. Badger, T.J. Andrews, S.M. Whitney, M. Ludwig, D.C. Yellowlees, W. Leggat, G.D. Price, The diversity and coevolution of Rubisco, plastids, pyrenoids, and chloroplast-based CO₂-concentrating mechanisms in algae, Can. J. Bot. 76 (1998) 1052–1071. https://doi.org/10.1139/cjb-76-6-1052.

[30] L. Zhu, Biorefinery as a promising approach to promote microalgae industry: An innovative framework, Renew. Sustain. Energy Rev. 41 (2015) 1376–1384. https://doi.org/10.1016/j.rser.2014.09.040.

[31] A.R.C. Morais, A.M. Da Costa Lopes, R. Bogel-Łukasik, Carbon dioxide in biomass processing: Contributions to the green biorefinery concept, Chem. Rev. 115 (2015) 3–27. https://doi.org/10.1021/cr500330z.

[32] J.D. Tibocha-Bonilla, C. Zuñiga, R.D. Godoy-Silva, K. Zengler, Advances in metabolic modeling of oleaginous microalgae Mike Himmel, Biotechnol. Biofuels. 11 (2018) 1–16. https://doi.org/10.1186/s13068-018-1244-3.

[33] Z. Ramazanov, M. Rawat, M.C. Henk, C.B. Mason, S.W. Matthews, J. V Moroney, The induction of the CO2-concentrating mechanism is correlated with the formation of the starch sheath around the pyrenoid of Chlamydomonas reinhardtii, Planta. 195 (1994) 210–216. https://doi.org/10.1007/BF00199681.

[34] X. Johnson, J. Alric, Interaction between starch breakdown, acetate assimilation, and photosynthetic cyclic electron flow in Chlamydomonas reinhardtii, J. Biol. Chem. 287 (2012) 26445–26452. https://doi.org/10.1074/jbc.M112.370205.

[35] M. Toyoshima, N. Sato, High-Level Accumulation of Triacylglycerol and Starch in Photoautotrophically Grown Chlamydomonas debaryana NIES-2212, Plant Cell Physiol. 56 (2015) 2447–2456. https://doi.org/10.1093/pcp/pcv163.

[36] L.M. Schüler, P.S.C. Schulze, H. Pereira, L. Barreira, R. León, J. Varela, Trends and strategies to enhance triacylglycerols and high-value compounds in microalgae, Algal Res. 25 (2017) 263–273. https://doi.org/10.1016/j.algal.2017.05.025.

[37] W.C. Chang, H.Q. Zheng, C.N.N. Chen, Comparative transcriptome analysis reveals a potential photosynthate partitioning mechanism between lipid and starch biosynthetic pathways in green microalgae, Algal Res. 16 (2016) 54–62. https://doi.org/10.1016/j.algal.2016.03.007.

[38] A. Andreeva, E. Budenkova, O. Babich, S. Sukhikh, E. Ulrikh, S. Ivanova, A. Prosekov, V. Dolganyuk, Production, purification, and study of the amino acid composition of microalgae proteins, Molecules. 26 (2021) 1–15. https://doi.org/10.3390/molecules26092767.

[39] M. Giordano, A. Norici, J. Beardall, Impact of inhibitors of amino acid, protein, and RNA synthesis on C allocation in the diatom Chaetoceros muellerii: A FTIR approach, Algae. 32 (2017) 161–170. https://doi.org/10.4490/algae.2017.32.6.6.

[40] F. V. Winck, D.O.P. Melo, D.M. Riaño-Pachón, M.C.M. Martins, C. Caldana, A.F.G. Barrios, Analysis of Sensitive CO2 Pathways and Genes Related to Carbon Uptake and Accumulation in Chlamydomonas reinhardtii through Genomic Scale Modeling and Experimental Validation, Front. Plant Sci. 7 (2016) 1–12.

https://doi.org/10.3389/fpls.2016.00043.

[41] S. Tripathi, S. Choudhary, A. Meena, K.M. Poluri, Carbon capture, storage, and usage with microalgae: a review, Springer International Publishing, 2023. https://doi.org/10.1007/s10311-023-01609-y.

[42] A. Solovchenko, O. Gorelova, I. Selyakh, O. Baulina, L. Semenova, M. Logacheva, O. Chivkunova, P. Scherbakov, E. Lobakova, Nitrogen availability modulates CO2 tolerance in a symbiotic chlorophyte, Algal Res. 16 (2016) 177–188. https://doi.org/10.1016/j.algal.2016.03.002.

[43] B. Zhao, Y. Su, Process effect of microalgal-carbon dioxide fixation and biomass production: A review, Renew. Sustain. Energy Rev. 31 (2014) 121–132. https://doi.org/10.1016/j.rser.2013.11.054.

[44] E.A. Laws, S.A. McClellan, Interactive effects of CO2, temperature, irradiance, and nutrient limitation on the growth and physiology of the marine cyanobacterium Synechococcus (Cyanophyceae), J. Phycol. 718 (2022) 703–718. https://doi.org/10.1111/jpy.13278.

[45] T.B. Bittar, Y. Lin, L.R. Sassano, B.J. Wheeler, S.L. Brown, W.P. Cochlan, Z.I. Johnson, Carbon allocation under light and nitrogen resource gradients in two model marine phytoplankton1, J. Phycol. 49 (2013) 523–535. https://doi.org/10.1111/jpy.12060.

[46] S.A. Kranz, D. Sültemeyer, K.-U. Richter, B. Rost, Carbon acquisition by *Trichodesmium*: the effect of pCO_2 and diurnal changes, Limnol. Oceanogr. 54 (2009) 548–559. https://doi.org/10.4319/lo.2009.54.2.0548.

[47] J.A.V. Costa, B.C.B. de Freitas, C.R. Lisboa, T.D. Santos, L.R. de F. Brusch, M.G. de Morais, Microalgal biorefinery from CO2 and the effects under the Blue Economy, Renew. Sustain. Energy Rev. 99 (2019) 58–65. https://doi.org/10.1016/j.rser.2018.08.009.

[48] L. Moreno-Garcia, K. Adjallé, S. Barnabé, G.S.V. Raghavan, Microalgae biomass production for a biorefinery system: Recent advances and the way towards sustainability, Renew. Sustain. Energy Rev. 76 (2017) 493–506. https://doi.org/10.1016/j.rser.2017.03.024.

[49] F. Hussain, S.Z. Shah, W. Zhou, M. Iqbal, Microalgae screening under CO2 stress: Growth and micro-nutrients removal efficiency, J. Photochem. Photobiol. B Biol. 170 (2017) 91–98. https://doi.org/10.1016/j.jphotobiol.2017.03.021.

[50] L. Yahya, R. Harun, L.C. Abdullah, Screening of native microalgae species for carbon fixation at the vicinity of Malaysian coal-fired power plant, Sci. Rep. 10 (2020) 1–14. https://doi.org/10.1038/s41598-020-79316-9.

[51] S. Gupta, S.B. Pawar, R.A. Pandey, G.S. Kanade, S.K. Lokhande, Outdoor microalgae cultivation in airlift photobioreactor at high irradiance and temperature conditions: effect of batch and fed-batch strategies, photoinhibition, and temperature stress, Bioprocess Biosyst. Eng. 0 (2018) 0. https://doi.org/10.1007/s00449-018-2037-6.

[52] M.C. Mitchell, M.T. Meyer, H. Griffiths, Dynamics of Carbon-Concentrating Mechanism Induction and Protein Relocalization during the Dark-to-Light Transition in Synchronized Chlamydomonas reinhardtii, Plant Physiol. 166 (2014) 1073–1082.

https://doi.org/10.1104/pp.114.246918.

[53] A.F. Esteves, O.S.G.P. Soares, V.J.P. Vilar, J.C.M. Pires, A.L. Gonçalves, The effect of light wavelength on CO2 capture, biomass production and nutrient uptake by green microalgae: A step forward on process integration and optimisation, Energies. 13 (2020). https://doi.org/10.3390/en13020333.

[54] S. Ma, Y. Huang, X. Zhu, A. Xia, X. Zhu, Q. Liao, Growth-based dynamic light transmission modeling and optimization in microalgal photobioreactors for high efficiency CO2 fixation, Renew. Sustain. Energy Rev. 197 (2024) 114414. https://doi.org/10.1016/j.rser.2024.114414.

[55] O. Sánchez, J. Mas, Measurement of light absorption and determination of the specific rate of light uptake in cultures of phototrophic microorganisms, Appl. Environ. Microbiol. 62 (1996) 620–624.

[56] W. Li, X. Xu, M. Fujibayashi, Q. Niu, N. Tanaka, O. Nishimura, Response of microalgae to elevated CO2 and temperature: impact of climate change on freshwater ecosystems, Environ. Sci. Pollut. Res. 23 (2016) 19847–19860. https://doi.org/10.1007/s11356-016-7180-5.

[57] J. Galmés, M. V. Kapralov, L.O. Copolovici, C. Hermida-Carrera, Niinemets, Temperature responses of the Rubisco maximum carboxylase activity across domains of life: Phylogenetic signals, trade-offs, and importance for carbon gain, Photosynth. Res. 123 (2015) 183–201. https://doi.org/10.1007/s11120-014-0067-8.

[58] O.B. Matoo, A. V. Ivanina, C. Ullstad, E. Beniash, I.I. Sokolova, Interactive effects of elevated temperature and CO2levels on metabolism and oxidative stress in two common marine bivalves (Crassostrea virginica and Mercenaria mercenaria), Comp. Biochem. Physiol. - A Mol. Integr. Physiol. 164 (2013) 545–553. https://doi.org/10.1016/j.cbpa.2012.12.025.

[59] J.J. Cole, Y.T. Prairie, Dissolved CO2 in Freshwater Systems☆, Ref. Modul. Earth Syst. Environ. Sci. (2014). https://doi.org/10.1016/b978-0-12-409548-9.09399-4.

[60] J.J. Cole, Y.T. Prairie, Dissolved CO2 in Freshwater Systems☆, Ref. Modul. Earth Syst. Environ. Sci. (2014). https://doi.org/10.1016/b978-0-12-409548-9.09399-4.

[61] Y. Matsuda, T. Hara, B. Colman, Regulation of the induction of bicarbonate uptake by dissolved CO2 in the marine diatom, Phaeodactylum tricornutum, Plant, Cell Environ. 24 (2001) 611–620. https://doi.org/10.1046/j.1365-3040.2001.00702.x.

[62] B.T. Nguyen, B.E. Rittmann, Predicting Dissolved Inorganic Carbon in Photoautotrophic Microalgae Culture via the Nitrogen Source, Environ. Sci. Technol. 49 (2015) 9826–9831. https://doi.org/10.1021/acs.est.5b01727.

[63] T. Li, C.E. Sharp, M. Ataeian, M. Strous, D. De Beer, Role of extracellular carbonic anhydrase in dissolved inorganic carbon uptake in alkaliphilic phototrophic biofilm, Front. Microbiol. 9 (2018) 1–12. https://doi.org/10.3389/fmicb.2018.02490.

[64] S. Hu, B. Zhou, Y. Wang, Y. Wang, X. Zhang, Y. Zhao, X. Zhao, X. Tang, Effect of CO2-induced seawater acidification on growth, photosynthesis and inorganic carbon acquisition of the harmful bloom-forming marine microalga, Karenia mikimotoi, PLoS One. 12 (2017) 1–19. https://doi.org/10.1371/journal.pone.0183289.

[65] M. Morales, L. Sánchez, S. Revah, The impact of environmental factors on carbon dioxide fixation by microalgae, FEMS Microbiol. Lett. 365 (2018) 1–11. https://doi.org/10.1093/femsle/fnx262.

[66] I. Havlik, P. Lindner, T. Scheper, K.F. Reardon, On-line monitoring of large cultivations of microalgae and cyanobacteria, Trends Biotechnol. 31 (2013) 406–414. https://doi.org/10.1016/j.tibtech.2013.04.005.

[67] A.L. Karam, C.C. McMillan, Y.C. Lai, F.L. De Los Reyes, H.W. Sederoff, A.M. Grunden, R.S. Ranjithan, J.W. Levis, J.J. Ducoste, Construction and setup of a bench-scale algal photosynthetic bioreactor with temperature, light, and pH monitoring for kinetic growth tests, J. Vis. Exp. 2017 (2017). https://doi.org/10.3791/55545.

[68] J. Legrand, A. Artu, J. Pruvost, A review on photobioreactor design and modelling for microalgae production, React. Chem. Eng. 6 (2021) 1134–1151. https://doi.org/10.1039/d0re00450b.

[69] A.D. Kroumov, A.N. Módenes, D.E.G. Trigueros, F.R. Espinoza-Quiñones, C.E. Borba, F.B. Scheufele, C.L. Hinterholz, A systems approach for CO2 fixation from flue gas by microalgae—Theory review, Process Biochem. 51 (2016) 1817–1832. https://doi.org/10.1016/j.procbio.2016.05.019.

[70] A. Kumar, S. Ergas, X. Yuan, A. Sahu, Q. Zhang, J. Dewulf, F.X. Malcata, H. Van Langenhove, Enhanced CO 2 fixation and biofuel production via microalgae : recent developments and future directions, Trends Biotechnol. 28 (2010) 371–380. https://doi.org/10.1016/j.tibtech.2010.04.004.

[71] Udaypal, R.K. Goswami, S. Mehariya, P. Verma, Advances in microalgae-based carbon sequestration: Current status and future perspectives, Environ. Res. 249 (2024) 118397. https://doi.org/10.1016/j.envres.2024.118397.

[72] W. Wu, L. Tan, H. Chang, C. Zhang, X. Tan, Q. Liao, N. Zhong, X. Zhang, Y. Zhang, S.H. Ho, Advancements on process regulation for microalgae-based carbon neutrality and biodiesel production, Renew. Sustain. Energy Rev. 171 (2023) 112969. https://doi.org/10.1016/j.rser.2022.112969.

[73] P. Xu, S. Shao, J. Qian, J. Li, R. Xu, J. Liu, W. Zhou, Scale-up of microalgal systems for decarbonization and bioproducts: Challenges and opportunities, Bioresour. Technol. 398 (2024) 130528. https://doi.org/10.1016/j.biortech.2024.130528.

[74] B. Le Gouic, H. Marec, J. Pruvost, J.F. Cornet, Investigation of growth limitation by CO2 mass transfer and inorganic carbon source for the microalga Chlorella vulgaris in a dedicated photobioreactor, Chem. Eng. Sci. 233 (2021) 116388. https://doi.org/10.1016/j.ces.2020.116388.

[75] E. Uggetti, B. Sialve, J. Hamelin, A. Bonnafous, J.P. Steyer, CO2 addition to increase biomass production and control microalgae species in high rate algal ponds treating wastewater, J. CO2 Util. 28 (2018) 292–298. https://doi.org/10.1016/j.jcou.2018.10.009.

[76] E.A. Laws, S.A. McClellan, U. Passow, Interactive Effects of CO2, Temperature, Irradiance, and Nutrient Limitation on the Growth and Physiology of the Marine Diatom Thalassiosira pseudonana (Coscinodiscophyceae), J. Phycol. 56 (2020) 1614–1624. https://doi.org/10.1111/jpy.13048.

[77] S. Ho, W. Lu, J. Chang, Bioresource Technology Photobioreactor strategies for improving the CO 2 fixation efficiency of indigenous Scenedesmus obliquus CNW-N : Statistical optimization of CO 2 feeding , illumination , and operation mode, Bioresour. Technol. 105 (2012) 106–113. https://doi.org/10.1016/j.biortech.2011.11.091.

[78] Y. Chen, C. Xu, S. Vaidyanathan, In fl uence of gas management on biochemical conversion of CO 2 by microalgae for biofuel production, Appl. Energy. 261 (2020) 114420. https://doi.org/10.1016/j.apenergy.2019.114420.

[79] A. Solovchenko, O. Gorelova, I. Selyakh, O. Baulina, L. Semenova, M. Logacheva, O. Chivkunova, P. Scherbakov, E. Lobakova, Nitrogen availability modulates CO2tolerance in a symbiotic chlorophyte, Algal Res. 16 (2016) 177–188. https://doi.org/10.1016/j.algal.2016.03.002.

[80] D. Shi, W. Li, B.M. Hopkinson, H. Hong, D. Li, S.J. Kao, W. Lin, Interactive effects of light, nitrogen source, and carbon dioxide on energy metabolism in the diatom Thalassiosira pseudonana, Limnol. Oceanogr. 60 (2015) 1805–1822. https://doi.org/10.1002/lno.10134.

[81] E.B. Young, J. Beardall, Modulation of photosynthesis and inorganic carbon acquisition in a marine microalga by nitrogen, iron, and light availability, Can. J. Bot. 83 (2005) 917–928. https://doi.org/10.1139/b05-081.

[82] X. Jin, S. Gong, Z. Chen, J. Xia, W. Xiang, Potential microalgal strains for converting flue gas CO2 into biomass, J. Appl. Phycol. (2020) 47–55. https://doi.org/10.1007/s10811-020-02147-8.

[83] R. Wang, X. Wang, T. Zhu, Research progress and application of carbon sequestration in industrial flue gas by microalgae :, J. Environ. Sci. (2024). https://doi.org/10.1016/j.jes.2024.04.018.

[84] H. Shang, T. Ouyang, F. Yang, Y. Kou, A biomass-supported Na2CO3 sorbent for flue gas desulfurization., Environ. Sci. Technol. 37 (2003) 2596–9. https://doi.org/10.1021/es021026o.

[85] H.M. Singh, R. Kothari, R. Gupta, V. V. Tyagi, H. Mohan, R. Kothari, R. Gupta, V. V. Tyagi, Bio-fixation of flue gas from thermal power plants with algal biomass: Overview and research perspectives, J. Environ. Manage. 245 (2019) 519–539. https://doi.org/10.1016/j.jenvman.2019.01.043.

[86] S.R. Ronda, C. Kethineni, L.C.P. Parupudi, V.B.S.C. Thunuguntla, S. Vemula, V.S. Settaluri, P.R. Allu, S.K. Grande, S. Sharma, C.V. Kandala, A growth inhibitory model with SOx influenced effective growth rate for estimation of algal biomass concentration under flue gas atmosphere, Bioresour. Technol. 152 (2014) 283–291. https://doi.org/10.1016/j.biortech.2013.10.091.

[87] S.Y. Chiu, C.Y. Kao, T.T. Huang, C.J. Lin, S.C. Ong, C. Da Chen, J.S. Chang, C.S. Lin, Microalgal biomass production and on-site bioremediation of carbon dioxide, nitrogen oxide and sulfur dioxide from flue gas using Chlorella sp. cultures, Bioresour. Technol. 102 (2011) 9135–9142. https://doi.org/10.1016/j.biortech.2011.06.091.

[88] K. Napan, L. Teng, J.C. Quinn, B.D. Wood, Impact of heavy metals from flue gas integration with microalgae production, Algal Res. 8 (2015) 83–8. https://doi.org/10.1016/j.algal.2015.01.003.

[89] J.H. Duarte, L.S. Fanka, J.A.V. Costa, Utilization of simulated flue gas containing CO2, SO2, NO and ash for Chlorella fusca cultivation, Bioresour. Technol. 214 (2016) 159–165. https://doi.org/10.1016/j.biortech.2016.04.078.

[90] J.A. Lara-Gil, M.M. Álvarez, A. Pacheco, Toxicity of flue gas components from cement plants in microalgae CO2 mitigation systems, J. Appl. Phycol. 26 (2014) 357–368. https://doi.org/10.1007/s10811-013-0136-y.

[91] C.M. Su, H.T. Hsueh, C.M. Tseng, D.T. Ray, Y.H. Shen, H. Chu, Effects of nutrient availability on the biomass production and CO2 fixation in a flat plate photobioreactor, Aerosol Air Qual. Res. 17 (2017) 1887–1897. https://doi.org/10.4209/aaqr.2016.09.0386.

[92] Y.C. a, C.X. a, How to narrow the CO2 gap from growth-optimal to flue gas levels by using microalgae for carbon capture and sustainable biomass production, J. Clean. Prod. 280 (2021) 124448. https://doi.org/10.1016/j.jclepro.2020.124448.

[93] S. Wu, W. Gu, S. Jia, L. Wang, L. Wang, X. Liu, L. Zhou, A. Huang, G. Wang, Proteomic and biochemical responses to different concentrations of CO2 suggest the existence of multiple carbon metabolism strategies in Phaeodactylum tricornutum, Biotechnol. Biofuels. 14 (2021) 1–17. https://doi.org/10.1186/s13068-021-02088-5.

[94] L. Patil, B. Kaliwal, Effect of CO2 Concentration on Growth and Biochemical Composition of Newly Isolated Indigenous Microalga Scenedesmus bajacalifornicus BBKLP-07, Appl. Biochem. Biotechnol. 182 (2017) 335–348. https://doi.org/10.1007/s12010-016-2330-2.

[95] W. Fang, Y. Si, S. Douglass, D. Casero, S.S. Merchant, M. Pellegrini, I. Ladunga, P. Liu, M.H. Spalding, Transcriptome-Wide Changes in Chlamydomonas reinhardtii Gene Expression Regulated by Carbon Dioxide and the CO2-Concentrating Mechanism Regulator CIA5/CCM1, Plant Cell. 24 (2012) 1876–1893. https://doi.org/10.1105/tpc.112.097949.

[96] M.L. Gerardo, S. Van Den Hende, H. Vervaeren, T. Coward, S.C. Skill, Harvesting of microalgae within a biorefinery approach: A review of the developments and case studies from pilot-plants, Algal Res. 11 (2015) 248–262. https://doi.org/10.1016/j.algal.2015.06.019.

[97] C. Zhu, R. Zhang, L. Cheng, Z. Chi, Biotechnology for Biofuels A recycling culture of Neochloris oleoabundans in a bicarbonate - based integrated carbon capture and algae production system with harvesting by auto - flocculation, Biotechnol. Biofuels. (2018) 1–11. https://doi.org/10.1186/s13068-018-1197-6.

[98] W. Farooq, M. Moon, B. gon Ryu, W.I. Suh, A. Shrivastav, M.S. Park, S.K. Mishra, J.W. Yang, Effect of harvesting methods on the reusability of water for cultivation of chlorella vulgaris, its lipid productivity and biodiesel quality, Algal Res. 8 (2015) 1–7. https://doi.org/10.1016/j.algal.2014.12.007.

[100] G. Muhammad, M.A. Alam, M. Mofijur, M.I. Jahirul, Y. Lv, W. Xiong, H.C. Ong, J. Xu, Modern developmental aspects in the field of economical harvesting and biodiesel production from microalgae biomass, Renew. Sustain. Energy Rev. 135 (2021) 110209. https://doi.org/10.1016/j.rser.2020.110209.

[101] N. Deconinck, K. Muylaert, W. Ivens, D. Vandamme, Innovative harvesting processes for microalgae biomass production: A perspective from patent literature, Algal Res. 31 (2018) 469–477. https://doi.org/10.1016/j.algal.2018.01.016.

[102] L. Xia, Y. Li, R. Huang, S. Song, Effective harvesting of microalgae by coagulation–flotation, R. Soc. Open Sci. 4 (2017). https://doi.org/10.1098/rsos.170867.

[103] J. Blockx, A. Verfaillie, W. Thielemans, K. Muylaert, Unravelling the Mechanism of Chitosan-Driven Flocculation of Microalgae in Seawater as a Function of pH, ACS Sustain. Chem. Eng. 6 (2018) 11273–11279. https://doi.org/10.1021/acssuschemeng.7b04802.

[104] N. Kumar, C. Banerjee, S. Negi, P. Shukla, Microalgae harvesting techniques: updates and recent technological interventions, Crit. Rev. Biotechnol. 43 (2023) 342–368. https://doi.org/10.1080/07388551.2022.2031089.

[105] G. Singh, S.K. Patidar, Microalgae harvesting techniques: A review, J. Environ. Manage. 217 (2018) 499–508. https://doi.org/10.1016/j.jenvman.2018.04.010.

[106] J.C. Beltrán-Rocha, C. Guajardo-Barbosa, H. Rodríguez-Fuentes, G.R. Reyna-Martínez, L. Osornio-Berthet, M. García-Martínez, I. Dagmar-Barceló Quintal, U.J. López-Chuken, Some implications of natural increase of pH in microalgae cultivation and harvest by autoflocculation, Lat. Am. J. Aquat. Res. 49 (2021) 836–842. https://doi.org/10.3856/vol49-issue5-fulltext-2691.

[107] K. Spilling, J. Seppälä, T. Tamminen, Inducing autoflocculation in the diatom Phaeodactylum tricornutum through CO2 regulation, J. Appl. Phycol. 23 (2011) 959–966. https://doi.org/10.1007/s10811-010-9616-5.

[108] A.A. Martins, F. Marques, M. Cameira, E. Santos, S. Badenes, L. Costa, V.V. Vieira, N.S. Caetano, T.M. Mata, Water footprint of microalgae cultivation in photobioreactor, Energy Procedia. 153 (2018) 426–431. https://doi.org/10.1016/j.egypro.2018.10.031.

[109] J. Yang, M. Xu, X. Zhang, Q. Hu, M. Sommerfeld, Y. Chen, Life-cycle analysis on biodiesel production from microalgae: Water footprint and nutrients balance, Bioresour. Technol. 102 (2011) 159–165. https://doi.org/10.1016/j.biortech.2010.07.017.

[110] A. Pugazhendhi, S. Nagappan, R.R. Bhosale, P.C. Tsai, S. Natarajan, S. Devendran, L. Al-Haj, V.K. Ponnusamy, G. Kumar, Various potential techniques to reduce the water footprint of microalgal biomass production for biofuel—A review, Sci. Total Environ. 749 (2020) 142218. https://doi.org/10.1016/j.scitotenv.2020.142218.

[111] A. Rempel, J.P. Gutkoski, M.T. Nazari, G.N. Biolchi, V.A.F. Cavanhi, H. Treichel, L.M. Colla, Current advances in microalgae-based bioremediation and other technologies for emerging contaminants treatment, Sci. Total Environ. 772 (2021) 144918. https://doi.org/10.1016/j.scitotenv.2020.144918.

[112] Z. Lu, S. Loftus, J. Sha, W. Wang, M.S. Park, X. Zhang, Z.I. Johnson, Q. Hu, Water reuse for sustainable microalgae cultivation: Current knowledge and future directions, Resour. Conserv. Recycl. 161 (2020) 104975. https://doi.org/10.1016/j.resconrec.2020.104975.

[113] W. Farooq, S.R. Naqvi, M. Sajid, A. Shrivastav, K. Kumar, Monitoring lipids profile,

CO2 fixation, and water recyclability for the economic viability of microalgae Chlorella vulgaris cultivation at different initial nitrogen, J. Biotechnol. 345 (2022) 30–39. https://doi.org/10.1016/j.jbiotec.2021.12.014.

[114] S.E. Loftus, Z.I. Johnson, Reused Cultivation Water Accumulates Dissolved Organic Carbon and Uniquely Influences Different Marine Microalgae, Front. Bioeng. Biotechnol. 7 (2019) 1–13. https://doi.org/10.3389/fbioe.2019.00101.

[115] M. Molazadeh, H. Ahmadzadeh, H.R. Pourianfar, S. Lyon, P.H. Rampelotto, The use of microalgae for coupling wastewater treatment with CO2 biofixation, Front. Bioeng. Biotechnol. 7 (2019). https://doi.org/10.3389/fbioe.2019.00042.

[116] G. Yadav, B.K. Dubey, R. Sen, A comparative life cycle assessment of microalgae production by CO2 sequestration from flue gas in outdoor raceway ponds under batch and semi-continuous regime, J. Clean. Prod. 258 (2020) 120703. https://doi.org/10.1016/j.jclepro.2020.120703.

[117] V. Balan, J. Pierson, H. Husain, S. Kumar, C. Saffron, V. Kumar, Potential of using microalgae to sequester carbon dioxide and processing to bioproducts, Green Chem. (2023). https://doi.org/10.1039/d3gc02286b.

[118] J. Fu, Y. Huang, Q. Liao, A. Xia, Q. Fu, X. Zhu, Photo-bioreactor design for microalgae: A review from the aspect of CO2 transfer and conversion, Bioresour. Technol. 292 (2019) 121947. https://doi.org/10.1016/j.biortech.2019.121947.

[119] A. Shekh, A. Sharma, P.M. Schenk, G. Kumar, S. Mudliar, Microalgae cultivation: photobioreactors, CO2 utilization, and value-added products of industrial importance, J. Chem. Technol. Biotechnol. 97 (2022) 1064–1085. https://doi.org/10.1002/jctb.6902.

[120] E. Ono, J.L. Cuello, Feasibility Assessment of Microalgal Carbon Dioxide Sequestration Technology with Photobioreactor and Solar Collector, Biosyst. Eng. 95 (2006) 597–606. https://doi.org/10.1016/j.biosystemseng.2006.08.005.

[121] J.H. De Vree, R. Bosma, M. Janssen, M.J. Barbosa, R.H. Wijffels, Biotechnology for Biofuels Comparison of four outdoor pilot - scale photobioreactors, Biotechnol. Biofuels. (2015) 1–12. https://doi.org/10.1186/s13068-015-0400-2.

[122] G. Yadav, A. Karemore, S.K. Dash, R. Sen, Performance evaluation of a green process for microalgal CO2 sequestration in closed photobioreactor using flue gas generated in-situ, Bioresour. Technol. 191 (2015) 399–406. https://doi.org/10.1016/j.biortech.2015.04.040.

[123] C. Lu, K. Rao, D. Hall, A. Vonshak, Production of eicosapentaenoic acid (EPA) in Monodus subterraneus grown in a helical tubular photobioreactor as affected by cell density and light intensity, J. Appl. Phycol. 13 (2001) 517–522. https://doi.org/10.1023/A:1012515500651.

[124] R. Münkel, U. Schmid-Staiger, A. Werner, T. Hirth, Optimization of outdoor cultivation in flat panel airlift reactors for lipid production by Chlorella vulgaris, Biotechnol. Bioeng. 110 (2013) 2882–2893. https://doi.org/10.1002/bit.24948.

[125] G.G. Satpati, R. Pal, Biomass to Biodiesel: A Review, J. Algal Biomass Util. 9 (2018) 11–37. https://www.researchgate.net/publication/329424285_Microalgae-_Biomass_to_Biodiesel_A_Review.

[126] E.G. Nwoba, D.A. Parlevliet, D.W. Laird, K. Alameh, N.R. Moheimani, Light management technologies for increasing algal photobioreactor efficiency, Algal Res. 39 (2019) 101433. https://doi.org/10.1016/j.algal.2019.101433.

[127] Z. Chen, X. Zhang, B. Su, Influence of arc baffle configuration on gas–liquid mass transfer in flat-plate bubble column, Chem. Eng. Res. Des. 165 (2021) 129–136. https://doi.org/10.1016/j.cherd.2020.10.024.

[128] V. Mortezaeikia, R. Yegani, O. Tavakoli, Membrane-sparger vs. membrane contactor as a photobioreactors for carbon dioxide biofixation of Synechococcus elongatus in batch and semi-continuous mode, J. CO2 Util. 16 (2016) 23–31. https://doi.org/10.1016/j.jcou.2016.05.009.

[129] X. You, L. Yang, H. Chu, L. Zhang, Y. Hong, Y. Lin, X. Zhou, Y. Zhang, Micro-nano-bubbles and their application in microalgae production: Wastewater treatment, carbon capture and microalgae separation, Algal Res. 78 (2024) 103398. https://doi.org/10.1016/j.algal.2024.103398.

[130] S. Dey, A. Bhattacharya, P. Kumar, A. Malik, High-rate CO2sequestration using a novel venturi integrated photobioreactor and subsequent valorization to microalgal lipids, Green Chem. 22 (2020) 7962–7973. https://doi.org/10.1039/d0gc02552f.

[131] K. Kim, J. Yoo, W.G. Lee, Recent advances in photobioreactor systems for sustainable and enhanced microalgal biofuel production, Sustain. Energy Fuels. 6 (2022) 5459–5473. https://doi.org/10.1039/d2se01345b.

[132] Y. Sun, D. Hu, H. Chang, S. Li, S.H. Ho, Recent progress on converting CO2 into microalgal biomass using suspended photobioreactors, Bioresour. Technol. 363 (2022) 127991. https://doi.org/10.1016/j.biortech.2022.127991.

[133] K. Xin, R. Guo, X. Zou, M. Rao, Z. Huang, C. Kuang, J. Ye, C. Chen, C. Huang, M. Zhang, W. Yang, J. Cheng, CO2 gradient domestication improved high-concentration CO2 tolerance and photoautotrophic growth of Euglena gracilis, Sci. Total Environ. 868 (2023). https://doi.org/10.1016/j.scitotenv.2023.161629.

[134] C.A. Arroyo, J.L. Contreras, B. Zeifert, C.C. Ramírez, CO2 capture of the gas emission, using a catalytic converter and airlift bioreactors with the microalga Scenedesmus dimorphus, Appl. Sci. 9 (2019). https://doi.org/10.3390/app9163212.

[135] R. García-Cubero, J. Moreno-Fernández, M. García-González, Modelling growth and CO2 fixation by Scenedesmus vacuolatus in continuous culture, Algal Res. 24 (2017) 333–339. https://doi.org/10.1016/j.algal.2017.04.018.

[136] A. Pandey, S. Srivastava, S. Kumar, Carbon dioxide fixation and lipid storage of Scenedesmus sp. ASK22: A sustainable approach for biofuel production and waste remediation, J. Environ. Manage. 332 (2023) 117350. https://doi.org/10.1016/j.jenvman.2023.117350.

[137] J. Cabello, M. Morales, S. Revah, Carbon dioxide consumption of the microalga Scenedesmus obtusiusculus under transient inlet CO2 concentration variations, Sci. Total Environ. 584–585 (2017) 1310–1316. https://doi.org/10.1016/j.scitotenv.2017.02.002.

[138] M. Rao, X. Zou, J. Ye, C. Kuang, C. Chen, C. Huang, G. Chen, S. Qin, Z. Wang, L. Feng, Y. Tang, J. Tian, J. Cheng, Light Conditions Determine Optimal

CO2Concentrations for Nannochloropsis oceanica Growth with Carbon Fixation, ACS Sustain. Chem. Eng. 10 (2022) 8799–8814. https://doi.org/10.1021/acssuschemeng.2c01179.

[139] J.N. Lee, J.S. Lee, C.S. Shin, S.C. Park, S.W. Kim, Methods to enhance tolerances of Chlorella KR-1 to toxic compounds in flue gas, Appl. Biochem. Biotechnol. - Part A Enzym. Eng. Biotechnol. 84–86 (2000) 329–342. https://doi.org/10.1385/ABAB:84-86:1-9:329.

[140] J.S. Lee, D.K. Kim, J.P. Lee, S.C. Park, J.H. Koh, H.S. Cho, S.W. Kim, Effects of SO2 and NO on growth of Chlorella sp. KR-1, Bioresour. Technol. 82 (2002) 1–4. https://doi.org/10.1016/S0960-8524(01)00158-4.

[141] H. Tang, M. Chen, K.Y. Simon Ng, S.O. Salley, Continuous microalgae cultivation in a photobioreactor, Biotechnol. Bioeng. 109 (2012) 2468–2474. https://doi.org/10.1002/bit.24516.

[142] J. Cheng, Y. Huang, J. Feng, J. Sun, J. Zhou, K. Cen, Mutate Chlorella sp. by nuclear irradiation to fix high concentrations of CO2, Bioresour. Technol. 136 (2013) 496–501. https://doi.org/10.1016/j.biortech.2013.03.072.

[143] A. Azari, H. Tavakoli, B.D. Barkdoll, O.B. Haddad, Predictive model of algal biofuel production based on experimental data, Algal Res. 47 (2020) 101843. https://doi.org/10.1016/j.algal.2020.101843.

[144] C. Van T. Do, C.T. Dinh, M.T. Dang, T. Dang Tran, T. Giang Le, A novel flat-panel photobioreactor for simultaneous production of lutein and carbon sequestration by Chlorella sorokiniana TH01, Bioresour. Technol. 345 (2022) 126552. https://doi.org/10.1016/j.biortech.2021.126552.

[145] A. Estrada-Graf, S. Hernández, M. Morales, Biomitigation of CO2 from flue gas by Scenedesmus obtusiusculus AT-UAM using a hybrid photobioreactor coupled to a biomass recovery stage by electro-coagulation-flotation, Environ. Sci. Pollut. Res. 27 (2020) 28561–28574. https://doi.org/10.1007/s11356-020-08240-2.

[146] J.B. Beigbeder, J.M. Lavoie, Effect of photoperiods and CO2 concentrations on the cultivation of carbohydrate-rich P. kessleri microalgae for the sustainable production of bioethanol, J. CO2 Util. 58 (2022) 101934. https://doi.org/10.1016/j.jcou.2022.101934.

[147] M. Mondal, A. Ghosh, K. Gayen, G. Halder, O.N. Tiwari, Carbon dioxide bio-fixation by Chlorella sp. BTA 9031 towards biomass and lipid production: Optimization using Central Composite Design approach, J. CO2 Util. 22 (2017) 317–329. https://doi.org/10.1016/j.jcou.2017.10.008.

[148] G. Yadav, S.P. Panda, R. Sen, Strategies for the effective solid, liquid and gaseous waste valorization by microalgae: A circular bioeconomy perspective, J. Environ. Chem. Eng. 8 (2020) 104518. https://doi.org/10.1016/j.jece.2020.104518.

[149] X. Liu, G. Chen, Y. Tao, J. Wang, Application of effluent from WWTP in cultivation of four microalgae for nutrients removal and lipid production under the supply of CO2, Renew. Energy. 149 (2020) 708–715. https://doi.org/10.1016/j.renene.2019.12.092.

[150] L.I. Rodas-Zuluaga, L. Castañeda-Hernández, E.I. Castillo-Vacas, A. Gradiz-Menjivar, I.Y. López-Pacheco, C. Castillo-Zacarías, L. Boully, H.M.N. Iqbal, R.

Parra-Saldívar, Bio-capture and influence of CO2on the growth rate and biomass composition of the microalgae Botryococcus braunii and Scenedesmus sp, J. CO2 Util. 43 (2021). https://doi.org/10.1016/j.jcou.2020.101371.

[151] M.A. Kassim, T.K. Meng, Carbon dioxide (CO2) biofixation by microalgae and its potential for biorefinery and biofuel production, Sci. Total Environ. 584–585 (2017) 1121–1129. https://doi.org/10.1016/j.scitotenv.2017.01.172.

[152] R. Tripathi, J. Singh, I.S. Thakur, Characterization of microalga Scenedesmus sp. ISTGA1 for potential CO2 sequestration and biodiesel production, Renew. Energy. 74 (2015) 774–781. https://doi.org/10.1016/j.renene.2014.09.005.

[153] S. Basu, A. Sarma Roy, A.K. Ghoshal, K. Mohanty, Operational strategies for maximizing CO2utilization efficiency by the novel microalga Scenedesmus obliquus SA1 cultivated in lab scale photobioreactor, Algal Res. 12 (2015) 249–257. https://doi.org/10.1016/j.algal.2015.09.010.

[154] Z. Wang, J. Cheng, W. Song, X. Du, W. Yang, CO2 gradient domestication produces gene mutation centered on cellular light response for efficient growth of microalgae in 15% CO2 from flue gas, Chem. Eng. J. 429 (2022) 131968. https://doi.org/10.1016/j.cej.2021.131968.

[155] H.H. Chou, H.Y. Su, X. Di Song, T.J. Chow, C.Y. Chen, J.S. Chang, T.M. Lee, Biotechnology for Biofuels Isolation and characterization of Chlorella sp . mutants with enhanced thermo - and - tolerances for - CO 2 sequestration and utilization of flue gases, Biotechnol. Biofuels. (2019) 1–14. https://doi.org/10.1186/s13068-019-1590-9.

[156] J.A. Lara-Gil, C. Senés-Guerrero, A. Pacheco, Cement flue gas as a potential source of nutrients during CO2 mitigation by microalgae, Algal Res. 17 (2016) 285–292. https://doi.org/10.1016/j.algal.2016.05.017.

[157] C.L. Cheng, Y.C. Lo, K. Lou Huang, D. Nagarajan, C.Y. Chen, D.J. Lee, J.S. Chang, Effect of pH on biomass production and carbohydrate accumulation of Chlorella vulgaris JSC-6 under autotrophic, mixotrophic, and photoheterotrophic cultivation, Bioresour. Technol. 351 (2022) 127021. https://doi.org/10.1016/j.biortech.2022.127021.

[158] J. Li, X. Tang, K. Pan, B. Zhu, Y. Li, X. Ma, Y. Zhao, The regulating mechanisms of CO2 fixation and carbon allocations of two Chlorella sp. strains in response to high CO2 levels, Chemosphere. 247 (2020) 125814. https://doi.org/10.1016/j.chemosphere.2020.125814.

[159] A. Satoh, N. Kurano, H. Senger, S. Miyachi, Regulation of energy balance in photosystems in response to changes in CO2 concentrations and light intensities during growth in extremely-high-CO2-tolerant green microalgae., Plant Cell Physiol. 43 (2002) 440–451. https://doi.org/10.1093/pcp/pcf054.

[160] Y. Chen, C. Xu, How to narrow the CO2 gap from growth-optimal to flue gas levels by using microalgae for carbon capture and sustainable biomass production, J. Clean. Prod. 280 (2021) 124448. https://doi.org/10.1016/j.jclepro.2020.124448.

[161] L. Ramanna, I. Rawat, F. Bux, Light enhancement strategies improve microalgal biomass productivity, Renew. Sustain. Energy Rev. 80 (2017) 765–773. https://doi.org/10.1016/j.rser.2017.05.202.

[162] A. Contreras, F. García, E. Molina, J.C. Merchuk, Interaction between CO2-mass transfer, light availability, and hydrodynamic stress in the growth of Phaeodactylum tricornutum in a concentric tube airlift photobioreactor, Biotechnol. Bioeng. 60 (1998) 317–325. https://doi.org/10.1002/(SICI)1097-0290(19981105)60:3<317::AID-BIT7>3.0.CO;2-K.

[163] D. Soletto, L. Binaghi, L. Ferrari, A. Lodi, J.C.M. Carvalho, M. Zilli, A. Converti, Effects of carbon dioxide feeding rate and light intensity on the fed-batch pulse-feeding cultivation of Spirulina platensis in helical photobioreactor, Biochem. Eng. J. 39 (2008) 369–375. https://doi.org/10.1016/j.bej.2007.10.007.

[164] B. Clément-Larosière, F. Lopes, A. Gonçalves, B. Taidi, M. Benedetti, M. Minier, D. Pareau, Carbon dioxide biofixation by Chlorella vulgaris at different CO2 concentrations and light intensities, Eng. Life Sci. 14 (2014) 509–519. https://doi.org/10.1002/elsc.201200212.

[165] K.E. Dickinson, C.G. Lalonde, P.J. McGinn, Effects of spectral light quality and carbon dioxide on the physiology of Micractinium inermum: growth, photosynthesis, and biochemical composition, J. Appl. Phycol. 31 (2019) 3385–3396. https://doi.org/10.1007/s10811-019-01880-z.

[166] T. Yamano, T. Tsujikawa, K. Hatano, S.I. Ozawa, Y. Takahashi, H. Fukuzawa, Light and low-CO2-dependent LCIBLCIC complex localization in the chloroplast supports the carbon-concentrating mechanism in Chlamydomonas reinhardtii, Plant Cell Physiol. 51 (2010) 1453–1468. https://doi.org/10.1093/pcp/pcq105.

[167] C.M. Su, H.T. Hsueh, T.Y. Li, L.C. Huang, Y.L. Chu, C.M. Tseng, H. Chu, Effects of light availability on the biomass production, CO2fixation, and bioethanol production potential of Thermosynechococcus CL-1, Bioresour. Technol. 145 (2013) 162–165. https://doi.org/10.1016/j.biortech.2013.02.092.

[168] F.F. Li, Z.H. Yang, R. Zeng, G. Yang, X. Chang, J.B. Yan, Y.L. Hou, Microalgae capture of CO2from actual flue gas discharged from a combustion chamber, Ind. Eng. Chem. Res. 50 (2011) 6496–6502. https://doi.org/10.1021/ie200040q.

[169] R.T. Smith, D.J. Gilmour, The influence of exogenous organic carbon assimilation and photoperiod on the carbon and lipid metabolism of Chlamydomonas reinhardtii, Algal Res. 31 (2018) 122–137. https://doi.org/10.1016/j.algal.2018.01.020.

[170] E. Jacob-Lopes, C.H.G. Scoparo, L.M.C.F. Lacerda, T.T. Franco, Effect of light cycles (night/day) on CO2 fixation and biomass production by microalgae in photobioreactors, Chem. Eng. Process. Process Intensif. 48 (2009) 306–310. https://doi.org/10.1016/j.cep.2008.04.007.

[171] C. Holdmann, U. Schmid-Staiger, H. Hornstein, T. Hirth, Keeping the light energy constant — Cultivation of Chlorella sorokiniana at different specific light availabilities and different photoperiods, Algal Res. 29 (2018) 61–70. https://doi.org/10.1016/j.algal.2017.11.005.

[172] B.A. Cho, M.Á. de C. Servia, E.A. del R. Chanona, R. Smith, D. Zhang, Synergising biomass growth kinetics and transport mechanisms to simulate light/dark cycle effects on photo-production systems, Biotechnol. Bioeng. (2021) 1–11. https://doi.org/10.1002/bit.27707.

[173] A.K. Minhas, S. Gaur, A. Adholeya, Influence of light intensity and photoperiod on the pigment and, lipid production of Dunaliella tertiolecta and Nannochloropsis oculata under three different culture medium, Heliyon. 9 (2023) e12801. https://doi.org/10.1016/j.heliyon.2023.e12801.

[174] S. Srirangan, M.L. Sauer, B. Howard, M. Dvora, J. Dums, P. Backman, H. Sederoff, Interaction of temperature and photoperiod increases growth and oil content in the marine microalgae Dunaliella viridis, PLoS One. 10 (2015) 1–32. https://doi.org/10.1371/journal.pone.0127562.

[175] S. Sivakaminathan, B. Hankamer, J. Wolf, J. Yarnold, High-throughput optimisation of light-driven microalgae biotechnologies, Sci. Rep. 8 (2018) 1–13. https://doi.org/10.1038/s41598-018-29954-x.

[176] Y. -K Lee, H. -M Tan, C. -S Hew, The effect of growth temperature on the bioenergetics of photosynthetic algal cultures, Biotechnol. Bioeng. 27 (1985) 555–561. https://doi.org/10.1002/bit.260270502.

[177] G. Torzillo, A. Sacchi, R. Materassi, Temperature as an important factor affecting productivity and night biomass loss in Spirulina platensis grown outdoors in tubular photobioreactors, Bioresour. Technol. 38 (1991) 95–100. https://doi.org/10.1016/0960-8524(91)90137-9.

[178] R.J. GEIDER, LIGHT AND TEMPERATURE DEPENDENCE OF THE CARBON TO CHLOROPHYLL a RATIO IN MICROALGAE AND CYANOBACTERIA: IMPLICATIONS FOR PHYSIOLOGY AND GROWTH OF PHYTOPLANKTON, New Phytol. 106 (1987) 1–34. https://doi.org/10.1111/j.1469-8137.1987.tb04788.x.

[179] J.F. Dye, Calculation of Effect of Temperature on pH, Free Carbon Dioxide, and the Three Forms of Alkalinity, J. Am. Water Works Assoc. 44 (1952) 356–372. https://doi.org/10.1002/j.1551-8833.1952.tb15363.x.

[180] S. Hindersin, M. Leupold, M. Kerner, D. Hanelt, Irradiance optimization of outdoor microalgal cultures using solar tracked photobioreactors, Bioprocess Biosyst. Eng. 36 (2013) 345–355. https://doi.org/10.1007/s00449-012-0790-5.

[181] S.P. Singh, P. Singh, Effect of temperature and light on the growth of algae species: A review, Renew. Sustain. Energy Rev. 50 (2015) 431–444. https://doi.org/10.1016/j.rser.2015.05.024.

[182] R. Praveenkumar, B. Kim, E. Choi, K. Lee, J.Y. Park, J.S. Lee, Y.C. Lee, Y.K. Oh, Improved biomass and lipid production in a mixotrophic culture of Chlorella sp. KR-1 with addition of coal-fired flue-gas, Bioresour. Technol. 171 (2014) 500–505. https://doi.org/10.1016/j.biortech.2014.08.112.

[183] L.R. Dahlin, A.T. Gerritsen, C.A. Henard, S. Van Wychen, J.G. Linger, Y. Kunde, B.T. Hovde, S.R. Starkenburg, M.C. Posewitz, M.T. Guarnieri, Development of a high-productivity, halophilic, thermotolerant microalga Picochlorum renovo, Commun. Biol. 2 (2019) 1–9. https://doi.org/10.1038/s42003-019-0620-2.

[184] Y. Zheng, T. Li, X. Yu, P.D. Bates, T. Dong, S. Chen, High-density fed-batch culture of a thermotolerant microalga chlorella sorokiniana for biofuel production, Appl. Energy. 108 (2013) 281–287. https://doi.org/10.1016/j.apenergy.2013.02.059.

[185] S. Abu-Ghosh, Z. Dubinsky, D. Iluz, Acclimation of thermotolerant algae to light and

temperature interaction1, J. Phycol. 56 (2020) 662–670. https://doi.org/10.1111/jpy.12964.

[186] E. Krivina, M. Sinetova, T. Savchenko, E. Degtyaryov, E. Tebina, A. Temraleeva, Micractinium lacustre and M. thermotolerans spp. nov. (Trebouxiophyceae, Chlorophyta): Taxonomy, temperature-dependent growth, photosynthetic characteristics and fatty acid composition, Algal Res. 71 (2023) 103042. https://doi.org/10.1016/j.algal.2023.103042.

[187] R. Serra-Maia, O. Bernard, A. Gonçalves, S. Bensalem, F. Lopes, Influence of temperature on Chlorella vulgaris growth and mortality rates in a photobioreactor, Algal Res. 18 (2016) 352–359. https://doi.org/10.1016/j.algal.2016.06.016.

[188] N. Hajinajaf, A. Fallahi, E. Eustance, A. Sarnaik, A. Askari, M. Najafi, R.W. Davis, B.E. Rittmann, A.M. Varman, Managing carbon dioxide mass transfer in photobioreactors for enhancing microalgal biomass productivity, Algal Res. 80 (2024) 103506. https://doi.org/10.1016/j.algal.2024.103506.

[189] A. Chrachri, B.M. Hopkinson, K. Flynn, C. Brownlee, G.L. Wheeler, Dynamic changes in carbonate chemistry in the microenvironment around single marine phytoplankton cells, Nat. Commun. 9 (2018) 74. https://doi.org/10.1038/s41467-017-02426-y.

[190] Mook W, Chemistry of carbonic acid in water, Environ. Isot. Hydrol. Cycle Princ. Appl. (2000) 143–165. http://www-naweb.iaea.org/napc/ih/documents/global_cycle/vol I/cht_i_09.pdf.

[191] P.C. Chen, C.F. Huang, H.W. Chen, M.W. Yang, C.M. Tsao, Capture of CO2 from coal-fired power plant with NaOH solution in a continuous pilot-scale bubble-column scrubber, Energy Procedia. 61 (2014) 1660–1664. https://doi.org/10.1016/j.egypro.2014.12.186.

[192] S.A. Razzak, M. Ilyas, S.A.M. Ali, M.M. Hossain, Effects of CO2Concentration and pH on mixotrophic growth of Nannochloropsis oculata, Appl. Biochem. Biotechnol. 176 (2015) 1290–1302. https://doi.org/10.1007/s12010-015-1646-7.

[193] Y. Yang, K.S. Gao, Effects of CO2 concentrations on the freshwater microalgae, Chlamydomonas reihardtii, Chlorella pyrenoidosa and Scenesdesmus obliquus (Chlorophyta), J. Appl. Phycol. 15 (2003) 379–389.

[194] M.A. Kassim, T.K. Meng, Carbon dioxide (CO2) biofixation by microalgae and its potential for biorefinery and biofuel production, Sci. Total Environ. 584–585 (2017) 1121–1129. https://doi.org/10.1016/j.scitotenv.2017.01.172.

[195] E. Van Hunnik, H. Van den Ende, K.R. Timmermans, P. Laan, J.W. De Leeuw, A comparison of CO2 uptake by the green algae Tetraedron minimum and Chlamydomonas monoica, Plant Biol. 2 (2000) 624–627. https://doi.org/10.1055/s-2000-16637.

[196] B. Chen, D. Zou, H. Jiang, Elevated CO2 exacerbates competition for growth and photosynthesis between Gracilaria lemaneiformis and Ulva lactuca, Aquaculture. 443 (2015) 49–55. https://doi.org/10.1016/j.aquaculture.2015.03.009.

[197] E.M. Nithiya, J. Tamilmani, K.K. Vasumathi, M. Premalatha, Improved CO2fixation with Oscillatoria sp. in response to various supply frequencies of CO2supply, J. CO2

Util. 18 (2017) 198–205. https://doi.org/10.1016/j.jcou.2017.01.025.

[198] Y. Sheng, T. Mathimani, K. Brindhadevi, S. Basha, A. Elfasakhany, C. Xia, A. Pugazhendhi, Combined effect of CO2 concentration and low-cost urea repletion/starvation in Chlorella vulgaris for ameliorating growth metrics, total and non-polar lipid accumulation and fatty acid composition, Sci. Total Environ. 808 (2022) 151969. https://doi.org/10.1016/j.scitotenv.2021.151969.

[199] C. Shene, Y. Chisti, M. Bustamante, M. Rubilar, Effect of CO2 in the aeration gas on cultivation of the microalga Nannochloropsis oculata: Experimental study and mathematical modeling of CO2 assimilation, Algal Res. 13 (2016) 16–29. https://doi.org/10.1016/j.algal.2015.11.005.

[200] A. Solovchenko, O. Gorelova, I. Selyakh, S. Pogosyan, O. Baulina, L. Semenova, O. Chivkunova, E. Voronova, I. Konyukhov, P. Scherbakov, E. Lobakova, A novel CO2-tolerant symbiotic Desmodesmus (Chlorophyceae, Desmodesmaceae): Acclimation to and performance at a high carbon dioxide level, Algal Res. 11 (2015) 399–410. https://doi.org/10.1016/j.algal.2015.04.011.

[201] R. Moghimifam, V. Niknam, H. Ebrahimzadeh, M.A. Hejazi, The influence of different CO2 concentrations on the biochemical and molecular response of two isolates of Dunaliella sp. (ABRIINW-CH2 and ABRIINW-SH33), J. Appl. Phycol. (2019). https://doi.org/10.1007/s10811-019-01914-6.

[202] A. Vadlamani, S. Viamajala, B. Pendyala, S. Varanasi, Cultivation of Microalgae at Extreme Alkaline pH Conditions: A Novel Approach for Biofuel Production, ACS Sustain. Chem. Eng. 5 (2017) 7284–7294. https://doi.org/10.1021/acssuschemeng.7b01534.

[203] A. Vadlamani, B. Pendyala, S. Viamajala, S. Varanasi, High Productivity Cultivation of Microalgae without Concentrated CO 2 Input, ACS Sustain. Chem. Eng. 7 (2019) 1933–1943. https://doi.org/10.1021/acssuschemeng.8b04094.

[204] N. Coulombier, P. Blanchier, L. Le Dean, V. Barthelemy, N. Lebouvier, T. Jauffrais, The effects of CO2-induced acidification on Tetraselmis biomass production, photophysiology and antioxidant activity: A comparison using batch and continuous culture, J. Biotechnol. 325 (2021) 312–324. https://doi.org/10.1016/j.jbiotec.2020.10.005.

[205] M.L. Scherholz, W.R. Curtis, Achieving pH control in microalgal cultures through fed-batch addition of stoichiometrically-balanced growth media, BMC Biotechnol. 13 (2013). https://doi.org/10.1186/1472-6750-13-39.

[206] S. Singhasuwan, W. Choorit, S. Sirisansaneeyakul, N. Kokkaew, Y. Chisti, Carbon-to-nitrogen ratio affects the biomass composition and the fatty acid profile of heterotrophically grown Chlorella sp. TISTR 8990 for biodiesel production, J. Biotechnol. 216 (2015) 169–177. https://doi.org/10.1016/j.jbiotec.2015.10.003.

[207] B.R. Björnsäter, P.A. Wheeler, Effect of Nitrogen and Phosphorus Supply on Growth and Tissue Composition of Ulva Fenestrata and Enteromorpha Intestinalis (Ulvales, Chlorophyta), J. Phycol. 26 (1990) 603–611. https://doi.org/10.1111/j.0022-3646.1990.00603.x.

[208] C.Y. Ma, J.M. Zhao, L.H. Liu, L. Zhang, Growth-dependent radiative properties of Chlorella vulgaris and its influence on prediction of light fluence rate in

photobioreactor, J. Appl. Phycol. 31 (2019) 235–247. https://doi.org/10.1007/s10811-018-1499-x.

[209] J.M. Cho, Y.K. Oh, W.K. Park, Y.K. Chang, Effects of nitrogen supplementation status on co2 biofixation and biofuel production of the promising microalga chlorella sp. ABC-001, J. Microbiol. Biotechnol. 30 (2020) 1235–1243. https://doi.org/10.4014/jmb.2005.05039.

[210] K. Kumari, S. Samantaray, D. Sahoo, B.C. Tripathy, Nitrogen, phosphorus and high CO2 modulate photosynthesis, biomass and lipid production in the green alga Chlorella vulgaris, Photosynth. Res. 148 (2021) 17–32. https://doi.org/10.1007/s11120-021-00828-0.

[211] J.C. Goldman, M.R. Dennett, C.B. Riley, Effect of Nitrogen-Mediated Changes i n Alkalinity on pH Control and COZ Supply i n Intensive Microalgal Cultures, XXIV (1982) 619–631.

[212] Y. Liu, D. Wei, High-efficient CO2-to-protein bioconversion by oleaginous Coccomyxa subellipsoidea using light quality shift and nitrogen supplementation strategy, Chem. Eng. J. 473 (2023) 145166. https://doi.org/10.1016/j.cej.2023.145166.

[213] A. Solovchenko, I. Khozin-Goldberg, I. Selyakh, L. Semenova, T. Ismagulova, A. Lukyanov, I. Mamedov, E. Vinogradova, O. Karpova, I. Konyukhov, S. Vasilieva, P. Mojzes, C. Dijkema, M. Vecherskaya, I. Zvyagin, L. Nedbal, O. Gorelova, Phosphorus starvation and luxury uptake in green microalgae revisited, Algal Res. 43 (2019) 101651. https://doi.org/10.1016/j.algal.2019.101651.

[214] F. Chu, J. Cheng, X. Zhang, Q. Ye, J. Zhou, Enhancing lipid production in microalgae Chlorella PY-ZU1 with phosphorus excess and nitrogen starvation under 15% CO2 in a continuous two-step cultivation process, Chem. Eng. J. 375 (2019) 121912. https://doi.org/10.1016/j.cej.2019.121912.

[215] S.J. Yu, X.F. Shen, H.Q. Ge, H. Zheng, F.F. Chu, H. Hu, R.J. Zeng, Role of sufficient phosphorus in biodiesel production from diatom Phaeodactylum tricornutum, Appl. Microbiol. Biotechnol. 100 (2016) 6927–6934. https://doi.org/10.1007/s00253-016-7641-2.

[216] F. Chu, J. Cheng, K. Li, Y. Wang, X. Li, W. Yang, Enhanced Lipid Accumulation through a Regulated Metabolic Pathway of Phosphorus Luxury Uptake in the Microalga Chlorella vulgaris under Nitrogen Starvation and Phosphorus Repletion, ACS Sustain. Chem. Eng. 8 (2020) 8137–8147. https://doi.org/10.1021/acssuschemeng.9b07447.

[217] S.J. Yu, H. Hu, H. Zheng, Y.Q. Wang, S.B. Pan, R.J. Zeng, Effect of different phosphorus concentrations on biodiesel production from Isochrysis zhangjiangensis under nitrogen sufficiency or deprivation condition, Appl. Microbiol. Biotechnol. 103 (2019) 5051–5059. https://doi.org/10.1007/s00253-019-09814-y.

[218] M. Muthuraj, V. Kumar, B. Palabhanvi, D. Das, Evaluation of indigenous microalgal isolate Chlorella sp. FC2 IITG as a cell factory for biodiesel production and scale up in outdoor conditions, J. Ind. Microbiol. Biotechnol. 41 (2014) 499–511. https://doi.org/10.1007/s10295-013-1397-9.

[219] C. Yao, J. Jiang, X. Cao, Y. Liu, S. Xue, Y. Zhang, Phosphorus Enhances

Photosynthetic Storage Starch Production in a Green Microalga (Chlorophyta) Tetraselmis subcordiformis in Nitrogen Starvation Conditions, J. Agric. Food Chem. 66 (2018) 10777–10787. https://doi.org/10.1021/acs.jafc.8b04798.

[220] O.Q.F. Araújo, C.N. Gobbi, R.M. Chaloub, M.A.Z. Coelho, Assessment of the impact of salinity and irradiance on the combined carbon dioxide sequestration and carotenoids production by Dunaliella Salina: A mathematical model, Biotechnol. Bioeng. 102 (2009) 425–435. https://doi.org/10.1002/bit.22079.

[221] M.A.J. Parry, A.J. Keys, P.J. Madgwick, A.E. Carmo-Silva, P.J. Andralojc, Rubisco regulation: A role for inhibitors, J. Exp. Bot. 59 (2008) 1569–1580. https://doi.org/10.1093/jxb/ern084.

[222] H. Yan, Z. Han, H. Zhao, S. Zhou, N. Chi, M. Han, X. Kou, Y. Zhang, L. Xu, C. Tian, S. Qin, Characterization of calcium deposition induced by Synechocystis sp. PCC6803 in BG11 culture medium, Chinese J. Oceanol. Limnol. 32 (2014) 503–510. https://doi.org/10.1007/s00343-014-3150-2.

[223] H. Zhao, Y. Han, M. Liang, Z. Han, J. Woo, L. Meng, X. Chi, M.E. Tucker, C. Han, Y. Zhao, Y. Zhao, H. Yan, Effect of Magnesium and Ferric Ions on the Biomineralization of Calcium Carbonate Induced by Synechocystis sp. PCC 6803, Minerals. 13 (2023) 1486. https://doi.org/10.3390/min13121486.

[224] J.G. Comley, J.A. Scott, C.A. Laamanen, Utilizing CO2 in industrial off-gas for microalgae cultivation: considerations and solutions, Crit. Rev. Biotechnol. 0 (2023) 1–14. https://doi.org/10.1080/07388551.2023.2233692.

[225] T. Li, G. Xu, J. Rong, H. Chen, C. He, M. Giordano, Q. Wang, The acclimation of Chlorella to high-level nitrite for potential application in biological NOx removal from industrial flue gases, J. Plant Physiol. 195 (2016) 73–79. https://doi.org/10.1016/j.jplph.2016.03.006.

[226] F. Liang, X. Wen, L. Luo, Y. Geng, Y. Li, Physicochemical effects on sulfite transformation in a lipid- rich Chlorella sp . strain, Chinese J. Oceanol. Limnol. 32 (2014) 1288–1296.

[227] P.K. Kumar, S.V. Krishna, S.S. Naidu, K. Verma, D. Bhagawan, V. Himabindu, Biomass production from microalgae Chlorella grown in sewage, kitchen wastewater using industrial CO2 emissions: Comparative study, Carbon Resour. Convers. 2 (2019) 126–133. https://doi.org/10.1016/j.crcon.2019.06.002.

[228] R.S. Wodzinski, D.P. Labeda, M. Alexander, Toxicity of so2and nox: selective inhibition of blue-green algae by bisulfite and nitrite, J. Air Pollut. Control Assoc. 27 (1977) 891–893. https://doi.org/10.1080/00022470.1977.10470510.

[229] A. Galván, J. Rexach, V. Mariscal, E. Fernández, Nitrite transport to the chloroplast in Chlamydomonas reinhardtii: molecular evidence for a regulated process., J. Exp. Bot. 53 (2002) 845–853. https://doi.org/10.1093/jexbot/53.370.845.

[230] G. De Bhowmick, A.K. Sarmah, R. Sen, Performance evaluation of an outdoor algal biorefinery for sustainable production of biomass, lipid and lutein valorizing flue-gas carbon dioxide and wastewater cocktail, Bioresour. Technol. 283 (2019) 198–206. https://doi.org/10.1016/j.biortech.2019.03.075.

[231] M.K. Ji, H.S. Yun, S. Park, H. Lee, Y.T. Park, S. Bae, J. Ham, J. Choi, Effect of food

wastewater on biomass production by a green microalga Scenedesmus obliquus for bioenergy generation, Bioresour. Technol. 179 (2015) 624–628. https://doi.org/10.1016/j.biortech.2014.12.053.

[232] A.M. Lizzul, P. Hellier, S. Purton, F. Baganz, N. Ladommatos, L. Campos, Combined remediation and lipid production using Chlorella sorokiniana grown on wastewater and exhaust gases, Bioresour. Technol. 151 (2014) 12–18. https://doi.org/10.1016/j.biortech.2013.10.040.

[233] D. Mohler, M.H. Wilson, S. Kesner, J.Y. Schambach, D. Vaughan, M. Frazar, J. Stewart, J. Groppo, R. Pace, M. Crocker, Beneficial re-use of industrial CO2 emissions using microalgae: Demonstration assessment and biomass characterization, Bioresour. Technol. 293 (2019). https://doi.org/10.1016/j.biortech.2019.122014.

[234] S. Lage, F.G. Gentili, Chemical composition and species identification of microalgal biomass grown at pilot-scale with municipal wastewater and CO2 from flue gases, Chemosphere. 313 (2023) 137344. https://doi.org/10.1016/j.chemosphere.2022.137344.

[235] G. Yadav, S.K. Dash, R. Sen, A biorefinery for valorization of industrial waste-water and flue gas by microalgae for waste mitigation, carbon-dioxide sequestration and algal biomass production, Sci. Total Environ. 688 (2019) 129–135. https://doi.org/10.1016/j.scitotenv.2019.06.024.

[236] C.Y. Kao, T.Y. Chen, Y. Bin Chang, T.W. Chiu, H.Y. Lin, C. Da Chen, J.S. Chang, C.S. Lin, Utilization of carbon dioxide in industrial flue gases for the cultivation of microalga Chlorella sp., Bioresour. Technol. 166 (2014) 485–493. https://doi.org/10.1016/j.biortech.2014.05.094.

[237] B.S. Yu, Y.J. Sung, H. Il Choi, R. Sirohi, S.J. Sim, Concurrent enhancement of CO2 fixation and productivities of omega-3 fatty acids and astaxanthin in Haematococcus pluvialis culture via calcium-mediated homeoviscous adaptation and biomineralization, Bioresour. Technol. 340 (2021) 125720. https://doi.org/10.1016/j.biortech.2021.125720.

[238] T. Mogany, V. Bhola, L. Ramanna, F. Bux, Photosynthesis and pigment production: elucidation of the interactive effects of nutrients and light on Chlamydomonas reinhardtii, Bioprocess Biosyst. Eng. 45 (2022) 187–201. https://doi.org/10.1007/s00449-021-02651-2.

[239] M.D. Ooms, P.J. Graham, B. Nguyen, E.H. Sargent, D. Sinton, Light dilution via wavelength management for efficient high-density photobioreactors, Biotechnol. Bioeng. 114 (2017) 1160–1169. https://doi.org/10.1002/bit.26261.

[240] H.S. Lee, M.W. Seo, Z.H. Kim, C.G. Lee, Determining the best specific light uptake rates for the lumostatic cultures in bubble column photobioreactors, Enzyme Microb. Technol. 39 (2006) 447–452. https://doi.org/10.1016/j.enzmictec.2005.11.038.

[241] R. Dineshkumar, G. Subramanian, S. Kumar, Development of an optimal light-feeding strategy coupled with semi-continuous reactor operation for simultaneous improvement of microalgal photosynthetic efficiency , lutein production and CO 2 sequestration, Biochem. Eng. J. 113 (2016) 47–56. https://doi.org/10.1016/j.bej.2016.05.011.

[242] S.L. Choi, I.S. Suh, C.G. Lee, Lumostatic operation of bubble column photobioreactors for Haematococcus pluvialis cultures using a specific light uptake rate as a control parameter, Enzyme Microb. Technol. 33 (2003) 403–409. https://doi.org/10.1016/S0141-0229(03)00137-6.

[243] S. Tachihana, N. Nagao, T. Katayama, F.M. Yusoff, S. Banerjee, M. Shariff, Y. Yamada, Y. Imaizumi, T. Toda, K. Furuya, High productivity of fucoxanthin and eicosapentaenoic acid in a marine diatom Chaetoceros gracilis by perfusion culture under high irradiance, Algal Res. 72 (2023) 103123. https://doi.org/10.1016/j.algal.2023.103123.

[244] A.W. Farahin, I. Natrah, N. Nagao, T. Katayama, Y. Imaizumi, N.Z. Mamat, F.M. Yusoff, M. Shariff, High intensity of light: A potential stimulus for maximizing biomass by inducing photosynthetic activity in marine microalga, Tetraselmis tetrathele, Algal Res. 60 (2021) 102523. https://doi.org/10.1016/j.algal.2021.102523.

[245] Y. Xie, S. Ho, C. Chen, C.N. Chen, C. Liu, I. Ng, K. Jing, S. Yang, C. Chen, J. Chang, Y. Lu, Simultaneous enhancement of CO 2 fixation and lutein production with thermo-tolerant Desmodesmus sp . F51 using a repeated fed-batch cultivation strategy, Biochem. Eng. J. 86 (2014) 33–40. https://doi.org/10.1016/j.bej.2014.02.015.

[246] H.F. Jin, B.R. Lim, K. Lee, Influence of nitrate feeding on carbon dioxide fixation by microalgae, J. Environ. Sci. Heal. - Part A Toxic/Hazardous Subst. Environ. Eng. 41 (2006) 2813–2824. https://doi.org/10.1080/10934520600967928.

[247] H. Rismani-Yazdi, B.Z. Haznedaroglu, C. Hsin, J. Peccia, Transcriptomic analysis of the oleaginous microalgaNeochloris oleoabundans reveals metabolic insightsinto triacylglyceride accumulation, Biotechnol. Biofuels. (2012) 74. http://www.scopus.com/inward/record.url?eid=2-s2.0-84866498955&partnerID=40&md5=9855617f1695efaf03134d5aa5c65ec9.

[248] B. Sajjadi, W.Y. Chen, A.A.A. Raman, S. Ibrahim, Microalgae lipid and biomass for biofuel production: A comprehensive review on lipid enhancement strategies and their effects on fatty acid composition, Renew. Sustain. Energy Rev. 97 (2018) 200–232. https://doi.org/10.1016/j.rser.2018.07.050.

[249] X. Wang, Z.H. Qin, T. Bin Hao, G. Bin Ye, J.H. Mou, S. Balamurugan, X.Y. Bin, J. Buhagiar, H.M. Wang, C.S.K. Lin, W.D. Yang, H.Y. Li, A combined light regime and carbon supply regulation strategy for microalgae-based sugar industry wastewater treatment and low-carbon biofuel production to realise a circular economy, Chem. Eng. J. 446 (2022) 137422. https://doi.org/10.1016/j.cej.2022.137422.

[250] Q. Fu, H.X. Chang, Y. Huang, Q. Liao, X. Zhu, A. Xia, Y.H. Sun, A novel self-adaptive microalgae photobioreactor using anion exchange membranes for continuous supply of nutrients, Bioresour. Technol. 214 (2016) 629–636. https://doi.org/10.1016/j.biortech.2016.04.081.

[251] H.W. Kim, R. Vannela, C. Zhou, B.E. Rittmann, Nutrient acquisition and limitation for the photoautotrophic growth of Synechocystis sp. PCC6803 as a renewable biomass source, Biotechnol. Bioeng. 108 (2011) 277–285. https://doi.org/10.1002/bit.22928.

[252] N.S. Garcia, J.A. Bonachela, A.C. Martiny, Interactions between growth-dependent changes in cell size, nutrient supply and cellular elemental stoichiometry of marine Synechococcus, ISME J. 10 (2016) 2715–2724. https://doi.org/10.1038/ismej.2016.50.

[253] J. Fu, Y. Huang, Q. Liao, A. Xia, Q. Fu, X. Zhu, Photo-bioreactor design for microalgae: A review from the aspect of CO2 transfer and conversion, Bioresour. Technol. 292 (2019) 121947. https://doi.org/10.1016/j.biortech.2019.121947.

[254] W. Levasseur, P. Perré, V. Pozzobon, A review of high value-added molecules production by microalgae in light of the classification, Biotechnol. Adv. 41 (2020) 107545. https://doi.org/10.1016/j.biotechadv.2020.107545.

[255] W. Guo, J. Cheng, Y. Song, S. Kumar, K.A. Ali, C. Guo, Z. Qiao, Developing a CO 2 bicarbonation absorber for promoting microalgal growth rates with an improved photosynthesis pathway, RSC Adv. 9 (2019) 2746–2755. https://doi.org/10.1039/c8ra09538h.

[256] W. Guo, J. Cheng, K.A. Ali, S. Kumar, C. Guo, Conversion of NaHCO3 to Na2CO3 with a growth of Arthrospira platensis cells in 660 m2 raceway ponds with a CO2 bicarbonation absorber, Microb. Biotechnol. 13 (2020) 470–478. https://doi.org/10.1111/1751-7915.13497.

[257] B.B. Cardias, M.G. de Morais, J.A.V. Costa, CO2conversion by the integration of biological and chemical methods: Spirulina sp. LEB 18 cultivation with diethanolamine and potassium carbonate addition, Bioresour. Technol. 267 (2018) 77–83. https://doi.org/10.1016/j.biortech.2018.07.031.

[258] Q. Yin, W. Mao, D. Chen, C. Song, Effect of adding tertiary amine TMEDA and space hindered amine DACH on the CO2 chemical absorption-microalgae conversion system, Energy. 263 (2023) 125726. https://doi.org/10.1016/j.energy.2022.125726.

[259] W. Mao, P. Li, D. Wang, Z. Hu, S. Wei, C. Song, Effect of DACH-K2CO3 Mixed Absorbent on the Performance of a CO2 Absorption and Microalgae Conversion (CAMC) System, ACS Sustain. Chem. Eng. 12 (2024) 120–129. https://doi.org/10.1021/acssuschemeng.3c04955.

[260] G. Kim, W. Choi, C.H. Lee, K. Lee, Enhancement of dissolved inorganic carbon and carbon fixation by green alga Scenedesmus sp. in the presence of alkanolamine CO2absorbents, Biochem. Eng. J. 78 (2013) 18–23. https://doi.org/10.1016/j.bej.2013.02.010.

[261] Q.I. Zheng, Efficient CO 2 delivery from flue gas to microalgae ponds through a novel membrane system, (2017). https://minerva-access.unimelb.edu.au/.../Efficient%2520CO2%25.

[262] Z. Yang, H. Pei, F. Han, Y. Wang, Q. Hou, Y. Chen, Effects of air bubble size on algal growth rate and lipid accumulation using fine-pore diffuser photobioreactors, Algal Res. 32 (2018) 293–299. https://doi.org/10.1016/j.algal.2018.04.016.

[263] Y. Huang, S. Zhao, Y. dong Ding, Q. Liao, Y. Huang, X. Zhu, Optimizing the gas distributor based on CO2 bubble dynamic behaviors to improve microalgal biomass production in an air-lift photo-bioreactor, Bioresour. Technol. 233 (2017) 84–91. https://doi.org/10.1016/j.biortech.2017.02.071.

[264] Y. Song, J. Cheng, W. Guo, S. Liu, L. Zhang, S. Kumar, K.A. Ali, Microporous Diaphragm Aerator Improves Flue Gas CO 2 Dissolution and Photosynthetic Characteristics of Arthrospira Cells in 660 m 2 Raceway Ponds , ACS Sustain. Chem. Eng. 8 (2020) 11558–11568. https://doi.org/10.1021/acssuschemeng.0c02714.

[265] Y.A. Lim, I.M.S.K. Ilankoon, M.N. Chong, S.C. Foo, Improving microalgae growth and carbon capture through micro-size bubbles generation in flat-panel photobioreactors: Impacts of different gas sparger designs on mixing performance, Renew. Sustain. Energy Rev. 171 (2023) 113001. https://doi.org/10.1016/j.rser.2022.113001.

[266] H. Kim, J. Cheng, B.E. Rittmann, Bioresource Technology Direct membrane-carbonation photobioreactor producing photoautotrophic biomass via carbon dioxide transfer and nutrient removal, Bioresour. Technol. 204 (2016) 32–37. https://doi.org/10.1016/j.biortech.2015.12.066.

[267] H.W. Kim, A.K. Marcus, J.H. Shin, B.E. Rittmann, Advanced control for photoautotrophic growth and CO2-utilization efficiency using a membrane carbonation photobioreactor (MCPBR), Environ. Sci. Technol. 45 (2011) 5032–5038. https://doi.org/10.1021/es104235v.

[268] S. Mishra, K. Mohanty, Comprehensive characterization of microalgal isolates and lipid-extracted biomass as zero-waste bioenergy feedstock: An integrated bioremediation and biorefinery approach, Bioresour. Technol. 273 (2018) 177–184. https://doi.org/10.1016/J.BIORTECH.2018.11.012.

[269] M. Gebremedhin, S. Mishra, K. Mohanty, Augmentation of native microalgae based biofuel production through statistical optimization of campus sewage wastewater as low-cost growth media, J. Environ. Chem. Eng. 6 (2018) 6623–6632. https://doi.org/10.1016/j.jece.2018.08.061.

[270] S. Gupta, R.A. Pandey, S.B. Pawar, Bioremediation of synthetic high–chemical oxygen demand wastewater using microalgal species Chlorella pyrenoidosa, Bioremediat. J. 21 (2017) 38–51. https://doi.org/10.1080/10889868.2017.1282936.

[271] M. Sati, M. Verma, J.P.N. Rai, Phycoremediation of Heavy Metals by Chlorella pyrenoidosa and Spirogyra communis, Int. J. Curr. Microbiol. Appl. Sci. 5 (2016) 920–930. https://doi.org/10.20546/ijcmas.2016.510.099.

[272] S. Basu, A. Sarma, K. Mohanty, A.K. Ghoshal, Bioresource Technology Enhanced CO 2 sequestration by a novel microalga : Scenedesmus obliquus SA1 isolated from bio-diversity hotspot region of Assam , India, Bioresour. Technol. 143 (2013) 369–377. https://doi.org/10.1016/j.biortech.2013.06.010.

[273] E.W. Rice, R.B. Baird, A.D. Eaton, eds., Standard Methods for the Examination of Water and Wastewater, 23rd ed., American Water Works Association/American Public Works Association/Water Environment Federation., Washington, DC, 2017. https://www.awwa.org/Store/Product-Details/productId/65266295.

[274] B. Ketheesan, N. Nirmalakhandan, Bioresource Technology Feasibility of microalgal cultivation in a pilot-scale airlift-driven raceway reactor, Bioresour. Technol. 108 (2012) 196–202. https://doi.org/10.1016/j.biortech.2011.12.146.

[275] P.S.C. Schulze, H.G.C. Pereira, T.F.C. Santos, L. Schueler, R. Guerra, L.A. Barreira, J.A. Perales, J.C.S. Varela, Effect of light quality supplied by light emitting diodes (LEDs) on growth and biochemical pro fi les of Nannochloropsis oculata and Tetraselmis chuii, ALGAL. 16 (2016) 387–398. https://doi.org/10.1016/j.algal.2016.03.034.

[276] H.K. Lichtenthaler, Chlorophylls and Carotenoids: Pigments of Photosynthetic

Biomembranes, Methods Enzymol. 148 (1987) 350–382. https://doi.org/10.1016/0076-6879(87)48036-1.

[277] J. Zhu, W. Chen, H. Chen, X. Zhang, C. He, J. Rong, Q. Wang, Improved productivity of neutral lipids in Chlorella sp. A2 by minimal nitrogen supply, Front. Microbiol. 7 (2016) 1–11. https://doi.org/10.3389/fmicb.2016.00557.

[278] U. Schreiber, U. Schliwa, W. Bilger, Continuous recording of photochemical and non-photochemical chlorophyll fluorescence quenching with a new type of modulation fluorometer, Photosynth. Res. 10 (1986) 51–62. https://doi.org/10.1007/BF00024185.

[279] M. Dubios, K.A. Gilles, J.K. Hamilton, P.A. Rebers, F. Smith, Colorimetric Method for Determination of Sugars and Related susbstances, Anal. Chem. 28 (1956) 350–356. https://doi.org/10.1021/ac60111a017.

[280] O.H. Lowry, N.J. Rosebrough, A.L. Farr, R.J. Randall, Protein measurement with the Folin phenol reagent, J. Biol. Chem. 193 (1951) 265–275.

[281] D.S. Chauhan, G. Goswami, G. Dineshbabu, B. Palabhanvi, D. Das, Evaluation and optimization of feedstock quality for direct conversion of microalga Chlorella sp. FC2 IITG into biodiesel via supercritical methanol transesterification, Biomass Convers. Biorefinery. (2019). https://doi.org/10.1007/s13399-019-00432-2.

[282] B. Ravi Kiran, S. Venkata Mohan, Photosynthetic transients in Chlorella sorokiniana during phycoremediation of dairy wastewater under distinct light intensities, Bioresour. Technol. 340 (2021) 125593. https://doi.org/10.1016/j.biortech.2021.125593.

[283] O. Osundeko, A.P. Dean, H. Davies, J.K. Pittman, Acclimation of microalgae to wastewater environments involves increased oxidative stress tolerance activity, Plant Cell Physiol. 55 (2014) 1848–1857. https://doi.org/10.1093/pcp/pcu113.

[284] E.H. Murchie, T. Lawson, Chlorophyll fluorescence analysis: A guide to good practice and understanding some new applications, J. Exp. Bot. 64 (2013) 3983–3998. https://doi.org/10.1093/jxb/ert208.

[285] T. Zakar, E. Herman, S. Vajravel, L. Kovacs, J. Knoppová, J. Komenda, I. Domonkos, M. Kis, Z. Gombos, H. Laczko-Dobos, Lipid and carotenoid cooperation-driven adaptation to light and temperature stress in Synechocystis sp. PCC6803, Biochim. Biophys. Acta - Bioenerg. 1858 (2017) 337–350. https://doi.org/10.1016/j.bbabio.2017.02.002.

[286] W. Maneechote, B. Cheirsilp, Stepwise-incremental physicochemical factors induced acclimation and tolerance in oleaginous microalgae to crucial outdoor stresses and improved properties as biodiesel feedstocks, Bioresour. Technol. 328 (2021) 124850. https://doi.org/10.1016/j.biortech.2021.124850.

[287] H. Sun, Y. Ren, X. Mao, X. Li, H. Zhang, Y. Lao, F. Chen, Harnessing C/N balance of Chromochloris zofingiensis to overcome the potential conflict in microalgal production, Commun. Biol. 3 (2020) 1–13. https://doi.org/10.1038/s42003-020-0900-x.

[288] A.K. Minhas, P. Hodgson, C.J. Barrow, A. Adholeya, A review on the assessment of stress conditions for simultaneous production of microalgal lipids and carotenoids, Front. Microbiol. 7 (2016) 1–19. https://doi.org/10.3389/fmicb.2016.00546.

[289] E.C. Camargo, A.T. Lombardi, Correction to: Effect of cement industry flue gas simulation on the physiology and photosynthetic performance of Chlorella sorokiniana, J. Appl. Phycol. 235 (2017) 1. https://doi.org/10.1007/s10811-017-1353-6.

[290] S. Van Den Hende, H. Vervaeren, N. Boon, Flue gas compounds and microalgae: (Bio-)chemical interactions leading to biotechnological opportunities, Biotechnol. Adv. 30 (2012) 1405–1424. https://doi.org/10.1016/j.biotechadv.2012.02.015.

[291] S.A. Channiwala, P.P. Parikh, A unified correlation for estimating HHV of solid, liquid and gaseous fuels, Fuel. 81 (2002) 1051–1063. https://doi.org/10.1016/S0016-2361(01)00131-4.

[292] M.H.A. Michels, J. Camacho-Rodríguez, M.H. Vermuë, R.H. Wijffels, Effect of cooling in the night on the productivity and biochemical composition of Tetraselmis suecica, Algal Res. 6 (2014) 145–151. https://doi.org/10.1016/j.algal.2014.11.002.

[293] J. Cabello, A. Toledo-Cervantes, L. Sánchez, S. Revah, M. Morales, Effect of the temperature, pH and irradiance on the photosynthetic activity by Scenedesmus obtusiusculus under nitrogen replete and deplete conditions, Bioresour. Technol. 181 (2015) 128–135. https://doi.org/10.1016/j.biortech.2015.01.034.

[294] K. Xu, X. Zou, H. Wen, Y. Xue, Y. Qu, Y. Li, Effects of multi-temperature regimes on cultivation of microalgae in municipal wastewater to simultaneously remove nutrients and produce biomass, Appl. Microbiol. Biotechnol. 103 (2019) 8255–8265. https://doi.org/10.1007/s00253-019-10051-6.

[295] K. Spilling, P. Ylöstalo, S. Simis, J. Seppälä, Interaction effects of light, temperature and nutrient limitations (N, P and Si) on growth, stoichiometry and photosynthetic parameters of the cold-water diatom Chaetoceros wighamii, PLoS One. 10 (2015) 1–18. https://doi.org/10.1371/journal.pone.0126308.

[296] M. Ras, J.P. Steyer, O. Bernard, Temperature effect on microalgae: A crucial factor for outdoor production, Rev. Environ. Sci. Biotechnol. 12 (2013) 153–164. https://doi.org/10.1007/s11157-013-9310-6.

[297] D. Singh, L. Sahoo, K. Mohanty, Bioresource Technology Maximize microalgal carbon dioxide utilization and lipid productivity by using toxic flue gas compounds as nutrient source, Bioresour. Technol. 348 (2022) 126784. https://doi.org/10.1016/j.biortech.2022.126784.

[298] S.H. Seo, J.S. Ha, C. Yoo, A. Srivastava, C.Y. Ahn, D.H. Cho, H.J. La, M.S. Han, H.M. Oh, Light intensity as major factor to maximize biomass and lipid productivity of Ettlia sp. in CO2-controlled photoautotrophic chemostat, Bioresour. Technol. 244 (2017) 621–628. https://doi.org/10.1016/j.biortech.2017.08.020.

[299] A. León-Vaz, R. León, J. Vigara, C. Funk, Exploring Nordic microalgae as a potential novel source of antioxidant and bioactive compounds, N. Biotechnol. 73 (2023) 1–8. https://doi.org/10.1016/j.nbt.2022.12.001.

[300] M.J. Raeesossadati, H. Ahmadzadeh, M.P. Mchenry, N.R. Moheimani, Review article CO 2 bioremediation by microalgae in photobioreactors : Impacts of biomass and CO 2 concentrations , light , and temperature, ALGAL. 6 (2014) 78–85. https://doi.org/10.1016/j.algal.2014.09.007.

[301] X. Li, S. Slavens, D.W. Crunkleton, T.W. Johannes, Interactive effect of light quality and temperature on Chlamydomonas reinhardtii growth kinetics and lipid synthesis, Algal Res. 53 (2021) 102127. https://doi.org/10.1016/j.algal.2020.102127.

[302] Y. Maltsev, K. Maltseva, Fatty acids of microalgae: diversity and applications, Springer Netherlands, 2021. https://doi.org/10.1007/s11157-021-09571-3.

[303] C. Chen, F. Tao, T. Han, F. Gao, T. Dong, W. Jiang, H. Lu, Y. Zhang, B. Li, Photoacclimation caused by high frequency flashing light assists Chlorella sp. M-12 wastewater treatment and biomass accumulation in dark color biogas slurry, J. Appl. Phycol. 34 (2022) 2929–2940. https://doi.org/10.1007/s10811-022-02840-w.

[304] Y. Wang, D.J. Stessman, M.H. Spalding, The CO<inf>2</inf> concentrating mechanism and photosynthetic carbon assimilation in limiting CO<inf>2</inf>: How Chlamydomonas works against the gradient, Plant J. 82 (2015) 429–448. https://doi.org/10.1111/tpj.12829.

[305] T. Jakob, H. Wagner, K. Stehfest, C. Wilhelm, A complete energy balance from photons to new biomass reveals a light- and nutrient-dependent variability in the metabolic costs of carbon assimilation, J. Exp. Bot. 58 (2007) 2101–2112. https://doi.org/10.1093/jxb/erm084.

[306] A. Lei, H. Chen, G. Shen, Z. Hu, L. Chen, J. Wang, Expression of fatty acid synthesis genes and fatty acid accumulation in haematococcus pluvialis under different stressors, Biotechnol. Biofuels. 5 (2012) 1–11. https://doi.org/10.1186/1754-6834-5-18.

[307] P. Varshney, S. Sohoni, P.P. Wangikar, J. Beardall, Effect of high CO 2 concentrations on the growth and macromolecular composition of a heat- and high-light-tolerant microalga, J. Appl. Phycol. (2016) 2631–2640. https://doi.org/10.1007/s10811-016-0797-4.

[308] N. Schiffrine, J.É. Tremblay, M. Babin, Interactive effects of temperature and nitrogen source on the elemental stoichiometry of a polar diatom, Limnol. Oceanogr. (2022) 2750–2762. https://doi.org/10.1002/lno.12235.

[309] Q. He, H. Yang, L. Wu, C. Hu, Effect of light intensity on physiological changes, carbon allocation and neutral lipid accumulation in oleaginous microalgae, Bioresour. Technol. 191 (2015) 219–228. https://doi.org/10.1016/j.biortech.2015.05.021.

[310] V. da S. Braga, J.B. Moreira, J.A.V. Costa, M.G. de Morais, Potential of Chlorella fusca LEB 111 cultivated with thermoelectric fly ashes, carbon dioxide and reduced supply of nitrogen to produce macromolecules, Bioresour. Technol. 277 (2019) 55–61. https://doi.org/10.1016/j.biortech.2019.01.035.

[311] J.U. Grobbelaar, N. Kurano, Use of photoacclimation in the design of a novel photobioreactor to achieve high yields in algal mass cultivation, J. Appl. Phycol. 15 (2003) 121–126. https://doi.org/10.1023/A:1023802820093.

[312] D. McGee, L. Archer, G.T.A. Fleming, E. Gillespie, N. Touzet, Influence of spectral intensity and quality of LED lighting on photoacclimation, carbon allocation and high-value pigments in microalgae, Photosynth. Res. 143 (2020) 67–80. https://doi.org/10.1007/s11120-019-00686-x.

[313] S.H. Seo, J.S. Ha, C. Yoo, A. Srivastava, C.Y. Ahn, D.H. Cho, H.J. La, M.S. Han, H.M. Oh, Light intensity as major factor to maximize biomass and lipid productivity of

Ettlia sp. in CO2-controlled photoautotrophic chemostat, Bioresour. Technol. 244 (2017) 621–628. https://doi.org/10.1016/j.biortech.2017.08.020.

[314] G. Torzillo, A. Sacchi, R. Materassi, A. Richmond, Effect of temperature on yield and night biomass loss in Spirulina platensis grown outdoors in tubular photobioreactors, J. Appl. Phycol. 3 (1991) 103–109. https://doi.org/10.1007/BF00003691.

[315] K. Tanaka, M. Kishi, H. Assaye, T. Toda, Low temperatures in dark period affect biomass productivity of a cyanobacterium Arthrospira platensis, Algal Res. 52 (2020) 102132. https://doi.org/10.1016/j.algal.2020.102132.

[316] D.A. Cataldo, M.H. Haroon, L.E. Schrader, V.L. Youngs, Rapid colorimetric determination of nitrate in plant tissue by nitration of salicylic acid, Commun. Soil Sci. Plant Anal. 6 (1975) 71–80. https://doi.org/10.1080/00103627509366547.

[317] F.S. Watanabe, S.R. Olsen, Test of an Ascorbic Acid Method for Determining Phosphorus in Water and NaHCO 3 Extracts from Soil 1 A NEED EXISTS for a more suitable method to determine, Soil Sci. Soc. Proc. (1965) 677–678.

[318] H. Chen, J. Wang, Y. Zheng, J. Zhan, C. He, Q. Wang, Algal biofuel production coupled bioremediation of biomass power plant wastes based on Chlorella sp. C2 cultivation, Appl. Energy. 211 (2018) 296–305. https://doi.org/10.1016/j.apenergy.2017.11.058.

[319] G. De Bhowmick, L. Koduru, R. Sen, Metabolic pathway engineering towards enhancing microalgal lipid biosynthesis for biofuel application - A review, Renew. Sustain. Energy Rev. 50 (2015) 1239–1253. https://doi.org/10.1016/j.rser.2015.04.131.

[320] F. Shuhaili, M. Segura-Noguera, Mathumathy, R. Vijayaraghavan, S. Thilagar, U. Lakshmanan, D. Prabaharan, S. Vaidyanathan, Nitrate and phosphate uptake dynamics in two halotolerant strains of Chlorella vulgaris is differentially influenced by carbon, nitrogen and phosphorus supply, Chem. Eng. J. 458 (2023) 141433. https://doi.org/10.1016/j.cej.2023.141433.

[321] S.K. Hoi, B.N.R. Winayu, H.T. Hsueh, H. Chu, Light factors and nitrogen availability to enhance biomass and C-phycocyanin productivity of Thermosynechococcus sp. CL-1, Biochem. Eng. J. 167 (2021) 107899. https://doi.org/10.1016/j.bej.2020.107899.

[322] B. Mueller, J. Den Haan, P.M. Visser, M.J.A. Vermeij, F.C. Van Duyl, Effect of light and nutrient availability on the release of dissolved organic carbon (DOC) by Caribbean turf algae, Sci. Rep. 6 (2016) 1–9. https://doi.org/10.1038/srep23248.

[323] L. Fu, X. Cui, Y. Li, L. Xu, C. Zhang, R. Xiong, D. Zhou, J.C. Crittenden, Excessive phosphorus enhances Chlorella regularis lipid production under nitrogen starvation stress during glucose heterotrophic cultivation, Chem. Eng. J. 330 (2017) 566–572. https://doi.org/10.1016/j.cej.2017.07.182.

[324] Y. Imaizumi, N. Nagao, F.M. Yusoff, N. Kurosawa, N. Kawasaki, T. Toda, Lumostatic operation controlled by the optimum light intensity per dry weight for the effective production of Chlorella zofingiensis in the high cell density continuous culture, Algal Res. 20 (2016) 110–117. https://doi.org/10.1016/j.algal.2016.09.015.

[325] L. Xin, H. Hong-ying, G. Ke, S. Ying-xue, Effects of different nitrogen and phosphorus concentrations on the growth, nutrient uptake, and lipid accumulation of a freshwater microalga Scenedesmus sp., Bioresour. Technol. 101 (2010) 5494–5500.

https://doi.org/10.1016/j.biortech.2010.02.016.

[326] Y. Zhou, B.T. Nguyen, C. Zhou, L. Straka, Y.J.S. Lai, S. Xia, B.E. Rittmann, The distribution of phosphorus and its transformations during batch growth of Synechocystis, Water Res. 122 (2017) 355–362. https://doi.org/10.1016/j.watres.2017.06.017.

[327] Y. Xia, M. Kishi, Y. Sugai, T. Toda, Microalgal flocculation and sedimentation: spatiotemporal evaluation of the effects of the pH and calcium concentration, Bioprocess Biosyst. Eng. 45 (2022) 1489–1498. https://doi.org/10.1007/s00449-022-02758-0.

[328] Y. Li, Engineering whiting events in culture: A microalgae-driven calcium carbonate and biomass production process at high pH and alkalinity with the marine microalga Nannochloropsis oceanica IMET1, J. CO2 Util. 80 (2024) 102669. https://doi.org/10.1016/j.jcou.2024.102669.

[329] D.R. Wybenga, J. Di Giorgio, V.J. Pileggi, Manual and automated methods for urea nitrogen measurement in whole serum., Clin. Chem. 17 (1971) 891–895. https://doi.org/10.1093/clinchem/17.9.891.

[330] W.C. Sun, C.B. Yong, M.H. Li, Kinetics of the absorption of carbon dioxide into mixed aqueous solutions of 2-amino-2-methyl-l-propanol and piperazine, Chem. Eng. Sci. 60 (2005) 503–516. https://doi.org/10.1016/j.ces.2004.08.012.

[331] S. Basu, A. Sarma, K. Mohanty, A.K. Ghoshal, Bioresource Technology CO 2 biofixation and carbonic anhydrase activity in Scenedesmus obliquus SA1 cultivated in large scale open system, Bioresour. Technol. 164 (2014) 323–330. https://doi.org/10.1016/j.biortech.2014.05.017.

[332] N. Rashid, M. Nayak, B. Lee, Y. Chang, Ef fi cient microalgae harvesting mediated by polysaccharides interaction with residual calcium and phosphate in the growth medium, J. Clean. Prod. 234 (2019) 150–156. https://doi.org/10.1016/j.jclepro.2019.06.154.

[333] D.S. Chauhan, K. Mohanty, Exploring microalgal nutrient-light synergy to enhance CO2 utilization and lipid productivity in sustainable long-term water recycling cultivation, J. Environ. Manage. 356 (2024) 120631. https://doi.org/10.1016/j.jenvman.2024.120631.

[334] R.M. Rosa, M. Machado, M.G.M.V. Vaz, R. Lopes-Santos, A.G. do Nascimento, W.L. Araújo, A. Nunes-Nesi, Urea as a source of nitrogen and carbon leads to increased photosynthesis rates in Chlamydomonas reinhardtii under mixotrophy, J. Biotechnol. 367 (2023) 20–30. https://doi.org/10.1016/j.jbiotec.2023.03.009.

[335] A.D. Batista, R.M. Rosa, M. Machado, A.S. Magalhães, B.A. Shalaguti, P.F. Gomes, L. Covell, M.G.M.V. Vaz, W.L. Araújo, A. Nunes-Nesi, Increased urea availability promotes adjustments in C/N metabolism and lipid content without impacting growth in Chlamydomonas reinhardtii, Metabolomics. 15 (2019) 1–14. https://doi.org/10.1007/s11306-019-1496-3.

[336] H. Liu, T.J. Liu, H.W. Guo, Y.J. Wang, R. Ji, L. Le Kang, Y.T. Wang, X. Guo, J.G. Li, L.Q. Jiang, Z. Fang, A review of the strategy to promote microalgae value in CO2 conversion-lipid enrichment-biodiesel production, J. Clean. Prod. 436 (2024) 140538.

https://doi.org/10.1016/j.jclepro.2023.140538.

[337] J. Li, X. Tang, K. Pan, B. Zhu, Y. Li, Z. Wang, Y. Zhao, Energy metabolism and intracellular pH regulation reveal different physiological acclimation mechanisms of Chlorella strains to high concentrations of CO2, Sci. Total Environ. 853 (2022) 158627. https://doi.org/10.1016/j.scitotenv.2022.158627.

[338] D. Singh Chauhan, L. Sahoo, K. Mohanty, Acclimation-driven microalgal cultivation improved temperature and light stress tolerance, CO2 sequestration and metabolite regulation for bioenergy production, Bioresour. Technol. 385 (2023) 129386. https://doi.org/10.1016/j.biortech.2023.129386.

[339] D. Singh Chauhan, L. Sahoo, K. Mohanty, Maximize microalgal carbon dioxide utilization and lipid productivity by using toxic flue gas compounds as nutrient source, Bioresour. Technol. 348 (2022) 126784. https://doi.org/10.1016/j.biortech.2022.126784.

[340] X. Chen, Q.Y. Goh, W. Tan, I. Hossain, W.N. Chen, R. Lau, Lumostatic strategy for microalgae cultivation utilizing image analysis and chlorophyll a content as design parameters, Bioresour. Technol. 102 (2011) 6005–6012. https://doi.org/10.1016/j.biortech.2011.02.061.

[341] Y. Su, Revisiting carbon, nitrogen, and phosphorus metabolisms in microalgae for wastewater treatment, Sci. Total Environ. 762 (2021) 144590. https://doi.org/10.1016/j.scitotenv.2020.144590.

[342] A. Ozkan, H. Berberoglu, Physico-chemical surface properties of microalgae, Colloids Surfaces B Biointerfaces. 112 (2013) 287–293. https://doi.org/10.1016/j.colsurfb.2013.08.001.

List of Publications

1. **D. Singh**, L. Sahoo, K. Mohanty, Maximize microalgal carbon dioxide utilization and lipid productivity by using toxic flue gas compounds as nutrient source, **Bioresource Technology**. 348 (2022) 126784. https://doi.org/10.1016/j.biortech.2022.126784.

2. [**D. Singh** , L. Sahoo, K. Mohanty, Acclimation-driven microalgal cultivation improved temperature and light stress tolerance, CO_2 sequestration and metabolite regulation for bioenergy production, **Bioresourse Technology** 385 (2023) 129386. https://doi.org/10.1016/j.biortech.2023.129386. **(Selected For The Cover Image)**

3. **D.Singh**, K. Mohanty, Exploring microalgal nutrient-light synergy to enhance CO_2 utilization and lipid productivity in sustainable long-term water recycling cultivation **Journol of Environemnt mangemnt** 356 (2024) 120631**.** https://doi.org/10.1016/j.jenvman.2024.120631

4. **D.Singh,** K. Mohanty**,** Revolutionizing CO_2 management strategy to maximize microalgal CO_2 fixation for high-density auto-sedimented value-added biomass production **(under Rervew process)**

Conference

1. **D.Singh**, K. Mohanty, *High cell density fed batch and Semi-continuous mode of microalgal cultivation for enhanced microalgal CO_2 and wastewater based nutrient utiliztation* .International Conference on Biotechnology for Sustainable Bioresources and Bioeconomy, 07th to 11th December 2022, jointly organized by Indian Institute of Technology Guwahati and The Biotech Research Society, India.

2. **D.Singh**, K. Mohanty, *Nutrient and Light syncretic effect on microalgal CO2 bio-mitigation and bioenergy production*. International Symposium on Advances in Algal Research, 12th to 14th June 2023, jointly organized by Indian Institute of Technology Guwahati and Denmark Technical University Denmark.

Bioresource Technology 348 (2022) 126784

Contents lists available at ScienceDirect

Bioresource Technology

journal homepage: www.elsevier.com/locate/biortech

Maximize microalgal carbon dioxide utilization and lipid productivity by using toxic flue gas compounds as nutrient source

Deepesh Singh Chauhan [a], Lingaraj Sahoo [a,b], Kaustubha Mohanty [a,c,*]

[a] School of Energy Science and Engineering, Indian Institute of Technology Guwahati, Guwahati 781039, India
[b] Department of Biosciences and Bioengineering, Indian Institute of Technology Guwahati, Guwahati 781039, India
[c] Department of Chemical Engineering, Indian Institute of Technology Guwahati, Guwahati 781039, India

HIGHLIGHTS

- Pre-acclimation is a useful approach for enhancing algae tolerance to NOx and SOx.
- Sulphur compounds were major inhibitors for CO_2 fixation and biomass production.
- High sulphate removal rate is crucial to maintain pH of media and CO_2 fixation.
- Pre-acclimated KMC8 cells could better mitigate CO_2 from real flue gas system.

GRAPHICAL ABSTRACT

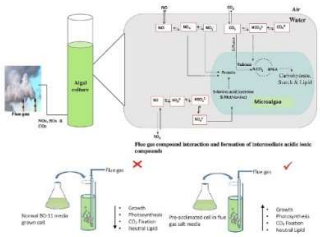

ARTICLE INFO

Keywords:
Microalgae
Acclimation
CO_2 fixation
Toxic flue gas compounds
Neutral lipid

ABSTRACT

NOx and SOx present in flue gas inhibit microalgal based CO_2 mitigation process. In this work, 13 microalgal strains were screened to evaluate their gradual acclimation capacity to toxic flue gas compounds, by testing their growth capability and photosynthetic ability in dissolved flue gas compounds. Six strains out of them were evaluated for their acclimation to bicarbonate and 15% CO_2 as sole carbon sources. Two strains, *Micractinium pusillum* KMC8 and *Scenedesmus acutus* NCIM5584 were found to accumulate nitrite as fixed nitrogen and showed improved growth performance in photobioreactor upon stepwise acclimation to bisulphite/sulphite. Notably, the strain KMC8 showed a high tolerance and rapidly acclimated dissolved flue gas compounds with higher biomass yield (1.32 g L^{-1}) and neutral lipid accumulation (32%), enhanced CO_2 utilization efficiency (3.07%) and CO_2 fixation rate (136.79 mg L^{-1} d^{-1}) post acclimation. KMC8 sustained its stability in biomass and lipid productivity while simultaneously bio-mitigated CO_2 under semi-continuous mode.

1. Introduction

Excessive combustion of conventional fossil fuels such as coal, oil and natural gas results in increased carbon dioxide (CO_2) emissions leading to global warming. The CO_2 emission recorded 33.1 Gt CO_2 in 2018, with 1% rise every year (Le Quéré et al., 2020). Flue gases released by various industries and power plants contribute the major proportion of CO_2 emission. It is inevitable that fossil fuel combustion

* Corresponding author at: School of Energy Science and Engineering, Indian Institute of Technology Guwahati, Guwahati 781039, India.
E-mail address: kmohanty@iitg.ac.in (K. Mohanty).

https://doi.org/10.1016/j.biortech.2022.126784
Received 13 December 2021; Received in revised form 22 January 2022; Accepted 24 January 2022
Available online 29 January 2022
0960-8524/

Bioresource Technology 385 (2023) 129386

Contents lists available at ScienceDirect

Bioresource Technology

journal homepage: www.elsevier.com/locate/biortech

Acclimation-driven microalgal cultivation improved temperature and light stress tolerance, CO_2 sequestration and metabolite regulation for bioenergy production

Deepesh Singh Chauhan [a], Lingaraj Sahoo [a,b], Kaustubha Mohanty [a,c,*]

[a] School of Energy Science and Engineering, Indian Institute of Technology Guwahati, Guwahati 781039, India
[b] Department of Biosciences and Bioengineering, Indian Institute of Technology Guwahati, Guwahati 781039, India
[c] Department of Chemical Engineering, Indian Institute of Technology Guwahati, Guwahati 781039, India

HIGHLIGHTS

- Light and temperature alter *M. pussilum* primary metabolites, C/N stichometry.
- Positive correlation exists between N fixation and photosynthetic carbon accumulation.
- Neutral lipid and cellular bioenergy increased when temperature and light levels increase.
- *M. pusillum* seems to be excellent for carbon fixation and bioenergy production.

GRAPHICAL ABSTRACT

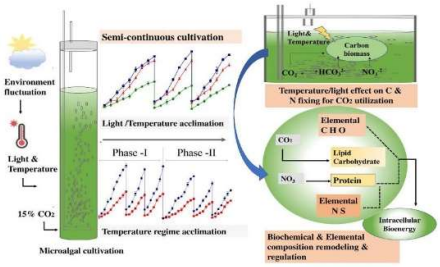

ARTICLE INFO

Keywords:
Photosynthesis
Acclimation
CO_2 sequestration
Primary metabolite
Bioenergy

ABSTRACT

This study investigates temperature and light impact on the ability of *Micractinium pusillum* microalgae to mitigate CO_2 and produce bioenergy in semi-continuous mode. Microalgae were exposed to temperatures (15, 25, and 35 °C) and light intensities (50, 350, and 650 μmol m^{-2} s^{-1}), including two temperature cycles, 25 °C had the maximum growth rate, with no significant difference at 35 °C and light intensities of 350 and 650 μmol m^{-2} s^{-1}. 15 °C temperature and 50 μmol m^{-2} s^{-1} light intensity reduced growth. Increased light intensity accelerated growth, CO_2 utilization with carbon and bioenergy accumulation. Microalgae demonstrate rapid primary metabolic adjustment and acclimation reactions in response to changes in light and temperature conditions. Temperature correlated positively with carbon and nitrogen fixation, CO_2 fixation, and carbon accumulation in the biomass, whereas there was no correlation found between light. In the temperature regime experiment, higher light intensity boosted nutrient and CO_2 utilization, carbon buildup, and biomass bioenergy.

* Corresponding author at: Department of Chemical Engineering, Indian Institute of Technology Guwahati, Guwahati 781039, India
E-mail address: kmohanty@iitg.ac.in (K. Mohanty).

https://doi.org/10.1016/j.biortech.2023.129386
Received 26 May 2023; Received in revised form 19 June 2023; Accepted 21 June 2023
Available online 25 June 2023

Journal of Environmental Management 356 (2024) 120631

Contents lists available at ScienceDirect

Journal of Environmental Management

journal homepage: www.elsevier.com/locate/jenvman

Research article

Exploring microalgal nutrient-light synergy to enhance CO_2 utilization and lipid productivity in sustainable long-term water recycling cultivation

Deepesh Singh Chauhan [a], Kaustubha Mohanty [a,b,*]

[a] School of Energy Science and Engineering, Indian Institute of Technology Guwahati, Guwahati, 781039, India
[b] Department of Chemical Engineering, Indian Institute of Technology Guwahati, Guwahati, 781039, India

ARTICLE INFO

Handling editor: Raf Dewil

Keywords:
CO_2 utilization
Nitrogen fixation
Lipid productivity
Repeated-fed-batch
Water recycling

ABSTRACT

In this work the effects of nutrient availability and light conditions on CO_2 utilization and lipid production in *Micractinium pusillum* KMC8 is reported. The study investigated the ideal nitrogen concentrations for growth and nitrogen utilization in a 15% CO_2 environment. Logistic and Gompertz models were employed to analyze the kinetics of KMC8 cell growth. Compared to 17.6 mmol L^{-1} control nitrogen, which generated 1.6 g L^{-1} growth, doubling and quadrupling nitrogen concentrations boosted biomass growth by 12.5% and 28.78%. At 8.6 mmol L^{-1} nitrogen, the growth decreased but lipid productivity increased to 18.62 mg L^{-1} day^{-1}. At 70.6 mmol L^{-1} nitrogen, elevated nitrogen levels maintained an alkaline pH above 7 and enhanced CO_2 mitigation, achieving 2.27% CO_2 utilization efficiency. Nitrogen shows a positive correlation with higher rates of carbon and nitrogen fixation. The investigation extends to find out the influence of phosphorus and light conditions on microalgae. Increasing light intensity incrementally from 150 to 1200 µmol m^{-2} s^{-1} with more phosphorus increased biomass productivity by 85% (255 mg L^{-1} day^{-1}) and lipid productivity by 2.5-fold (84.76 mg L^{-1} day^{-1}), with 3.3% CO_2 utilization efficiency compared to directly using 1200 µmol m^{-2} s^{-1}. This study suggests a water recycling-fed batch cycle with gradual light feeding, which results in high CO_2 fixation (1.1 g L^{-1} day^{-1}), 7% CO_2 utilization, and significant biomass and lipid productivity (577.23 and 150 mg L^{-1} day^{-1}). This approach promotes lipid synthesis, maintains carbon fixation, and minimizes biomass loss, thus supporting sustainable bioenergy development in a circular bio-economy framework.

1. Introduction

Microalgae are the subject of extensive research due to their potential use in a wide range of environmental applications along with attaining carbon neutrality and advancing the circular bioeconomic paradigm (Xu et al., 2023). They are capable of efficiently capturing carbon dioxide through photosynthesis and converting it into valuable biomass for bioenergy production. Microalgae possess distinct metabolic abilities that offer significant opportunities for tackling environmental and energy issues, such as producing biofuels and sequestering carbon. Optimizing CO_2 utilization and ensuring long-term stability and sustainability in biofuel production are crucial for harnessing the potential of microalgae and overcoming key challenges in microalgal cultivation.

Microalgae have a wide range of utilization patterns for light, nitrate, phosphate, and carbon dioxide. The observed patterns are shaped by the presence of carbon, nitrogen, and phosphorus, in addition to the feeding tactics adopted. Furthermore, these interactions have a substantial influence on the efficiency of carbon dioxide fixation during photosynthesis (Kumari et al., 2021; Shuhaili et al., 2023). It is difficult to effectively use increased CO_2 levels, such as those found in industrial exhaust gas (ranging from 10% to 20% CO_2). To successfully capture carbon, it is necessary to effectively control the surplus CO_2 and ensure its accessibility to microalgal cells for carbon fixation, thereby preventing its release into the environment (Galès et al., 2020). However, some microalgae exhibit efficient CO_2 sequestration and biomass accumulation at higher CO_2 concentrations, but inhibitory effects arise beyond a certain threshold (Wang et al., 2022; Xin et al., 2023). A high level of CO_2 to the cultivation of microalgae leads to medium acidification (Choi et al., 2021). The degree of acidification is closely tied to the composition of the growth medium, specifically affected by the presence of nitrogen sources (Goldman et al., 1982). Previous investigation has established a direct correlation between elevated CO_2 levels and the impact of nitrate metabolism on the regulation of dissolved inorganic carbon (DIC) (Nguyen and Rittmann, 2015). Therefore, in

* Corresponding author. School of Energy Science and Engineering, Indian Institute of Technology Guwahati, Guwahati, 781039, India.
E-mail address: kmohanty@iitg.ac.in (K. Mohanty).

https://doi.org/10.1016/j.jenvman.2024.120631
Received 13 October 2023; Received in revised form 1 February 2024; Accepted 10 March 2024
Available online 23 March 2024